Identification of genes regulating glucocorticoid-induced and antigen-mediated thymocyte apoptosis

Martin J. Woodward

A thesis submitted for the Degree of Doctor of Philosophy

Institute of Child Health
University College London

2007

ProQuest LLC
789 East Eisenhower Parkway
P.O. Box 1346
Ann Arbor, MI 48106-1346

I, Martin Woodward, confirm that the work presented in this thesis is my own. Where information has been derived from other sources, I confirm that this has been indicated in the thesis.

Abstract.

The default pathway for developing thymocytes is apoptosis; they must be actively instructed to survive and proliferate. Approximately 95% of developing thymocytes undergo apoptosis; only 5% survive to enter the periphery. Thymocytes commit to apoptosis either because of a lack of survival signalling (death by neglect), or by encountering high avidity T cell receptor signalling that might predicate potential autoimmunity (negative selection).

We have performed two Affymetrix DNA microarray screens to attempt to identify candidate regulatory genes for thymocytes undergoing apoptosis; in response to the synthetic glucocorticoid dexamethasone and in the F5 TCR$^{-/-}$ Rag-1$^{-/-}$ Tap-1$^{-/-}$ transgenic model for antigen-mediated negative selection. The up-regulation and expression of genes identified in these screens has been confirmed by qPCR. The action of these genes was assayed in both foetal thymic organ culture (FTOC) and OP9-Delta-Like 1 (OP9-DL1) thymocyte co-culture systems. We have used modified pMSCV (murine stem cell virus) over-expression and knockdown retroviral vectors to infect haematopoietic progenitor cells (HPCs). These cells were then used to reconstitute depleted FTOCs or placed into culture on OP9-DL1 stromal cell layers. Transduced HPCs then differentiate into thymocytes, allowing us to assay the effect of target genes upon apoptosis and the T cell development program.

We assayed target genes from both screens for their effect on thymocyte apoptosis in the presence and absence of apoptosis inducing agents, and have identified several that may be critical in the context of thymocyte apoptosis. One gene, *Tnfaip8*, has been shown to markedly enhance apoptosis in response to dexamethasone, and to inhibit apoptosis when knocked down using RNA interference. This gene is both up-regulated at the double negative (DN) to double positive (DP) transition and highly up-regulated by glucocorticoids.

We have also demonstrated that *Krox24*, a highly induced gene in our F5 TCR$^{-/-}$ Rag-1$^{-/-}$ Tap-1$^{-/-}$ antigen screen, appears to have a role in enhancing apoptosis induced by negative selection in over-expression studies.

Acknowledgements.

I would like to thank Hugh Brady, my Supervisor for all his help, support and encouragement over the years. I would also like to thank Mike Hubank and Owen Williams for all their help, support and encouragement also.

I would also like to thank all the members of the MHCBU lab during my time at ICH, for their help, support, advice and encouragement over the years.

I would also like to thank my wife Shaoni for all her love and support, and for giving me such a wonderful son, Indra.

Contents

Figures

1. Introduction.

2. Materials and Methods.

3. Results (1).

4. Results (2).

5. Results (3).

Tables

2. Materials and Methods.

3. Results (1).

4. Results (2).

5. Results (3).

CHAPTER 1

INTRODUCTION

1. Introduction.

Developing thymocytes are ultimately derived from haematopoietic stem cells (HSCs) of the foetal liver or adult bone marrow. HSCs and other thymic precursors migrate to the thymus and differentiate to become T cells. The process of thymocyte development is not autonomous and requires signalling from both haematopoietic and non-haematopoietic components of the thymic architecture. Traffic of the developing thymocyte through distinct regions of the thymus is required to receive different types of signalling at different points of development in order to generate a mature T cell. The initial steps in development of the thymocyte begin much earlier however, in the bone marrow, with haematopoiesis.

1.1. Haematopoiesis.

All of the mature cells of the haematopoietic blood system have a finite lifespan and are continually replenished, with approximately 3×10^{11} new haematopoietic blood cells produced every day, or 10^{16} in a human lifetime (Spangrude, Heimfeld et al. 1988). The lifespan of a blood cell varies enormously, from less than a week in the case of neutrophils and monocytes, to 120 days in the case of erythrocytes, to many years in the case of mature T cells.

All of these cells are generated from the proliferation and differentiation of a small, relatively constant number of HSCs. One in every 10,000 to 15,000 bone marrow cells is thought to be a stem cell, while in the blood stream the proportion falls to one in ≈100,000 blood cells (Kondo, Wagers et al. 2003; Lensch and Daley 2004). In mice, just 30 of these HSCs are sufficient both to save, and to restore the entire blood system of 50% of lethally irradiated mice (Spangrude, Heimfeld et al. 1988).

Haematopoiesis occurs in discrete organs during development, and occurs in two separate phases defined as primitive (embryonic or yolk sac) and definitive (adult) haematopoiesis. Primitive or embryonic haematopoiesis occurs first in aggregated regions of the extraembryonic yolk sac called blood islands at about 7 days gestation (E7) (Moore and Metcalf 1970). Definitive or adult haematopoiesis occurs from day 11-12 of gestation and generates both the myeloid and lymphoid lineages in the foetal liver (Lensch and Daley 2004), which is subsequently replaced by the bone marrow (particularly of the long bones such as the femurs, but also spongy bone like the ribs and sternum) as the primary site of haematopoiesis after birth.

Haematopoiesis is a hierarchical system. HSCs reside at the pinnacle of all haematopoietic lineages, and can asymmetrically divide and produce both HSCs and progeny more restricted in their pluripotency. These progeny divide, differentiate and proliferate to become the lymphoid, myeloid, and erythroid cells of the haematopoietic system (**Figure 1.1**).

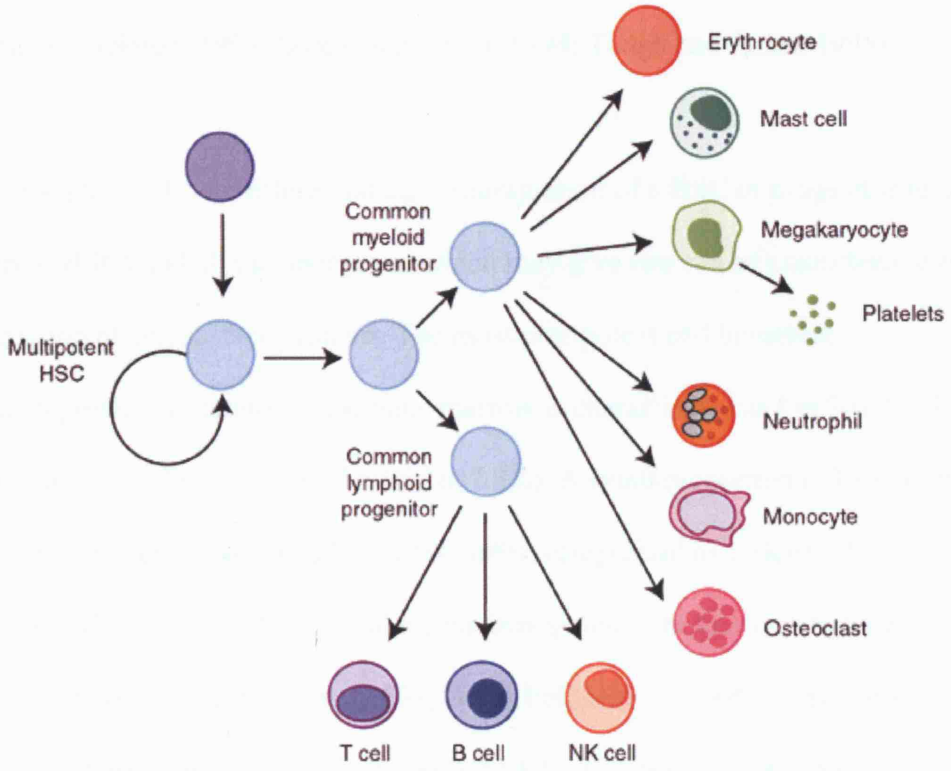

Figure 1.1. Overview of haematopoiesis.
Haematopoiesis produces all the cells of the blood and immune systems. HSCs asymmetrically divide to produce progeny that, although more restricted and committed to a particular cell fate, are hierarchically closer to a defined haematopoietic lineage. Figure adapted from Expert Reviews in Molecular Medicine, Cambridge University Press ©2004.

1.2. Haematopoiesis to thymopoiesis.

T cells are not generated in the bone marrow like other blood cells. The main site of thymopoiesis is the thymus. T cells can also be distinguished from other haematopoietic lineages by their much greater proliferative lifespans. Mature T cells can survive and give rise to proliferative progeny many years after originally exiting the thymus (Sprent 1993; Sprent and Tough 1994; Tough and Sprent 1995).

The first step in T cell differentiation is immigration of a HSC or progenitor to the thymus. HSCs and all the lineages to which they give rise can be characterised by the expression of cell surface proteins. The most pluripotent and immature haematopoietic progenitor of the bone marrow is characterised as $Lin^{-}Sca\text{-}1^{+}c\text{-}Kit^{+}$ ($Lineage^{-}$ Stem Cell Antigen-1^{+} c-Kit^{+} or LSK). A small proportion (≈30%) of these cells also lack expression of Flt-3. These cells, categorised as $LSKFLT3^{-}$, are the self-renewing HSCs that give rise to all the haematopoietic lineages (Spangrude, Heimfeld et al. 1988; Ikuta and Weissman 1992; Baba, Pelayo et al. 2004; Pelayo, Welner et al. 2005; Bhandoola and Sambandam 2006). LSKFLT3+ cells are multipotent progenitors (MPPs) that while still multipotent, lack the self-renewing capacity of true HSCs (Adolfsson, Borge et al. 2001) (**Figure 1.2A**).

HSCs and MPPs are not the only characterised haematopoietic progenitors found in the bone marrow. Also found are the MPP-derived myeloerythroid-restricted common myeloid progenitors (CMPs) (Akashi, Traver et al. 2000), characterised at the cell surface as Lin^{-} Stem Cell Antigen-1^{-} c-Kit^{high} IL-7Rα^{-} Fc$\gamma R^{low}CD34^{+}$, and the lymphoid restricted common lymphoid progenitors (CLPs) (Kondo, Weissman et al.

1997), characterised at the cell surface as Lin^- Stem Cell Antigen-1^{low} c-Kit^{low} IL-$7R\alpha^{high}$ $FLT3^{high}$ (**Figure 1.2A**).

Recent studies have identified a further class of MPP that disputes the classic linear decision between myeloerythroid and lymphoid cell fates. The LMPP, or lymphoid-primed multipotent progenitor ($LSKFLT3^-CD34^+$) exhibits a lymphoid-enhanced and myeloerythroid-reduced multipotency, and is perhaps an intermediate stage between MPPs and CLPs (Adolfsson, Mansson et al. 2005; Jacobsen 2007). HSCs, MPPs, LMPPs and CLPs can all give rise to thymocyte development in the context of the thymus, and will all initiate thymopoiesis.

The earliest T cell progenitors of the thymus have classically been sub-divided according to expression of two cell surface proteins, CD44 (pgp-1) and CD25 (IL-2 receptor α-chain) (Godfrey, Kennedy et al. 1993). The earliest thymic immigrants will reside in the double negative 1 subset (DN1), which is characterised as $CD44^+$ $CD25^-$ $CD3^-$ $CD4^-$ $CD8^-$ (**Figure 1.2B**). DN1 cells of the thymus maintain a great deal of multipotency and lineage plasticity, and can still give rise to many haematopoietic lineages including B cells, T cells, myeloid cells, NK (natural killer) cells and dendritic cells (Ardavin, Wu et al. 1993; Matsuzaki, Gyotoku et al. 1993; Moore and Zlotnik 1995; Shortman, Vremec et al. 1998; Lee, Kim et al. 2001).

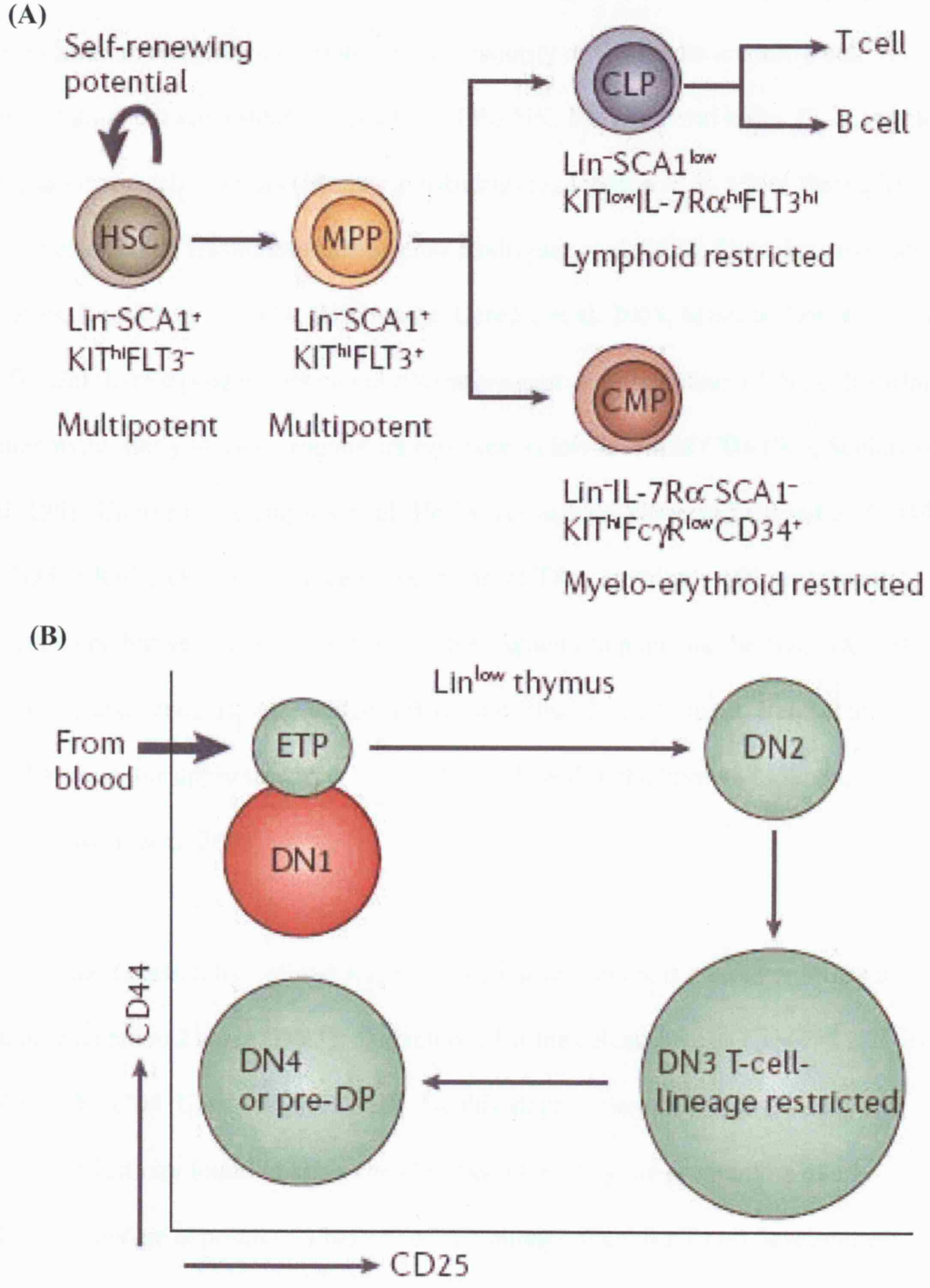

Figure 1.2A and B. Thymocyte development. (A) Development of T and B lineage cells from pluripotent progenitors, as characterised by cell surface markers. Expression of FLT-3 receptor marks transition from self-renewing HSC to more committed multipotent progenitors. **(B)** Early stages of thymocyte development, from immigration (DN1), to specification and commitment (DN3) to pre-DP (DN4). Figure adapted from (Bhandoola and Sambandam 2006).

The definition of DN1 is incomplete when referring to the earliest thymic progenitors. In addition to retaining multipotency, the majority of DN1 cells are not T cell progenitors, but are instead progenitors of the NK, NKT (natural killer T), B, myeloid and dendritic cell lineages (Montecino-Rodriguez, Johnson et al. 1996; Benlagha, Kyin et al. 2002; Hashimoto, Montecino-Rodriguez et al. 2002; Shen, Lu et al. 2003; Porritt, Rumfelt et al. 2004; Balciunaite, Ceredig et al. 2005; Masuda, Itoi et al. 2005). Efficient thymic progenitors can also exist without demonstrating a DN1 cell surface phenotype. Early thymic progenitors can express low levels of CD4 (Wu, Scollay et al. 1991; Chervenak, Dempsey et al. 1993). These cells, characterised as Lin^- $CD44^+$ $CD25^-$ c-Kit^+ $CD4^{low}$ early T cell progenitors (ETPs), are highly efficient thymic precursors, but yet retain the differentiation capacity to populate the NK, NKT, B, myeloid and dendritic cell lineages (Benz and Bleul 2005; Heinzel, Benz et al. 2007). ETPs constitute approximately 1 in 10,000 cells within the thymus (Allman, Sambandam et al. 2003).

The second classically defined stage of T cell development is characterised as the double negative 2 stage (DN2), characterised at the cell surface as $CD44^+$ $CD25^+$c-Kit^+ $CD3^-$ $CD4^-$ $CD8^-$ (**Figure 1.2B**). By this stage some of the multipotency and lineage plasticity found in DN1 cells has been lost. Thymic progenitors of all descriptions are exposed to a battery of signalling critical for T cell development, including Delta-like Notch ligands (Schmitt and Zuniga-Pflucker 2002), C-KIT, IL-7 and WNT factors, and an increased oxygen tension (Ivanov, Merkenschlager et al. 1993). Notch signalling rapidly degrades the B cell potential of thymic progenitors (Pui, Allman et al. 1999; Radtke, Wilson et al. 1999; Wilson, MacDonald et al. 2001;

Hashimoto, Montecino-Rodriguez et al. 2002). DN2 thymic progenitors can however still give rise to NK and dendritic cells (Ardavin, Wu et al. 1993; Shen, Lu et al. 2003).

Final T cell lineage specification and commitment does not occur until stage double negative 3 (DN3, characterised as $CD44^-$ $CD25^+$c-Kit^- $CD3^-$ $CD4^-$ $CD8^-$), at which point thymic progenitors undergo proliferative expansion and *TCRβ*, *TCRγ* and *TCRδ* gene rearrangement (Ismaili, Antica et al. 1996; Capone, Hockett et al. 1998; Livak, Tourigny et al. 1999) (**Figure 1.2B**). The boundary between stages DN2 and DN3 is not as clear as other transitions. *TCR* rearrangement is initiated by induction of the recombinase-activating genes 1 and 2 (*Rag-1* and *Rag-2*). There is also induction of the LCK tyrosine kinase needed for pre-TCR and TCR signalling (Shimizu, Kawamoto et al. 2001), and of the CD3γ and ε chains of the TCR and pre-TCR complexes (Wurch, Biro et al. 1998) and pTα (Yamasaki and Saito 2007) . Full commitment to the T cell lineage can be extensively delayed, and may require 7-10 cycles of proliferation and approximately 2 weeks in the thymus to occur. Typical expansion from a thymic precursor may involve a 10^5-fold expansion in numbers, with a 10^3 fold expansion occurring prior to DN4 β-selection (Kawamoto, Ohmura et al. 2003).

Until the DN3 stage is reached, apparently committed T lineage progenitors can still be induced to change fate and become myeloid, B or NK cells (Taghon, David et al. 2005). Removal of cells from the thymus and exposure to alternative conditions, whether *in vitro* culture or an irradiated mouse host, has been shown to be able to reverse commitment in DN2 thymocytes, even once *Rag* activation and *TCR* α, β and

γ gene rearrangement has commenced (Igarashi, Gregory et al. 2002). The B cell alternative is lost earliest, becoming undetectable within the DN1 subset as the sustained Notch/Delta-like 1 signalling of the thymic microenvironment blocks B cell fate (Hozumi, Abe et al. 2003; Taghon, David et al. 2005).

TCRα, *TCRβ* and *TCRγ* gene rearrangement, governed by expression of the linked *Rag* genes and transcription factor-mediated opening of the *TCR* loci, must occur for successful T cell development (Shinkai, Koyasu et al. 1993; Godfrey, Kennedy et al. 1994; Guidos, Williams et al. 1995; Diamond, Ward et al. 1997; Shockett, Zhou et al. 2004). Rearrangement of the immunoglobulin gene segments is critically important for T cell maturation; if the rearrangement is unsuccessful in manufacturing a translatable protein, this will be detected by the transcription of genes encoding the signalling components of the TCR complex. *TCR* gene rearrangement which generates a non-functional, non-translatable TCR chain leads to apoptosis (Falk, Nerz et al. 2001). The pre-Tα, CD3 and ζ proteins combine with the successfully translated TCRβ, γ or δ chain to form the pre-TCR, which stimulates proliferation, β-selection (or γδ-selection) (Fehling and von Boehmer 1997) and DN3 to DN4 transition.

Successful pre-TCR signalling drives the down-regulation of the *CD25*, *pre-Tα* and *Rag* genes, allelic exclusion of the non-rearranged *TCRβ* locus and the appearance of DN4 cells (characterised as $CD44^-$ $CD25^-$ c-Kit^- $CD3^-$ $CD4^-$ $CD8^-$) (**Figure 1.2B**). β-selected cells (cells that have successfully rearranged their *TCRβ* gene to form a translatable TCR protein) undergo a burst of proliferation followed by up-regulation of *CD8* and *CD4* genes to become quiescent $CD4^+$ $CD8^+$ DP cells. The *Rag* genes then undergo a second cycle of expression to drive *TCRα* gene rearrangement.

Transcriptional control of the *TCRα* chain gene is similar to that of the *TCRβ* gene, and if rearrangement is successful, leads to the formation of a complete αβ TCR, which is expressed on the surface of the αβ lineage $CD4^+$ $CD8^+$ $CD3^+$ (DP) T cell as a complex with CD3 and ζ proteins (Huesmann, Scott et al. 1991). Once expressing a complete TCR complex, these DP cells become responsive to antigen, and therefore susceptible to both positive and negative selection.

A diagram demonstrating the major steps in thymocyte development is shown in **Figure 1.3**.

1.3. Molecular regulators of T cell lymphoid development.

T cell development requires a specific set of transcription factors and signalling molecules to occur, both throughout maturation to confirm T cell identity and later to delineate between subset specifications (**Figure 1.4**). One of the earliest acting factors is Notch1, and its downstream effector RbpSuh (**Figure 1.4**) (Han, Tanigaki et al. 2002). *Notch1* knockout cells cannot commit to the T cell lineage, and B cells generate in the thymus instead (Radtke, Wilson et al. 1999; Wilson, MacDonald et al. 2001), while *Notch* gain of function mutation (expression of NotchIC, a constitutively active mutant) enhances T cell development at the expense of B cell development, so much so that DP thymocytes form in the bone marrow (Pui, Allman et al. 1999).

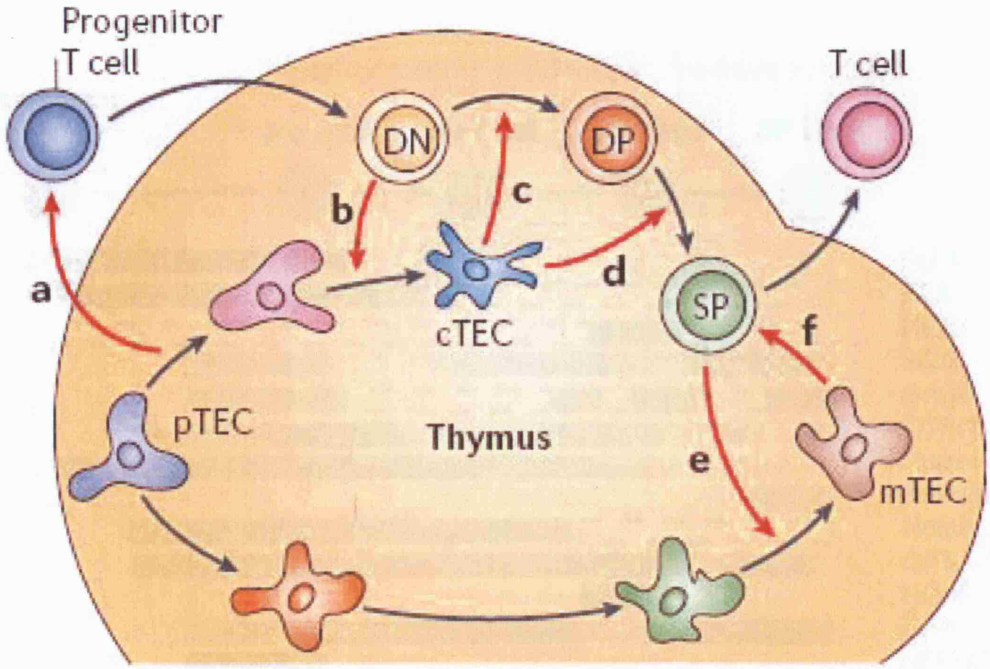

Figure 1.3. Overview of thymocyte development.
Diagram demonstrating development of a T cell precursor from immigration to exit as a mature T cell. A, immigration; B, DN thymocytes conditioning cortical TECs; C, DP formation; D, positive selection; E, SP thymocytes conditioning medullary TECs; F, SP export to periphery. Figure adapted from (Takahama 2006).

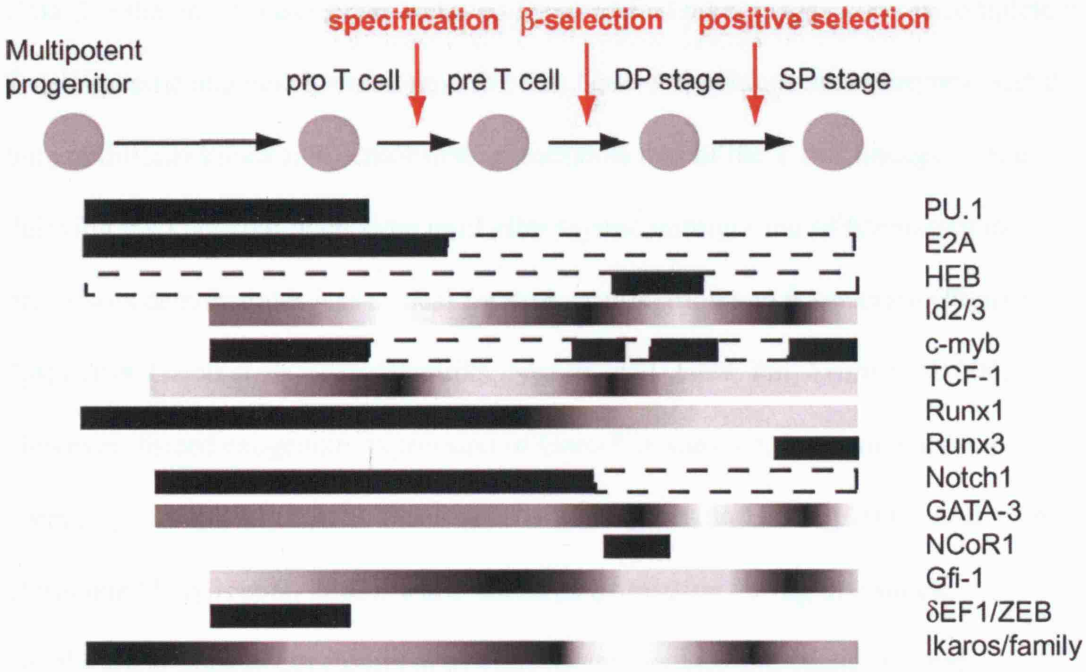

Figure 1.4. Gene expression during thymocyte development.
Diagram outlining temporal control of expression of T cell developmental genes. Shading intensity represents relative level of expression. Figure adapted from (Rothenberg and Taghon 2005).

Notch1/RbpSuh signalling is also required for *TCRβ* rearrangement and proliferation prior to β-selection (**Figure 1.4**) (Wolfer, Wilson et al. 2002). However, constitutive expression of Notch1 later in T cell development (Notch1 is down-regulated at the DN to DP transition (Huang, Gallegos et al. 2003)) perturbs the choices made by β-selected T cells (Fowlkes and Robey 2002), and favours generation of CD8 SP thymocytes over CD4 SP thymocytes.

Gata-3 is the only transcription factor so far identified whose expression is completely T-cell specific amongst haematopoietic cells. *Gata-3* knockouts are embryonic lethal, but conditional knockouts demonstrate a complete loss of the T cell lineage, while delaying the knockout phenotype until after thymic immigration of haematopoietic precursors demonstrates it is critical for both proliferation and β-selection (**Figure 1.4**) (Ting, Olson et al. 1996; Hendriks, Nawijn et al. 1999; Pai, Truitt et al. 2003). However, forced exogenous expression of Gata-3 in non-thymic haematopoietic precursors completely blocks T cell specification (Chen and Zhang 2001; Anderson, Hernandez-Hoyos et al. 2002), while enforced expression during thymocyte development impairs development of CD8 SP thymocytes and causes thymic lymphoma (Nawijn, Ferreira et al. 2001). Gata-3 can exert multiple molecular and biochemical effects in thymocytes, including chromatin remodelling, and both transcriptional activation and repression (Lee, Fields et al. 2001; Ranganath and Murphy 2001; Klein-Hessling, Jha et al. 2003).

Developing thymocytes also share essential regulatory genes with B cells, one such gene being *E2A*, which is known to regulate several vital target genes including *CD4*, *pTα* and the *Rag* genes, and to co-ordinate with IL-7 in promoting survival (**Figure**

1.4) (Kee, Bain et al. 2002). *E2A* has also been shown to control the accessibility of the *TCRβ*, *TCRγ*, and *TCRδ* loci to the Rag recombinase machinery (Bain, Romanow et al. 1999). Over-expression of Id proteins, which heterodimerize with E2A to block E2A DNA-binding domains, completely abrogates T cell specification (Heemskerk, Blom et al. 1997).

The cytokine IL-7 is of paramount importance in thymocyte development, governing the DN2 stage-associated burst of proliferation in particular. Loss of the *IL-7* gene reduces thymic cellularity 20-fold, splenic cellularity 10-fold, and was the first example of a cytokine-deficient mice to exhibit severe lymphopaenia (von Freeden-Jeffry, Vieira et al. 1995). C-Kit receptor expression is also vital. Loss of c-Kit reduces thymic cellularity and affects both the structure of the thymus and development of thymic epithelial cells. Without T cell development the thymus develops aberrantly, with both cortical and medullary TECs failing to form properly (**Figure 1.3B** and **E**) (Asamoto and Mandel 1981; Takahama 2006).

Runx family proteins are also of great importance in T cell development. *Runx1* knockouts are embryonic lethal because of its importance in haematopoiesis (Tracey and Speck 2000; Nishimura, Fukushima-Nakase et al. 2004), but targeted conditional transgenics and knockouts have determined that Runx factors are crucially important for many aspects of the T cell developmental program, including proliferation, β-selection and CD8 SP cell specification (**Figure 1.4**) (Taniuchi, Osato et al. 2002; Woolf, Xiao et al. 2003). *Ikaros* is essential for both T and B cell development; global inhibition of all isoforms inhibits T, B and NK cell formation. Ikaros family isoforms act at successive stages of T cell development, including HSC maintenance and β-

selection, and may also play a role in negative selection (**Figure 1.4**) (Cortes, Wong et al. 1999; Nichogiannopoulou, Trevisan et al. 1999; Winandy, Wu et al. 1999; Georgopoulos 2002; Papathanasiou, Perkins et al. 2003; Abrams, Robertson et al. 2004; Urban and Winandy 2004). Ikaros and Runx family expression patterns and effects overlap, both families tending to drive CD8 expression and differentiation (Harker, Naito et al. 2002).

Pu.1, a member of the *ETS* family, is a transcription factor expressed very early on in maturation (Dahl and Simon 2003), where it acts in cohort with IL-7Rα expression in a mainly proliferative context (**Figure 1.4**) (DeKoter, Lee et al. 2002). Disruption of Pu.1 prevents T cell development, as does constitutive over-expression (McKercher, Torbett et al. 1996; Anderson, Weiss et al. 2002).

1.4. Thymocyte apoptosis.

Once T cells have gone through T lineage specification, *TCRβ* rearrangement, pre-TCR complex formation, proliferation and the DN to DP transition, *TCRα* rearrangement and TCRαβ complex formation and presentation, the resultant TCRαβ T cells are ready for TCR-based positive or negative selection.

DP thymocytes only survive in the thymus for 3-4 days (Guo, Hawwari et al. 2002), and are exquisitely sensitive to apoptotic stimuli (Screpanti, Morrone et al. 1989). Apoptosis is the default pathway for DP thymocytes, they must be actively instructed to survive and proliferate. The short-lived survival of DP thymocytes is maintained by gradually decreasing levels of Bcl-XL (Chao and Korsmeyer 1997). Loss of the Rorγ steroid transcription factor, which maintains Bcl-XL expression, ensures that

thymocytes enter the apoptotic 'death by neglect' pathway long before they have had an opportunity to be positively selected (Kurebayashi, Ueda et al. 2000; Sun, Unutmaz et al. 2000; Guo, Hawwari et al. 2002).

The DP T cell has also down-regulated Bcl-2 to negligible levels (Hockenbery, Zutter et al. 1991; Gratiot-Deans, Merino et al. 1994), and is therefore sensitive to apoptotic stimuli to which DN or SP cells are unresponsive (Wiegers, Knoflach et al. 2001). Less than 5% of DP thymocytes will survive this stage of development by being positively selected (**Figure 1.5A**), and ≈5% of DP T cells expressing a TCR with an excessively high avidity for self peptide:MHC complexes will be actively instructed to undergo apoptosis in a process termed negative selection (**Figure 1.5B**) (Rammensee and Bevan 1984; Kappler, Roehm et al. 1987; Sprent and Webb 1987; Sha, Nelson et al. 1988; Sebzda, Mariathasan et al. 1999). The remaining 90% or more will undergo apoptosis as a result of receiving no survival signalling, a consequence of their TCR not binding to self peptide:MHC complexes at all (**Figure 1.5C**) (Ashwell, Lu et al. 2000; Chung, Choi et al. 2002; Abrams, Robertson et al. 2004; Ko, Jang et al. 2004; Lepine, Sulpice et al. 2005; Herold, McPherson et al. 2006). This clonal deletion enables the formation of a fully functional, yet still self-tolerant peripheral T cell repertoire.

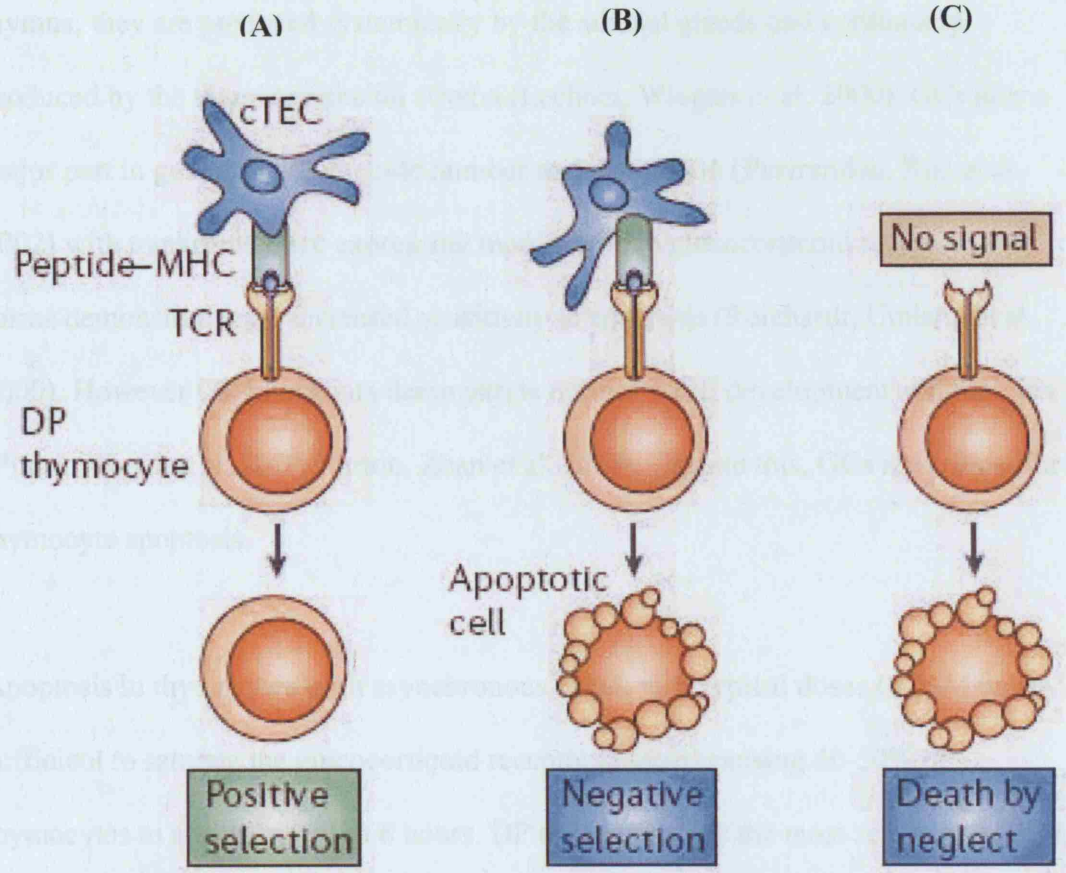

Figure 1.5. Thymocyte Apoptosis.
Diagram showing potential fates of an immature DP T cell; survival through positive selection as a result of moderate avidity TCR self-peptide:MHC signalling (A), apoptotic death through negative selection as a result of excessively high avidity TCR self-peptide:MHC signalling (B) or 'death by neglect' as a result of no TCR self-peptide:MHC signalling (C). Figure adapted from (Takahama 2006).

1.5. Glucocorticoid-induced thymocyte apoptosis.

DP thymocytes are non-cycling, quiescent TCRαβ cells that are exquisitely sensitive to many apoptotic stimuli including glucocorticoids (GCs), ionising radiation, heat shock, FAS, and etoposide. GC steroid hormones are continuously present in the thymus; they are produced systemically by the adrenal glands and continually produced by the thymic epithelial stroma (Lechner, Wiegers et al. 2000). GCs play a major part in governing thymocyte number and maturation (Pazirandeh, Xue et al. 2002) with transgenic mice expressing more sensitive glucocorticoid receptor (GR) forms demonstrating an increased sensitivity to apoptosis (Reichardt, Umland et al. 2000). However GR knockouts demonstrate normal T cell development and function (Purton, Boyd et al. 2000; Purton, Zhan et al. 2002). Despite this, GCs are critical for thymocyte apoptosis.

Apoptosis in thymocytes is an asynchronous event, with typical doses (0.5μM being sufficient to saturate the glucocorticoid receptor *in vitro*) causing 40-50% of thymocytes to apoptose within 6 hours. DP thymocytes are the most sensitive to GCs, with CD4 SP cells and CD8 SP cells less so, while DN thymocytes are completely resistant (Screpanti, Morrone et al. 1989; Wiegers, Knoflach et al. 2001). GR expression is highest in DN cells, lowest in DP cells with SP expression lying intermediate between the two. GC regulation *in vivo* follows a circadian pattern, as does the expression of several GC target genes (Mitsui, Yamaguchi et al. 2001). Elevated concentrations during stress responses are sufficient to exert physiological effects on thymocyte number.

GCs are involved in the regulation of a wide variety of biological processes, including inflammation, metabolism, proliferation, differentiation, and reproduction. GCs are also highly important in the treatment of lymphoid malignancies because of their pro-apoptotic effects upon lymphoid cells (Frankfurt and Rosen 2004; Schmidt, Rainer et al. 2004). GCs exert an apoptotic response in GC-sensitive cells, inducing mitochondrial permeabilization, caspase activation, cell shrinkage and membrane blebbing, phosphatidylserine exposure, chromatin condensation, endonuclease activation and DNA fragmentation (Kerr, Wyllie et al. 1972; Wyllie 1980; Wyllie, Morris et al. 1984; McConkey, Nicotera et al. 1989; Howie, Harrison et al. 1994; Lepine, Sulpice et al. 2005).

Apoptosis as a defined program of controlled cell death is highly important in thymocyte development, not only as it serves to clonally delete potentially harmful or useless thymocyte clones from the T cell repertoire, but it does so in a way that does not provoke an inflammatory response. If 95% of the DP cells in the thymus were to die by necrosis, with the associated release of toxic cellular components and debris, this would provoke inflammation. Instead the thymocyte undergoing apoptosis presents phosphatidylserine molecules on its cell surface that act as a signal to macrophages to clear the cell by phagocytosis (Fadok, Bratton et al. 2000).

The actions of lipophilic GCs are first initiated by passively crossing the cell membrane and binding to the cytosolic GR, a member of the nuclear receptor family of ligand-binding transcription factors. GR is normally sequestered in the cytosol in association with 'chaperone' heat shock proteins including Hsp90, Hsp70, and the immunophilins Hsp56, Cyp-40 and Fkbp51 in a hetero-oligomeric complex. Once a

GC ligand is bound, the GR undergoes conformational change and dimerization that leads to its release. Homodimerized GR translocates to the nucleus where it binds to DNA sequences called glucocorticoid-response elements (GREs, consensus sequence GGT ACA NNN TGT TCT) from which it can transactivate or transrepress GRE-regulated genes (Luisi, Xu et al. 1991). Nuclear GR can also bind to other transcription factors including NF-κB (De Bosscher, Schmitz et al. 1997; Heck, Bender et al. 1997; De Bosscher, Vanden Berghe et al. 2003), AP-1 (Jonat, Rahmsdorf et al. 1990) and Stat5 (Stoecklin, Wissler et al. 1997). The dual nature of GR activity was most clearly demonstrated by knock-in mice expressing GR with a A458T point mutation that prevents both dimerization and DNA binding (Reichardt, Kaestner et al. 1998). GR^{dim} mice are unable to induce transcription from GREs but still retain AP-1, Stat5 and NF-κB binding activity and effects (Reichardt, Tuckermann et al. 2001)

Apoptosis induced by GCs is reliant on *de novo* transcription and translation, and is blocked by inhibition of both RNA (actinomycin D) and protein (cycloheximide) synthesis (Wyllie, Morris et al. 1984). Glucocorticoid-induced thymocyte apoptosis is apparently mediated by the mitochondrial pathway, is inhibited by Bcl-2 and Bcl-XL (Siegel, Katsumata et al. 1992), and requires caspase cleavage and Apaf-1 (Hakem, Hakem et al. 1998; Kuida, Haydar et al. 1998). A rapid non-genomic effect of GCs induced by GC/GR interaction is activation of the ceramide pathway and production of ceramide, which is detectable within 5 minutes (Cifone, Migliorati et al. 1999). Ceramide is enzymatically converted to sphingosine, which provokes apoptosis in thymocytes by activating the JNK-MAPK pathway (Cuvillier 2002).

A major effect of GC induced apoptosis is the enhancement of Cdk2 activity (Gil-Gomez, Berns et al. 1998). The *Bcl-2* family members Bcl-2 and Bax both modulate Cdk2 activity in thymocytes (Brady, Gil-Gomez et al. 1996; Brady and Gil-Gomez 1998; Brady and Gil-Gomez 1999) (**Section 1.7**). GCs also trigger the proteasome pathway, which is important for degrading some of the products of GC-induced apoptosis in addition to degrading some anti-apoptotic molecules.

1.6. Bcl-2 family members.

The *Bcl-2* family consists of a group of proteins which share BH (Bcl-2 homology) domains, some members sharing three domains while a group of pro-apoptotic members share only the shortest BH3 domain (**Figure 1.7**). Different pro-apoptotic and anti-apoptotic family members demonstrate different expression patterns and sub-cellular localisation. As stated previously, Bcl-2 is almost completely down-regulated at the DN to DP transition, and DP thymocytes express negligible levels of Bcl-2 (a major reason why DP thymocytes are so sensitive to apoptotic stimuli) (Hockenbery, Zutter et al. 1991; Gratiot-Deans, Merino et al. 1994). Bcl-XL is conversely up-regulated (which explains the spontaneous survival of DP thymocytes without Bcl-2) (Linette, Grusby et al. 1994; Ma, Pena et al. 1995; Chao and Korsmeyer 1997). As Bcl-XL expression gradually decreases over time, non-selected thymocytes go into the apoptotic 'death by neglect' pathway.

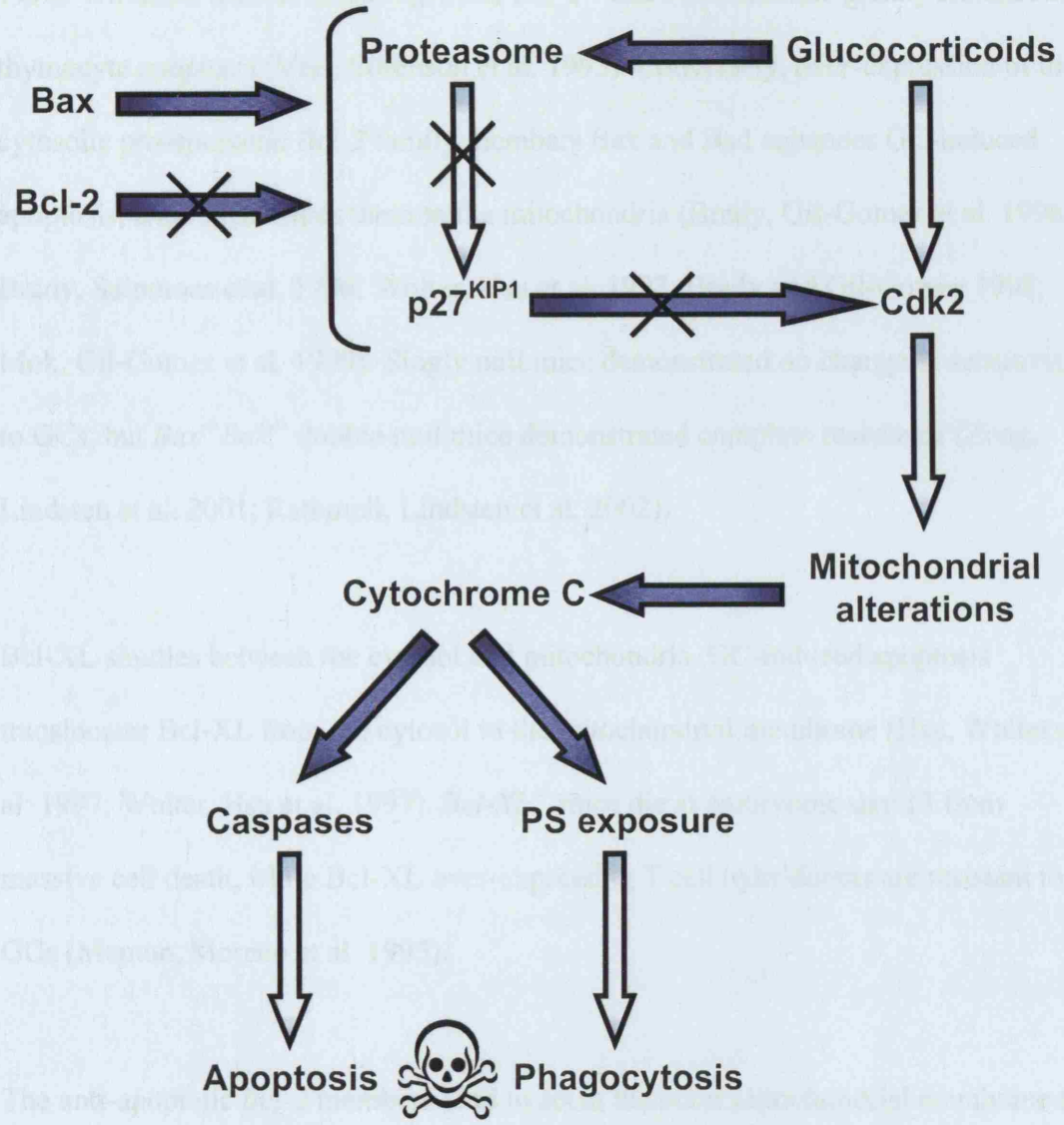

Figure 1.6. Cdk2 in thymocyte apoptosis.
Central importance of Cdk2 in glucocorticoid-induced thymocyte apoptosis. Figure adapted from (Lepine, Sulpice et al. 2005).

Bcl-2 is an anti-apoptotic, membrane-bound member of the *Bcl-2* family that resides in the mitochondrial membrane. Bcl-2 over-expression completely abrogates GC-induced thymocyte apoptosis (Memon, Moreno et al. 1995; Williams, Norton et al. 1998; Williams, Mok et al. 2001), while *Bcl-2*$^{-/-}$ mice demonstrate greatly enhanced thymocyte apoptosis (Veis, Sorenson et al. 1993). Conversely, over-expression of the cytosolic pro-apoptotic *Bcl-2* family members Bax and Bad enhances GC-induced apoptosis, and redistributes them to the mitochondria (Brady, Gil-Gomez et al. 1996; Brady, Salomons et al. 1996; Wolter, Hsu et al. 1997; Brady and Gil-Gomez 1998; Mok, Gil-Gomez et al. 1999). Singly null mice demonstrated no change in sensitivity to GCs, but *Bax*$^{-/-}$*Bak*$^{-/-}$ double null mice demonstrated complete resistance (Zong, Lindsten et al. 2001; Rathmell, Lindsten et al. 2002).

Bcl-XL shuttles between the cytosol and mitochondria. GC-induced apoptosis translocates Bcl-XL from the cytosol to the mitochondrial membrane (Hsu, Wolter et al. 1997; Wolter, Hsu et al. 1997). *Bcl-XL*$^{-/-}$ mice die at embryonic day 13 from massive cell death, while Bcl-XL over-expressing T cell hybridomas are resistant to GCs (Memon, Moreno et al. 1995).

The anti-apoptotic *Bcl-2* members tend to act at the outer mitochondrial membrane to inhibit cytochrome c release, while the pro-apoptotic members react to an apoptotic stimulus by shuttling to the outer mitochondrial membrane to promote cytochrome c release and apoptosis. The levels of *Bcl-2* family members are generally unaffected by GC administration, with the exception of Bad and Bax which are up-regulated (Mok, Gil-Gomez et al. 1999). Over-expression of Bax and Bad both accelerate apoptosis and cell cycle entry in response to GC, while Bcl-2 over-expression retards cell cycle

entry (Brady, Gil-Gomez et al. 1996; Brady, Salomons et al. 1996; Brady and Gil-Gomez 1998; Gil-Gomez, Berns et al. 1998; Mok, Gil-Gomez et al. 1999).

The Bim isoforms are up-regulated by glucocorticoids in lymphoid models (Wang, Malone et al. 2003), in addition to being of crucial importance in negative selection (Bouillet, Purton et al. 2002). RNAi-mediated knockdown of various isoforms reduces or abrogates glucocorticoid-induced thymocyte apoptosis (Abrams, Robertson et al. 2004). Constitutively active forms of Bim are unable to induce apoptosis in the absence of *Bak* and *Bax*, implying that these pro-apoptotic multi-domain *Bcl-2* family members are required for Bim function (Zong, Lindsten et al. 2001) (**Figure 1.7**).

1.7. Cdk2 and thymocyte apoptosis.

Cdk2 is most often associated with cell cycle progression through cell cycle checkpoints in counterpart with the cyclins and the cyclin-dependent kinase inhibitors. However there is a crossover between the cell cycle and apoptotic programs on the part of *Cdk2*, which acts as a juncture between both pathways (Gil-Gomez, Berns et al. 1998; Hakem, Sasaki et al. 1999; Granes, Roig et al. 2004). This is particularly important in the case of quiescent cells such as thymocytes where the activity of Cdk2 in each program can be delineated (**Figure 1.8**).

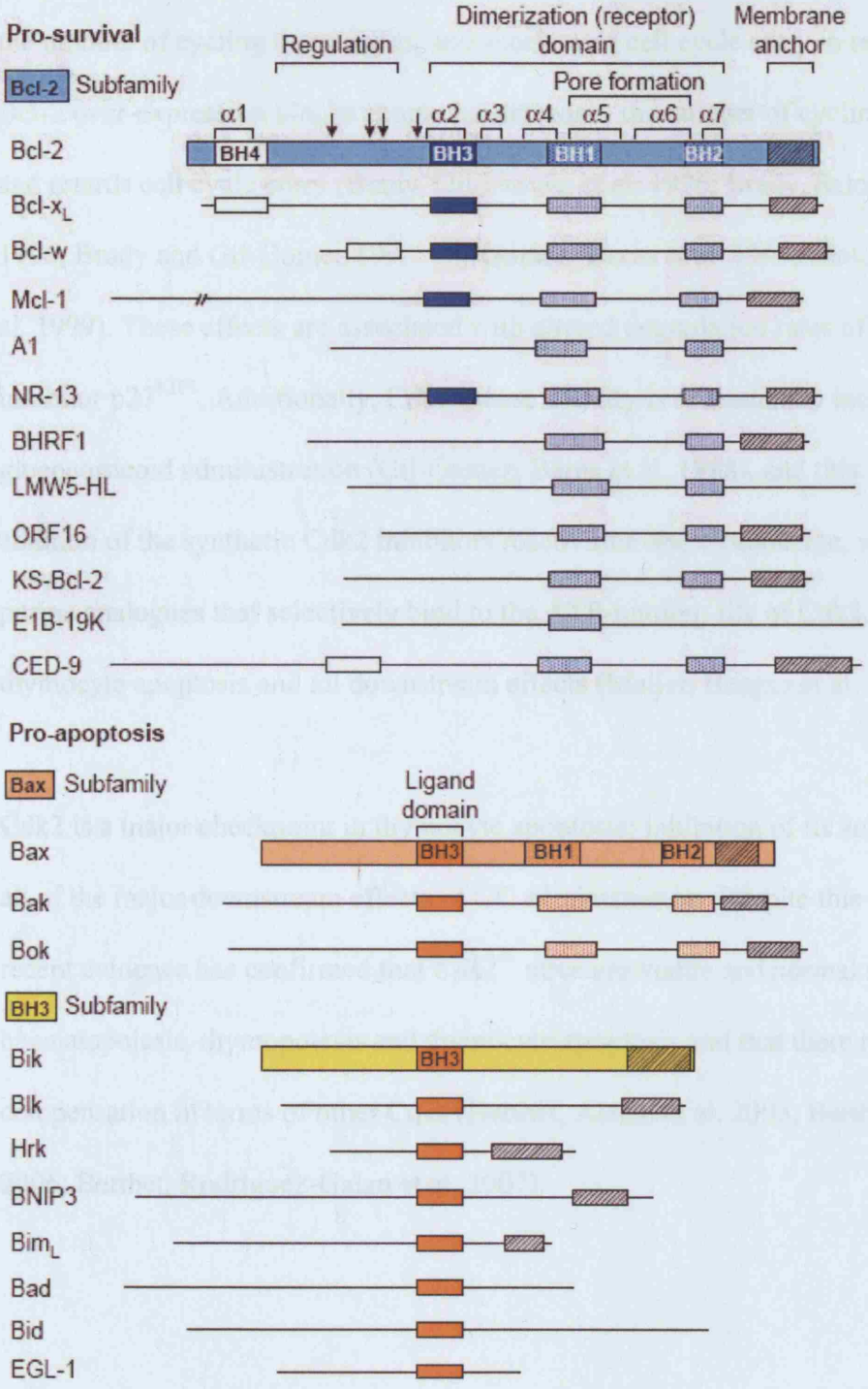

Figure 1.7. Bcl-2 family members.
Bcl-2 family members and their protein domains. BH1 to BH4 are conserved domains. Anti-apoptotic members of the Bcl-2 sub-group possess all four BH domains, while all Bcl-2 family members share the BH3 domain. The Bax sub-group resembles the Bcl-2 sub-group but lacks a functional BH4 domain. Includes orthologous members Nr-13 (*gallus gallus*), Ced-9, and Egl-1 (*C. elegans*), viral proteins Bhrf1, Lmw5-hl, Orf16, Ks-Bcl-2, and E1B- 19K. Adapted from (Adams and Cory 1998).

As stated previously, over-expression of Bax and Bad enhances apoptosis, increases the number of cycling thymocytes, and accelerates cell cycle entry in response to GC. Bcl-2 over-expression blocks apoptosis, decreases the number of cycling thymocytes and retards cell cycle entry (Brady, Gil-Gomez et al. 1996; Brady, Salomons et al. 1996; Brady and Gil-Gomez 1998; Gil-Gomez, Berns et al. 1998; Mok, Gil-Gomez et al. 1999). These effects are associated with altered degradation rates of the Cdk2 inhibitor $p27^{KIP1}$. Additionally, Cdk2 kinase activity is dramatically increased upon glucocorticoid administration (Gil-Gomez, Berns et al. 1998), and this is blocked by addition of the synthetic Cdk2 inhibitors roscovitine and olomoucine, which are purine analogues that selectively bind to the ATP-binding site of Cdk2, and abolish thymocyte apoptosis and all downstream effects (Meijer, Borgne et al. 1997).

Cdk2 is a major checkpoint in thymocyte apoptosis; inhibition of its activity precludes all of the major downstream effects of GC administration. Despite this however, recent evidence has confirmed that *Cdk2*$^{-/-}$ mice are viable and normal in terms of haematopoiesis, thymopoiesis and thymocyte apoptosis and that there might be compensation in terms of other Cdks (Berthet, Aleem et al. 2003; Berthet and Kaldis 2006; Berthet, Rodriguez-Galan et al. 2007).

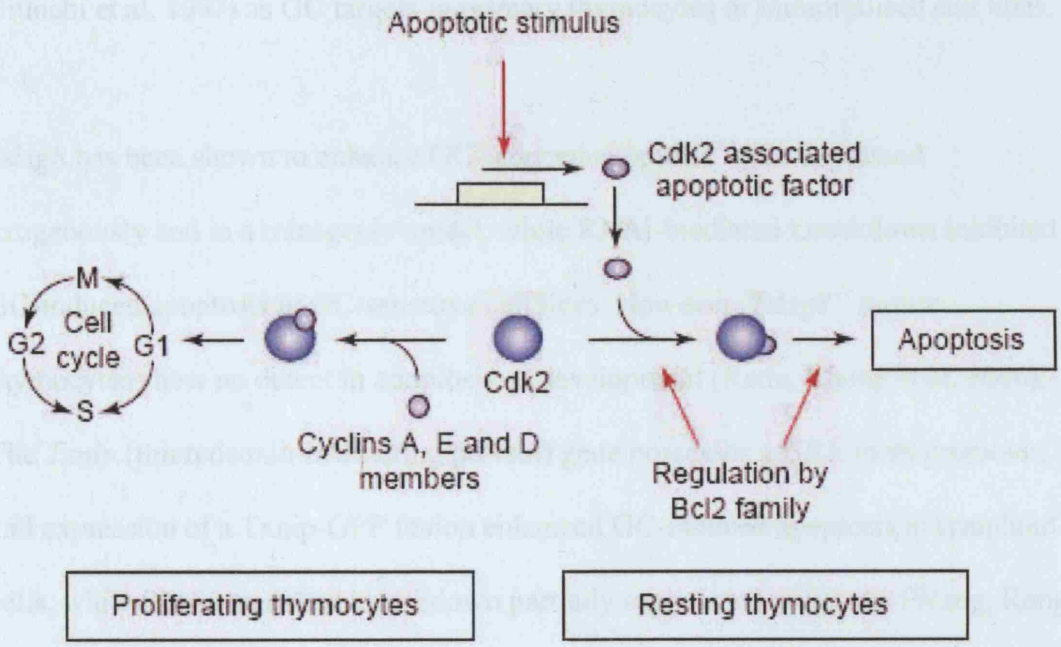

Figure 1.8. Role of Cdk2 in resting and proliferating thymocytes.
Diagram delineating divergent role of Cdk2 in proliferating and quiescent thymocytes, and potential novel Cdk2 associated apoptotic factor involved in apoptosis. Figure taken from (Williams and Brady 2001).

1.8. Previously identified targets of glucocorticoids.

Previous studies have identified several transcriptional targets of glucocorticoid exposure in thymocytes. Although aspects of the pathway induced by GCs remains uncertain, recent studies have identified *Bim* (Wang, Malone et al. 2003), *Tdag8* (Tosa, Murakami et al. 2003; Malone, Wang et al. 2004), *dig2* (Wang, Malone et al. 2003), *Txnip* (Wang, Rong et al. 2006), *Gilz* (D'Adamio, Zollo et al. 1997), *puma* (Han, Flemington et al. 2001), *IκB* (Deroo and Archer 2001) and *Gitr* (Nocentini, Giunchi et al. 1997) as GC targets in primary thymocytes or immortalised cell lines.

Tdag8 has been shown to enhance GC-induced apoptosis when expressed exogenously and in a transgenic model, while RNAi-mediated knockdown inhibited GC-induced apoptosis in GC-sensitive cell lines. However, *Tdag8*$^{-/-}$ mouse thymocytes show no defect in apoptosis or development (Radu, Cheng et al. 2006). The *Txnip* (thioredeoxin-interacting protein) gene possesses a GRE in its promoter, and expression of a Txnip-GFP fusion enhanced GC-induced apoptosis in lymphoid cells, while RNAi-mediated knockdown partially suppressed apoptosis (Wang, Rong et al. 2006). *Dig2* was demonstrated to be a novel anti-apoptotic GC target gene whose expression was shown to block apoptosis in lymphoid cell lines (Wang, Malone et al. 2003).

Gilz (glucocorticoid-induced leucine zipper protein) is rapidly induced by dexamethasone, and when over-expressed in lymphoid cells lines increases apoptosis (D'Adamio, Zollo et al. 1997). This is caused by a Gilz-mediated reduction in Bcl-XL expression and increase in caspase activation (Delfino, Agostini et al. 2004). Gilz also reduces TCR-mediated apoptosis by down-regulating FAS expression at the cell

surface, and may be involved in the mutual antagonism of GR and TCR signalling (D'Adamio, Zollo et al. 1997). Gilz has been demonstrated to interact with AP-1 and NF-κB, both targets of GR (Ayroldi, Migliorati et al. 2001). *Bax* and *Bad* are also known GC targets (Brady, Gil-Gomez et al. 1996; Mok, Gil-Gomez et al. 1999), as is *E4bp4*, which has been shown to possess a GRE (Wallace, Wheeler et al. 1997). The full spectrum of genes regulating the glucocorticoid-induced apoptotic cascade is however incomplete.

1.9. Negative selection.

DP T cells that express αβ TCR heterodimers on their cell surface are susceptible to both positive and negative selection. T cells that express MHC class II restricted TCRs can be positively selected to the CD4 SP helper T cell lineage (Berg, Pullen et al. 1989; Kaye, Hsu et al. 1989), while T cells that express MHC class I restricted TCRs can be positively selected to the CD8 SP cytotoxic T cell lineage (Sha, Nelson et al. 1988; Teh, Kisielow et al. 1988). It is the strength of the interaction between TCR and self peptide:MHC that governs whether the cell is positively or negatively selected. Too strong an interaction might predicate autoimmunity, and therefore cells exhibiting an excessively strong avidity for self-peptide:MHC are negatively selected, and directed to undergo apoptosis. A moderate avidity reaction indicates a potentially viable and productive T cell clone, and these cells are positively selected for further differentiation and subsequent export to the periphery as mature functional T cells. Too weak an interaction and the cells receive insufficient survival signalling and die by apoptosis (Kappler, Staerz et al. 1988; Kisielow, Bluthmann et al. 1988; Sha, Nelson et al. 1988; Sebzda, Mariathasan et al. 1999; Huseby, White et al. 2005).

Negative selection occurs primarily in the thymic medulla, via presentation of self-antigen-peptide:MHC complexes upon antigen-presenting cells (APCs) (Gallegos and Bevan 2004). For a fully self-tolerant, yet viable and productive immune system to form, developing thymocytes must be exposed to a massive battery of peptide:MHC complexes, including both ubiquitous antigens and those that might not be expressed in the thymus, whose expression is otherwise tissue-specific (Kyewski and Derbinski 2004). In addition to dendritic cells, medullary thymic epithelial cells (TECS) are also active as APCs, although less efficiently. Individual medullary TECs can express greater than 400 non-thymic antigens (typically genes grouped on chromosomes) (Gotter, Brors et al. 2004), and many thousands of non-thymic antigens may be expressed overall (Derbinski, Schulte et al. 2001; Derbinski, Gabler et al. 2005). mTECs share antigens with dendritic cells for the purposes of negative selection, taking advantage of the dendritic cells supreme efficiency as an APC (Gallegos and Bevan 2004).

Developing thymocytes must contact several APCs to be exposed to the entire self-peptide repertoire, as the number of APCs expressing any given peptide within the thymus is relatively small. Defects in the catalogue of presentation are highlighted by autoimmune deficiencies in *AIRE*$^{-/-}$ individuals, which in humans is categorised by those with the rare disorder autoimmune polyendocrinopathy syndrome type 1 (APS-1) (Anderson, Venanzi et al. 2002; Anderson, Venanzi et al. 2005). Sufferers lack expression of ≈ 500 non-thymic antigens on mTECs. *Aire*$^{-/-}$ mice develop a similar syndrome. The disorder leads to a serious gap in negative selection and a plethora of autoimmune reactions, as a whole repertoire of self-antigens are not presented in the thymus.

The mechanics of negative selection relies upon discrimination between high and low avidity TCR interactions (Siggs, Makaroff et al. 2006). Therefore decisions must be made regarding the signal strength generated by TCR/self-peptide:MHC interactions. Mutations in genes that enhance TCR/self-peptide:MHC signalling produce an increase in negative selection (Thien, Blystad et al. 2005), while mutations that enhance positive selection simultaneously impair negative selection (Sakaguchi, Takahashi et al. 2003). TCR/self-peptide:MHC interactions that induce positive or negative selection induce the same conformational change in TCR. These decisions are therefore made downstream of TCR engagement (Gil, Schrum et al. 2005).

The decision between positively selecting and negatively selecting signal intensities has been hypothesised to occur at the level of ERK and JNK signalling and phosphorylation, or p38 activation. Disruption of calcineurin and ERK activity specifically affects positive selection (Neilson, Winslow et al. 2004), while inhibition of JNK and p38 phosphorylation specifically targets negative selection (Rincon, Whitmarsh et al. 1998; Bommhardt, Scheuring et al. 2000), as demonstrated by knockdown of the MINK kinase misshapen NIKs-related kinase, which impairs negative selection by selectively reducing phosphorylation of JNK and up-regulating Bim (McCarty, Paust et al. 2005). Bim is one of the key effector molecules in negative selection; loss of *Bim* renders thymocytes refractory to negative selection, preventing the interaction with Bcl-XL that inhibits survival (Bouillet, Purton et al. 2002). A similar phenotype is seen in $Bax^{-/-}Bak^{-/-}$ mice, downstream effectors of Bim (Rathmell, Lindsten et al. 2002) (**Figure 1.9**).

The Nur77 orphan nuclear receptor is one of the key effector molecules in antigen-mediated negative selection, and one of the most highly induced genes in experimental models. *Nur77*$^{-/-}$ mice exhibit no defect in TCR-mediated apoptosis (Lee, Wesselschmidt et al. 1995), there being functional redundancy with other *nur77* family members *Nurr1* and *Nor1* (Cheng, Chan et al. 1997), but Nur77 can render the archetypal anti-apoptotic molecule Bcl-2 pro-apoptotic by enforcing a conformational change (**Figure 1.9**). This interaction is required for Nur77 mitochondrial translocation and apoptosis (Lin, Kolluri et al. 2004). The mechanism of action of Nur77 is thought to be reliant upon TCR-mediated nuclear exclusion of Hdac7, which would otherwise inhibit Nur77 expression (Dequiedt, Kasler et al. 2003; Dequiedt, Van Lint et al. 2005). Hdacs have also been implicated in regulating *bim* expression through TCR signals that exclude Hdacs from the nucleus and prevent inhibition of *Bim* expression (Zhao, Tan et al. 2005). Pro-apoptotic Bim and Nur77 expression may co-ordinate with TCR-mediated nuclear exclusion of Hdacs to regulate negative selection (**Figure 1.9**).

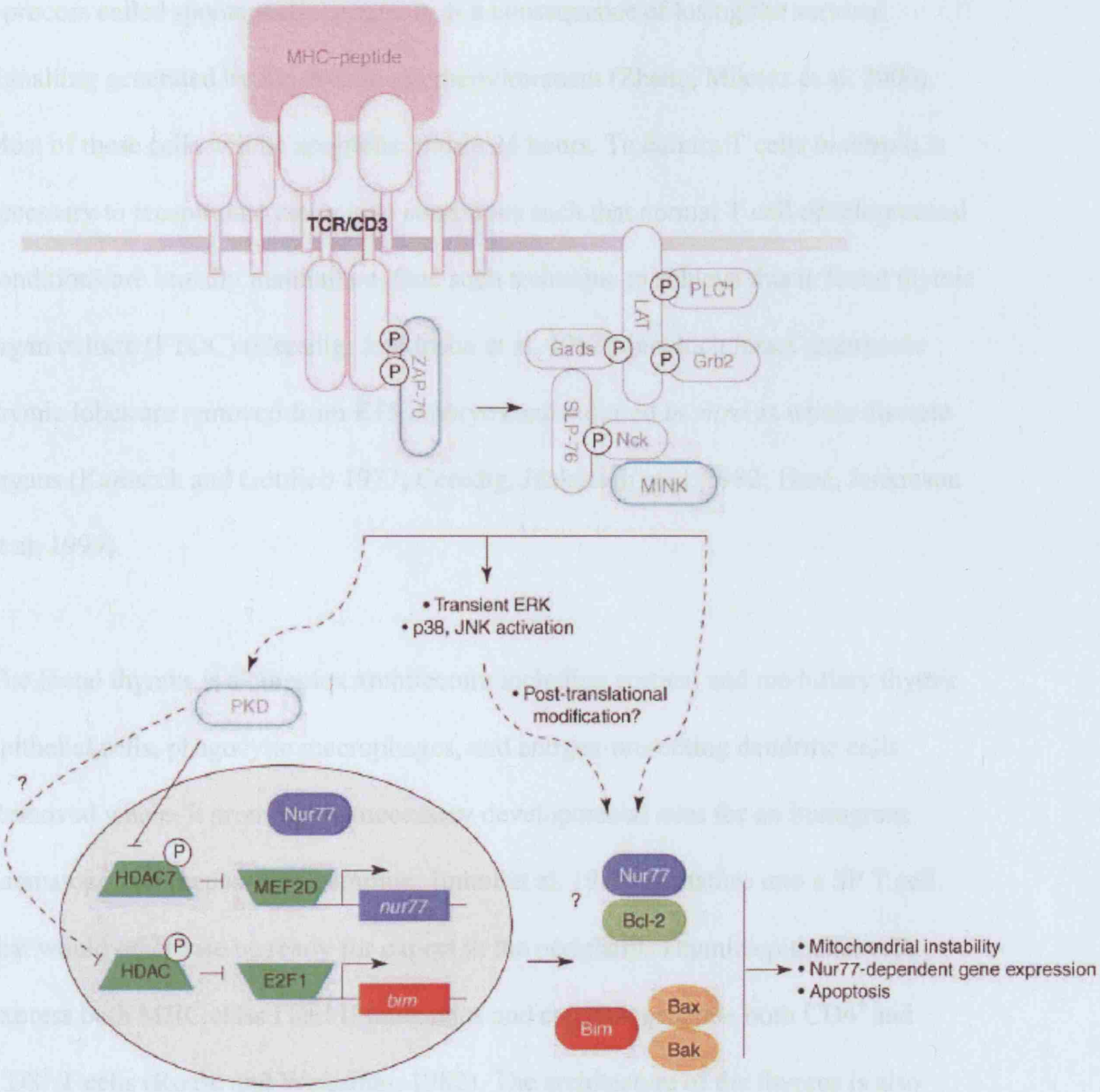

Figure 1.9. Negative Selection.
Schematic highlighting possible molecular regulation of antigen-mediated negative selection, highlighting BIM and NUR77. Figure adapted from (Siggs, Makaroff et al. 2006).

1.10. Tools for analysis – FTOC (foetal thymic organ culture).

Culturing T cells *in vitro* requires specialised tissue culture techniques. If removed from the thymus and placed into suspension culture conditions, DP thymocytes enter a process called spontaneous apoptosis as a consequence of losing the survival signalling generated by the thymic microenvironment (Zhang, Mikecz et al. 2000). Most of these cells will be apoptotic within 24 hours. To culture T cells *in vitro* it is necessary to recapitulate the *in vivo* conditions such that normal T cell developmental conditions are broadly maintained. One such technique to achieve this is foetal thymic organ culture (FTOC) (Ceredig, Jenkinson et al. 1982), in which intact embryonic thymic lobes are removed from E15 embryos and cultured *in vitro* as whole discrete organs (Kamarck and Gottlieb 1977; Ceredig, Jenkinson et al. 1982; Hare, Jenkinson et al. 1999).

The foetal thymus is a complex architecture including cortical and medullary thymic epithelial cells, phagocytic macrophages, and antigen-presenting dendritic cells. Removed whole, it provides the necessary developmental cues for an immigrant haematopoietic precursor (Champion, Imhof et al. 1986) to mature into a SP T cell that would otherwise be ready for export to the periphery. Thymic epithelial cells express both MHC class I and II molecules and can thus generate both $CD4^+$ and $CD8^+$ T cells (Rouse and Weissman 1982). The architecture of the thymus is also responsible for generating the signals that propel vulnerable thymocytes into apoptosis. The *F5 TCR Rag-1$^{-/-}$ Tap-1$^{-/-}$* transgenic system has been used to clonally delete DP thymocytes expressing the F5 TCR transgene using antigenic NP68 peptide presented upon thymic APCs, and these cells have been shown to die by apoptosis in FTOC (Tarazona, Williams et al. 1998).

The FTOC system is used as a model system for studying T cell development, and most relevant to us, apoptosis *in vitro*. When explanted, the cells within the FTOC continue to develop normally, producing mature T cells with similar kinetics to that seen in vivo (Zhang, Gong et al. 2007). A powerful adaptation to this technique is the use of the selective toxicity of 2-deoxyguanosine (2dGuo) to kill rapidly-dividing cells within the FTOC, preferentially depleting thymic lobes of developing T cells (Jenkinson, Franchi et al. 1982; Kingston, Jenkinson et al. 1985). By culturing FTOCs on filters floating on medium with the addition of 1.5mM 2dGuo for 4-7 days, the developing T cells are selectively deleted and the alymphoid FTOC structure is left intact. The empty FTOC can be repopulated with thymic progenitors which will migrate into the FTOC detecting chemotactic cues (Champion, Imhof et al. 1986; Ivanov, Merkenschlager et al. 1993; Wilkinson, Owen et al. 1999) and be exposed to the signalling that will direct T cell differentiation.

Adapting this technique still further, thymic precursors can be initially infected with retrovirus to introduce bicistronic reporter constructs that enable investigation of the effects of over-expressing or knocking down target genes with simultaneous reporter gene expression permitting tracking of the infected cells and their fate in the FTOC (Hare, Jenkinson et al. 1999). This combined approach allows the reconstitution of a T cell pool from infected precursors, and once DP thymocytes appear, the use of inhibitors and apoptotic stimuli can be studied for their effect on thymocyte apoptosis against a background of transgene expression or knockdown (**Figure 1.10**).

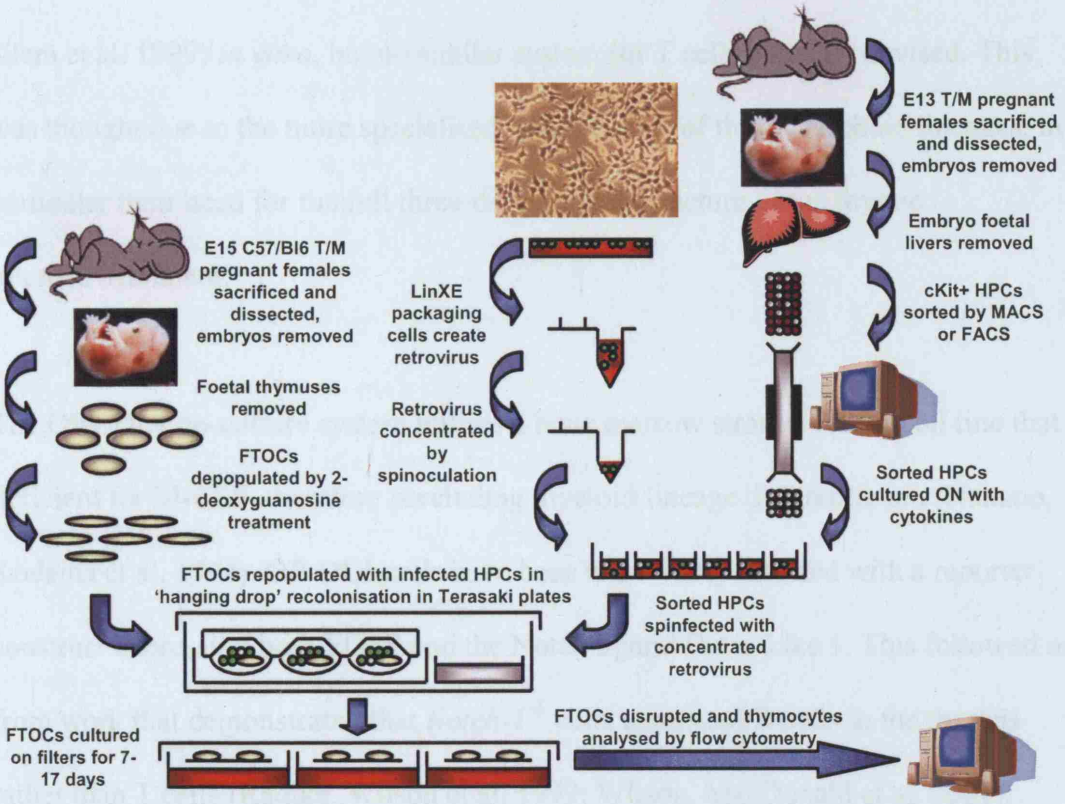

Figure 1.10. Foetal thymic organ culture (FTOC).
Diagram showing FTOC protocol used in our analyses. E15 FTOCs are depleted and repopulated with retrovirally infected HPCs which differentiate into T cells in FTOC.

1.11. Tools for analysis – OP9-DL1 bone marrow stromal cell co-culture system.

The powerful FTOC and associated RTOC (reaggregate thymic organ culture) (Hare, Jenkinson et al. 1999) systems are the principal techniques for recapitulating T cell development *in vitro*, enabling progression of a thymic progenitor from immigration to mature T cell. Previously, bone marrow stromal cell co-culture systems have been developed that enable the culture and development of B (Ray, Paige et al. 1996; Milne, Fleming et al. 2004) and NK cells (Williams, Moore et al. 1997; Williams, Klem et al. 1999) *in vitro*, but no similar system for T cells could be devised. This was thought due to the more specialised requirements of the T lymphoid lineages, in particular their need for the full three-dimensional structure of the thymic microenvironment.

The OP9-DL1 co-culture system utilises a bone marrow stromal feeder cell line that is deficient for M-CSF, therefore precluding myeloid lineage differentiation (Nakano, Kodama et al. 1994). OP-DL1 cells have been retrovirally infected with a reporter construct expressing both EGFP and the Notch ligand Delta-Like 1. This followed on from work that demonstrated that *Notch-1*$^{-/-}$ cells generated B cells in the thymus rather than T cells (Radtke, Wilson et al. 1999; Wilson, MacDonald et al. 2001), while BM cells transduced with a constitutively active form of Notch-1 produced DP T cells in the bone marrow (Pui, Allman et al. 1999). Therefore constitutive expression of one of the Notch ligands was thought to provide an aspect of the critical T-lineage signalling provided in the thymus.

OP9-DL1 cells ectopically expressing the Delta-Like 1 protein actively support the differentiation of DP and SP (CD8 only, as OP9-DL1 cells express only MHC class I)

cells from HSCs, HPCs (Schmitt and Zuniga-Pflucker 2002), embryonic stem cells (Schmitt, de Pooter et al. 2004) or human cord-blood derived HSCs (La Motte-Mohs, Herer et al. 2005). Thymocyte progenitors cultured on OP9-DL1 exhibit similar stage-specific development into DP and SP cells to that seen *in vivo* and in the FTOC system. This system therefore provides an alternative to FTOC as a means of developing and culturing T cells, and accompanies our use of FTOC in this study (**Figure 1.11**).

1.12. Strategy for the identification of genes regulating glucocorticoid and antigen-mediated thymocyte apoptosis.

Affymetrix GeneChip® probe arrays were used to identify genes differentially regulated in both glucocorticoid-induced and antigen-mediated apoptosis. In our first screen, primary thymocytes were incubated with a synthetic glucocorticoid (dexamethasone or DEX) in the presence of Roscovitine (ROSC) to induce apoptosis while blocking the downstream response by Cdk2 inhibition. Therefore only target genes upstream of Cdk2 will be induced. Preliminary candidate genes were confirmed by real-time qPCR.

The effect of these genes upon thymocyte development and thymocyte apoptosis was then studied using a combined FTOC/retroviral and OP9-DL1/retrovirus system to identify target genes which have an effect upon thymocyte apoptosis when either over-expressed or knocked down. Functionally confirmed targets were then further studied using the same techniques.

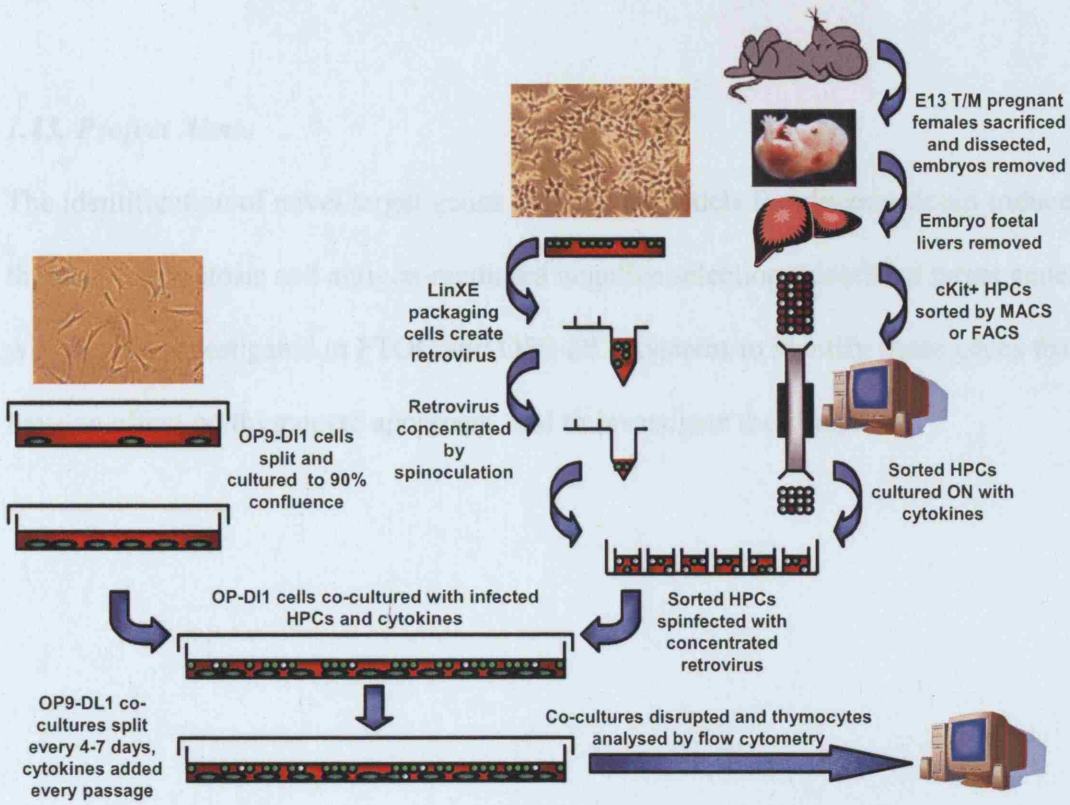

Figure 1.11. OP9-DL1 co-culture protocol.
Diagram showing OP9-DL1 protocol we used in our analyses. OP9-DL1 co-cultures were initiated with retrovirally infected HPCs which differentiate into T cells in co-culture.

For our second screen, F5 TCR Rag-$1^{-/-}$ Tap-$1^{-/-}$ transgenic thymocytes were exposed to NP68 cognate antigen *in vivo*, and differentially regulated genes again identified by Affymetrix GeneChip® probe arrays. Target genes were investigated to identify genes which had an effect upon negative selection when over-expressed, and currently ongoing, knocked down.

1.13. Project Aims.

The identification of novel target genes induced in models for glucocorticoid-induced thymocyte apoptosis and antigen-mediated negative selection. Identified target genes will then be investigated in FTOC and OP9-DL1 systems to identify those genes that have an effect on thymocyte apoptosis, and to investigate their function.

CHAPTER 2

MATERIALS & METHODS

2. Materials and Methods.

Chemicals were obtained from Sigma (Milwaukee, WI, USA). Antibodies were obtained from eBiosciences (San Diego, CA, USA), Caltag (Burlingame, CA, USA) and Pharmingen (San Diego, CA, USA). Tissue culture reagents were obtained from Invitrogen (Paisley, UK). Restriction enzymes were obtained from Promega (Madison, WI, USA). Oligos were obtained from Sigma Genosys (Haverhill, UK). Cytokines were obtained from Peprotech EC (London, UK).

2.1. Reagents, kits and solutions.

Table 2.1. Buffers and Solutions.

Solution	Components and Concentration
LB Agar	LB Broth + 15g/l Agar
LB Broth	1% tryptone, 0.5% yeast extract, 1 % NaCl (pH 7)
LB Low Salt Agar	LB Broth + 15g/l Agar
LB Low Salt Broth	1% tryptone, 0.5% yeast extract, 0.5 % NaCl (pH 7)
TAE buffer	40mM Tris-acetate, 1mM EDTA pH 8.3
TBE buffer	45mM Tris-borate, 1mM EDTA pH 8.3
Orange G loading buffer	30% Glycerol, 2mg/ml Orange G
Ethidium Bromide	10mg/ml
TBS	20mM Tris-HCl (pH 7.5), 150mM Nacl
TBS-T	20mM Tris-HCl (pH 7.5), 150mM Nacl, 0.1% Tween-20
Protein (SDS-PAGE) running buffer	25mM Tris, 250mM glycine pH 8.3, 0.1% SDS
Protein (SDS-PAGE) transfer buffer	39mM glycine, 48mM Tris base, 0.037% SDS, 20% methanol
5 x SDS gel-loading buffer	250mM Tris pH 6.8, 100mM dithiothreitol, 10% SDS, 2.5% bromophenol blue, 50% glycerol
RIPA lysis buffer	50mM Tris-HCl pH 7.4, 1% NP-40, 0.25% Na-deoxycholate, 150mM NaCl, 1mM EDTA, + protease inhibitors (Roche)
NP40 lysis buffer	50mM Tris-HCl pH 8.0, 1% NP-40, 150mM NaCl, + protease inhibitors (Roche)
Sequencing loading buffer	Formamide 5:1 25mM EDTA (pH8.0) + 50 mg/ml Blue Dextran
Premixed sequencing packs	Long Ranger Singel Packs – ABI 377- Cat No. 50691
TFBI	100mM $RbCl_2$, 50mM $MnCl_2$, 30mM, KOAc, 10mM $CaCl_2$, 15% glycerol. pH to 5.8 with AcOH
TFBII	10mM 3-[N-morpholino]-2-hydroxypropanesulfonic acid (MOPS), 10mM $RbCl_2$, 75mM $CaCl_2$, 15% glycerol. pH to 7.0 with NaOH
TBS	20mM Tris-HCl (pH 7.5), 150mM NaCl
TBS-T	20mM Tris-HCl (pH 7.5), 150mM NaCl, 0.1% Tween 20 (Sigma)
FACS Staining Buffer	PBS (Invitrogen), 2% FCS, 0.1% NaN_3

2.2. Cell culture.

For cell culture, all cell lines were maintained in 37^0c humidified incubators (Galaxy R, Wolf Laboratories) with 5% CO_2 unless otherwise stated.

Table 2.2. Cell Culture Reagents.

Tissue culture reagent	Supplier	Cat. No.
DMEM	Invitrogen	41965-039
RPMI	Invitrogen	31870-025
αMEM	Invitrogen	32561-029
PBS	Invitrogen	14190-094
1 x Trypsin	Sigma	T3924
10 x Trypsin	Invitrogen	15400-054
FCS (normal)	Sigma	F7524 Lot: 064K3395
FCS (OP9-DL1)	Invitrogen	10270-106 Lot: 40F4053K
FCS (stem cell)	Stem Cell Technologies	O6200
L-glutamine	Invitrogen	25030-024
Penicillin/streptomycin	Invitrogen	15140-122
2-mercaptoethanol	Invitrogen	31350-010
Hygromycin B	Calbiochem	400052
HBSS	Invitrogen	24020-091
HEPES	Invitrogen	15630-056
Sodium Pyruvate	Invitrogen	11360-039
Gentamicin	Invitrogen	15750-037
Glutamax	Invitrogen	35050-038
Optimem	Invitrogen	51985-042
Lipofectamine	Invitrogen	18324-012

2.2.1. LinX E retroviral packaging cell line

LinX E (E – ecotropic, therefore rodent cell specific infection) cells are a HEK293 derived, human embryonic kidney cell line, stably transduced by amphotropic infection with an expression cassette encoding the viral *GAG*, *POL* and *ENV* genes in addition to a hygromycin resistance gene for stable selection. LinXE cells were maintained in DMEM: 10% FCS, 100U/ml penicillin, 100μg/ml streptomycin, 2mM L-glutamine and 75μg/ml hygromycin B. LinX E cultures were split 1:5 every 2-3 days for maintenance, and split 1:25 three days prior to transfection to achieve 50-75% confluence.

2.2.2. 3T3 murine cell line

3T3 cells are a murine immortalised cell line used for test retroviral infections and control experiments. 3T3 cells were maintained in DMEM: 10% FCS, 100U/ml penicillin, 100µg/ml streptomycin and 2mM L-glutamine, split 1:10 every 2-3 days. 3T3 cells were split 1:5 the day preceding test infections to ensure cells were actively dividing at the point of retroviral infection.

2.2.3. S49.1 DP thymoma cells.

S49.1 cells are a murine double positive thymoma cell line that is exquisitely sensitive to glucocorticoid treatment. S49.1 cells were maintained in RPMI: 10% FCS, 100U/ml penicillin, 100µg/ml streptomycin, 2mM L-glutamine and 50µM 2-mercaptoethanol, spilt 1:5 every 2-3 days.

2.2.4. OP9-DL1 bone marrow stromal cells.

OP9-DL1 cells are a murine $MCSF^{-/-}$ bone marrow-derived stromal cell line retrovirally infected to over-express the Notch ligand Delta-Like 1 (pMSCV-IRES-EGFP-'Delta-Like 1'). Over-expression of Delta-Like 1 drives development of DP T cells in co-cultures with haematopoietic progenitor cells (HPCs) supplemented with cytokines. OP9-DL1 cells are maintained in αMEM:20%FCS (Invitrogen Cat. No. 10270-106 Lot. 40F4053K), 100U/ml penicillin, 100µg/ml streptomycin, 50µM 2-mercaptoethanol, 10mM HEPES, 1mM Sodium Pyruvate, 50µg/ml Gentamicin, 2µM Glutamax, split 1:5 every 2-3 days.

2.2.5. OP9-GFP bone marrow stromal cells.

OP9-GFP cells are a murine $MCSF^{-/-}$ bone marrow-derived stromal cell line that has been retrovirally infected to act as a vector control for OP9-DL1 cells, expressing only EGFP. OP9-GFP cells are maintained in αMEM:20%FCS (Invitrogen Cat. No. 10270-106 Lot. 40F4053K), 100U/ml penicillin, 100μg/ml streptomycin, 50μM 2-mercaptoethanol, 10mM HEPES, 1mM Sodium Pyruvate, 50μg/ml Gentamicin, 2μM Glutamax, split 1:5 every 2-3 days.

2.3. Primary Cells.

All primary cultures were maintained in 37^0c humidified incubators (Galaxy R, Wolf Laboratories) with 5% CO_2 unless otherwise stated.

2.3.1. Culture of primary murine thymocytes.

For experiments, thymuses were removed from sacrificed ($C0_2$ asphyxiation or cervical dislocation) C57/BL10 or C57/BL6 4-6 week old female mice. Single cell thymocyte suspensions were prepared in air-buffered HBSS:1mM HEPES by filtering through nylon mesh cell strainers (70 μM). Cultures were maintained in RPMI 1640: 10% FCS, 100U/ml penicillin, 100μg/ml streptomycin, 2mM L-glutamine and 50μM 2-mercaptoethanol for experiments.

2.3.2. Time-mated pregnant females.

E12 (left to mature to E13 or E15 as required) time-mated pregnant C57/BL6 females were ordered from Harlan, and maintained in animal facilities at ICH, UCL, London or Windeyer Institute, UCL, London. Pregnant females were sacrificed by cervical dislocation, embryos removed using sterile technique and placed in ice-cold HBSS:

1mM HEPES. Foetal thymuses or livers were dissected and removed using a Zeiss Stemi 1000 microscope, Schott KL1500 LCD and Dumont No.5 jewellers forceps (Sigma, Cat. No. F6521).

2.4. Molecular biology techniques – DNA and cloning.

Protocols, solutions, buffers and general reagents were as detailed in *Molecular Cloning: A Laboratory Manual, Sambrook et al.*

2.4.1. Cloning – minipreps and small-scale plasmid preps.

Overnight cultures (16-24 hours, 37^0C incubators, 300rpm shaking) of LB Broth plus relevant antibiotics (ampicillin, zeocin, kanamycin, etc.) were inoculated with single bacterial colonies from LB agar plates. Plasmid DNA was extracted with the Qiagen Spin Miniprep kit (Cat. No. 27106) according to manufacturer's protocols. DNA was eluted in 75µl EB Buffer (10mM Tris:HCl; pH 8) and stored at -20^0C.

2.4.2. Cloning – maxipreps and large-scale plasmid preps.

For large-scale preps of plasmid DNA, 5ml starter cultures of LB broth with relevant antibiotic were inoculated with single bacterial colonies and cultured for 6 hours at 37^0C with vigorous shaking (300rpm). 400 ml of LB broth with antibiotic was then inoculated with the starter culture and incubated overnight as before. Plasmid DNA was extracted from pelleted bacteria with Qiagen Hi-Speed MaxiPrep kits (Cat. No. 12663) according to the manufacturers protocols, with DNA eluted in 500µl EB Buffer (10mM Tris:HCl; pH 8) and stored at -20^0C.

2.4.3. Preparation of competent bacteria.

For preparation of chemically competent bacteria, a 5ml starter culture of LB broth was inoculated with a DH10β *Escherichia Coli* colony and cultured overnight at 37^{0}C with vigorous shaking (300rpm). The next day the starter culture was used to inoculate 100ml of 37^{0}C LB broth and cultured at 37^{0}C with vigorous shaking for 1-2 hours. At approximately 20 minute intervals, aliquots were tested until a visual absorbance of 0.48 at 550nm was achieved, representing a bacterial culture in the log phase of growth. All subsequent steps were performed at 4^{0}C in a cold room. The log phase culture was transferred to pre-chilled 50ml Falcon tubes and incubated on ice for 10 minutes. Cells were then centrifuged at 2500rpm, 10 minutes, 4^{0}C, aspirated and resuspended in 30ml ice-cold TFBI buffer, and incubated on ice for a further 20 minutes. Cells were then again centrifuged at 2500rpm, 10 minutes, 4^{0}C, aspirated and resuspended in 4ml ice-cold TFBII buffer. Of this 4ml, 100µl and 50µl aliquots were dispensed into 1.5ml eppendorfs in a dry ice/ethanol bath using a repeat pipettor and rapidly transferred to storage at -80^{0}C. For use, 100µl and 50µl aliquots were thawed on wet ice.

2.4.4. Transformation of prepared chemically competent cells.

For transformation, 100µl or 50µl aliquots were thawed on wet ice and then gently mixed with either 10ng or 1-2µl of ligation reaction in 14ml Falcon© 2059 polypropylene tubes, and incubated on ice for 30 minutes. Chilled transformation mixes were then heat shocked at 42^{0}C for 30 (50µl) or 45 (100µl) seconds and placed back on ice to cool for 2 minutes. 0.45mls (50µl) or 0.9mls (100µl) of SOC media was then added to the transformation mix and incubated at 37^{0}C for 1 hour with

vigorous shaking (225rpm). 100-200µl of transformation mix was then plated onto LB-agar plates with relevant antibiotics and incubated overnight at 37^0C.

2.4.5. Commercially prepared competent bacteria.

Commercially available competent bacteria were used for specific cloning applications.

Table 2.3. Commercially Obtained Bacteria.

Commercial Bacteria	Supplier	Cat. No.	Type and application
DH10β ElectroMax	**Invitrogen**	**18290-015**	**Difficult cloning**
DH10β Library efficiency	**Invitrogen**	**18263-012**	**Library cloning**
DH10β sub-cloning efficiency	**Invitrogen**	**18365-017**	**General cloning**

All commercially obtained bacteria were used according to manufacturers' instructions.

2.4.6. Cloning vectors and construction of cDNAs for gene expression.

Polymerase Chain Reaction (PCR) was used to amplify cDNAs for expression analysis, and for the incorporation of epitope tags and specific flanking restriction enzyme sites to facilitate cloning of cDNAs into expression vectors. PCR was carried out on MJ Research Engine Alpha PTC-0200 PCR machines, with 50µl volume reactions containing 10ng template DNA (typically murine thymocyte cDNA), 1x *Pfx* amplification buffer (Invitrogen Platinum Pfx, Cat. No. 11708-021), 0.3mM dNTPs (Promega, Cat. No. U1330), 1mM MgSO4, 0.3µM primers, 1x Enhancer solution and 2.5U Platinum *Pfx* DNA polymerase. Cycling conditions were 94^0c for 2 minutes initial denaturation, then 30-36 cycles of 94^0C for 30 seconds denaturation, 50^0C to 60^0C annealing across a gradient block for 30 seconds, 68^0C extension for 1 minute per kilobase (kb), followed by 68^0C for 5 minutes final extension with a final hold at 4^0C.

For PCR to incorporate 5' or 3' epitope tags using longer primers, two-step cycling conditions were used. First step cycling conditions were 94^0c for 2 minutes initial denaturation, then 4 cycles of 94^0C for 30 seconds denaturation, 45^0C to 55^0C annealing across a gradient block for 30 seconds, 68^0C extension for 1 minute per kilobase (kb), then 30-36 cycles of 94^0C for 30 seconds denaturation, 50^0C to 60^0C annealing across a gradient block for 30 seconds, 68^0C extension for 1 minute per kilobase (kb), followed by 68^0C for 5 minutes final extension with a final hold at 40C. HA and Myc epitope tags were incorporated if possible into cDNAs at 5' and 3' ends using the Roche Guide, *Addition of an Epitope Tag Sequence to a Target Gene by PCR.* (Epitope Tagging Basic Laboratory Methods, J.Keesey 2000)

PCR products were electrophoresed on 1.5% TAE (Tris-acetate EDTA buffer) agarose gels containing 0.5µg/ml ethidium bromide and visualised with an UviTec UVI-DOC gel documentation system. Correctly sized PCR products were excised using sterile clean scalpels and purified using a Qiagen Gel Extraction kit (Qiagen, Cat. No. 28704) and resuspended in 30µl EB Buffer (10mM Tris:HCl; pH 8) and stored at -20^0C.Purified PCR products were digested using relevant restriction enzymes to create compatible 'sticky ends' in the 5' and 3' flanking sequences, and ligated into the pZero-1 cloning vector (Invitrogen, Cat. No. K2500-01) with T4 DNA ligase (NEB, Cat. No. M0202T) according to manufacturers instructions. PCR products were excised from pZero-1 following sequencing to ensure accurate amplification and religated into pMSCV vectors dependent on the specific flanking restriction sites.

2.4.7. Expression vectors and vector construction.

For high-level, long-term expression of transduced genes in haematopoietic progenitor cells (HPCs) and derived thymocytes, the pMSCV-neo (Clontech, Cat. No. 634401) was extensively modified. The phosphoglycerate kinase promoter (PGK) and neomycin resistance cassette was replaced with an internal ribosome entry site (IRES) –hCD2'tailless' cassette amplified by PCR from the pMI-IRES-hCD2'tailless' vector (gift from Dr M. J. Bevan, Department of Immunology, University of Washington, Seattle, USA). The MCS then consisted of only the EcoR1 restriction site; this was extended by the addition of further restriction sites by annealing 2 sets of 2 oligos (Sigma-Genosys) together to form linkers (annealing at 65^0C, cooled to RT and used for ligation at 3 serial dilutions), which were then cloned into the EcoR1-Sal1 (Sal1 not unique in pMSCV constructs) site at the MCS. This resulted in 2 constructs, pMSCV-IRES-hCD2-'tailless'-LK1 and pMSCV-IRES-hCD2-'tailless'-LK2 respectively.

Expression of the tailless form of the human CD2 gene produces a protein that is targeted to the cell membrane and can be detected using cell-surface antibodies, but lacks the cytoplasmic domain that would signal any downstream effects of ligand-receptor interaction. The pMSCV-IRES-EGFP construct (gift from Dr O. Williams, Molecular Haematology and Cancer Biology Unit, Camelia Botnar Labs, Institute of Child Health, University College London, UK) was also used in test experiments.

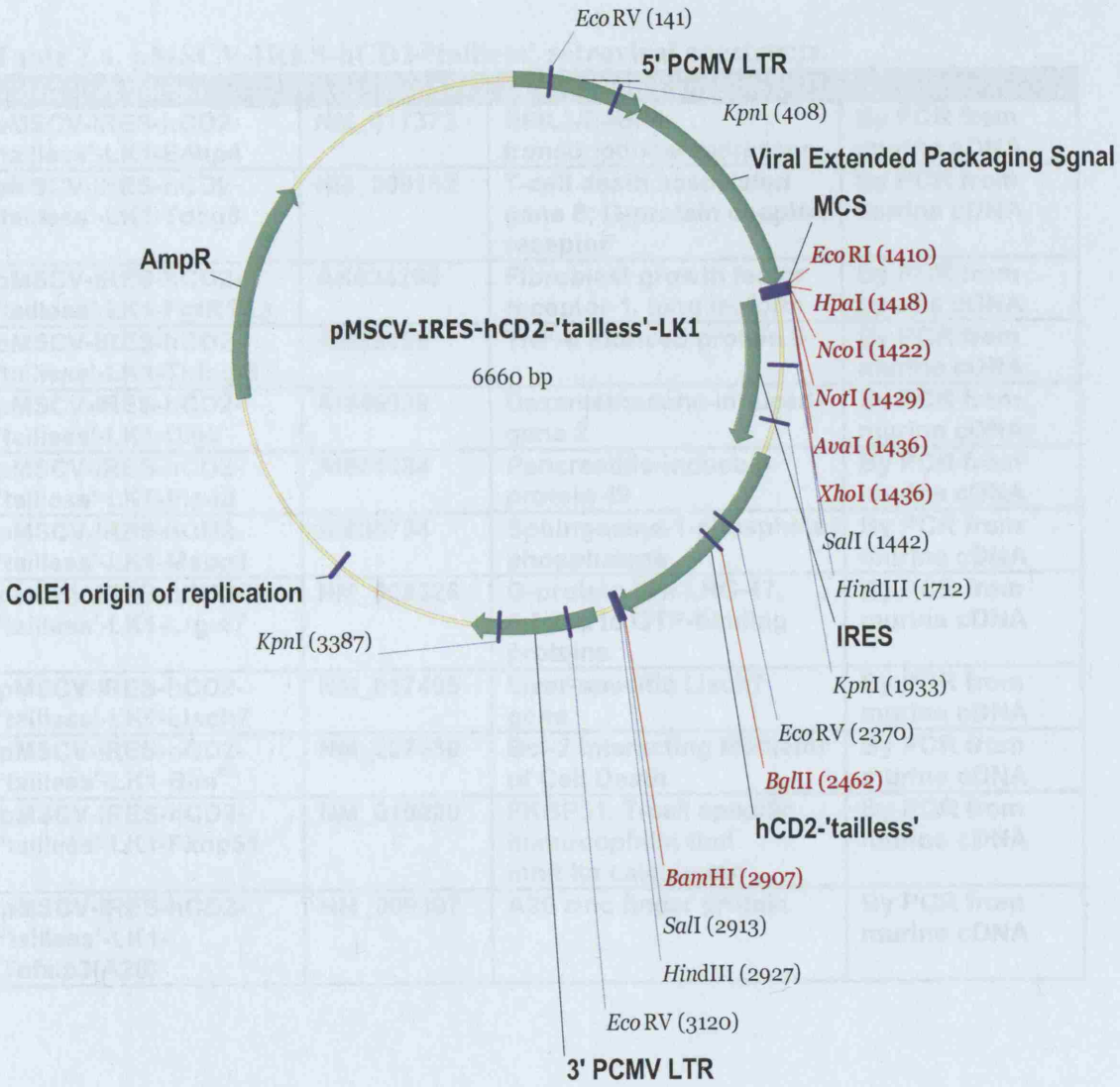

Figure 2.1. pMSCV-IRES-hCD2-'tailless'-LK1.
Plasmid map of the pMSCV-IRES-hCD2-'tailless'-LK1 retroviral vector.

2.4.8. Constructs.

The following over-expression constructs were prepared by amplifying the ORF from murine cDNA and cloning into pMSCV-IRES-hCD2-'tailless' vectors. All constructs were sequenced.

Table 2.4. pMSCV-IRES-hCD2-'tailless' retroviral constructs.

cDNA and Vector	Accession	Description/Function	Generated?
pMSCV-IRES-hCD2-'tailless'-LK1-E4bp4	NM_017373	NFIL3/E4BP4 transcriptional repressor	By PCR from murine cDNA
pMSCV-IRES-hCD2-'tailless'-LK1-Tdag8	NM_008152	T-cell death associated gene 8; G-protein coupled receptor	By PCR from murine cDNA
pMSCV-IRES-hCD2-'tailless'-LK1-FgfR1(L)	AK034295	Fibroblast growth factor receptor-1, long isoform	By PCR from murine cDNA
pMSCV-IRES-hCD2-'tailless'-LK1-Tnfaip8	AI839109	TNF-α induced protein 8	By PCR from murine cDNA
pMSCV-IRES-hCD2-'tailless'-LK1-Dig2	AI849939	Dexamethasone-induced-gene 2	By PCR from murine cDNA
pMSCV-IRES-hCD2-'tailless'-LK1-Pip49	AI841484	Pancreatitis-induced-protein 49	By PCR from murine cDNA
pMSCV-IRES-hCD2-'tailless'-LK1-Mspp1	AI835784	Sphingosine-1-phosphate phosphatase	By PCR from murine cDNA
pMSCV-IRES-hCD2-'tailless'-LK1-Lrg-47	NM_008326	G-protein-like LRG-47, related to GTP-binding proteins	By PCR from murine cDNA
pMSCV-IRES-hCD2-'tailless'-LK1-Lisch7	NM_017405	Liver-specific Lisch7 gene	By PCR from murine cDNA
pMSCV-IRES-hCD2-'tailless'-LK1-Bim^{EL}	NM_207680	Bcl-2 Interacting Mediator of Cell Death	By PCR from murine cDNA
pMSCV-IRES-hCD2-'tailless'-LK1-Fkbp51	NM_010220	FKBP51, T-cell specific immunophilin that inhibits calcineurin	By PCR from murine cDNA
pMSCV-IRES-hCD2-'tailless'-LK1-Tnfaip3(A20)	NM_009397	A20 zinc finger protein	By PCR from murine cDNA

Table 2.5. pMSCV-IRES-hCD2-'tailless' retroviral construct controls.

cDNA and Vector	Accession	Description/Function	Generated?
pMSCV-IRES-hCD2-'tailless'-LK1-Bcl-2	NM_009741	B-cell leukaemia/lymphoma 2	By PCR from murine cDNA
pMSCV-IRES-hCD2-'tailless'-Bax	NM_007527	Bcl2-associated X protein	Obtained from O. Williams.
pMSCV-IRES-hCD2-'tailless'-LK1-Bim^{EL}	NM_207680	Bcl-2 Interacting Mediator of Cell Death	By PCR from murine cDNA
pMSCV-IRES-hCD2-'tailless'-Bcl-XL	NM_009743	Bcl2-like 1	Obtained from O. Williams.
pMSCV-IRES-hCD2-'tailless'-LK1-Dig2	AI849939	Dexamethasone-induced-gene 2	By PCR from murine cDNA
pMSCV-IRES-hCD2-'tailless'-Mcl-1	NM_008562	myeloid cell leukaemia sequence 1	Obtained from J. Zhuang.
pMSCV-IRES-hCD2-'tailless'-LK1-Gilz	AF024519	Glucocorticoid-induced leucine zipper protein	By PCR from murine cDNA

2.4.9. RNAi Vectors

The pMSCV-LTRmiR30-PIG (LMP) RNAi vector was obtained from Open Biosystems (Open Biosystems, Cat. No. EAV4071). This expresses the shRNA^{mir} from the retroviral LTR promoter, while expressing the 'puromycin resistance-IRES-EGFP' (PIG) transcript from the PGK promoter. This vector was also adapted to express the hCD2-'tailless' protein instead of EGFP by removing the EGFP cDNA with Nco1-Sal1, and replacing it with a PCR product amplified from pMSCV-IRES-hCD2-'tailless'-LK1 containing the hCD2-'tailless' ORF flanked by Nco1-Sal1 restriction sites.

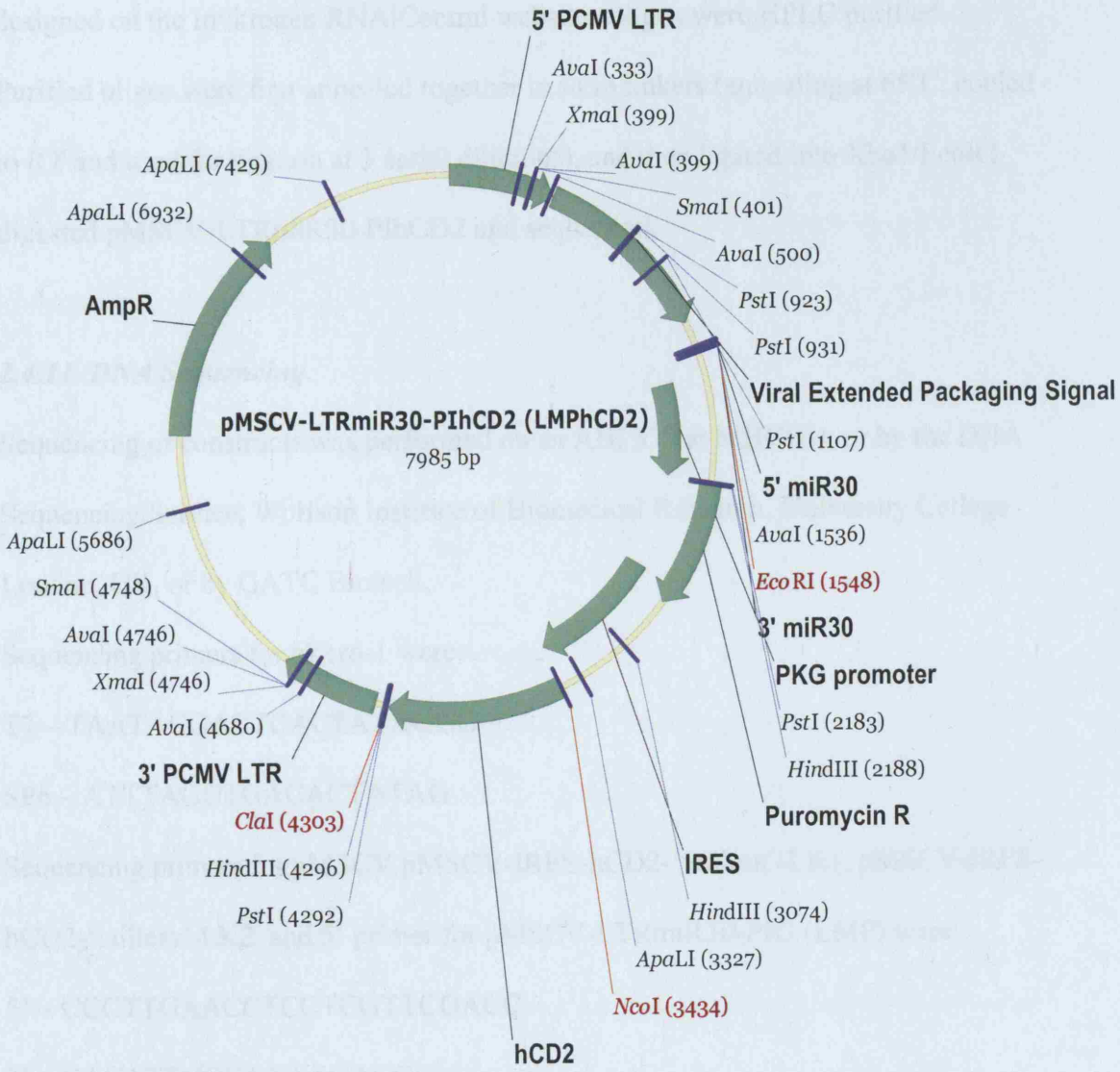

Figure 2.2. pMSCV-LTRmiR30-PIhCD2.
Plasmid map of the pMSCV-LTRmiR30-PIhCD2 retroviral vector.

2.4.10. RNAi cloning

The pMSCV-LTRmiR30-PIG (LMP) RNAi vector was adapted to express the hCD2(tailless) cDNA instead of EGFP (pMSCV-LTRmiR30-PIhCD2). The shRNA^{mir} oligo hairpins were generated by Sigma-Genosys, Haverhill, UK, and were originally designed on the Invitrogen RNAiCentral website. Oligos were HPLC purified. Purified oligos were first annealed together to form linkers (annealing at 65^{0}C, cooled to RT and used for ligation at 3 serial dilutions), and then ligated into Xho1/EcoR1 digested pMSCV-LTRmiR30-PIhCD2 and sequenced.

2.4.11. DNA Sequencing

Sequencing of constructs was performed on an ABI 377 at MHCBU, or by the DNA Sequencing Service, Wolfson Institute of Biomedical Research, University College London, UK, or by GATC Biotech.

Sequencing primers for pZero-1 were:-

T7 – TAATACGACTCACTATAGGG

SP6 – ATTTAGGTGACACTATAG

Sequencing primers for pMSCV pMSCV-IRES-hCD2-'tailless'-LK1, pMSCV-IRES-hCD2-'tailless'-LK2, and 5' primer for pMSCV-LTRmiR30-PIG (LMP) were:-

5' – CCCTTGAACCTCCTCGTTCGACC

3' – CACATTGCCAAAAGACGG

2.5. Molecular biology techniques – isolation of total RNA.

Total RNA was extracted from cells using Trizol® Reagent (Invitrogen, Cat. No. 15596-026) according to the manufacturer's instructions. For Affymetrix GeneChip®

probe array and Northern Blot analysis, cell pellets were flash frozen in liquid nitrogen, and subsequently lysed in 1ml Trizol per 10^7 cells and left to homogenise at RT for 10 minutes. 0.2ml of chloroform per 1ml of Trizol was then added, mixed by vigorous shaking and centrifuged at 12000g for 15 minutes at 4^0C. The upper aqueous phase was then transferred to a fresh polypropylene tube and 0.5ml of isopropanol added per 1ml of Trizol originally used, with the addition of 1µg glycogen (Roche, Cat. No. 10901393001) carrier per sample. RNA was left to precipitate at RT for 10 minutes and then centrifuged at 12000g for 30 minutes at 4^0C. RNA pellets were aspirated and washed in 70% ethanol:DEPC-H_20 at 12000g for 10 minutes at 4^0C. RNA pellets were than allowed to partially air-dry before resuspension in diethyl-pyrocarbonate (DEPC)-treated dd H_20 for storage at -80^0C. For Affymetrix GeneChip® probe array analysis, RNA was further purified over RNeasy mini columns (Qiagen, Cat. No. 74104) according to manufacturers instructions.

2.6. Molecular biology techniques – northern blotting.

For Northern blotting, 10µg total RNA or 3µg poly^{A+} RNA prepared using Trizol® and the Qiagen Oligotex mRNA midi kit (Qiagen, Cat. No. 70022) was electrophoresed in a denaturing 1.2% formaldehyde/agarose gel made with diethyl pyrocarbonate-treated ddH20 in 1 x MOPS buffer. RNA samples were initially checked for integrity and concentration using an Agilent 2100 bioanalyser, denatured in RNA sample buffer, mixed with RNA loading buffer and loaded onto a pre-run gel. Successful electrophoresis was checked using a transilluminator. RNA was then transferred onto nitrocellulose membranes by capillary action (Sambrook et al, 1989), and cross-linked under UV light. Pre-hybridised membranes were probed with ^{32}-P

labelled probes and reprobed with housekeeping genes (murine *β-actin* or *GAPDH*), and visualised using a Typhoon 8600 phosphoimager (Amersham)

2.7. Molecular biology techniques – Affymetrix GeneChip® probe array analysis.

2.7.1. Sample preparation

To isolate differentially regulated transcripts during glucocorticoid-induced apoptosis and antigen-mediated negative selection, experiments were performed independently and in triplicate. For the glucocorticoid screen, thymuses were removed from sacrificed C57/Bl10 4-6 week old female mice. Single cell thymocyte suspensions were prepared in complete RPMI:10% FCS, 2mM L-glutamine, penicillin/streptomycin, 50μM 2-mercaptoethanol by filtering through 70μM nylon mesh cell strainers. Thymocyte suspensions in RPMI complete medium at 1 $x10^6$ cells/ml were incubated with 25μM roscovitine (CalbioChem, Cat. No. 557364), and either untreated or exposed to 5μM dexamethasone (Sigma, Cat. No. D2915). After 4 hours incubation at 37^0C in 5% CO_2 incubators, cell suspensions were harvested and flash-frozen in liquid nitrogen. Duplicate samples were prepared at 0, 4 and 6 hours for flow cytometric analysis to determine the apoptotic profile on a Beckman Coulter Epics XL flow cytometer. For the antigen screen, 6 x F5 TCR Rag-$1^{-/-}$ Tap-$1^{-/-}$ female mice were IP injected with 1μM NP68 cognate antigen, 6 x F5 TCR Rag-$1^{-/-}$ Tap-$1^{-/-}$ female mice were IP injected with PBS as controls and left for 6 hours. After 6 hours thymuses were removed from sacrificed F5 TCR $Rag^{-/-}$ $TAP^{-/-}$ female mice, single cell thymocyte suspensions were prepared and lysed directly in Trizol.

2.7.2. Affymetrix GeneChip® probe arrays.

RNA was extracted in Trizol according to the manufacturer's instructions. Samples were further purified over RNeasy mini columns (Qiagen, Cat. No. 74104), and checked for integrity, concentration and the presence of genomic DNA contamination using an Agilent 2100 Bioanalyser. RNA templates (10μg) were used for the multi-step synthesis of biotin-labelled cRNA, which was then hybridized to Affymetrix GeneChip® probe arrays according to protocols outlined in the Affymetrix Gene Expression Technical Manual. Affymetrix GeneChip® probe arrays were then probed, washed, and bound probe detected with a GeneChip® 3000 Array scanner, as specified in Affymetrix protocols. One Affymetrix GeneChip® probe array was used for each sample, with experiments performed in triplicate. Data was analysed using Affymetrix Microarray Suite version 5.0, with normalisation performed using Genespring 5.0 to allow comparison across panels of multiple arrays. Transcripts that were scored as detected in ≥ 2 arrays per triplicate; scored as increased, marginally increased, decreased or marginally decreased; and exhibited a ≥ 1.5-fold difference in RNA levels compared with controls were considered to be regulated. Statistical t-testing was used to confirm differentially regulated transcripts, and Benjamini-Hochberg multiple testing corrections used to reduce the incidence of false positives.

2.8. Molecular biology techniques – real-time qPCR.

To confirm Affymetrix GeneChip® probe array results and for further expression analysis, Taqman real-time qPCR assays were performed according to the manufacturers instructions (Applied Biosystems). Total RNA was prepared from discretely prepared murine thymocytes treated in triplicate using Trizol and Qiagen RNeasy mini columns (Qiagen, Cat. No. 74104), which was checked for integrity,

concentration and the presence of genomic DNA contamination using an Agilent 2100 Bioanalyser. Single-stranded cDNA was prepared according to Affymetrix protocols. Primers and probes were designed using Primer Express (Applied Biosystems). Probes were designed across intron-exon boundaries in all possible cases to ensure maximum specificity and to preclude the possibility of amplifying genomic DNA. Probes were labelled at the 5' end with FAM (6-carboxyfluorescin) reporter dye and TAMRA (6-carboxyl-N-N-N'-N'-tetramethylrhodramine) quencher dye at the 3' end. Assays for each gene were designed following the submission guidelines, as dictated by the Assays-by-Design® Service. For qPCR reactions 5-10ng of cDNA was used and added to a pre-prepared Taqman Mastermix. Housekeeper assays were prepared in separate tubes. Due to the nature of transcription during thymocyte apoptosis it was not possible to utilise any commonly used housekeeper gene i.e. Gapdh, β-actin, Tubulin. *Mus musculus* poly(A)-specific ribonuclease (deadenylation nuclease) (Parn), was identified from Affymetrix GeneChip® probe array data across several different parallel Affymetrix GeneChip® probe array screens as a gene whose expression did not vary during the time course of thymocyte apoptosis studied, and used as a loading control. HPRT was also used as a loading control in later experiments. Quadruplicate singleplex reactions were performed in 96 well plates using the ABI PRISM 7700 or the 7900 HT Fast Real Time qPCR systems (Applied Biosystems). Changes in expression relative to each of the treatments were determined by the ΔΔCT method of absolute quantitation. Primer sequences are detailed below.

Assays on demand

Mm00452942_m1	-	PARN
Mm00506554_m1	-	TNFAIP8
Mm00480144_m1	-	PIP49
Mm00438923_m1	-	FGFR-1
Mm00440911_m1	-	MUPAR1

Mm00473016_m1 - MSPP-1
Mm00433695_m1 - TDAG8
CCCTCCAGAAACAGGGAAACATGAC Mm00433695_m1 TDAG8
GCCCGAACAAGCTCAGCCCTGGGGA Mm00438923_m1 FGFR-1
CAGGGAAGTGGCTACAGATGTCTTC Mm00506554_m1 TNFAIP8
ACCTGTGTCCCAGCCTCCCAGGGCC Mm00440911_m1 MUPAR1 NM_011113
CTATCCTGGATGTCATTGCTGGATT Mm00473016_m1 MSPP1 NM_030750
AGGTGGTGATCTGCGACCAGTACCG Mm00480144_m1 PIP49 NM_019833
CCCTGCCTGCGGACCTGAATGAGTT Mm00452942_m1 PARN NM_028761
AACACACAGGACTTTTGCGCAGATC Mm00487425_m1 C-FOS NM_010234
GGGCTGTCCTGCCTCTGGTGCTTGC Mm00433237_m1 FAS NM_007987
CGGAGTGGCGGGAGATGGCATGATC Mm00456650_m1 EGR2 (Krox20) NM_010118
GTCTAAAATGAAGGTACAGGCGAAG Mm00438084_m1 CYCLIN G1 NM_009831
AGCCGCCTCCCGTCTACACCAACCT Mm00492781_s1 JUN-B NM_008416
TTCCTGGCAAGTTGGGGCTAAAGAA Mm00497029_m1 GTSE NM_013882
GCAAGCCAAATTCCCTGGTGGTTGA Mm00479445_m1 NFAT-c1 NM_016791
TAACGGAGGCTGGGATGCCTTTGTG Mm00477631_m1 BCL2 NM_009741
AGTATGTCAGAGGCCAGAGGAGCTG Mm00435532_m1 PD-1 NM_008798
CATCACTGATCGACACGGGCTCCAG Mm00439358_m1 NR4A1 (Nur77) NM_010444
AACCCAGATTCAAGGCAAGTGCCCC Mm00476267_m1 NAB2 NM_008668
CCGTGAAGAGTGAGCCGGTGGAGCC Mm00435245_m1 NOTCH1 NM_008714

2.9. Molecular biology techniques – western blotting.

2.9.1. SDS-PAGE

For Western Blots, cell pellets were washed twice in 4^0C PBS and lysed in RIPA or NP40 Lysis buffer containing protease inhibitors (Roche, Cat. No. 11836153001), and protein quantified using Bradford Reagent (BioRad, Cat No. 500-0006). Protein lysates containing 10-20µg protein were electrophoresed in 10-15% SDS-PAGE gels. SDS-PAGE was carried out using Bio-Rad apparatus according to the manufacturer's protocols. 10 and 12.5% polyacrylamide resolving gels contained 375mM Tris-HCl (pH 8.8), 0.1% SDS, 0.1% ammonium persulphate (Sigma, Cat No. A3678) and 0.4% N,N,N',N'-tetramethylethylenediamine (TEMED) (Sigma, Cat No. T9281). Stacking gels contained 5% polyacrylamide, 125mM Tris-HCl (pH 6.8), 0.1% SDS, 0.1% ammonium persulphate and 0.4% N,N,N',N'-tetramethylethylenediamine (TEMED). Polyacrylamide gels were electrophoresed at 80-150V in standard SDS-PAGE electrophoreis buffer.

2.9.2. Western blotting

Electrophoresed samples were transferred to PVDF (polyvinylidene fluoride) membranes in Transfer buffer using Bio-Rad or Hoefer transfer apparatus according to manufacturers protocols. Gels were transferred either for 1 hour at 100V at RT, or 40V overnight at 4^0C.

2.9.3. Antibody analysis.

Membranes were initially checked for even transfer with Ponceau S Solution (Sigma, Cat. No. P7170), blocked with TBS-T (**Table 2.1**) containing 5% Marvel milk powder for 1 hour at room temperature, and then probed for proteins in TBS-T containing 5% Marvel milk powder for either 1 hour at room temperature or overnight at 4^0C with gentle agitation. Membranes were then washed with TBS-T three times at ten minute intervals, before subsequent incubation with secondary antibodies in 5% Marvel milk/TBS-T for 30 minutes. Again membranes were washed three times with TBS-T at ten minute intervals, before protein visualisation with ECL (Amersham, Cat No. RPN3004).

Table 2.6. Antibodies used for Western Blotting.

Antibody	Supplier	Cat. No.	Clone, Isotype	Dilution
Myc	**Roche**	**11 667 149 001**	**9E10, Mouse IgG1,κ**	**1/1000**
HA	**Roche**	**11 867 423 001**	**3F10, rat IgG1**	**1/1000**
Tubulin	**Serotec**	**MCA77G, YL1/2**	**IgG2a**	**1/2000**
Bim	**Chemicon**	**AB17003**		**1/1000**
Parp	**Santa Cruz**	**sc-7150**	**rabbit IgG**	**1/1000**
Tnfaip8	**Abnova**	**H00025816-A01**		**1/1000**

2.10. Tissue culture techniques – transfection of retroviral vectors and concentration of retrovirus.

2.10.1. Transfection of retroviral rectors

The pMSCV-based expression and knock-down vectors were constructed as detailed in section **2.4**. Maxipreps were performed using the Qiagen Hi-Speed Maxi-Prep Kit (Qiagen, Cat No. 12663) and DNA quantified and checked for quality using a NanoDrop spectrophotometer. LinX E packaging cells were split 1:25 72 hours prior to transfection to achieve 50-75% confluence, and transfected with Lipofectamine (Invitrogen, Cat No. 18324-012)/Optimem (Invitrogen, Cat No. 51985-042) complexes. 2 solutions were prepared:

Solution A – 900µl optimem + 10µg DNA

Solution B – 855µl optimem + 45µl lipofectamine

Solution A was added dropwise to solution B and left for 30 to 45 minutes. LinXE plates were then washed with 5mls Optimem, while 8ml Optimem was added to each transfection mix. The 10ml Optimem was then added to a plate of LinXE cells and incubated at 37^0C for 4-5 hours. 10 ml of DMEM: 20% FCS, 100U/ml penicillin, 100µg/ml streptomycin, 2mM L-glutamine was then added and the cultures left at 37^0C overnight. After 24 hours, the transfection mix was removed and replaced with 7ml DMEM: 10% FCS, 100U/ml penicillin, 100µg/ml streptomycin, 2mM L-glutamine and left at 37^0C for a further 24 hours.

2.10.2. Concentration of retroviral particles.

Retroviral supernatant (7ml) was harvested at 48 hrs post transfection and cleared of cellular debris by centrifugation at 1500rpm for 7 minutes at 4^0C. Retroviral particles

were then concentrated 10-fold by centrifugation at 16,000g at 4^0C for 60 minutes followed by resuspension in 1/10 volume target media.

2.10.3. Infection of haematopoietic progenitor cells (HPCs).

Haematopoietic progenitor cells (HPCs) were obtained from E12 or E13 murine embryonic foetal livers, dissected from C57Bl6/J time-mated pregnant females (Harlan). $cKit^+$ HPCs were purified by magnetic-activated cell sorting (MACS) (Miltenyi Biotech) using anti-cKit (clone 2B8, Cat. No. 553352, Pharmingen) antibody covalently linked to Streptavidin, with the second step utilising anti-Biotin microbeads. Following purification, $cKit^+$ HPCs were assayed by flow cytometry for purity (secondary stain, Streptavidin-PE, Cat. No. 349023, Pharmingen), with $90\%^+$ purity typically achieved. Purified $cKit^+$ HPCs were either frozen in 90% FCS (Stem Cell Technology, Cat. No. O6200), 10% DMSO (Sigma, Cat. No. D8418) or cultured overnight at 0.5 x 10^6 cells/ml in RPMI: 10% FCS (Stem Cell Technology), 100U/ml penicillin, 100µg/ml streptomycin, 2mM L-glutamine, 50µM 2-mercaptoethanol, 100ng/ml SCF (Peprotech, Cat. No. 250-03), 20ng/ml IL-7 (Peprotech, Cat. No. 217-17), 10ng/ml IL-6 (Peprotech, Cat. No. 216-16), and 10ng/ml IL-3 (Peprotech, Cat. No. 213-13). Infections of cultured HPCs were performed in 96-well TC plates. Concentrated retrovirus were resuspended in 1/10 original volume RPMI: 20% FCS (Stem Cell Technology, Cat. No. O6200), 100U/ml penicillin, 100µg/ml streptomycin, 2mM L-glutamine, 50µM 2-mercaptoethanol, 100ng/ml SCF, 20ng/ml IL-7, 10ng/ml IL-6, and 10ng/ml IL-3 and 5µg/ml polybrene (Hexadimethrine bromide, Sigma, Cat. No. H9268). HPCs were added to infection mixes, and plated at 1 x 10^4 cells/well of a 96-well plate. Infection was then performed by centrifugation at

700 x *g* for 45 minutes at RT, followed by overnight culture at 37^0C, with infected cells harvested at 24 hours for subsequent procedures.

2.11. Tissue culture techniques – foetal thymic organ culture (FTOC).

For cell culture, FTOCs were maintained in 37^0c humidified incubators (Galaxy R, Wolf Laboratories) with 5% CO_2 unless otherwise stated.

Foetal thymic organ cultures (FTOCs) were used to generate T cells for analysis. FTOC lobes were obtained by dissection from C57Bl6 E15 time-mated pregnant females (Harlan). Mice were sacrificed by cervical dislocation, and embryos removed and placed into ice-cold HBSS:1mM HEPES. In sterile conditions, embryos were dissected from amniotic sacs using a Zeiss Stemi 1000 microscope, Schott KL1500 LCD light source and Dumont No.5 jewellers forceps (Sigma Cat. No. F6521). Embryos were first severed across the midsection at diaphragm level, heart and lungs were removed from the thorax and the thymic lobes removed into clean HBSS:1mM HEPES for fine dissection. Thymic lobes were separated, and each lobe cultured for five days (10 lobes per filter) on autoclaved Whatman Nuclepore Track-Etch Polycarbonate Membranes (Whatman, Cat. No. 110409) floating on 3ml RPMI: 10% FCS (Stem Cell Technology), 100U/ml penicillin, 100µg/ml streptomycin, 2mM L-glutamine, 50µM 2-mercaptoethanol supplemented with 1.5mM 2-deoxyguanosine (2dGuo) (Sigma, Cat. No. D0901) in 6-well TC dishes. After 5 days depopulation, FTOC filters were moved to media without 2dGuo to rest for 24 hours. Each FTOC lobe was then reconstituted with 1-3 x 10^4 retrovirally infected (24 hours past infection) $cKit^+$ HPCs in a well of a Terasaki 6 x 10 Mini Tray TC plate (Fisher, Cat. No. DIS-980-010X), inverted and placed inside a 150mM TC plate containing a

35mM TC plate containing 4ml PBS to maintain humidity levels, and left to reconstitute at the oxygen-enriched interface overnight (Ivanov, Merkenschlager et al. 1993). 1-2 x 10^5 $cKit^+$ HPCs were also maintained in RPMI complete media and cytokines for a further 24 hrs to check hCD2 expression, and thus transfection/infection efficiency. After 24 hrs, the reconstituted FTOCs were transferred to fresh Whatman Nuclepore Track-Etch Polycarbonate Membranes floating on 3ml RPMI: 10% FCS (Stem Cell Technology), 100U/ml penicillin, 100µg/ml streptomycin, 2mM L-glutamine, 50µM 2-mercaptoethanol in 12-well TC plates and left to culture at 37^0C for 7-17 days, with 1 media change at 7-10 days. After 7-17 days incubation, the FTOCs were mechanically disrupted using a plastic pestle or by repeat pipetting in 300µl PBS:2%FCS:0.1% sodium azide and stained for cell surface markers or permeabilized for combination cell surface marker/intracellular DNA staining.

2.12. Tissue culture techniques – OP9-Dl1 co-cultures.

For cell culture, OP9-DL1 co-cultures were maintained in 37^0c humidified incubators (Galaxy R, Wolf Laboratories) with 5% CO2 unless otherwise stated.

OP9-DL1 bone marrow-derived stromal cells were maintained in αMEM:20%FCS (Invitrogen Cat. No. 10270-106, Lot No. Lot: 40F4053K), 100U/ml penicillin, 100µg/ml streptomycin, 50µM 2-mercaptoethanol, 10mM HEPES, 1mM Sodium Pyruvate, 50µg/ml Gentamicin, 2µM Glutamax, split 1:5 every 2-3 days as stated previously. For co-cultures, OP9-DL1 cells were split 1:5 into 6-well TC plates 2 days prior to co-culture initiation, achieving ≈75% confluence. HPCs were placed into co-culture 24 hours post retroviral infection. OP9-DL1 cells were first washed and

replenished with fresh media with the addition of 1ng/ml IL-7 (Peprotech, Cat. No. 217-17) and 5ng/ml Flt-3 ligand (Peprotech, Cat. No. 250-31L). Each well was initially inoculated with 1 x 10^4 HPCs. Co-cultures were then incubated for 7 days at 37^0C, with one media change at 4 days. After 7 days, co-cultures were split to fresh OP9-DL1 stromal cell feeder layers. Co-cultures were disrupted by repeat pipetting with a P1000 barrier tip and then filtered through a 70μM nylon mesh strainer to remove OP9-DL1 cell layers. Developing thymocytes were then placed into new OP9-DL1 co-cultures at a 1:10 split. Further 1:4 splits were performed at 12, 16 and 20 days. At each split cultured thymocytes were analysed by flow cytometry to check development.

2.13. Molecular biology techniques – flow cytometry and FACS.

For flow cytometry, cells (typically 0.5-1 x 10^6 cells/stain or for FTOCs, ≈ 1 x 10^5 cells/stain) were stained with fluorescein isothiocyanate (FITC)-, phycoerythrin (PE)-, TriColor (TC)-, allophycocyanin (APC)-, allophycocyanin-Cy7 (APC-Cy7)-, peridinin-chlorophyll-protein Complex (PerCP)-, or biotin (Bio)-conjugated monoclonal antibodies specific for cell surface markers. Cells were pre-blocked with unlabelled anti-Fcγ III/II receptor $mAb^{2.4G2}$ diluted in FACS staining buffer (PBS:2% FCS: 0.1% sodium azide). Cells were then stained with antibodies in 100μl FACS staining buffer for 30 minutes on ice in dark conditions, then washed in FACS staining buffer. For secondary antibodies (Strepavidin-PE or Streptavidin-PerCP), cells were again stained in 100μl FACS staining buffer for 30 minutes on ice in dark conditions, then again washed in FACS staining buffer. For intracellular DNA staining with 7AAD, cells were permeabilized with 0.03% saponin following cell surface staining, incubating with 0.03% saponin (Sigma Cat. No. S4521), 2.5μg/ml

7AAD (Sigma Cat. No. A9400) in FACS staining buffer at 37^0c for 30 minutes, then stored until analysis at 4^0C. For DRAQ5 staining, cells were first stained for cell surface markers and then resuspended in 300µl FACS staining buffer containing 20µM DRAQ5. For flow cytometry, cells were resuspended in 300µl FACS staining buffer and analysed using an EPICS© XL™ flow cytometer or a Dako CyAn™ flow cytometer.

Table 2.7. Antibodies used for flow cytometry.

Antibody	Supplier	Clone	Isotype	Cat. No.	Working dilution
hCD2-PE (LFA-2)	ebiosciences	RPA-2.10	Mouse IgG1, κ	12-0029-71	1/100
CD4-PE (L3T4)	ebiosciences	RM4-5	Rat IgG2a, κ	12-0042-85	1/100
CD44-APC	ebiosciences	IM7	Rat IgG2b, κ	17-0441-81	1/100
CD8α-FITC (Ly-2)	ebiosciences	53-6.7	Rat IgG2a, κ	11-0081-85	1/100
CD25-FITC (IL-2Rα)	ebiosciences	PC61.5	Rat IgG1, λ	11-0251-81	1/100
hCD4-APC	ebiosciences	RPA-T4	Mouse IgG1, κ	17-0049-71	1/100
CD4-APC	ebiosciences	RM4-5	Rat IgG2a, κ	17-0042-83	1/100
hCD4 (L3T4)	ebiosciences	RPA-T4	Mouse IgG1, κ	11-0049-71	1/100
CD25-APC	ebiosciences	PC61.5	Rat IgG1, λ	17-0251-81	1/100
CD44-APC	ebiosciences	GK1.5	Rat IgG2b, κ	11-0041-81	1/100
TCR β chain-Biotin	BD Pharmingen	H57-597	Armenian Hamster IgG 2, l1	553169	1/100
CD24 Heat Stable Antigen	BD Pharmingen	M1/69	Rat IgG_{2b}, k	553260	1/100
CD3ε- Biotin	ebiosciences	145-2C11	Armenian Hamster IgG	13-0031-85	1/100
CD4-TC	Caltag	CT-CD4	Rat IgG2a	RM2506	1/100
CD4-PerCP (L3T4)	BD Pharmingen	RM4-5	Rat IgG_{2a}, k	553052	1/100
Streptavidin-PerCP	BD Pharmingen	Strept avidin		554064	1/250
Streptavidin-PE	BD Pharmingen	Strept avidin		554061	1/250
Annexin V-APC	Invitrogen			A35110	1/100

CHAPTER 3

RESULTS (1)

3.1. Background.

3.1.1. Introduction.

The initial objective of this work was to identify candidate genes involved in the regulation of thymocyte apoptosis in two model systems. The first screen was designed to identify candidate genes regulated in glucocorticoid (GC)-induced thymocyte apoptosis, while the second screen was designed to identify genes regulated in a transgenic mouse model for antigen-mediated negative selection. The results from both screens would also be compared to determine any overlap.

The multigenic pathways induced in both systems in response to apoptotic stimuli are as yet only partially understood. Both GC-induced and antigen-mediated apoptosis are transcriptionally dependent, and require the synthesis of new RNA transcripts to occur. Therefore we used Affymetrix GeneChip® probe arrays to compare the RNA profile of thymocytes induced to undergo apoptosis with untreated controls. We can therefore identify potential candidate genes involved in regulating thymocyte apoptosis to investigate further in functional studies.

3.1.2. Affymetrix GeneChip® probe array analysis.

Affymetrix GeneChip® probe array technology enables 'molecular snapshots' to be taken of the transcriptional profile of cells across thousands of genes. Groups of arrays can be directly compared for the effect on transcription of a particular stimulus, the expression of a particular protein or the knockdown of a specific transcript. Affymetrix GeneChip® probe arrays contain millions of copies of an oligonucleotide probe anchored to specific locations on the chip (called a probe cell), in groups of eleven to sixteen probes for each transcript. Each probe is associated with a mismatch

probe, identical except for a single central nucleotide. These mismatch probes act as controls to identify non-specific hybridization and act as guides for the relative amount of RNA loaded on the chips.

All probe sets on Affymetrix GeneChip® probe arrays, and the information pertaining to their sequence, ontology, accession numbers etc. are publicly available on frequently updated databases. For our Affymetrix GeneChip® probe array screens we used the murine genome U74a chip, which contains probe sites for more than 12,000 genes and expressed sequence tags (ESTs) from the Unigene Build 74 database. A schematic overview of the protocol for preparing material for hybridization to Affymetrix GeneChip® probe arrays is shown in **Figure 3.1**.

3.1.3. Sample preparation for Affymetrix GeneChip® probe arrays.

Total RNA from triplicate experimental and control samples was extracted, checked for integrity and concentration using an Agilent 2100 Bioanalyser, and reverse transcribed to cDNA. This cDNA is then used in an *in vitro transcription* reaction as a template for the generation of biotin-labelled complementary RNA (cRNA). cRNA is fragmented and added to a hybridization cocktail for overnight annealing to DNA microarrays. Microarrays are washed and stained with a streptavidin-PE conjugate which binds to the cRNA. This is visualised using an Affymetrix probe scanner, which quantifies the fluorescence emitted when the fluorophore is excited by a Nd:YAG Green Laser. The level of fluorescence is directly proportional to the absolute amount of fragmented cRNA bound at each location. It is therefore possible to compare expression levels and perform statistical analyses to determine which genes are differentially regulated.

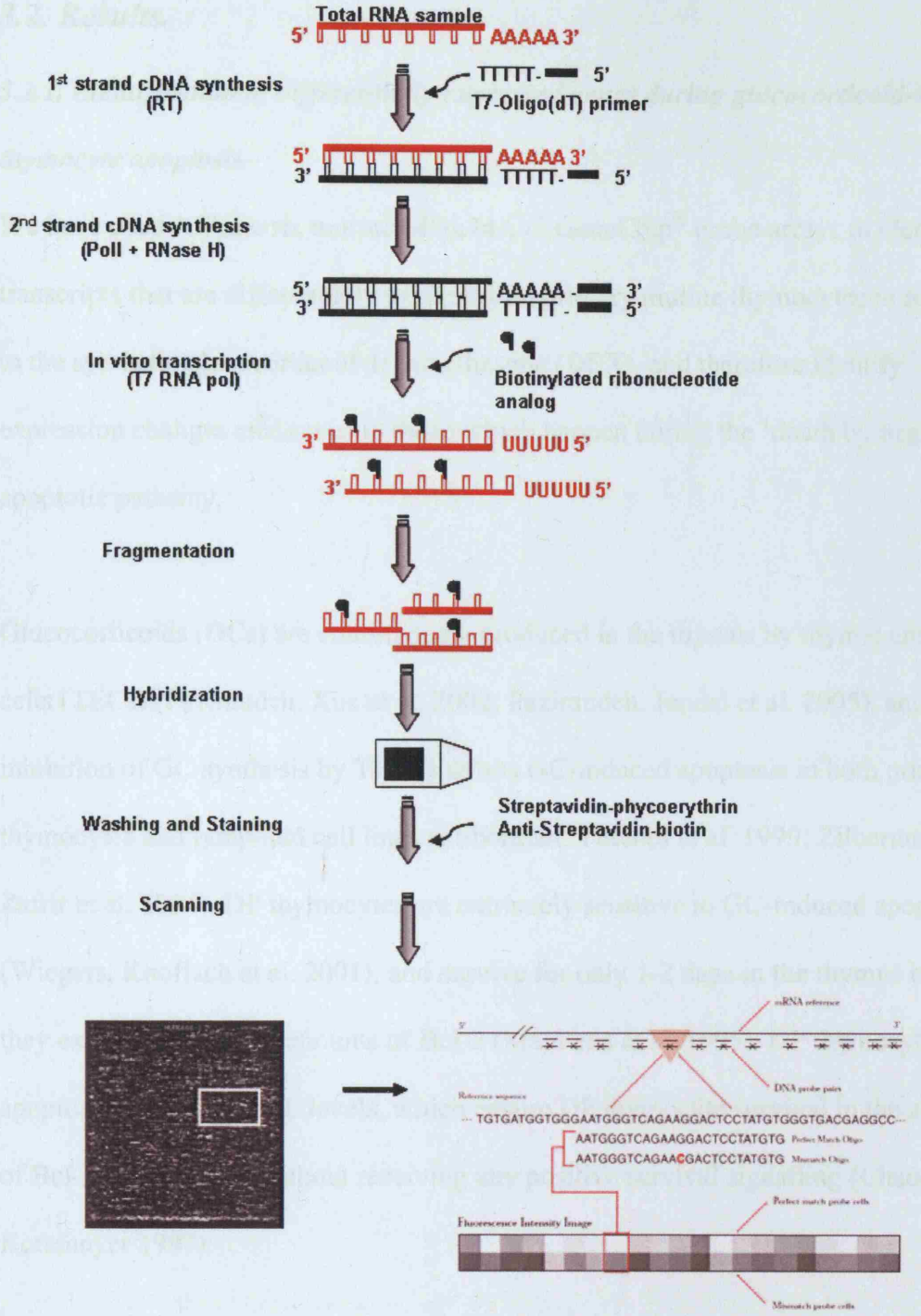

Figure 3.1. Overview of Affymetrix Array GeneChip® Technology.
Affymetrix GeneChip® probe arrays consist of nucleic acid probes attached to a quartz matrix. The precise location where each probe is synthesised is called a feature, each array containing millions of features. Labelled nucleic acids from experimental and control samples are hybridized to GeneChip® probe arrays, and the amount of bound label analysed at each feature, enabling comparison between samples on a whole-genome scale. Adapted from Affymetrix website.

3.2. Results.

3.2.1. Identification of differentially expressed genes during glucocorticoid-induced thymocyte apoptosis.

We have used Affymetrix murine MGu74Av2 GeneChip® probe arrays to identify transcripts that are differentially expressed in primary murine thymocytes in response to the synthetic glucocorticoid dexamethasone (DEX), and therefore identify expression changes analogous to those which happen during the 'death by neglect' apoptotic pathway.

Glucocorticoids (GCs) are continuously produced in the thymus by thymic epithelial cells (TECs) (Pazirandeh, Xue et al. 2002; Pazirandeh, Jondal et al. 2005), and inhibition of GC synthesis by TECs inhibits GC-induced apoptosis in both primary thymocytes and lymphoid cell lines (Zilberman, Yefenof et al. 1999; Zilberman, Zafrir et al. 2004). DP thymocytes are extremely sensitive to GC-induced apoptosis (Wiegers, Knoflach et al. 2001), and survive for only 1-2 days in the thymus because they express negligible amounts of Bcl-2 (Ma, Pena et al. 1995). DP thymocytes enter apoptosis as their Bcl-XL levels, which ensure DP thymocyte survival in the absence of Bcl-2, also decline without receiving any positive survival signalling (Chao and Korsmeyer 1997).

GC-induced apoptosis is transcriptionally dependent, and is blocked by both RNA and protein synthesis inhibitors (Wyllie, Morris et al. 1984). To identify genes that are transcriptionally regulated during the initial stages of GC-induced apoptosis, but before the loss of mitochondrial membrane stability, cytochrome c release and caspase activation, we used the Cdk2 inhibitor Roscovitine (ROSC). ROSC is a

chemically synthesised purine analogue that selectively binds to the ATP-binding site of Cdk2 and Cdc2 (and to a far lesser extent, Cdk1 and Cdk5), blocking Cdk kinase activity and activation, and abolishing thymocyte apoptosis (De Azevedo, Leclerc et al. 1997; Meijer, Borgne et al. 1997).

Cdk2 inhibition, using pharmacological inhibitors, has previously been shown to block thymocyte apoptosis induced by GCs (p53-independent) and γ-irradiation (p53-dependent), but not CD95 signalling (Gil-Gomez *et al,* EMBO 1998, Williams *et* al, Eur J Immunol 2000, Granes *et al*, Eur J Immunol 2004). Cdk2 activation resides at a critical juncture in thymocyte apoptosis, upstream of cytochrome c release, apical caspase activation and phosphatidylserine exposure, downstream of Bax and Bcl-2 activity. An increase in Cdk2 kinase activity is intrinsically associated with thymocyte apoptosis, closely correlating to cell death (**Figure 3.3A, Taken from (Gil-Gomez, Berns et al. 1998)**).

To prepare RNA for DNA microarray analysis, primary thymocytes were harvested from C57/BL6 mice and cultured *in vitro* for 4 hours with or without 5μM DEX in the presence of 25μM ROSC to arrest the apoptotic response at the stage of Cdk2 activation (**Figure 3.2**). Duplicate samples at 4 and 6 hours were stained with propidium iodide and analysed by flow cytometry to check the extent of apoptosis and the extent of inhibition in the presence of ROSC (**Figure 3.3B**). Flow cytometric analysis revealed that 25μM ROSC efficiently blocked apoptosis induced by 5μM DEX at both 4 and 6 hours.

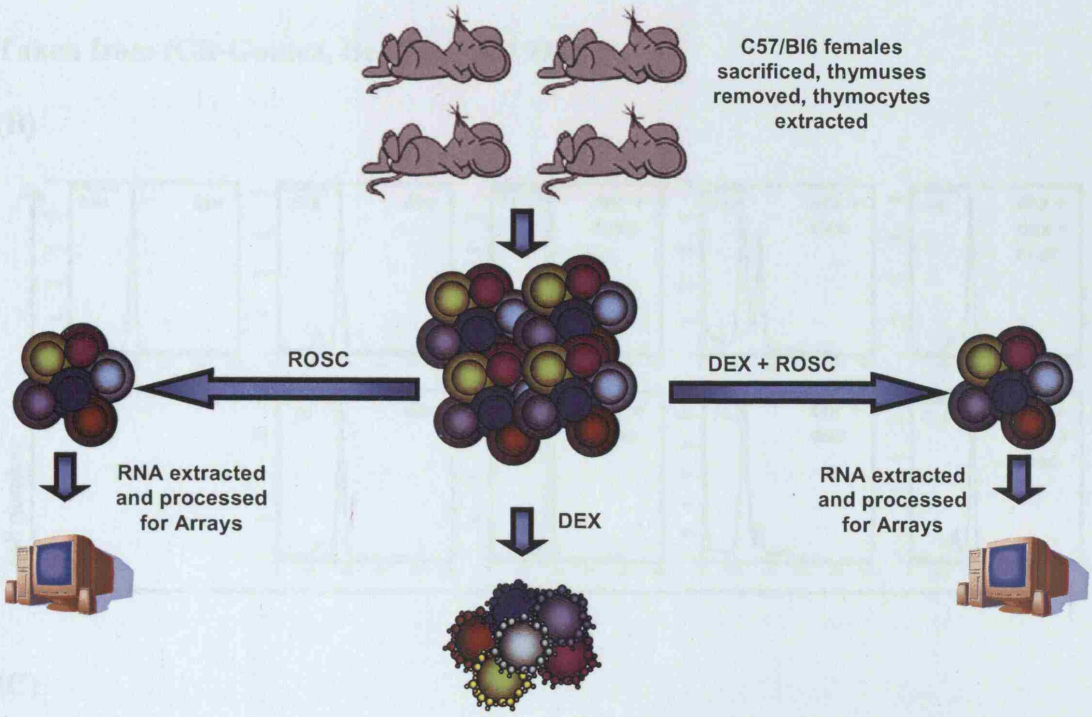

Figure 3.2. Experimental plan – glucocorticoid screen.
Diagram of Affymetrix GeneChip® probe array analysis. Experimental samples from thymocytes treated with DEX in the presence of ROSC were compared with thymocytes treated with ROSC alone.

(A)

Taken from (Gil-Gomez, Berns et al. 1998)

(B)

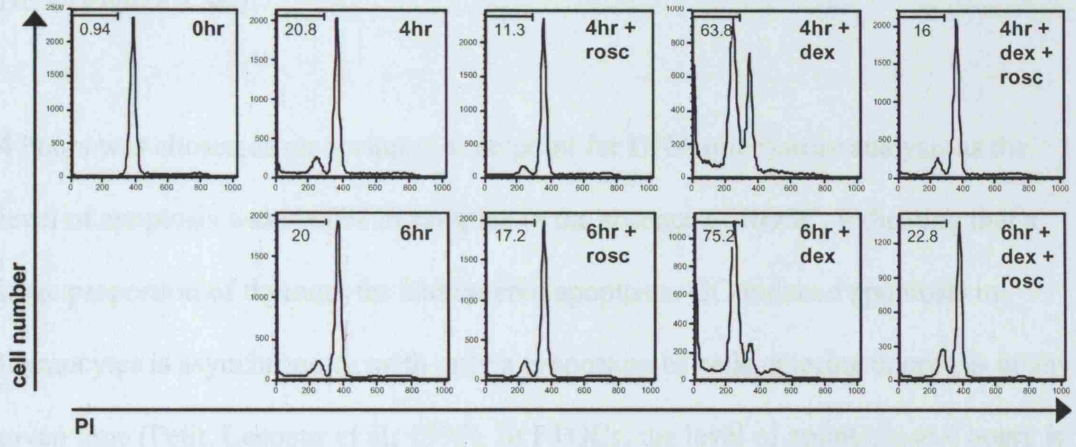

(C)

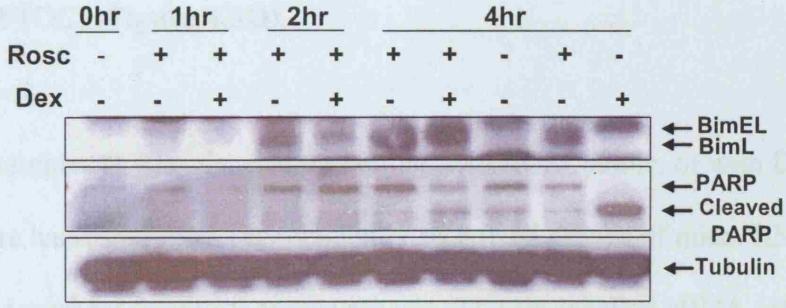

Figure 3.3. Cdk2 inhibition by ROSC abrogates thymocyte apoptosis in response to DEX (A) Thymocytes from wild-type mice treated with DEX and γ-irradiation tested for Cdk2 kinase activity in kinase assays. **Taken from (Gil-Gomez, Berns et al. 1998) (B)** Flow cytometry of murine thymocytes cultured *in vitro* +/- DEX, +/- ROSC. Cells were stained with CD8-FITC, CD4-PE, then permeabilized with 0.03% saponin and intracellular DNA stained with 7AAD **(C)** Western blots of parallel samples used for GeneChip® probe array analysis.

A duplicate experiment was performed to check the induction or cleavage of apoptosis-related proteins Parp and Bim under similar conditions. Partial abrogation of Parp cleavage, a known caspase substrate and marker of the executioner phase of thymocyte apoptosis (Ivanov and Nikolic-Zugic 1998), is evident when thymocytes are incubated with 5μM DEX in the presence of 25μM ROSC (**Figure 3.3C**).

Induction of Bim^{EL} (Wang, Malone et al. 2003), a known target of GCs in several lymphoid model systems, is also evident when thymocytes are incubated with 5μM DEX (**Figure 3.3C**).

4 hours was chosen as an optimum time point for DNA microarray analysis as the level of apoptosis was ≈ 60% in samples in the absence of ROSC, indicating that a large proportion of thymocytes had entered apoptosis. GC-induced apoptosis in thymocytes is asynchronous, with only a proportion of cells entering apoptosis at any given time (Petit, Lecoeur et al. 1995). In FTOCs, the level of apoptosis at 4 hours is ≈ 12% (reduced because of phagocytic clearance of apoptotic cells by macrophages within the FTOC) (**Figure 4.3D**).

Triplicate samples at 4 hours, cultured either with ROSC alone, or with DEX and ROSC, were harvested from independently sacrificed groups of mice. RNA was isolated and used for the multi-step synthesis of biotin-labelled cRNA, which was hybridized to Affymetrix MGu74a GeneChip® probe arrays. Quality control among samples was maintained by checks at relevant steps for integrity and concentration using an Agilent 2100 Bioanalyser (**Figure 3.4A**).

Primary data analysis was performed using Affymetrix Microarray Suite software Version 5, and normalisation carried out using Genespring 5.0. Each Affymetrix chip was normalised to the median of the triplicate and each gene normalised to the control sample, to allow for direct pairwise comparison of gene expression levels. Data was also filtered to only include genes that were detected as expressed in both control and test samples.

3.2.2 Transcripts regulated by glucocorticoids.

Upon analysis, 301 transcripts were found to be up-regulated in murine thymocytes cultured with both 5μM DEX and 25μM ROSC. 54 were found to be statistically significant following more stringent Benjamini-Hochberg false discovery rate (FDR) multiple testing corrections. The FDR-selected genes up-regulated by DEX in the presence of ROSC were changed up to 87-fold (*mouse endogenous proviral superantigen Mtv-7 sag*, a known target of GCs), and those with the highest degree of regulation were investigated regarding their biological role. The target genes most up-regulated by DEX (those with an induction greater than 4-fold) are detailed in **Table 3.1,** while the most down-regulated genes (those with a reduction greater than 2-fold) are detailed in **Table 3.2**. For full tables of all regulated genes, please see **Appendices A.1 and A.2**.

64 transcripts were found to be significantly down-regulated by DEX, but we have found that upon treatment with DEX there is a global down-regulation in transcription, most evident in the down-regulation of the housekeeping genes *β-actin* and *Gapdh* (**Figure 3.4B**). Genes that were down-regulated against a background of global down-regulation were therefore excluded from further study.

(A)

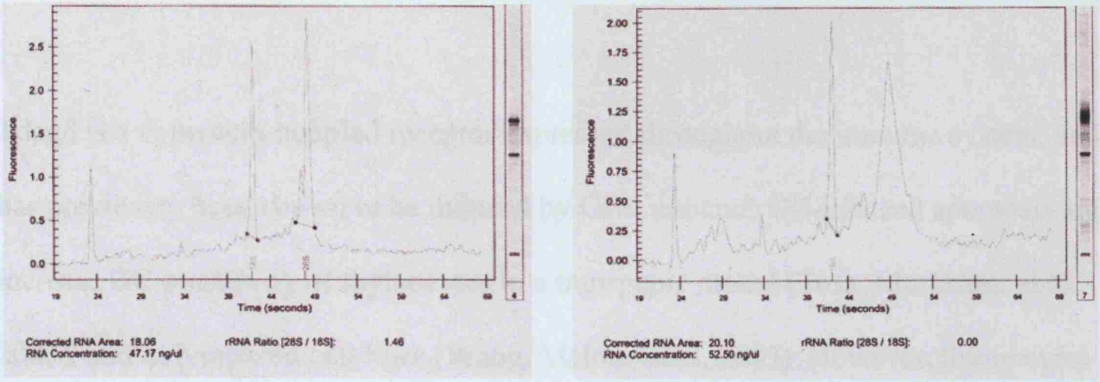

(B)

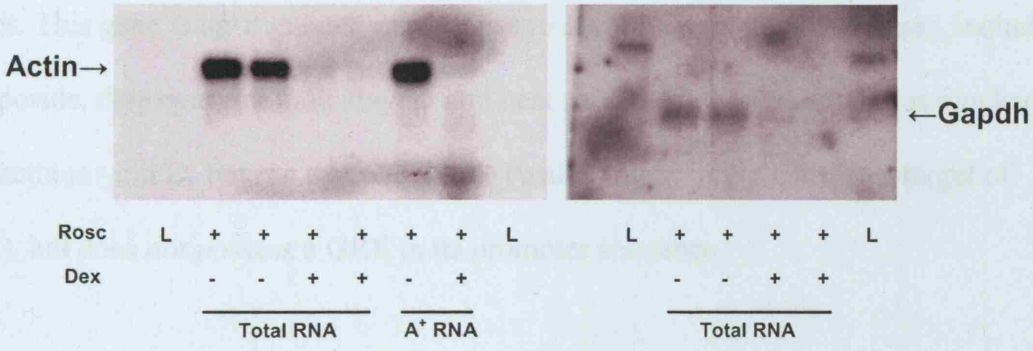

Figure 3.4. RNA integrity of samples extracted for glucocorticoid screen and down-regulation of housekeeping genes in response to DEX. **(A)** Agilent 2100 Bioanalyser plots of RNA extracted for Affymetrix DNA microarray analysis, two samples, ROSC and ROSC + DEX. **(B)** Northern blots demonstrating down-regulation of *actin* and *GAPDH* following DEX treatment (L=RNA Ladder).

Regulation of many of the GC-induced genes found in this study has previously been reported in similar screens, including *Tdag8* (Tosa, Murakami et al. 2003; Malone, Wang et al. 2004), *Fkbp51* (Malone, Wang et al. 2004), *Tnfaip3/A20* (DeRyckere, Mann et al. 2003), *Dig2* (Wang, Malone et al. 2003) and *Bim* (Wang, Malone et al. 2003; Malone, Wang et al. 2004).

Tdag8 is a G-protein-coupled receptor expressed throughout the immune system, and has previously been shown to be induced by GCs, enhance GC-induced apoptosis and increase GC sensitivity of thymocytes in a transgenic model (Tosa, Murakami et al. 2003), and in lymphoid cell lines (Wang, Malone et al. 2003). However, thymocytes from $Tdag8^{-/-}$ mice show normal levels of apoptosis in response to GCs both *in vivo* and *in vitro* (Radu, Cheng et al. 2006). *Dig2* is a novel stress response gene also known to be up-regulated in GC-induced apoptosis, but which demonstrates an anti-apoptotic effect when over-expressed (Wang, Malone et al. 2003) in lymphoid cell lines. This gene is up-regulated in response to several other cellular stresses, including etoposide, thapsigargin, tunicamycin and heat shock. *Dig2* up-regulation is blocked by actinomycin D, but not cycloheximide (which might imply a primary target of GR), but does not possess a GRE in its promoter sequence.

Bim^{EL} (Bcl-2 interacting mediator of cell death) is a BH3-only, pro-apoptotic member of the *Bcl-2* family. Bim acts at the mitochondria, activating Bax and Bak and promoting cytochrome c release, active at a critical juncture of the executioner stage of apoptosis (O'Connor, Strasser et al. 1998; Letai, Bassik et al. 2002; Rathmell, Lindsten et al. 2002). RNAi-mediated knockdown of Bim isoforms blocks GC-

induced apoptosis, with RNAi constructs effective against multiple isoforms (Bim^{EL}, Bim^{L} and Bim^{S}) more effective (Abrams, Robertson et al. 2004).

The immunophilin *Fkbp51* is a glucocorticoid co-chaperone molecule that, similar to heat shock protein Hsp90, binds to and inactivates glucocorticoid receptor (GR) by sequestrating GR in a protein complex (Reynolds, Ruan et al. 1999). Fkbp51 binding to GR can therefore regulate sensitivity to GC-induced apoptosis. Intriguingly, some of the most up-regulated genes in our screen were absent in data produced by previous DNA microarray screens to identify genes regulating GC-induced apoptosis. *E4bp4*, one of the most up-regulated genes, is a transcriptional repressor known to possess a glucocorticoid-response element in its promoter (Wallace, Wheeler et al. 1997). E4bp4 was originally identified as a transcriptional activator of the human interleukin-3 promoter in T cells (Cowell, Skinner et al. 1992; Zhang, Zhang et al. 1995), is ubiquitously expressed and has been implicated in control of circadian rhythm (glucocorticoid levels also demonstrate circadian rhythm patterns) and hormone responses (Lai and Ting 1999; Cowell 2002).

Tnfaip8 is a novel death-effector domain (DED) containing protein found to be induced in several screens isolating genes up-regulated in response to TNF-α stimulation (Kumar, Whiteside et al. 2000), while Tnfaip3(A20) is a TNF-α inducible cytoplasmic zinc finger domain protein known to act as a potent NF-κB signalling inhibitor. Tnfaip3(A20) attenuates TNF signalling by inhibiting NF-κB, and is up-regulated in *in vivo* models for negative selection (DeRyckere, Mann et al. 2003). $Tnfaip3(A20)^{-/-}$ mice display widespread inflammation and cachexia as they are

unable to attenuate NF-κB responses to endogenous Tnf-α signalling (Lee, Boone et al. 2000).

Table 3.1. Genes up-regulated by glucocorticoids in presence of roscovitine.

	Probe set ID	Gene Title	Gene Symbol	Description	Fold change
1	92780_f_at	Mammary gland RCB-0526 Jyg-MC(A) cDNA, RIKEN full-length enriched library, clone:G830022P11 product:unclassifiable, full insert sequence		Mammary tumor virus locus 43	87.721 (83.847 to 92.419)
2	93928_f_at	hypothetical protein LOC624610	LOC624610		25.25 (19.269 to 34.599)
3	102663_at	plasminogen activator, urokinase receptor	Plaur	M.musculus muPAR1 mRNA.	24.745 (23.936 to 25.323)
4	102955_at	nuclear factor, interleukin 3, regulated	Nfil3	Mus musculus NFIL3/E4BP4 transcription factor mRNA, complete cds.	**21.17 (14.468 to 26.46)**
5	92925_at	CCAAT/enhancer binding protein (C/EBP), beta	Cebpb	Mouse alpha-1-acid glycoprotein (AGP/EBP) mRNA, complete cds.	**18.154 (9.792 to 28.171)**
6	96553_at	G-protein coupled receptor 65	Gpr65	putative G protein-coupled receptor; Mus musculus putative G protein-coupled receptor TDAG8 (TDAG8) mRNA, complete cds.	**16.609 (6.518 to 28.918)**
7	97509_f_at	fibroblast growth factor receptor 1	Fgfr1	FGFR1(L); similar to mouse FGFR-1 encoded by GenBank Accession Number M28998 and to human FGFR-1 encoded by GenBank Accession Numbers M34187 and M34188; Mus musculus fibroblast growth factor receptor-1 mRNA, long isoform precursor, complete cds.	**14.174 (10.57 to 17.964)**
8	160246_at	tumor necrosis factor, alpha-induced protein 8	Tnfaip8	UI-M-AO0-ach-a-08-0-UI.s1 NIH_BMAP_MPG Mus musculus cDNA clone UI-M-AO0-ach-a-08-0-UI 3', mRNA sequence.	**7.994 (7.125 to 8.821)**
9	93316_at	oxysterol binding protein-like 1A	Osbpl1a	putative; Mus musculus mRNA for oxysterol-binding protein, complete cds.	**7.871 (5.492 to 12.02)**
10	101805_f_at	nuclear factor, interleukin 3, regulated	Nfil3	similar to human transcriptional repressor E4BP4, PIR Accession Number S18995; belongs to CREB-ATF subfamily of bZIP family of transcription factors; Mus musculus strain BALB/c transcription factor E4BP4 mRNA, partial cds.	**7.861 (5.593 to 9.11)**
11	103460_at	DNA-damage-inducible transcript 4	Ddit4	UI-M-BG0-ahz-g-03-0-UI.s1 NIH_BMAP_MSC Mus musculus cDNA clone UI-M-BG0-ahz-g-03-0-UI 3', mRNA sequence.	**7.292 (4.224 to 9.064)**
12	92356_at	protein tyrosine phosphatase, non-receptor type 22 (lymphoid)	Ptpn22	Mouse protein tyrosine phosphatase (70zpep) mRNA, complete cds.	**7.26 (5.942 to 8.64)**
13	160904_at	RIKEN cDNA B230317C12 gene	B230317C12Rik	UI-M-AH0-acy-c-05-0-UI.s1 NIH_BMAP_MCE Mus musculus cDNA clone UI-M-AH0-acy-c-05-0-UI 3', mRNA sequence.	**7.161 (6.049 to 9.074)**
14	94501_at	sphingosine-1-phosphate phosphatase 1	Sgpp1	UI-M-AI0-aaq-b-10-0-UI.s1 NIH_BMAP_MBS Mus musculus cDNA clone UI-M-AI0-aaq-b-10-0-UI 3', mRNA sequence.	**6.89 (3.306 to 10.533)**
15	160547_s_at	thioredoxin interacting protein	Txnip	UI-M-AO0-ach-d-06-0-UI.s1 NIH_BMAP_MPG Mus musculus cDNA clone UI-M-AO0-ach-d-06-0-UI 3', mRNA sequence.	**6.647 (5.47 to 7.546)**
16	97409_at	immunity-related GTPase family, M	Irgm	related to GTP-binding proteins; Mus musculus G-protein-like LRG-47 mRNA, complete cds.	**6.275 (2.712 to 8.304)**
17	97349_at	FERM domain containing 6	Frmd6	vu99g08.r1 Stratagene mouse skin (#937313) Mus musculus cDNA clone IMAGE:1210334 5', mRNA sequence.	**6.093 (3.097 to 9.299)**
18	99452_at	lipolysis stimulated lipoprotein receptor	Lsr	liver-specific gene; Mus musculus B6CBA Lisch7 mRNA, partial cds.	**5.981 (4.509 to 6.98)**
19	92778_i_at	Coronin, actin binding protein 2A	Coro2a	M.musculus membrane glycoprotein gene.	**5.921 (4.564 to 7.666)**
20	104058_at	coiled-coil domain containing 128	Ccdc128	UI-M-BH1-ama-d-09-0-UI.s1 NIH_BMAP_M_S2 Mus musculus cDNA clone UI-M-BH1-ama-d-09-0-UI 3', mRNA sequence.	**5.796 (3.938 to 8.334)**
21	95024_at	ubiquitin specific peptidase 18	Usp18	UI-M-BH1-alo-a-12-0-UI.s1 NIH_BMAP_M_S2 Mus musculus cDNA clone UI-M-BH1-alo-a-12-0-UI 3', mRNA sequence.	**5.733 (3.994 to 7.14)**
22	103891_i_at	elongation factor RNA polymerase II 2	Ell2	ue51h10.r1 Soares_mammary_gland_NMLMG Mus musculus cDNA clone IMAGE:1494691 5', mRNA sequence.	**5.665 (3.783 to 8.076)**
23	103599_at	transformed mouse 3T3 cell double minute 1	Mdm1	Source: Mouse nuclear protein (mdm-1a) mRNA, complete cds.	**5.238 (4.334 to 6.587)**
24	103264_at	myotubularin related protein 1	Mtmr1	Mus musculus myotubularin related protein 1 (Mtmr1) mRNA, complete cds.	**5.155 (2.01 to 7.384)**
25	93360_at	phosphomannomutase 1	Pmm1	similar to yeast Sec53p; Mus musculus phosphomannomutase Sec53p homolog mRNA, complete cds.	**4.63 (3.527 to 5.705)**
26	102293_at	IKAROS family zinc finger 1	Ikzf1	Mouse Ikaros DNA binding protein (Ikaros) mRNA, complete cds.	**4.582 (1.666 to 6.938)**
27	104670_at	DENN/MADD domain containing 4C	Dennd4c	uj34a01.x1 Sugano mouse kidney mkia Mus musculus cDNA clone IMAGE:1921800 3', mRNA sequence.	**4.484 (4.223 to 4.619)**
28	160236_at	SLAIN motif family, member 1	Slain1	UI-M-AI0-aap-g-03-0-UI.s1 NIH_BMAP_MBS Mus musculus cDNA clone UI-M-AI0-aap-g-03-0-UI 3', mRNA sequence.	**4.425 (2.457 to 5.709)**
29	98923_at	RNA terminal phosphate cyclase-like 1	Rcl1	UI-M-BH0-aiu-d-07-0-UI.s1 NIH_BMAP_M_S1 Mus musculus cDNA clone UI-M-BH0-aiu-d-07-0-UI 3', mRNA sequence.	**4.327 (3.251 to 5.066)**
30	99419_g_at	Bcl2-like 11 (apoptosis facilitator)	Bcl2l11	pro-apoptotic BH3-containing Bcl-2 family member; Mus musculus BimEL mRNA, complete cds.	**4.278 (2.006 to 5.499)**
31	160273_at	zinc finger protein 36, C3H type-like 2	Zfp36l2	vw64d05.s1 Soares_mammary_gland_NMLMG Mus musculus cDNA clone IMAGE:1248585 3', mRNA sequence.	**4.259 (2.995 to 5.595)**
32	98440_at	leukotriene B4 12-hydroxydehydrogenase	Ltb4dh	vm60d08.r1 Stratagene mouse Tcell 937311 Mus musculus cDNA clone IMAGE:1002639 5' similar to TR:E212316 E212316 NADP DEPENDENT LEUKOTRIENE B4 12-HYDROXYDEHYDROGENASE. ;, mRNA sequence.	**4.234 (2.793 to 5.702)**
33	94297_at	FK506 binding protein 5	Fkbp5	T-cell specific immunophilin that inhibits calcineurin; Mus musculus immunophilin FKBP51 mRNA, complete cds.	**4.133 (3.261 to 5.127)**
34	99392_at	tumor necrosis factor, alpha-induced protein 3	Tnfaip3	Mus musculus zinc finger protein A20 (murine A20) mRNA, complete cds.	**4.085 (2.039 to 6.664)**
35	95057_at	homocysteine-inducible, endoplasmic	Herpud1	UI-M-AK1-aey-e-10-0-UI.s1 NIH_BMAP_MHY_N Mus	**4.077 (3.629**

		reticulum stress-inducible, ubiquitin-like domain member 1		*musculus cDNA clone UI-M-AK1-aey-e-10-0-UI 3', mRNA sequence.*	**to 4.413)**
36	99033_at	inositol 1,3,4-triphosphate 5/6 kinase	Itpk1	UI-M-AK0-adc-g-01-0-UI.s1 NIH_BMAP_MHY Mus musculus cDNA clone UI-M-AK0-adc-g-01-0-UI 3', mRNA sequence.	**4.028 (2.806 to 4.865)**

Table 3.2. Genes down-regulated by glucocorticoids in presence of roscovitine.

	Probe set ID	Gene Title	Gene Symbol	Description	Fold change
1	102921_s_at	Fas (TNF receptor superfamily member)	Fas	NGF/TNF-receptor-related protein; Mus musculus Fas antigen mRNA, complete cds.	**0.251 (0.155 to 0.439)**
2	102282_g_at	CD antigen 27	Cd27	Mus musculus CD27 antigen (Cd27) mRNA.	**0.299 (0.186 to 0.499)**
3	92832_at	suppressor of cytokine signaling 1	Socs1	Mus musculus suppressor of cytokine signalling-1 (SOCS-1) mRNA, complete cds.	**0.327 (0.24 to 0.427)**
4	102940_at	lymphotoxin B	Ltb	bp 1-11 were derived from genomic sequence; Mus musculus lymphotoxin-beta mRNA, complete cds.	**0.334 (0.139 to 0.52)**
5	99027_at	Bcl2-like 1	Bcl2l1	Mus musculus Bcl-xL mRNA, complete cds.	**0.348 (0.271 to 0.456)**
6	93285_at	dual specificity phosphatase 6	Dusp6	UI-M-AQ1-adx-c-06-0-UI.s1 NIH_BMAP_MHI_N Mus musculus cDNA clone UI-M-AQ1-adx-c-06-0-UI 3', mRNA sequence.	**0.354 (0.335 to 0.365)**
7	102123_at	Lysosomal acid lipase 1	Lip1	M.musculus (C57 Black/6X CBA) LAL mRNA for lysosomal acid lipase.	**0.358 (0.343 to 0.384)**
8	100011_at	Kruppel-like factor 3 (basic)	Klf3	UI-M-BH0-ain-f-03-0-UI.s1 NIH_BMAP_M_S1 Mus musculus cDNA clone UI-M-BH0-ain-f-03-0-UI 3', mRNA sequence.	**0.372 (0.224 to 0.48)**
9	94835_f_at	tubulin, beta 2a	Tubb2a	beta-tubulin; Mouse beta-tubulin gene M-beta-2, 3' end.	**0.372 (0.316 to 0.406)**
10	94345_at	interleukin 6 signal transducer	Il6st	UI-M-AK1-aer-e-08-0-UI.s1 NIH_BMAP_MHY_N Mus musculus cDNA clone UI-M-AK1-aer-e-08-0-UI 3', mRNA sequence.	**0.393 (0.275 to 0.592)**
11	103259_at	growth factor independent 1	Gfi1	zinc finger protein; Mus musculus growth factor independence (Gfi1) mRNA, complete cds.	**0.395 (0.198 to 0.715)**
12	96865_at	myristoylated alanine rich protein kinase C substrate	Marcks	putative; Mouse myristoylated alanine-rich C-kinase substrate (MARCKS) mRNA, complete cds.	**0.408 (0.19 to 0.817)**
13	101014_at	interferon (alpha and beta) receptor 2	Ifnar2	M.musculus mRNA for type I interferon receptor, IFNaR2b.	**0.413 (0.223 to 0.573)**
14	95665_at	SEC14-like 1 (S. cerevisiae)	Sec14l1	UI-M-BH0-aja-g-04-0-UI.s1 NIH_BMAP_M_S1 Mus musculus cDNA clone UI-M-BH0-aja-g-04-0-UI 3', mRNA sequence.	**0.414 (0.297 to 0.56)**
15	104372_at	abhydrolase domain containing 8	Abhd8	UI-M-AP0-abg-e-08-0-UI.s2 NIH_BMAP_MST Mus musculus cDNA clone UI-M-AP0-abg-e-08-0-UI 3', mRNA sequence.	**0.434 (0.339 to 0.59)**
16	161788_f_at	endothelial differentiation sphingolipid G-protein-coupled receptor 1	Edg1	AV347228 RIKEN full-length enriched, adult male olfactory bulb Mus musculus cDNA clone 6430594J09 3', mRNA sequence.	**0.436 (0.362 to 0.493)**
17	160462_f_at	tubulin, beta 3	Tubb3	UI-M-BH1-ans-b-12-0-UI.s1 NIH_BMAP_M_S2 Mus musculus cDNA clone UI-M-BH1-ans-b-12-0-UI 3', mRNA sequence.	**0.438 (0.349 to 0.561)**
18	160829_at	pleckstrin homology-like domain, family A, member 1	Phlda1	Mus musculus TDAG51 (TDAG51) mRNA, complete cds.	**0.439 (0.35 to 0.581)**
19	96096_f_at	hydroxysteroid dehydrogenase like 2	Hsdl2	uk39c03.x1 Sugano mouse kidney mkia Mus musculus cDNA clone IMAGE:1971364 3' similar to SW:DHB4_HUMAN P51659 ESTRADIOL 17 BETA-DEHYDROGENASE 4 ;, mRNA sequence.	**0.439 (0.376 to 0.501)**
20	97497_at	Notch gene homolog 1 (Drosophila)	Notch1	homologue of Drosophila neurogenic gene Notch; M.musculus notch-1 mRNA.	**0.441 (0.391 to 0.488)**
21	103970_at	AT rich interactive domain 3B (Bright like)	Arid3b	Mus musculus bright and dead ringer gene product homologous protein Bdp mRNA, complete cds.	**0.442 (0.366 to 0.49)**
22	96623_at	UDP-glucose ceramide glucosyltransferase	Ugcg	UI-M-BH0-ajh-b-06-0-UI.s1 NIH_BMAP_M_S1 Mus musculus cDNA clone UI-M-BH0-ajh-b-06-0-UI 3', mRNA sequence.	**0.444 (0.357 to 0.514)**
23	AFFX-MurFAS_at	Fas (TNF receptor superfamily member)	Fas	NGF/TNF-receptor-related protein; Mus musculus Fas antigen mRNA, complete cds.	**0.446 (0.375 to 0.54)**
24	96752_at	intercellular adhesion molecule	Icam1	Mouse intercellular adhesion molecule 1 (ICAM-1) gene, exons 6 and 7 and complete cds.	**0.448 (0.228 to 0.596)**
25	103946_at	proline-serine-threonine phosphatase-interacting protein 1	Pstpip1	similar to S. pombe Cdc15p, a protein associated with formation of the cleavage furrow during cytokinesis; actin interacting protein with C-terminal SH3 domain; PSTPIP; Mus musculus PEST phosphatase interacting protein mRNA, complete cds.	**0.461 (0.268 to 0.645)**
26	102978_at	RIKEN cDNA A430104N18 gene	A430104N18Rik	ub02f03.r1 Soares_mammary_gland_NbMMG Mus musculus cDNA clone IMAGE:1365821 5', mRNA sequence.	**0.464 (0.34 to 0.561)**
27	104645_at	Kruppel-like factor 7 (ubiquitous)	Klf7	UI-M-BH0-ajq-d-05-0-UI.s1 NIH_BMAP_M_S1 Mus musculus cDNA clone UI-M-BH0-ajq-d-05-0-UI 3', mRNA sequence.	**0.469 (0.32 to 0.593)**
28	102711_at	regulator of G-protein signaling 14	Rgs14	Mus musculus rap1/rap2 interacting protein mRNA, complete cds.	**0.471 (0.361 to 0.646)**
29	102871_at	Eph receptor B6	Ephb6	putative; Mus musculus MEP mRNA, complete cds.	**0.48 (0.294 to 0.737)**
30	93372_at	acidic (leucine-rich) nuclear phosphoprotein 32 family, member A	Anp32a	LANP; PHAPI; I1-PP2A; Mus musculus acidic nuclear phosphoprotein pp32 mRNA, complete cds.	**0.485 (0.323 to 0.598)**
31	92653_at	RIKEN cDNA D530037H12 gene	D530037H12Rik	vg38e09.x1 Soares_mammary_gland_NbMMG Mus musculus cDNA clone IMAGE:863656 3', mRNA sequence.	**0.485 (0.409 to 0.53)**
32	162410_s_at	CD8 antigen, beta chain 1	Cd8b1	AV316162 RIKEN full-length enriched, adult male thymus Mus musculus cDNA clone 5830434K21 3' similar to M19504 Mouse T-cell differentiation antigen (Ly-3) mRNA, mRNA sequence.	**0.485 (0.424 to 0.581)**
33	160359_at	RIKEN cDNA 1190002H23 gene	1190002H23Rik	UI-M-BG1-aic-e-02-0-UI.s1 NIH_BMAP_MSC_N Mus musculus cDNA clone UI-M-BG1-aic-e-02-0-UI 3', mRNA sequence.	**0.494 (0.286 to 0.764)**
34	92564_at	leucine rich repeat (in FLII) interacting protein 1	Lrrfip1	ul59a06.x1 Sugano mouse kidney mkia Mus musculus cDNA clone IMAGE:2123314 3', mRNA sequence.	**0.494 (0.357 to 0.62)**

3.2.3. Identification of differentially expressed genes during antigen-mediated negative selection.

We have also used Affymetrix DNA microarrays to identify transcripts involved in regulating antigen-mediated negative selection. A transgenic *in vivo* model was used in which mice transgenic for a TCR (F5) were specifically exposed to the cognate antigen NP68 from the A/NT/60/68 human influenza virus nucleoprotein in the context of class I MHC. F5 is a T-cell receptor specific for the 9 amino acid peptide NP68 presented in the context of H-2Db (Murphy, Heimberger et al. 1990; Mamalaki, Norton et al. 1992; Mamalaki, Elliott et al. 1993; Liblau, Tisch et al. 1996; Townsend, Rothbard et al. 2006). Acute administration of antigenic peptide to these mice leads to deletion of almost all double-positive thymocytes within 4 days (Tarazona, Williams et al. 1998). These mice were also Rag-$1^{-/-}$ (Spanopoulou, Roman et al. 1994), precluding TCR rearrangement at the DN3 stage of T cell development and therefore endogenous canonical T cell development, and Tap-$1^{-/-}$ (Transporter associated with Antigen Processing) (Tourne, van Santen et al. 1996), precluding efficient complexing of antigenic peptide fragments into MHC major groove during protein synthesis by preventing peptide transfer from the cytosol to the endoplasmic reticulum (ER).

Thymocytes from F5 Rag-$1^{-/-}$ Tap-$1^{-/-}$ mice therefore only express the F5 TCR, and transgenic mice do not have mature T-cells. The lack of mature peripheral T cells ensures there will be no peripheral T cell activation, which would stimulate release of cytokines, in particular TNF-α. TNF-α would act upon cells in the thymus to cause apoptosis independent of antigen-mediated negative selection (Martin and Bevan 1997). Intraperitoneal (IP) injection of the NP68 peptide into F5 TCR Rag-$1^{-/-}$ Tap-$1^{-/-}$

mice leads to up-regulation of MHC class I on thymic stroma and negative selection of thymocytes. Therefore this transgenic model can only recognise one cognate antigen, to which it is not exposed under normal circumstances. IP injection of these transgenic mice with NP68 antigenic peptide leads to depletion and apoptosis of immature double-positive (DP) thymocytes due to peptide-specific recognition, a process which mimics the typical negative selection response (Tarazona, Williams et al. 1998).

6 x F5 TCR/Rag$^{-/-}$/Tap$^{-/-}$ transgenic mice were used for Affymetrix DNA microarray analysis, 3 IP injected with 1μM NP68, 3 with PBS vehicle control (**Figure 3.5A**). Injected mice were then left for 6 hours, after which all were sacrificed, and thymuses removed and lysed directly in Trizol. RNA was isolated and used for the multi-step synthesis of biotin-labelled cRNA, which was hybridized to Affymetrix MGu74a GeneChip® probe arrays. Quality control among samples was maintained by checks at relevant steps for integrity and concentration using an Agilent 2100 Bioanalyser (**Figure 3.5B**).

Primary data analysis was performed using Affymetrix Microarray Suite software Version 5, and normalisation carried out using Genespring 5.0. Each Affymetrix chip was normalised to the median of the triplicate and each gene normalised to the control sample, to allow for direct pairwise comparison of gene expression levels. Data was also filtered to only include genes that were detected as expressed in both control and test samples.

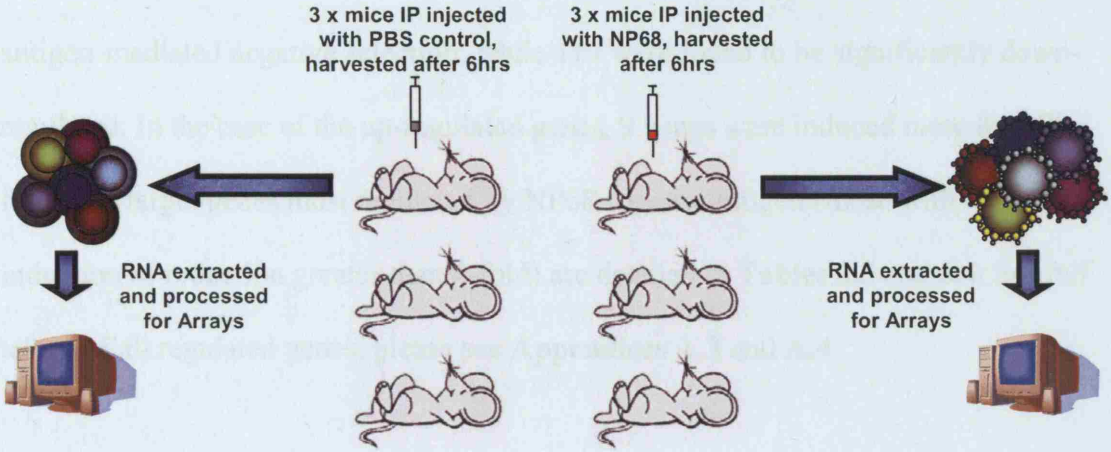

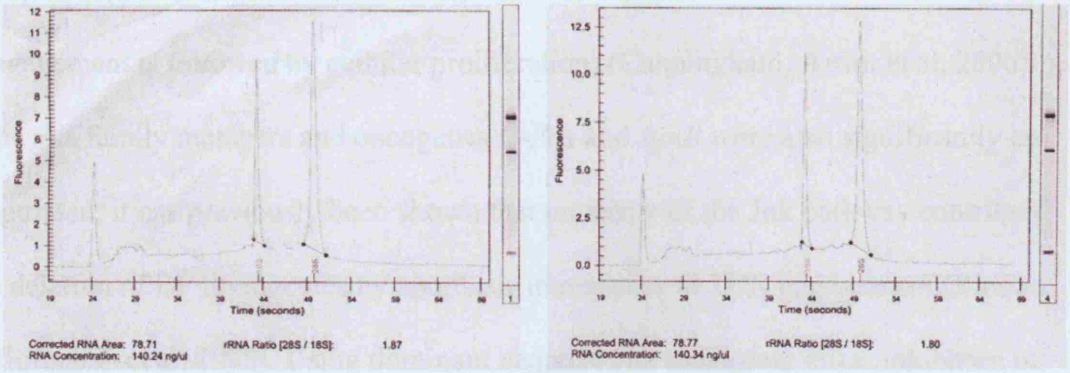

Figure 3.5. Experimental plan – antigen screen, and RNA integrity of samples extracted for antigen screen. (A) Diagram of Affymetrix GeneChip® probe array Analysis. 6 x F5 TCR Rag-$1^{-/-}$/Tap-$1^{-/-}$ transgenic mice were used, 3 IP injected with 1μM NP68, 3 with PBS vehicle control. Thymocytes were removed after 6 hours and RNA prepared for Affymetrix GeneChip® probe array analysis.**(B)** Agilent 2100 Bioanalyser plots of RNA extracted for Affymetrix GeneChip® probe array Analysis.

3.2.4 Transcripts regulated during antigen-mediated negative selection.

Following analysis 109 genes were found to be significantly up-regulated during antigen-mediated negative selection, while 119 were found to be significantly down-regulated. In the case of the up-regulated genes, 9 genes were induced more than 20-fold. The target genes most regulated by NP68 cognate antigen (those with an induction or reduction greater than 4-fold) are detailed in **Tables 3.3** and **3.4**. For full tables of all regulated genes, please see **Appendices A.3** and **A.4**.

One of the most up-regulated genes identified is *Nur77* (Nr4a1, the nuclear hormonal orphan steroid receptor), which is thought to be vital to TCR-mediated clonal deletion of immature DP thymocytes. It has been shown that immature thymocytes rapidly up-regulate nuclear Nur77 levels following TCR engagement, which is followed by apoptosis (unlike in mature SP T cells, where up-regulation of Nur77 following TCR engagement is followed by cellular proliferation) (Cunningham, Artim et al. 2006). The *Jnk* family members and oncogenes *C-Fos* and *JunB* were also significantly up-regulated; it has previously been shown that members of the Jnk pathway contribute to deletion of DP thymocytes by apoptosis in response to TCR engagement (Rincon, Whitmarsh et al. 1998). Using dominant negative *Jnk* transgenic mice, inhibition of the Jnk pathway was shown to reduce the *in vivo* deletion of DP thymocytes, and that this was in part mediated by the Map kinase Mkk7.

The two *Krox* family zinc finger transcription factors, Krox-20 and Krox-24 were also highly up-regulated during antigen-mediated negative selection in this study, 70-fold and 24-fold respectively. Krox-24 has been shown to have a role in positive selection, influencing the avidity thresholds required for thymocyte selection (Miyazaki and

Lemonnier 1998). Krox-24 has also been shown to be a downstream target of the Jnk pathway in other systems (Gururajan, Chui et al. 2005; Ke, Gururajan et al. 2006), and to interact at the protein level with another Affymetrix DNA microarray screen target C-Jun, part of the Jnk pathway (Levkovitz and Baraban 2002).

Krox20, *Nur77*, *cFos*, *Gadd45β* and *Bcl-2* have all been identified in a previous screen to characterise genes differentially regulated during negative selection (DeRyckere, Mann et al. 2003) using a similar *in vivo* model.

Table 3.3. Genes up-regulated by NP68 cognate antigen in F5 TCR Rag-1$^{-/-}$ Tap-1$^{-/-}$ transgenic mice.

	Probe set ID	Gene Title	Gene Symbol	Description	Fold change
1	101587_at	epoxide hydrolase 1, microsomal	Ephx1	Allele: b; Mus musculus microsomal expoxide hydrolase (Eph1) mRNA, allele b, complete cds.	80.2920413
2	102661_at	early growth response 2	Egr2	zinc finger protein A; zinc finger protein B; Mouse zinc finger protein (krox-20) gene, exon 2.	70.26385631
3	100962_at	Ngfi-A binding protein 2	Nab2	represses transcription mediated by NGFI-A/Egr-1 and Krox20; similar to NAB1 protein sequence; transcriptional co-repressor; Mus musculus NGFI-A binding protein 2 (NAB2) mRNA, complete cds.	55.7838096
4	102371_at	nuclear receptor subfamily 4, group A, member 1	Nr4a1	Mouse N10 gene for a nuclear hormonal binding receptor.	40.54992302
5	98579_at	early growth response 1	Egr1	Mus musculus zinc finger protein (Krox-24) gene, exon 2.	24.42272725
6	160901_at	FBJ osteosarcoma oncogene	Fos	Mouse c-fos oncogene.	24.05096348
7	103560_at	LysM, putative peptidoglycan-binding, domain containing 2	Lysmd2	UI-M-BH2.1-ape-d-04-0-UI.s1 NIH_BMAP_M_S3.1 Mus musculus cDNA clone UI-M-BH2.1-ape-d-04-0-UI 3', mRNA sequence.	23.879658
8	93637_at	CD5 antigen	Cd5	precursor; Mouse lymphocyte differentiation antigen Ly-1 mRNA, complete cds.	23.04372369
9	161666_f_at	growth arrest and DNA-damage-inducible 45 beta	Gadd45b	AV138783 Mus musculus C57BL/6J 10-11 day embryo Mus musculus cDNA clone 2810046L02, mRNA sequence.	22.73874092
10	98836_at	programmed cell death 1	Pdcd1	M.musculus PD-1 mRNA.	15.06922656
11	102209_at	nuclear factor of activated T-cells, cytoplasmic, calcineurin-dependent 1	Nfatc1	Mus musculus transcription factor NF-ATc isoform a (NF-ATca) mRNA, complete cds.	12.07189415
12	93915_at	POU domain, class 2, associating factor 1	Pou2af1	POU domain, class 2, associating factor 1	12.00437714
13	104445_at	RIKEN cDNA 4631408O11 gene	4631408O11Rik	UI-M-BH1-alm-d-07-0-UI.s1 NIH_BMAP_M_S2 Mus musculus cDNA clone UI-M-BH1-alm-d-07-0-UI 3', mRNA sequence.	11.33650486
14	95373_at	CD2 antigen	Cd2	precursor (-22 to -1); Murine mRNA for T11 protein.	10.74588323
15	95673_s_at	brain abundant, membrane attached signal protein 1	Basp1	UI-M-BH2.1-apr-b-09-0-UI.s1 NIH_BMAP_M_S3.1 Mus musculus cDNA clone UI-M-BH2.1-apr-b-09-0-UI 3', mRNA sequence.	10.5852837
16	93511_at	integral membrane protein 2A	Itm2a	putative; Mus musculus (E25) mRNA, complete cds.	9.868450032
17	92758_at	dual specificity phosphatase 2	Dusp2	Source: Mus musculus domesticus 129 tyrosine-threonine dual specificity phosphatase PAC-1 gene, complete cds.	7.881777013
18	92975_at	SH3-domain binding protein 2	Sh3bp2	PH domain, aa 25-133; SH2, aa 453-555; SH3 binding site, aa 201-210; putative; Mouse SH3 binding protein 3BP2 mRNA, complete cds.	7.675971445
19	98868_at	B-cell leukemia/lymphoma 2	Bcl2	bcl2-alpha; Mus musculus bcl-2 alpha gene, exon 2.	7.645360262
20	92534_at	GTP binding protein (gene overexpressed in skeletal muscle)	Gem	Mus musculus Gem GTPase (gem) mRNA, complete cds.	6.912092602
21	98282_at	inducible T-cell co-stimulator	Icos	Mus musculus mRNA for activation-inducible lymphocyte immunomediatory molecule AILIM, complete cds.	6.744154778
22	160629_at	regulator of G-protein signalling 10	Rgs10	UI-M-AI1-afr-f-03-0-UI.s1 NIH_BMAP_MBS_N Mus musculus cDNA clone UI-M-AI1-afr-f-03-0-UI 3', mRNA sequence.	6.63850231
23	102272_at	CD160 antigen	Cd160	similar to human natural killer cell BY55; Mus musculus natural killer cell BY55 precursor, mRNA, complete cds.	6.485392263
24	103629_g_at	lymphoid enhancer binding factor 1	Lef1	Mouse mRNA for LEF-1S, complete cds.	6.086040106
25	161765_f_at	regulator of G-protein signalling 10	Rgs10	AV335997 RIKEN full-length enriched, adult male medulla oblongata Mus musculus cDNA clone 6330579C12 3', mRNA sequence.	6.008065407
26	102362_i_at	Jun-B oncogene	Junb	Mus musculus transcription factor junB (junB) gene, 5' region and complete cds.	5.993565701
27	99109_at	immediate early response 2	Ier2	Mouse growth factor-inducible protein (pip92) mRNA, complete cds.	5.834417906
28	96596_at	N-myc downstream regulated gene 1	Ndrg1	differentially repressed by testosterone and dihydrotestosterone; Mus musculus TDD5 mRNA, complete cds.	5.778821475
29	99916_at	protein kinase C, eta	Prkch	Mouse mRNA for nPKC-eta.	5.368793767
30	94278_at	lymphocyte cytosolic protein 1	Lcp1	Mouse mRNA for 65-kDa macrophage cytosolic protein, complete cds.	5.289561186
31	160464_s_at	N-myc downstream regulated-like	Ndrl	Mus musculus cytoplasmic protein Ndr1 (Ndr1) mRNA, complete cds.	5.239062162
32	93869_s_at	B-cell leukemia/lymphoma 2 related protein A1a	Bcl2a1a	Mus musculus hematopoietic-specific early-response A1-d protein (A1d) gene, exon 2, and complete cds.	4.933908757
33	97834_g_at	phosphofructokinase, platelet	Pfkp	UI-M-BH0-ajg-h-01-0-UI.s1 NIH_BMAP_M_S1 Mus musculus cDNA clone UI-M-BH0-ajg-h-01-0-UI 3', mRNA sequence.	4.838037598
34	98869_g_at	B-cell leukemia/lymphoma 2	Bcl2	bcl2-alpha; Mus musculus bcl-2 alpha gene, exon 2.	4.734601164
35	97796_at	cofactor required for Sp1 transcriptional activation, subunit 2	Crsp2	similar to human EXLM1 gene; Mus musculus gene, complete cds, similar to EXLM1.	4.684658746
36	95733_at	solute carrier family 29 (nucleoside transporters), member 1	Slc29a1	UI-M-AO0-aby-a-05-0-UI.s1 NIH_BMAP_MPG Mus musculus cDNA clone UI-M-AO0-aby-a-05-0-UI 3', mRNA sequence.	4.453102386
37	97833_at	phosphofructokinase, platelet	Pfkp	UI-M-BH0-ajg-h-01-0-UI.s1 NIH_BMAP_M_S1 Mus musculus cDNA clone UI-M-BH0-ajg-h-01-0-UI 3', mRNA sequence.	4.426045673
38	92203_s_at	CD6 antigen	Cd6	Mus musculus T cell surface glycoprotein CD6 mRNA, complete cds.	4.299402604
39	92204_at	CD6 antigen	Cd6	Mus musculus mscd6 precursor (Cd6) mRNA, complete cds.	4.15336851
40	95102_at	scotin gene	Scotin	UI-M-BH2.1-apm-a-08-0-UI.s1 NIH_BMAP_M_S3.1 Mus musculus cDNA clone UI-M-BH2.1-apm-a-08-0-UI 3', mRNA sequence.	4.070119685

Table 3.4. Genes down-regulated by NP68 cognate antigen in F5 TCR Rag-1$^{-/-}$ Tap-1$^{-/-}$ transgenic mice.

	Probe set ID	Gene Title	Gene Symbol	Description	Fold change
1	93683_at	recombination activating gene 1	Rag1	recombination activating protein; Mouse recombination activating protein (Rag-1) mRNA, complete cds.	0.027494432
2	101163_at	recombination activating gene 2	Rag2	Mus musculus Rag-2 protein (Rag-2) mRNA, complete cds.	0.037772925
3	102397_at	core-binding factor, runt domain, alpha subunit 2, translocated to, 3 homolog (human)	Cbfa2t3h	Mus musculus ETO/MTG8-related protein ETO-2 mRNA, complete cds.	0.074067808
4	102692_s_at	histocompatibility 2, T region locus 18	H2-T18	Mouse mRNA for TL antigen, complete cds.	0.07890813
5	98354_at	pre T-cell antigen receptor alpha	Ptcra	aa 31 (Cys) potentially involved in intramolecular disulphide linkage; aa 91 (Cys) potentially involved in intramolecular disulphide linkage; aa 139 (Cys) potentially involved in intermolecular disulphide linkage to TCR-beta chain; aa 51-54 and aa 101-104 are potential N-linked glycosylation sites; Mus musculus pre-T cell receptor alpha-type chain precursor mRNA, complete cds.	0.08392641
6	162206_f_at	suppressor of cytokine signaling 3	Socs3	AV374868 RIKEN full-length enriched, adult male cecum Mus musculus cDNA clone 9130017A09 3' similar to U88328 Mus musculus suppressor of cytokine signalling-3 (SOCS-3) mRNA, mRNA sequence.	0.10155657
7	94246_at	E26 avian leukemia oncogene 2, 3' domain	Ets2	ets2 protein; Mouse erythroblastosis virus oncogene homolog 2 (ets-2) mRNA, complete cds.	0.102001658
8	93484_at	GRAM domain containing 3	Gramd3	UI-M-BH1-anw-d-01-0-UI.s1 NIH_BMAP_M_S2 Mus musculus cDNA clone UI-M-BH1-anw-d-01-0-UI 3', mRNA sequence.	0.135329021
9	162410_s_at	CD8 antigen, beta chain 1	Cd8b1	AV316162 RIKEN full-length enriched, adult male thymus Mus musculus cDNA clone 5830434K21 3' similar to M19504 Mouse T-cell differentiation antigen (Ly-3) mRNA, mRNA sequence.	0.139364259
10	101699_at	per-hexamer repeat gene 2	Phxr2	ORF (AA 1 - 65); Mouse period repetitive mRNA (lambda Sp28).	0.150353036
11	101470_at	WD repeat domain 78	Wdr78	UI-M-BH0-ajv-c-08-0-UI.s1 NIH_BMAP_M_S1 Mus musculus cDNA clone UI-M-BH0-ajv-c-08-0-UI 3', mRNA sequence.	0.151335149
12	99637_at	procollagen, type XV	Col15a1	Mus musculus type XV collagen mRNA, complete cds.	0.153905569
13	96712_at	SPARC related modular calcium binding 1	Smoc1	UI-M-AP1-agf-d-04-0-UI.s2 NIH_BMAP_MST_N Mus musculus cDNA clone UI-M-AP1-agf-d-04-0-UI 3', mRNA sequence.	0.156445029
14	92185_at	ADP-ribosylation factor-like 4C	Arl4c	UI-M-AP1-agl-g-02-0-UI.s1 NIH_BMAP_MST_N Mus musculus cDNA clone UI-M-AP1-agl-g-02-0-UI 3', mRNA sequence.	0.184044267
15	103961_s_at	deoxynucleotidyltransferase, terminal	Dntt	M.musculus mRNA for terminal deoxynucleotidyltransferase.	0.195832833
16	104014_at	hemochromatosis	Hfe	Hemochromatosis	0.197097651
17	102203_at	placental protein 11 related	Pp11r	Mus musculus T cell-specific protein (Tcl-30) mRNA, complete cds.	0.203079235
18	160413_at	neuron specific gene family member 2	Nsg2	Mus musculus p19 mRNA, complete cds.	0.2064935
19	161409_f_at	deoxynucleotidyltransferase, terminal	Dntt	AV312871 RIKEN full-length enriched, adult male thymus Mus musculus cDNA clone 5830406G23 3' similar to X68670 M.musculus mRNA for terminal deoxynucleotidyltransferase, mRNA sequence.	0.209585376
20	103971_at	purinergic receptor P2X, ligand-gated ion channel, 1	P2rx1	M.musculus mRNA for ATP receptor.	0.210824922
21	104745_at	ADP-ribosylation factor-like 6 interacting protein 2	Arl6ip2	vv48a12.r1 Soares_thymus_2NbMT Mus musculus cDNA clone IMAGE:1225630 5', mRNA sequence.	0.222616078
22	103480_at	CD4 antigen	Cd4	precursor; brain allele; Mouse T-cell differentiation antigen CD4 (L3T4) gene, exons 8-10.	0.226386483
23	99813_g_at	calpain 3	Capn3	M.musculus mRNA for skeletal muscle-specific calpain.	0.228542925
24	94977_at	inositol 1,4,5-triphosphate receptor 1	Itpr1	P400 protein; Mouse cerebellum mRNA for P400 protein.	0.23407998
25	92472_f_at	schlafen 2	Slfn2	mSLFN2; Mus musculus schlafen2 (Slfn2) mRNA, complete cds.	0.23537603
26	101410_at	claudin 4	Cldn4	Mus musculus mCPE-R mRNA for CPE-receptor, complete cds.	0.236887513
27	100928_at	fibulin 2	Fbln2	M.musculus mRNA for fibulin-2.	0.241046237

3.2.5. Validation of Affymetrix GeneChip® probe array data – glucocorticoid screen.

To confirm potential candidates identified from this Affymetrix DNA microarray screen and exclude false positives, real-time semi-quantitative PCR (qPCR) was performed for a selected sample of 10 up-regulated genes. These targets were selected on the basis of biological function, greatest up-regulation and a relevant biological role, with particular relevance given to those published to have an apoptosis-related phenotype. *Tdag8*, *Fkbp51* and *Mspp1* are previously implicated targets of GCs (Cifone, Migliorati et al. 1999; Lepine, Lakatos et al. 2004; Malone, Wang et al. 2004). *muPAR1* and *Pip49* have apoptosis related phenotypes (Samir, Ropolo et al. 2000; Crippa 2007). *Fgfr1(L)* and *Tnfaip8* interact with the GC target NF-κB (Byrd, Ballard et al. 1999; You, Ouyang et al. 2001), *E4bp4* possesses a GRE (Wallace, Wheeler et al. 1997), while *Agp/Ebp* and *Lisch7* are highly regulated.

In an independent experiment, triplicate samples of thymocytes were harvested and treated with or without DEX, in the presence of ROSC for 4 hours, in identical conditions as for the Affymetrix DNA microarray screen. Each triplicate was isolated in an independent experiment and qPCR performed in triplicate, with results quantified using the ΔΔCT method of absolute quantitation. Of 10 transcripts tested (Tdag8, E4bp4/Nfil3, Fgfr1(L), Tnfaip8, Mspp1, Pip49, MuPar1, Agp/Ebp, Fkbp51, Lisch7), 9 were found to be significantly up-regulated by real-time qPCR after 4 hours (**Figure 3.6A and B**).

(A)

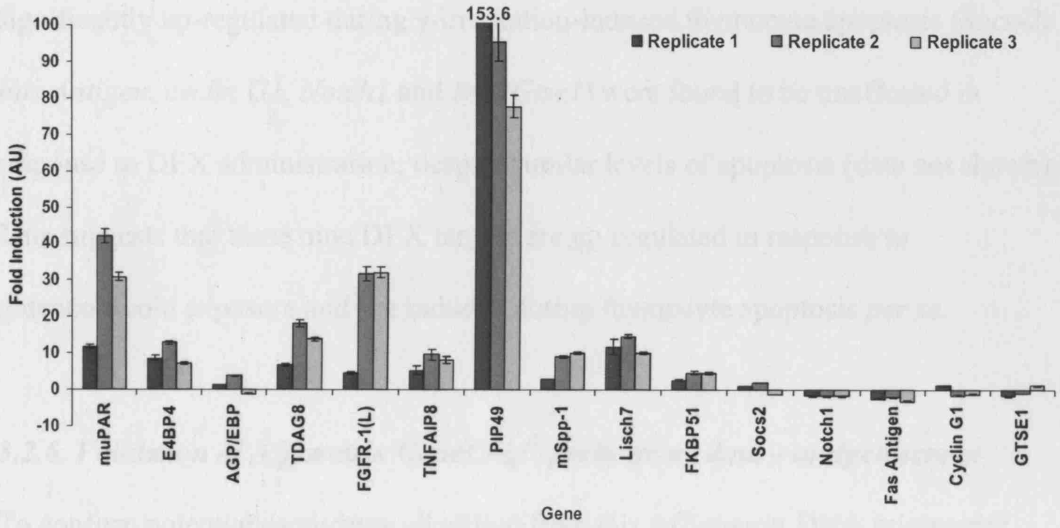

(B) Table 3.5.

Gene	Accession	Affymetrix GeneChip® probe array Fold change	Average real-time qPCR fold change	Confirmed Target?
Mupar1	X62700	24.7	28.2	Yes
E4bp4	U83148	21.2	9.5	Yes
Agp/Ebp	M61007	18.2	1.3	No
Tdag8	U39827	16.6	12.9	Yes
Fgfr1(L)	U22324	14.2	22.7	Yes
Tnfaip8	AI839109	8.0	5.2	Yes
Pip49	AI841484	7.2	153.6	Yes
Mspp1	AI835784	6.9	7.4	Yes
Lisch7	U49507	6.0	12.2	Yes
Fkbp51	U16959	4.1	4.0	Yes

Figure 3.6. qPCR of target genes – glucocorticoid screen. (A) Real-time qPCR of genes as indicated, indicating fold-change versus control. Error bars represent triplicates, fold-change ± upper/lower confidence limits, n=3 **(B)** Table of target genes showing both Affymetrix GeneChip® probe array and real-time qPCR fold changes.

The level of up-regulation for these target genes parallels that seen in Affymetrix DNA microarray analysis, with isolated examples of variation e.g. Pip49 levels of up-regulation from real-time qPCR are considerably greater than those seen in DNA microarray analysis. Five target genes identified from a parallel screen for genes significantly up-regulated during γ-irradiation-induced thymocyte apoptosis (*Socs-2*, *Fas Antigen*, *cyclin G1*, *Notch1* and *B99/Gtse1*) were found to be unaffected in response to DEX administration, despite similar levels of apoptosis (data not shown). This suggests that these nine DEX targets are up-regulated in response to glucocorticoid exposure and not induced during thymocyte apoptosis *per se*.

3.2.6. Validation of Affymetrix GeneChip® probe array data – antigen screen

To confirm potential candidates identified from this Affymetrix DNA microarray screen and exclude false positives, real-time semi-quantitative PCR (qPCR) was again performed for a selected sample of 10 up-regulated genes. These targets were again selected on the basis of biological function, greatest up-regulation and a relevant biological role, with particular relevance given to those published to have an apoptosis-related phenotype. *Nur77*, *c-Fos*, *Jun-B*, *Bcl-2*, *Nfat-cA*, *Pd-1* and *Lef-1* have all been implicated in negative selection or apoptosis (Ishida, Agata et al. 1992; Calnan, Szychowski et al. 1995; Wisniewska, Stanczyk et al. 1997; Rincon, Whitmarsh et al. 1998; Williams, Norton et al. 1998; Ioannidis, Beermann et al. 2001; Cunningham, Artim et al. 2006), while *Krox20*, *Krox24*, *Nab2* and *Nfat-cA* are both highly regulated and interact in related signalling pathways.

(A)

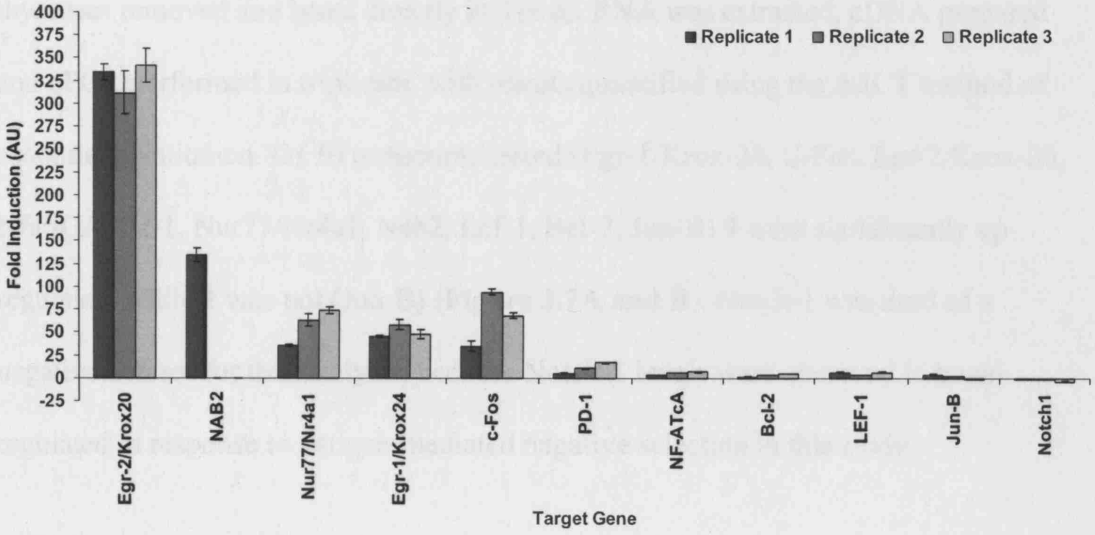

(B) Table 3.6.

Gene	Accession	Affymetrix GeneChip® probe array Fold change	Average real-time qPCR fold change	Confirmed Target?
Egr-2/Krox-20	M24377	70.3	329.1	Yes
Nab2	U47543	55.8	134.4	Yes
Nur77/Nr4a1	X16995	40.6	57.3	Yes
Egr-1/Krox-24	M28845	24.4	50.4	Yes
C-Fos	V00727	24.1	65.3	Yes
PD-1	X67914	15.1	10.9	Yes
Nfat-CA	AF087434	12.1	5.5	Yes
Bcl-2	L31532	7.6	3.0	Yes
Lef-1	D16503	6.1	5.5	Yes
Jun-B	U20735	6.0	1.7	No

Figure 3.7. qPCR of target genes – antigen screen. (A) Real-time qPCR of genes as indicated, indicating fold-change versus control. Error bars represent triplicates, fold-change ± upper/lower confidence limits, n=3 **(B)** Table of target genes showing both Affymetrix GeneChip® probe array and real-time qPCR fold changes.

In an independent experiment, 6 x F5 TCR/Rag$^{-/-}$/Tap$^{-/-}$ transgenic mice were used for real-time qPCR analysis; 3 IP injected with 1μM NP68, 3 with PBS vehicle control. Injected mice were then left for 6 hours, after which all were sacrificed, their thymuses removed and lysed directly in Trizol. RNA was extracted, cDNA prepared and qPCR performed in triplicate, with results quantified using the ΔΔCT method of absolute quantitation. Of 10 transcripts tested (Egr-1/Krox-24, C-Fos, Egr-2/Krox-20, Nfat-CA, Pd-1, Nur77/Nr4a1, Nab2, Lef-1, Bcl-2, Jun-B) 9 were significantly up-regulated, while 1 was not (Jun-B) (**Figure 3.7A and B**). Notch-1 was used as a negative control for this analysis, because Notch-1 levels were observed to be un-regulated in response to antigen-mediated negative selection in this study.

3.3. Discussion.

3.3.1. Identification of novel transcripts regulating glucocorticoid-induced thymocyte apoptosis.

GC-induced thymocyte apoptosis is transcriptionally dependent, and is blocked by both RNA and protein synthesis inhibitors (Wyllie, Morris et al. 1984). Therefore GC-induced cell death requires the synthesis of new RNA transcripts. Previous studies have implicated various signalling pathways that contribute to GC-induced apoptosis. Glucocorticoids trigger thymocyte apoptosis by increasing Cdk2 kinase activity (Hakem, Sasaki et al. 1999), and up-regulating the expression and altering the distribution of pro-apoptotic Bcl-2 family members (Brady, Gil-Gomez et al. 1996; Brady, Salomons et al. 1996; Gil-Gomez, Berns et al. 1998). However the initial targets of GR activation and nuclear translocation are still largely undetermined.

This study aims to identify candidate targets of GR translocation upstream of Cdk2 activation. Previously identified transcriptional targets of GR activation common to our screen include *Tdag8* (Tosa, Murakami et al. 2003; Malone, Wang et al. 2004), *Fkbp51* (Malone, Wang et al. 2004), *Tnfaip3/A20* (DeRyckere, Mann et al. 2003), *Dig2* (Wang, Malone et al. 2003) and *Bim* (Wang, Malone et al. 2003; Malone, Wang et al. 2004). The difference in the methodology of our screen to previous studies is the use of the Cdk2 inhibitor ROSC to block thymocyte apoptosis at the stage of Cdk2 activation, blocking effects downstream of Cdk2. Our use of ROSC identified both differences and similarities in the genes shown to be regulated. Most strikingly, both *E4bp4* and *Tnfaip8*, two of the most highly up-regulated genes identified in our DNA microarray screen, were absent from data published in previous studies.

E4bp4(nfil3) was initially identified as an adenovirus E4 promoter-binding protein and as a transcriptional activator of the human interleukin-3 promoter in T-cells (Cowell and Hurst 1994; Zhang, Zhang et al. 1995). E4bp4 is a widely expressed transcriptional repressor, and expression has previously been shown to be induced by GCs in ID13 murine fibroblasts (Wallace, Wheeler et al. 1997). E4bp4 has also been shown to possess a glucocorticoid-response-element (GRE) element in its promoter (Wallace, Wheeler et al. 1997), and recently demonstrated to protect motor neurons against apoptosis induced by removal of neurotrophic factors (Junghans, Chauvet et al. 2004)

Tnfaip8 (also termed *SCC-S2*, *NDED*, *Gg2-1*) is a novel death-effector-domain containing protein (198aa) identified by several differential display screens identifying genes induced by TNF-α (Kumar, Whiteside et al. 2000). In their system,

Tnfaip8 is induced by NF-κB and acts to protect against TNF-induced apoptosis. This was potentially interesting because of the apparent cross-talk evident between the glucocorticoid and TNF-induced apoptotic pathways, most specifically TNF-α priming of the GR (Costas, Trapp et al. 1996; Arzt, Kovalovsky et al. 2000; Refojo, Liberman et al. 2003). The GR and NF-κB signalling pathways are typically mutually antagonistic (Scheinman, Gualberto et al. 1995). There is no published data on the role of Tnfaip8 in thymocyte apoptosis or development. Fibroblast growth factors (FGFs, our target FGFR1 (L)) are heparin-binding proteins crucial to wound-healing, embryogenesis and angiogenesis. FGF-1 induces nuclear translocation of NF-κB binding proteins in Jurkat T cells, and this is enhanced in combination with TCR signalling (Byrd, Ballard et al. 1999). In our screen, *Ffgfr1(L)* was one of the most up-regulated genes, and may indicate the cross-talk between the GR, TCR and NF-κB signalling pathways.

Mspp1 (sphingosine-1-phosphate phosphohydrolase) is an enzymatic intermediate of the ceramide pathway, one of the earliest physiologically detectable consequences of GC administration. Increases in cellular ceramide levels can be detected within 5 minutes of GC signalling (Cifone, Migliorati et al. 1999; Lepine, Lakatos et al. 2004). Ceramide generation precedes GC/GR induced transcription and peptide synthesis, and is not blocked by cycloheximide or actinomycin D (Cifone, Migliorati et al. 1999). Ceramide is rapidly converted to sphingosine, the apoptotic mediator that contributes to GC-induced apoptosis in thymocytes. Mspp1 is the enzyme that converts sphingosine-1-phosphate (S1P, the inactive form) to sphingosine (SP, the active form). Additionally, exogenous S1P inhibits GC-induced thymocyte apoptosis.

Similar to Tdag8 and Bim^{EL}, this suggests a role for Mspp1 in the GC-induced apoptotic pathway (Lepine, Lakatos et al. 2004).

Identification of panels of 301 and 54 potential target genes, and confirming a selection by real-time qPCR provided a set of targets for functional validation. Initially a cut-off was set at 4-fold induction, and study was made of any previously published data on potential targets that might be suggestive of a role in thymocyte apoptosis, as outlined in section **3.2.5**. In this way, the following genes were selected for further functional analysis.

Table 3.7. Final target list – glucocorticoid screen.

Genes	Description/Function	Accession
E4bp4	NFIL3/E4BP4 transcriptional repressor	U83148
Tdag8	T-cell death associated gene 8; G-protein coupled receptor	U39827
Fgfr1(L)	Fibroblast growth factor receptor-1, long isoform	U22324
Tnfaip8	TNF-α induced protein 8	AI839109
Dig2	Dexamethasone-induced-gene 2	AI849939
Pip49	Pancreatitis-induced-protein 49	AI841484
Mspp1	Sphingosine-1-phosphate phosphatase	AI835784
Lrg-47	G-protein-like LRG-47, related to GTP-binding proteins	U19119
Lisch7	Liver-specific Lisch7 gene	U49507
Bim^{EL}	Bcl-2 Interacting Mediator of Cell Death	AF032459
Fkbp51	FKBP51, T-cell specific immunophilin that inhibits calcineurin	U16959
Tnfaip3(A20)	A20 zinc finger protein	U19463

3.3.2. Identification of novel transcripts regulating antigen-mediated negative selection.

Many of the signalling pathways that govern TCR-mediated apoptosis and selection have already been elucidated. Roles for the most proximal TCR signalling components, including the Fyn (p59Fyn) and Lck (p56Lck) SRC-family signalling kinases have been shown in both positive and negative selection (van Oers, Lowin-Kropf et al. 1996; Zamoyska, Basson et al. 2003). The pathways controlling the more distal signalling components are differentially required for positive and negative

selection. The Erk-MapK pathway is required for positive selection (Sugawara, Moriguchi et al. 1998), but is dispensable for negative selection, while the Jnk, p38 Mapk and Mek-(Erk) signalling pathways are required for negative selection (Rincon, Whitmarsh et al. 1998; Bommhardt, Scheuring et al. 2000). These signalling pathways converge on the nucleus where some of the proteins crucial to negative selection have so far been identified. *Nur77*, one of the most up-regulated genes in our DNA microarray screen, and member of the orphan steroid receptor family of ligand-dependent transcription factors, has been shown to be highly induced by TCR-mediated apoptosis. Disruption of Nur77 activity by antisense RNA or a dominant-negative form abrogates antigen-mediated apoptosis both *in vivo* (Liu, Smith et al. 1994; Woronicz, Calnan et al. 1994) and *in vitro* (Calnan, Szychowski et al. 1995; Zhou, Cheng et al. 1996). Nur77 is a transcription factor, but the DNA binding and transcriptional activation domains are not required for its apoptotic function. In response to TCR signalling, Nur77 is relocalised from the nucleus to the outer mitochondrial membrane where it causes cytochrome c release and membrane depolarisation (Li, Kolluri et al. 2000). Nur77 is up-regulated more than 40-fold in our DNA microarray screen for genes up-regulated during antigen-mediated apoptosis.

Krox-20 (Egr-2) and *Krox-24 (Egr-1)* genes express zinc finger transcription factors characterised by rapid and transient up-regulation to cellular stresses. In our DNA microarray screen, Krox-20 and Krox-24 were induced 70-fold and 24-fold respectively. Krox-24/Egr-1 has been shown to both influence avidity thresholds in positive selection, as stated previously, and affect positive selection by up-regulating ID3 and Bcl-2 (Miyazaki and Lemonnier 1998; Bettini, Xi et al. 2002). Egr-1 over-

expression in Egr-1/TCR H-Y double-transgenic mice permitted positive selection of thymocytes despite TCR-MHC interactions of extremely low avidity, but not when TCR-MHC interactions were absent. Increased numbers of self-reactive thymocytes were also positively selected in *Egr-1* transgenic mice, causing a significant increase in reactivity against self-MHC molecules. Krox-24 (and other *Egr* family members) has also previously been shown to be important in the DN to DP transition, with over-expression able to bypass defects in pre-TCR signalling that would otherwise prevent DP T cell formation (Carleton, Haks et al. 2002). The role of Krox-24 in positive selection in CD8 SP cell differentiation has also been investigated (Basson, Wilson et al. 2000).

The specific transcriptional co-repressor of Egr proteins, *Nab2*, was also highly induced in our DNA microarray screen (55-fold), suggestive of a feedback loop similar to that shown between Egr-1, p53 and p73 (Yu, Baron et al. 2007). *Nfat-CA*, another highly induced gene, has also been shown to form heterodimers with EGR proteins to regulate expression of proinflammatory cytokines IL-2 and TNFα, specifically in response to antigenic stimulation (Denny, Patai et al. 2000; Decker, Nehmann et al. 2003). This indicates several associated genes induced in conditions of negative selection.

Our DNA microarray screen identified an 8-fold induction in levels of Bcl-2. Over-expression of Bcl-2 in FTOC (Williams, Norton et al. 1998) and a transgenic mouse model (Strasser, Harris et al. 1994) inhibits negative selection, so induction upon TCR engagement might be suggestive of a feedback mechanism, which might parallel up-regulation both of Egr transcription factors and the functional co-repressor Nab2. Bcl-

2 up-regulation is however not a causal event in positive selection (Williams, Mok et al. 2001).

The down-regulation of several identified genes in our DNA microarray screen is indicative of negative selection. Both Rag-1 and Rag-2 proteins and the pre T-cell antigen receptor alpha (pTCRα) are significantly reduced in agreement with previous studies (Groves, Parsons et al. 1997), as are both CD4 and CD8α, which at the protein level is an early indicator of negative selection in transgenic models (Tarazona, Williams et al. 1998).

Our antigenic DNA microarray screen identified 109 potential up-regulated target genes, and a selection confirmed by real-time qPCR identified targets for functional validation. Initially a cut-off was again set at 4-fold induction, and study was made of any previously published data on potential targets that might be suggestive of a role in thymocyte apoptosis, as detailed above in section **3.2.6**. The following genes were selected for functional screening.

Table 3.8. Final target list – antigen screen.

Genes	Description/Function	Accession
Krox-20	Early growth response gene 2	M24377
Nab2	Ngfi-A binding protein 2	U47543
Nur77	Mouse N10 gene for a nuclear hormonal binding receptor.	X16995
Krox-24	Early growth response gene 1	M28845
C-Fos	FBJ osteosarcoma oncogene	V00727
PD-1	Programmed cell death 1 gene	X67914
Nfat-c	Mus musculus transcription factor NF-ATc isoform a (NF-ATca)	AF087434
E25	putative; Mus musculus (E25) mRNA	L38971
Bcl-2	Anti-apoptotic member of Bcl-2 family	L31532
Lef-1	LEF-1S	D16503

3.3.3. Identification of potentially interesting genes induced in both Affymetrix GeneChip® probe array screens.

Upon initial examination, there were no candidate genes common to both DNA microarray screens, most likely due to initial differences in the mechanism by which GC-induced and antigen-mediated thymocyte apoptotic signals are propagated by the target cell. However Bim^{EL}, a known target and effector in antigen-mediated negative selection and apoptosis (Bouillet, Purton et al. 2002) was also up-regulated in our glucocorticoid DNA microarray screen, and indicates the importance of the *Bcl-2* family members in the apoptotic response to both stimuli.

3.3.4. Further work.

Functional investigation of the candidate genes generated by the two DNA microarray studies was subsequently undertaken. Affymetrix DNA microarray targets, confirmed by real-time qPCR analysis, provided panels of suitable candidate genes. Relevant open reading frames pertaining to each candidate gene were cloned into pMSCV-based retroviral expression vectors. Transcriptional targets were then investigated to determine if they had functional phenotypes if over-expressed, or latterly knocked down, in foetal thymic organ culture (FTOC) and OP9-DL1 co-culture.

In this way any potential role of these candidate genes in thymocyte apoptosis might be elucidated.

CHAPTER 4

RESULTS (2)

4.1. Background.

4.1.1.Introduction.

In Chapter 3, two Affymetrix GeneChip® probe array screens were discussed in which candidate genes in GC-induced apoptosis and antigen-mediated negative selection were identified. DNA microarray targets were confirmed as regulated by qPCR. In this chapter the GC-induced candidates were investigated functionally to determine if any had a role in GC-induced apoptosis by using the FTOC and OP9-DL1 systems for generating DP thymocytes *in vitro*.

FTOC is the principal system for recapitulating thymocyte development *in vitro*, enabling thymocyte development from thymic progenitors to mature T cells. Combining this with retroviral infection of the haematopoietic progenitor cells (HPCs) used to reconstitute depleted FTOCs enabled study of the effect of candidate gene over-expression on thymocyte development and apoptosis. The OP9-DL1 co-culture system was also used to investigate the effect upon apoptosis of target gene over-expression, without the effect of apoptotic cell clearance by phagocytosis that is evident in FTOC. RNAi-mediated knockdown of candidates was used to determine if knockdown of targets produced the opposite phenotype to over-expression.

4.1.2. Foetal thymic organ culture (FTOC).

The thymus provides a specialised microenvironment for thymocyte development, providing both the necessary three-dimensional architecture, and the essential complex interactions required between developing thymocytes and cells of the thymic stroma (Anderson, Moore et al. 1996). Duplicating this process *in vitro* requires the use of specialised culture techniques, including both FTOC (foetal thymic organ

culture) and RTOC (reaggregate thymic organ culture) (Ceredig, Jenkinson et al. 1982; Jenkinson and Owen 1990; Hare, Jenkinson et al. 1999).

FTOC involves the removal of the intact foetal thymus from the top of the murine chest cavity, typically at day 15 of murine gestation, for culture *in vitro*. This provides an experimental system in which the both the normal *in vivo* thymic architecture, and the process of T cell development, is maintained. Thymocyte development in FTOC is comparative in both manner and kinetics to *in vivo* thymocyte development (Zhang, Gong et al. 2007). *In vivo*, the developing foetal thymus is colonised by haematopoietic stem cells (HSCs) at approximately 10-11 days of gestation (Owen and Ritter 1969). *In vitro*, the depleted FTOC was repopulated with HPCs 5 days after removal from E15 embryos.

For FTOC, explanted lobes can either be analysed as discrete organs with their endogenous thymocyte populations, or depleted of developing thymocytes using the selective toxicity of 2-deoxyguanosine, which acts specifically upon rapidly dividing cells . After 4-7 days 2-deoxyguanosine treatment, alymphoid, depleted FTOC lobes can be recolonised with haematopoietic progenitor cells (HPCs) or other thymic precursors (Kingston, Jenkinson et al. 1985). These precursor cells will then commit to, and develop along the T cell lineage. A powerful modification that we utilised is the use of bicistronic retroviral vectors to infect HPCs prior to recolonisation in FTOC (Hare, Jenkinson et al. 1999), enabling over-expression of target genes, reporter constructs, or knockdown microRNAs. A combined approach using retrovirally infected HPCs recolonised into depleted thymic lobes, therefore permitting normal thymocyte development against a backdrop of target gene-reporter construct over-

expression or target gene knockdown, enabled investigation of the effect of these target genes on T cell development and apoptosis.

The FTOC/retrovirus system was used to functionally validate targets isolated by our microarray screens. Initially, the bicistronic murine stem cell virus (pMSCV) retroviral system (Clontech) was modified to express reporter genes instead of antibiotic resistance genes (which would prove useless in FTOC studies, as although transduced target cells would become antibiotic-resistant following infection, the thymic lobe itself would remain susceptible) (Miller and Rosman 1989; Grez, Akgun et al. 1990; Hawley, Lieu et al. 1994). Analogous to the previously published pMIG (pMSCV-IRES-EGFP) retroviral vector (Persons, Allay et al. 1997; Morrow, Horton et al. 2004), a modified pMSCV-IRES-hCD2-'tailless' retroviral vector was constructed, which expresses as a reporter gene a truncated form of the human CD2 (hCD2) protein, lacking the cytoplasmic signalling domain but retaining the transmembrane domain (Melton, Sarner et al. 1996), under the control of an internal ribosome entry site (IRES) (Deftos, He et al. 1998). This enabled the infection efficiency of the integrated retrovirus to be determined using an anti-human CD2 antibody, which importantly does not cross-react with murine CD2.

pMSCV retroviral vectors are bicistronic, and express both target genes cloned into the multiple cloning site (MCS) and the hCD2 cDNA from the same RNA transcript, with expression driven by the 5' modified PCC4-cell-passaged myeloproliferative sarcoma virus (PCMV) long terminal repeat (LTR) promoter region (Grez, Akgun et al. 1990). Expression of the bicistronic transcript is driven from the MSCV viral 5' LTR promoter, described to be resistant to epigenetic silencing (Persons, Allay et al.

1997; Dickins, Hemann et al. 2005), a factor of vital importance in maintaining expression in stem cell populations. Expression of hCD2 detected on the cell surface by flow cytometry directly indicates target gene expression. To facilitate cloning, linker constructs providing an MCS were also added, into which target gene cDNAs amplified by PCR were cloned. cDNAs were epitope-tagged if possible with HA or MYC epitopes by secondary rounds of PCR. pMSCV-IRES-hCD2-'tailless' retroviral vectors constructed are detailed in **Figure 4.1**. A diagram of the FTOC/retrovirus protocol is shown in **Figure 4.2**.

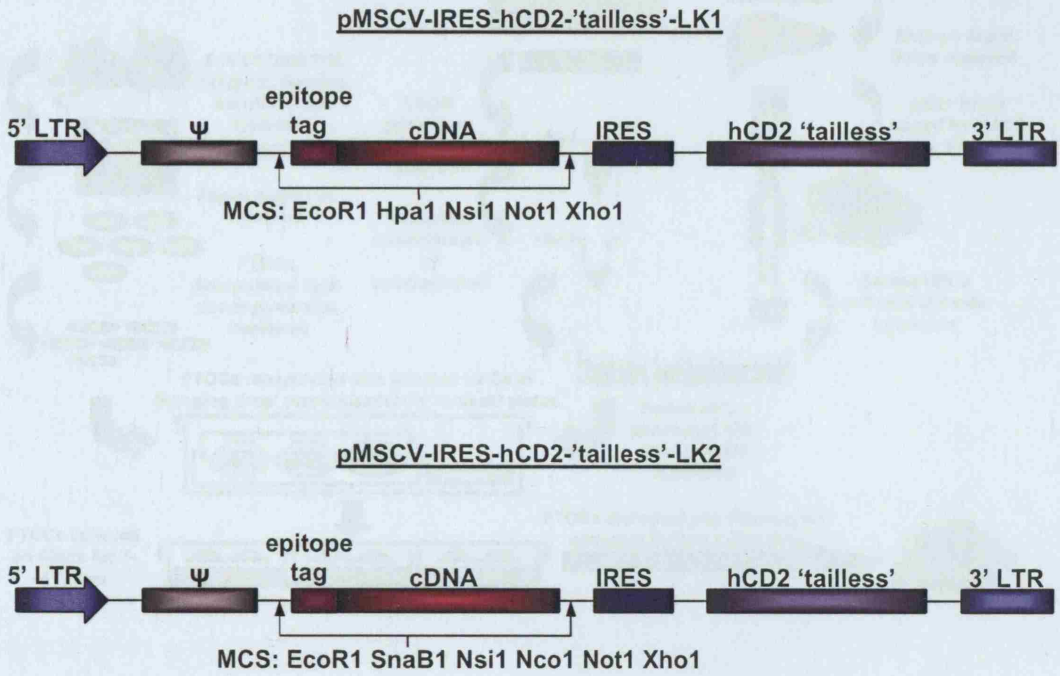

Figure 4.1. pMSCV-IRES-hCD2-'tailless' constructs used to transduce primary HPCs. cDNAs for functional validation were cloned into pZERO-1 for sequencing and sub-cloned into pMSCV-based retroviral vectors for expression. 5' and 3' LTR, long terminal repeat, also MSCV viral promoter. Ψ^+, viral packaging signal. MCS, multiple cloning site with restriction enzyme sites. IRES, internal ribosome entry site. hCD2, truncated human CD2 cDNA.

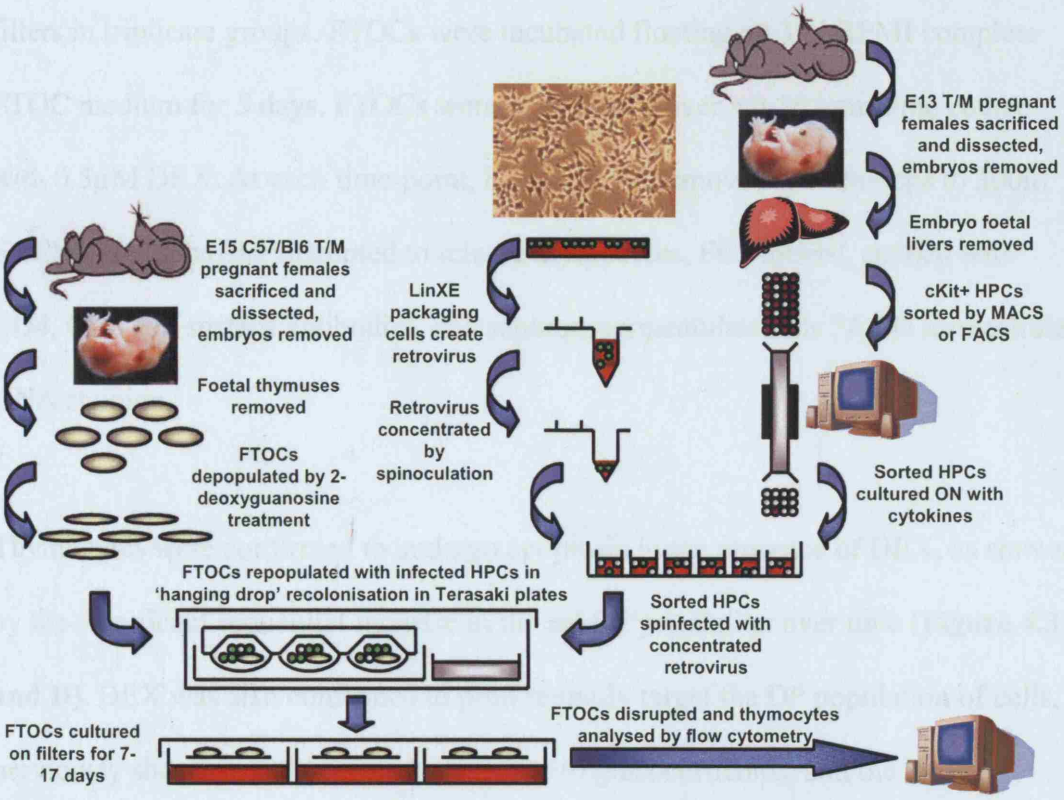

Figure 4.2. FTOC/retrovirus experimental strategy used to transduce primary HPCs and repopulate depleted FTOCs. cKit$^+$ HPCs obtained by MACS from E12 or E13 time-mated embryos are retrovirally infected with pMSCV retroviral vectors, used to repopulate 2-deoxyguanosine-depleted FTOCs, and cultured to produce DP T cells.

4.2. Results.

4.2.1. FTOCs are sensitive to glucocorticoid treatment in vitro.

To establish the sensitivity of FTOCs to DEX, whole thymuses were removed from time-mated (Harlan) C57/BL6 pregnant female mice and individual thymic lobes placed on to autoclaved Whatman Nuclepore Track-Etch Polycarbonate Membrane filters in triplicate groups. FTOCs were incubated floating on 3ml RPMI complete FTOC medium for 5 days. FTOCs were then treated over a 0-10 hour time course with 0.5μM DEX. At each time-point, FTOCs were removed with forceps to 300μl FACS staining buffer, disrupted to release thymocytes, FC blocked, stained with CD4, CD8 cell surface antibodies, and saponin-permeabilised for 7AAD intracellular DNA staining.

Thymocytes were confirmed to undergo apoptosis in the presence of DEX, as shown by the significant sequential increase in the subG1 population over time (**Figure 4.3A and D**). DEX was also confirmed to preferentially target the DP population of cells, previously shown to be exquisitely sensitive to glucocorticoids, and the most apoptotically sensitive of four thymocyte sub-populations (DN, DP, CD4 SP and CD8 SP) (**Figure 4.3A and C**) (Wiegers, Knoflach et al. 2001; Berki, Palinkas et al. 2002). A parallel experiment, again performed on whole FTOCs in triplicate groups, demonstrated that 0.5μM DEX sufficiently saturates the glucocorticoid receptor and induces a maximal apoptotic response (Wyllie, Morris et al. 1984) (**Figure 4.3E**).

(A)

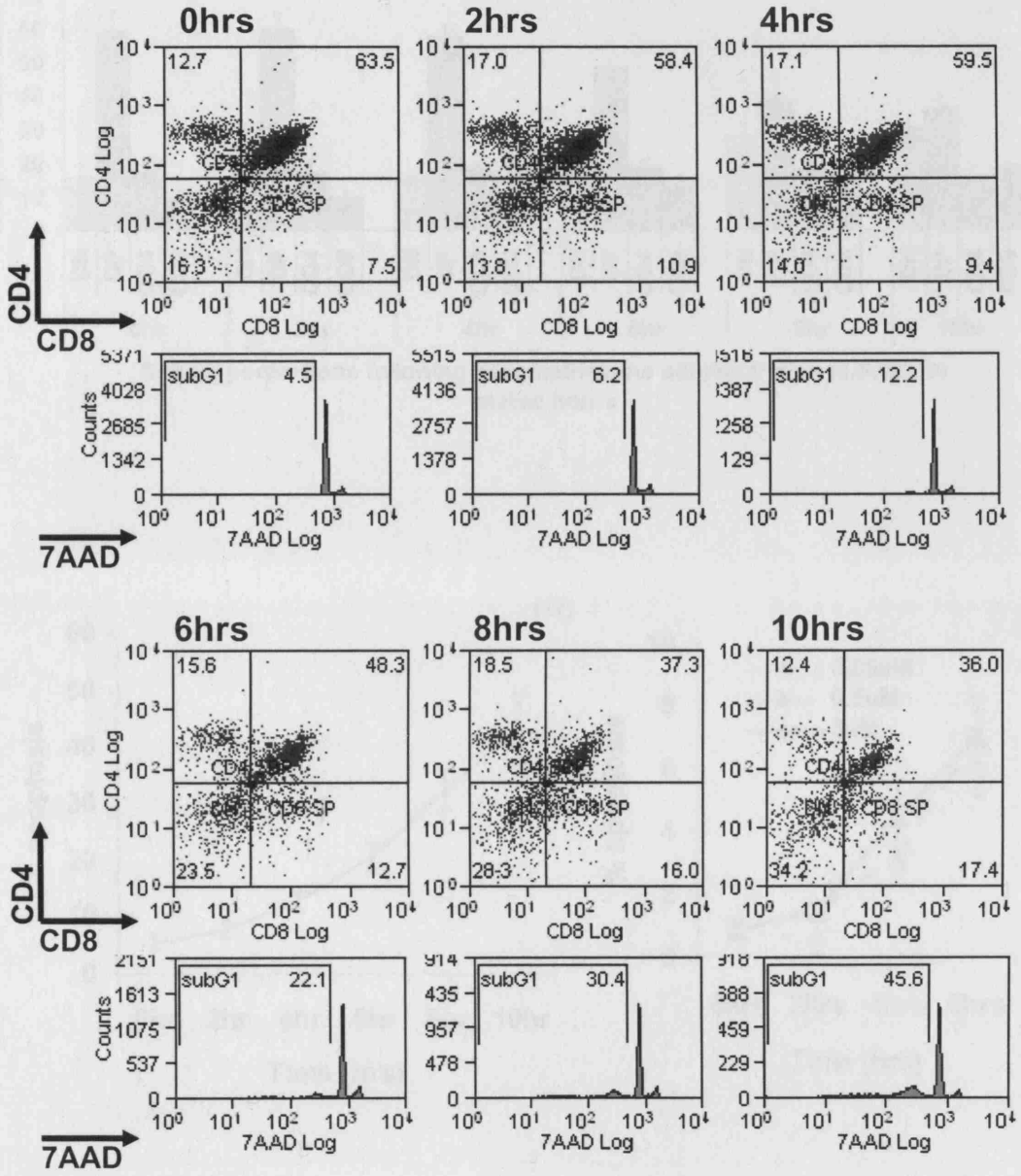

Figure 4.3A. FTOC thymocytes are sensitive to glucocorticoid treatment *in vitro*. **(A)** Flow cytometric (FC) analysis of FTOCs treated with 0.5μM DEX for stated hours, stained for CD4 and CD8, and saponin-permeabilised and intracellular-stained for DNA content

(B)

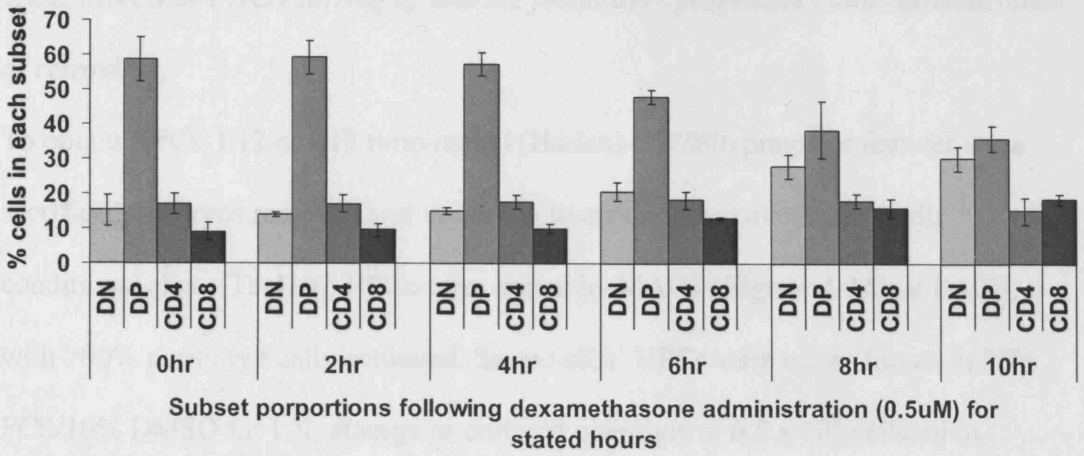

(D)

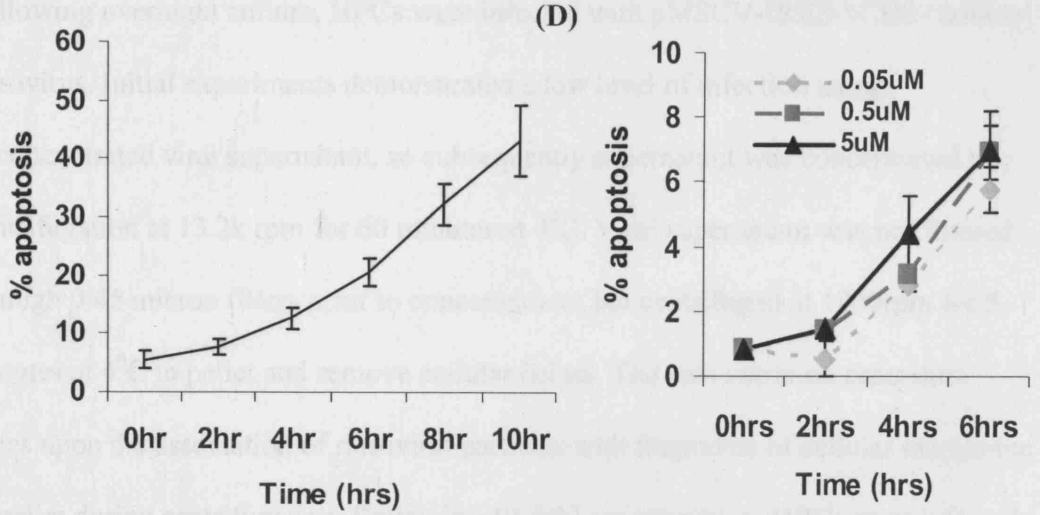

Figure 4.3B,C,D. FTOC thymocytes are sensitive to glucocorticoid treatment *in vitro*. **(B)** Graph of subset proportions within FTOCs treated with 0.5μM DEX. **(D)** Graph of apoptosis within FTOCs treated with 0.5μM DEX. **(E)** Dose dependence graph of FTOCs treated with 0.05μM, 0.5μM, and 5μM DEX.

4.2.2. MACS or FACS sorting of murine foetal liver progenitors and concentration of retrovirus.

To obtain HPCs, E12 or E13 time-mated (Harlan) C57/Bl6 pregnant females were sacrificed, embryos removed and the foetal livers dissected out under sterile conditions. $cKit^+$ ($Ter119^-$) HPCs were sorted by MACS (**Figure 4.4A**) or FACS, with >90% purity typically achieved. Sorted $cKit^+$ HPCs were either frozen in 90% FCS/10% DMSO for LN_2 storage or cultured overnight at 0.5 x 10^6 cells/ml in complete FTOC medium with SCF, IL-7, IL-6, and IL-3.

Following overnight culture, HPCs were infected with pMSCV-IRES-hCD2-'tailless' retrovirus. Initial experiments demonstrated a low level of infection using unconcentrated viral supernatant, so subsequently supernatant was concentrated by centrifugation at 13.2k rpm for 60 minutes at 4^0C. Viral supernatant was not filtered through 0.45 micron filters prior to concentration, but centrifuged at 1200rpm for 5 minutes at 4^0C to pellet and remove cellular debris. The concentration procedure relies upon the association of retroviral particles with fragments of cellular membrane to pellet during centrifugation. Following 10-fold concentration, HPCs were infected by spinoculation, which acts to increase the number of retroviral particles that bind to target cell surface as much as 40-fold (O'Doherty, Swiggard et al. 2000), with addition of polybrene (Manning, Hackett et al. 1971) (**Figure 4.4B**). Concentrated pMSCV retrovirus demonstrated an infection efficiency of as high as 90% upon freshly sorted cells, approximately 50% upon frozen and thawed HPCs.

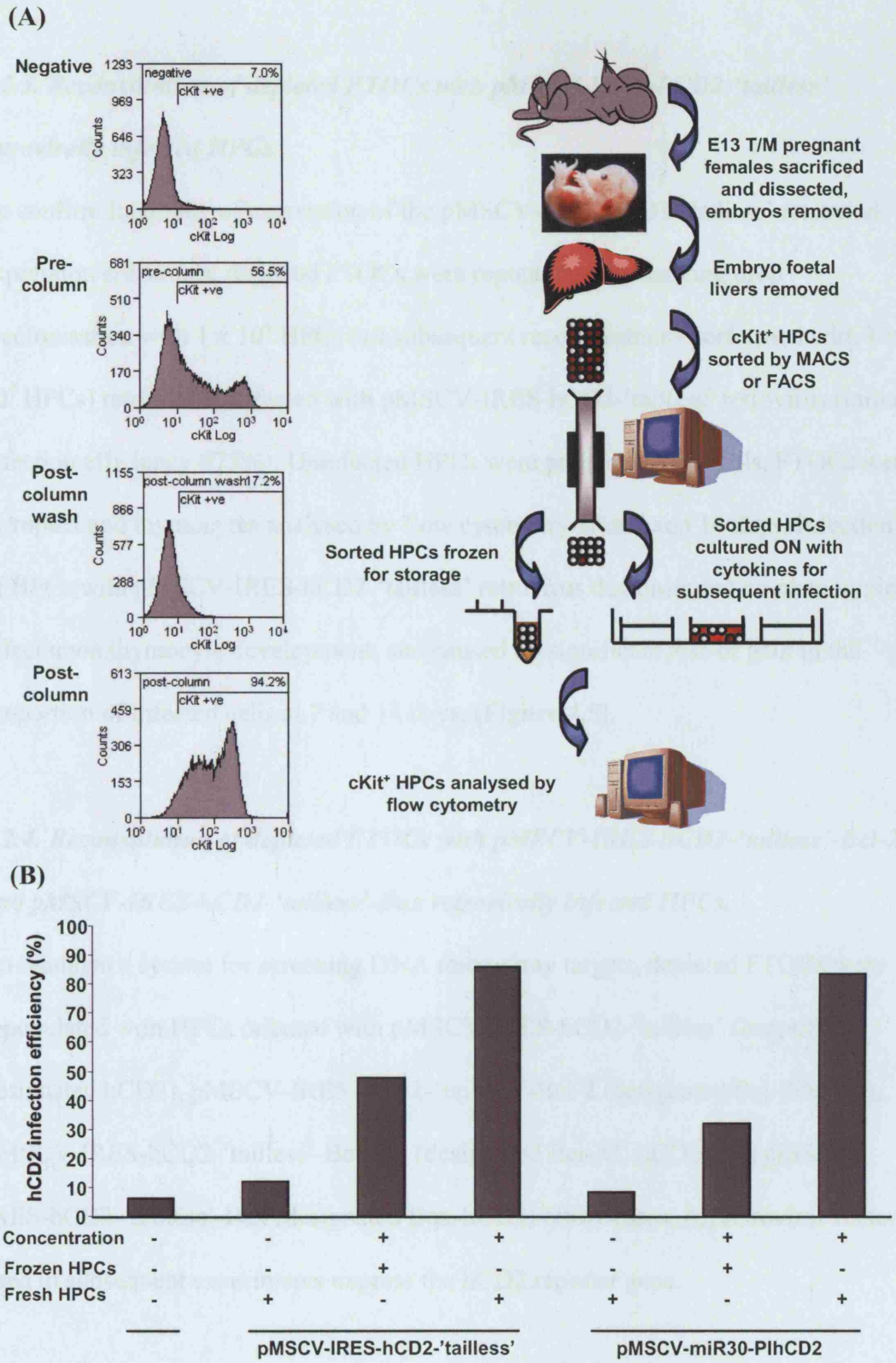

Figure 4.4. MACS sorting and infection of cKit$^+$ haematopoietic progenitor cells. **(A)** Diagram of MACS sorting protocol. Flow cytometric analysis of HPCs during MACS sort, showing samples stained with anti-CD117 (cKit) 2B8 biotin-conjugated antibody, secondary streptavidin-PE **(B)** Graph of FC analysis of infection efficiency of pMSCV-IRES-hCD2-'tailless' and pMSCV-miR30-PIhCD2 retroviral vectors upon isolated HPCs, with unconcentrated and concentrated retrovirus.

4.2.3. Reconstitution of depleted FTOCs with pMSCV-IRES-hCD2-'tailless' retrovirally infected HPCs.

To confirm longevity of expression of the pMSCV-IRES-hCD2-'tailless' retroviral expression constructs, depleted FTOCs were repopulated by hanging drop recolonisation with 1 x 10^4 HPCs (all subsequent recolonisations performed with 1 x 10^4 HPCs) retrovirally infected with pMSCV-IRES-hCD2-'tailless' retrovirus (initial infection efficiency ≈75%). Uninfected HPCs were prepared as controls. FTOCs were disrupted and thymocytes analysed by flow cytometry after 7 and 14 days. Infection of HPCs with pMSCV-IRES-hCD2-'tailless' retrovirus demonstrated no phenotypic effect upon thymocyte development, and caused no significant loss or gain in the proportion of infected cells at 7 and 14 days. (**Figure 4.5**).

4.2.4. Reconstitution of depleted FTOCs with pMSCV-IRES-hCD2-'tailless'-Bcl-2 and pMSCV-IRES-hCD2-'tailless'-Bax retrovirally infected HPCs.

To establish a system for screening DNA microarray targets, depleted FTOCs were repopulated with HPCs infected with pMSCV-IRES-hCD2-'tailless' (hereafter designated hCD2), pMSCV-IRES-hCD2-'tailless'-Bcl-2 (designated Bcl-2-hCD2), pMSCV-IRES-hCD2-'tailless'-Bcl-XL (designated Bcl-XL-hCD2) and pMSCV-IRES-hCD2-'tailless'-Bax (designated Bax-hCD2) retroviruses. All retroviral vectors used in subsequent experiments express the hCD2 reporter gene.

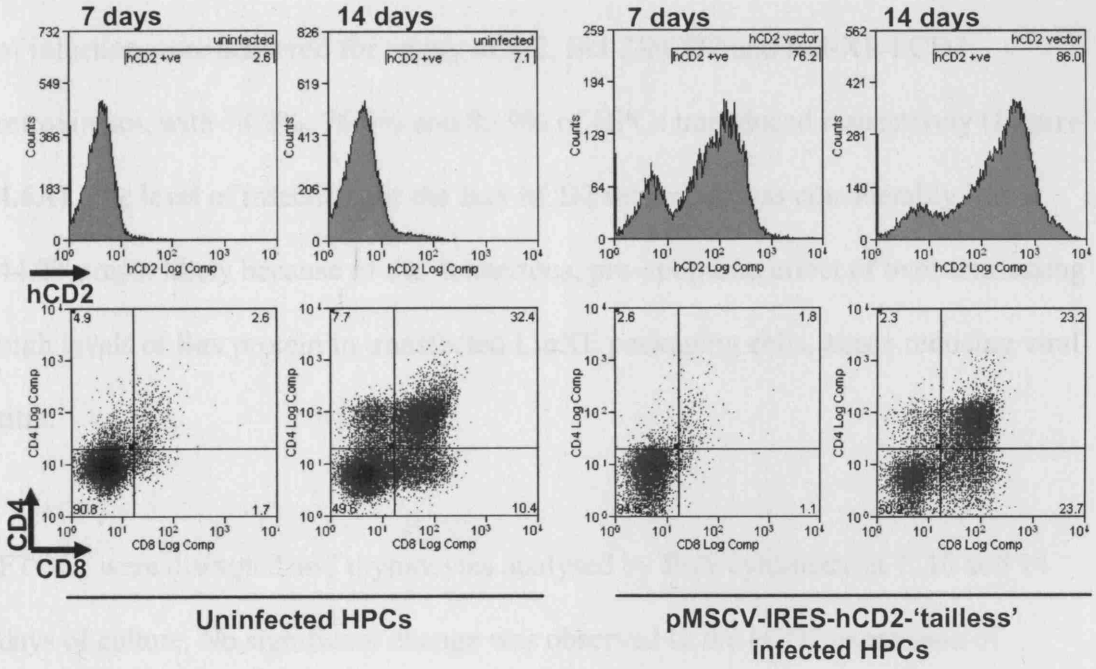

Figure 4.5. Time course of pMSCV-IRES-hCD2-'tailless' retrovirally infected HPCs differentiating in FTOCs. (A) Flow cytometric analysis of uninfected and pMSCV-IRES-hCD2-'tailless' infected FTOCs 7 and 14 days after plating onto filters.

It has previously been established that over-expression of anti-apoptotic Bcl-2 is protective against glucocorticoid-induced thymocyte apoptosis (Strasser, Harris et al. 1991; McColl, He et al. 1998), while over-expression of Bax sensitizes thymocytes to apoptotic stimuli (Gil-Gomez, Berns et al. 1998). Bcl-2-hCD2, Bcl-XL-hCD2 and Bax-hCD2 retroviruses were chosen as pro-apoptotic and anti-apoptotic controls.

To determine the infection efficiency of the retroviral constructs, the level of hCD2 expression was determined by flow cytometry 48 hours after infection (24 hours after hanging drop recolonisation, same day as FTOCs transferred to filters). Similar levels of infection were achieved for empty hCD2, Bcl-2-hCD2 and Bcl-XL-hCD2 retroviruses, with 74.9%, 76.9% and 85.9% of HPCs transduced respectively (**Figure 4.6A**). The level of infection for the Bax-hCD2 retrovirus was considerably less at 44.2%, most likely because of the deleterious, pro-apoptotic effect of over-expressing high levels of Bax protein in transfected LinXE packaging cells, hence reducing viral titre.

FTOCs were disrupted and thymocytes analysed by flow cytometry at 7, 10 and 14 days of culture. No significant change was observed in the hCD2 expression of developing thymocytes transduced with hCD2 retrovirus at 7, 10 and 14 days (**Figure 4.6B**). HPCs transduced by the Bcl-XL-hCD2 and Bcl-2-hCD2 retroviruses demonstrated successive enrichment in hCD2 expressing cells at 7, 10 and 14 days, while Bax-hCD2 infected HPCs showed a significant loss in hCD2 expressing cells.

FTOCs reconstituted with hCD2, Bcl-2-hCD2 and Bax-hCD2 cells were also analysed for their sensitivity to DEX. Groups of FTOCs were treated ± 0.5μM DEX

for four hours. FTOCs were assayed for apoptosis by subG1 DNA quantification. Bcl-2-hCD2 FTOCs proved almost completely resistant to DEX treatment, while Bax-hCD2 FTOCs showed a marked enhancement in apoptosis compared to vector control (**Figure 4.6C**). Infection efficiency in these apoptosis experiments was sufficiently high to preclude analysing uninfected cells in hCD2 and Bcl-2-hCD2 FTOCs as too few cells were present to generate representative DNA profiles.

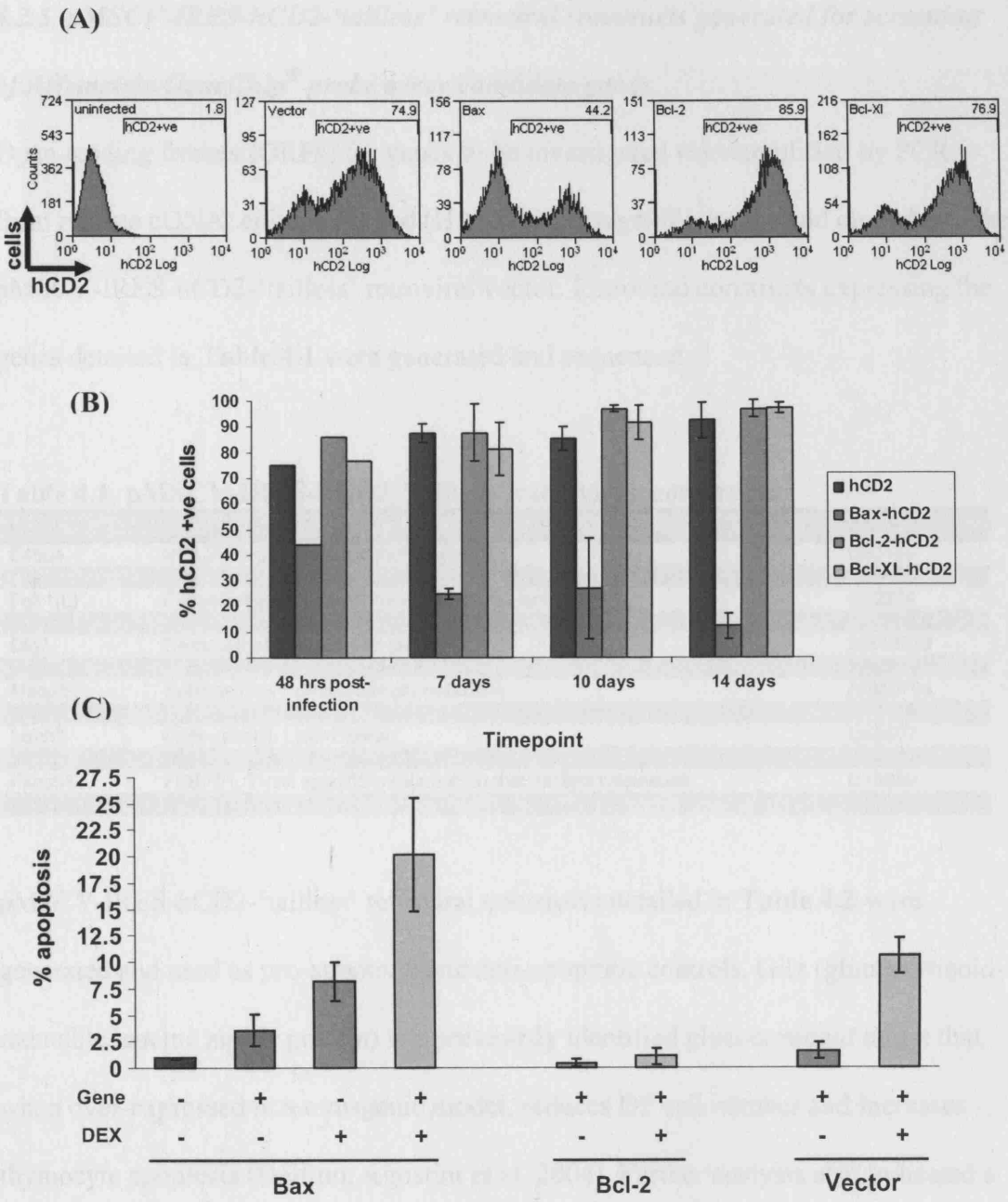

Figure 4.6. FTOCs repopulated with Bcl-2-hCD2, Bcl-XL-hCD2 and Bax-hCD2 retrovirally infected HPCs. (A) Flow cytometric analysis of HPCs used to repopulate FTOCs, stained for hCD2, 48 hours post infection. **(B)** Graph of hCD2 status determined by flow cytometry, of hCD2, Bax-hCD2, Bcl-2-hCD2 and Bcl-XL-hCD2 FTOCs 7, 10, and 14 days after plating. Mean ± S.D., n=3. Representative expt, n=3 **(C)** Graph of apoptosis in 13 day reconstituted FTOCs treated ± 0.5μM DEX for 4 hrs. Mean ± S.D., n=5. Representative expt, n=3.

4.2.5. pMSCV-IRES-hCD2-'tailless' retroviral constructs generated for screening of Affymetrix GeneChip® probe array candidate genes.

Open reading frames (ORFs) for genes to be investigated were amplified by PCR from murine cDNA, epitope-tagged (HA and Myc tags) if possible and cloned into the pMSCV-IRES-hCD2-'tailless' retroviral vector. Retroviral constructs expressing the genes detailed in **Table 4.1** were generated and sequenced.

Table 4.1. pMSCV-IRES-hCD2-'tailless' retroviral constructs.

cDNA	Description/Function	Accession
E4bp4	NFIL3/E4bp4 transcriptional repressor	U83148
Tdag8	T-cell death associated gene 8; G-protein coupled receptor	U39827
Fgfr1(L)	Fibroblast growth factor receptor-1, long isoform	U22324
Tnfaip8	TNF-α induced protein 8	AI839109
Dig2	Dexamethasone-induced-gene 2	AI849939
Pip49	Pancreatitis-induced-protein 49	AI841484
Mspp1	Sphingosine-1-phosphate phosphatase	AI835784
Lrg-47	G-protein-like LRG-47, related to GTP-binding proteins	U19119
Lisch7	Liver-specific Lisch7 gene	U49507
Bim^{EL}	Bcl-2 Interacting Mediator of Cell Death	AF032459
Fkbp51	FKBP51, T-cell specific immunophilin that inhibits calcineurin	U16959
Tnfaip3(A20)	A20 zinc finger protein	U19463

pMSCV-IRES-hCD2-'tailless' retroviral constructs detailed in **Table 4.2** were generated and used as pro-apoptotic and anti-apoptotic controls. Gilz (glucocorticoid-inducible leucine zipper protein) is a previously identified glucocorticoid target that, when over-expressed in a transgenic model, reduces DP cell number and increases thymocyte apoptosis (Delfino, Agostini et al. 2004). Further analysis also indicated a reduction in Bcl-XL expression and increased activation of caspase-3 and caspase-8.

Table 4.2. pMSCV-IRES-hCD2-'tailless' retroviral control constructs.

Controls	Description/Function	Accession
Bcl-2	B-cell leukemia/lymphoma 2	NM_009741
Bax	Bcl2-associated X protein	NM_007527
BIM^{EL}	Bcl-2 Interacting Mediator of Cell Death	AF032459
Bcl-XL	Bcl2-like 1	NM_009743
GILZ	Glucocorticoid-induced leucine zipper protein	AF024519

4.2.6. Screening of target genes in FTOCs.

Candidate genes were screened in FTOC. HPCs were infected with retrovirus expressing target genes and then used to repopulate depleted FTOCs in hanging drop recolonisations. FTOCs were then cultured for 13 days to determine the effect of target gene over-expression upon thymocyte development and apoptosis. hCD2, Bax-hCD2, Bcl-2-hCD2, and Bcl-XL-hCD2 FTOCs were used as controls.

Only the target genes *Tdag8*, *Tnfaip8*, *Tnfaip3(A20)* and *E4bp4* were confirmed to impose a net negative survival effect upon infected cells in FTOC, and that over-expression of these genes during thymocyte development within the competitive FTOC microenvironment appeared to be deleterious and potentially pro-apoptotic. These target genes were studied in further detail in the following sections.

4.2.7. Expression of specific target genes in HPC reconstituted FTOCs profoundly affects cell survival.

Several candidate genes (*tdag8*, *tnfaip8*, *tnfaip3(A20)* and *e4bp4*) were confirmed to affect the survival of developing thymocytes in FTOC. These target genes were investigated for their effect upon cell survival as pooled FTOCs over a series of experiments. FTOCs were prepared as pools (groups of FTOCs on filters, $n \geq 3$) over 6 experiments. Tdag8-hCD2, Tnfaip8-hCD2, Tnfaip3(A20)-hCD2, E4bp4-hCD2 and Mspp1-hCD2 FTOCs were included as target genes, and Bax-hCD2, Bcl-2-hCD2 and hCD2 as controls.

Tdag8-hCD2, Tnfaip8-hCD2 and E4bp4-hCD2 FTOCs showed a significant loss in $hCD2^+$ infected cells over 13 days FTOC. Tdag8-hCD2, Tnfaip8-hCD2 and E4bp4-hCD2 FTOCs also demonstrated a non-significant further loss in $hCD2^+$ infected cells specifically in DP cells (**Figure 4.7A**). As expected, Bcl-2-hCD2 FTOCS showed an enrichment in $hCD2^+$ infected cells during culture, increasing from an initial infection efficiency of 93% to 99.6% in 13-day DP cells, while Bax-hCD2 FTOCs showed a significant loss similar to the confirmed apoptotic targets.

hCD2 FTOCs demonstrated no significant change, as did Mspp1-hCD2 FTOCs. Tnfaip3(A20)-hCD2 FTOCs produced almost no infected cells following FTOC, suggesting as before a Tnfaip3(A20)-induced developmental block.

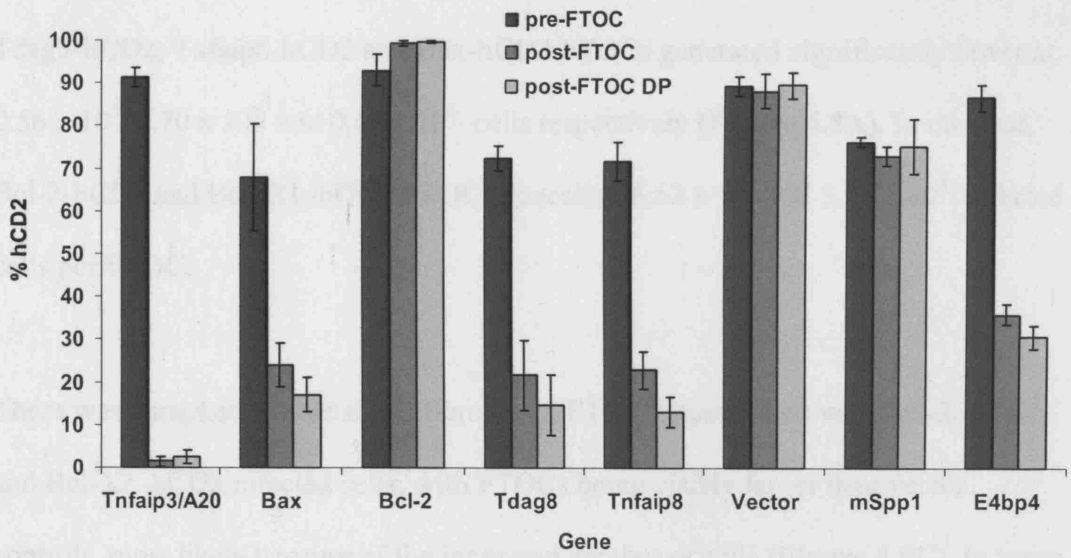

Figure 4.7. Expression of specific target genes in HPC reconstituted FTOCs profoundly affects cell survival. (A) Graph of % $hCD2^+$ cells pre and post FTOC. Pre-FTOC cells stained for bicistronic hCD2 expression 48 hours post retroviral infection. Post-FTOC (13 days) cells pooled from ≥3 FTOCs stained with CD8-FITC, CD4-TC, hCD2-PE. Error bars mean ± SD, n= 4-6, dependent on gene, pooled data from 6 independent experiments.

4.2.8. Reconstitution of depleted FTOCs with target gene infected HPCs affects FTOC cellularity and degree of expansion.

To study the effect of target gene over-expression upon the growth properties of HPCs as they develop in FTOC, the growth in numbers and relative expansion of infected cells was determined. Cell counts were performed upon individual FTOCs (in quintuplicate), taking into account the initial infection efficiency (at 48 hours, determining how many of the initial 1 x 10^4 cells per FTOC were infected), and the number of $hCD2^+$ infected cells at 13 days. hCD2 and mock (therefore total number) infected FTOCs generated 2.56 x 10^5 and 2.48 x 10^5 infected cells per FTOC, while Tdag8-hCD2, Tnfaip8-hCD2 and Bax-hCD2 FTOCs generated significantly fewer at 0.56 x 10^5, 0.70 x 10^5 and 0.42 x 10^5 cells respectively (**Figure 4.8A**). In contrast, Bcl-2-hCD2 and Bcl -XL-hCD2 FTOCs generated 5.52 x 10^5 and 5.58 x 10^5 infected cells per FTOC.

There was a marked visible size difference in FTOCs repopulated with Bcl-2-hCD2 and Bcl-XL-hCD2 infected cells, with FTOCs being visibly larger than vector controls, most likely because of the increased number of cells (**Figure 4.8C**). In terms of expansion in cell number, hCD2 FTOCs demonstrated an approximate 16-fold expansion in numbers of infected cells. Tdag8-hCD2, Tnfaip8-hCD2 and Bax-hCD2 FTOCs demonstrated an approximate 4, 6 and 4-fold expansion, while both Bcl-2-hCD2 and Bcl-XL-hCD2 showed a 27-fold expansion (**Figure 4.8B**). Despite the large differences in cell number however, the proportion of cells in each of four thymocyte sub-populations, DN, DP, CD4 SP and CD8 SP, in 13-day FTOCs demonstrated no significant differences in infected or total cells, irrespective of target

gene. The only exception was for the *Bcl-2* gene family members Bcl-2 and Bcl-XL, which displayed a shift towards CD4 SP cells and slightly increased numbers of DP cells (**Figure 4.8D**).

4.2.9. Over-expression of pro-apoptotic target genes markedly enhances FTOC sensitivity to DEX treatment in vitro.

HPCs infected with retroviral constructs were also used to repopulate FTOCs for use in apoptosis assays, to determine if the survival disadvantage data shown in Tdag8-hCD2, Tnfaip8-hCD2 and Bax-hCD2 FTOCs was accompanied by a demonstrable sensitivity to apoptotic stimuli. FTOCs were prepared in replicates of $n \geq 3$, cultured for 13 days and exposed ± 0.5μM DEX for 4 hours. Thymocytes were stained with CD8 and hCD2 cell surface markers, saponin-permeabilised and stained with 7AAD DNA dye. Gating was performed as demonstrated in **Figure 4.9A**. Cells were gated for $CD8^+$ thymocytes to exclude CD8-, DEX-resistant DN thymocytes, and separated on the basis of hCD2 expression (to separate infected and uninfected cells). The apoptotic response could therefore be quantified both within and between FTOCs, comparing distinct populations of cells.

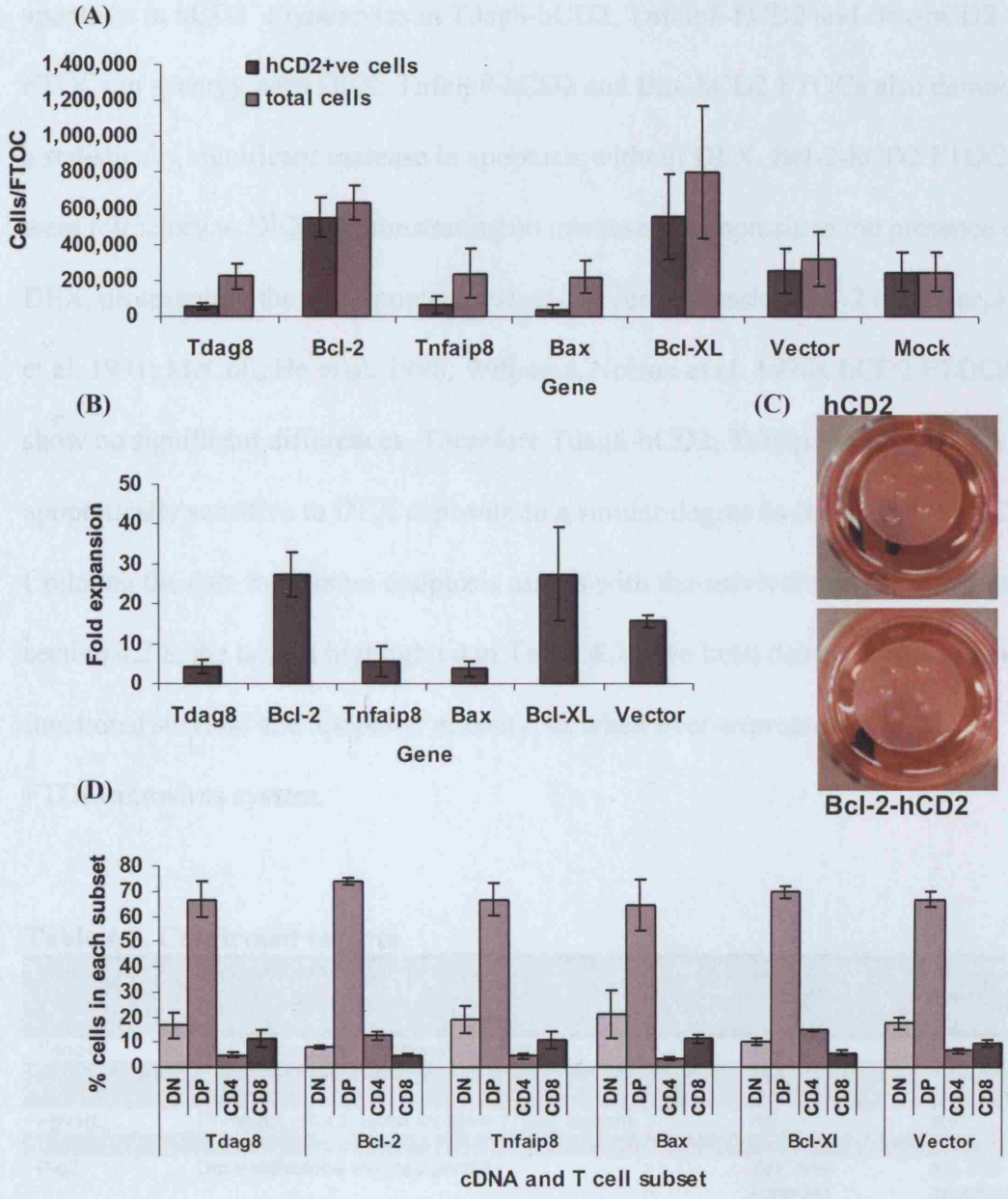

Figure 4.8. FTOCs repopulated with target gene infected HPCs affects FTOC cellularity and degree of expansion. (A) FTOC cell counts at 13 days, showing numbers of $hCD2^+$ and total cells. Mean ± S.D., n=5. Representative expt, n=2 **(B)** Fold-expansion of infected cells in hCD2, Bax-hCD2, Bcl-2-hCD2 and Bcl-XL-hCD2 FTOCs 13 days after plating. Mean ± S.D., n=5. Representative expt, n=2 **(C)** Digital photos of Bcl-2-hCD2 and hCD2 FTOCs at 13 days **(D)** Graph of subset proportions in reconstituted FTOCs. Mean ± S.D., n=5. Representative expt, n=2.

Figure 4.9B demonstrates a statistically significant ($p<0.05$) enhancement in apoptosis in $hCD2^+$ thymocytes in Tdag8-hCD2, Tnfaip8-hCD2 and Bax-hCD2 FTOCs in synergy with DEX. Tnfaip8-hCD2 and Bax-hCD2 FTOCs also demonstrate a statistically significant increase in apoptosis without DEX. Bcl-2-hCD2 FTOCs were refractory to DEX, demonstrating no increase in apoptosis in the presence of DEX, protected by the anti-apoptotic effect of over-expressing Bcl-2 (Strasser, Harris et al. 1991; McColl, He et al. 1998; Williams, Norton et al. 1998). hCD2 FTOCs show no significant differences. Therefore Tdag8-hCD2, Tnfaip8-hCD2 FTOCs are apoptotically sensitive to DEX exposure to a similar degree as Bax-hCD2 FTOCs. Collating the data from these apoptosis assays with the survival assays detailed in section 4.2.8, the targets highlighted in **Table 4.3** have been demonstrated to have functional survival and apoptotic phenotypes when over-expressed in the FTOC/retrovirus system.

Table 4.3. Confirmed targets.

Genes	Description/Function	Survival phenotype?	Pro-apoptotic Phenotype?
E4bp4	NFIL3/E4bp4 transcriptional repressor	Yes	No
Tdag8	T-cell death associated gene 8; G-protein coupled receptor	**Yes**	**Yes**
Fgfr1(L)	Fibroblast growth factor receptor-1, long isoform	No	No
Tnfaip8	TNF-α induced protein 8	**Yes**	**Yes**
Dig2	Dexamethasone-induced-gene 2	Yes, anti-apoptotic	No, anti-apoptotic
Pip49	Pancreatitis-induced-protein 49	No	No
Mspp1	Sphingosine-1-phosphate phosphatase	No	No
Lrg-47	G-protein-like LRG-47, related to GTP-binding proteins	No	No
Lisch7	Liver-specific Lisch7 gene	No	No
Bim^{EL}	Bcl-2 Interacting Mediator of Cell Death	Yes	Yes
Fkbp51	FKBP51, T-cell specific immunophilin that inhibits calcineurin	No	No
Tnfaip3(A20)	A20 zinc finger protein	Blocks T cell development	Blocks T cell development

(A)

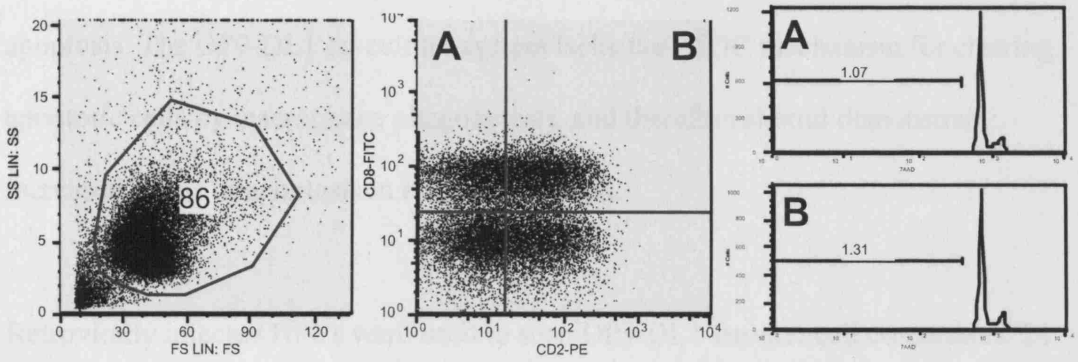

(B)

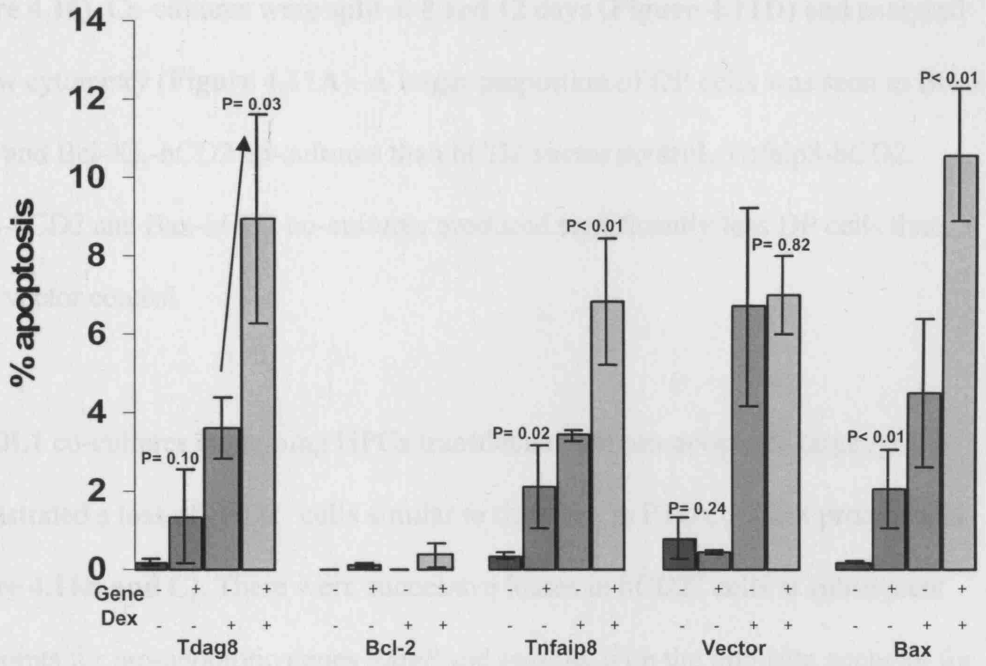

Figure 4.9. Expression of specific target genes in HPC reconstituted FTOCs markedly enhances sensitivity to DEX. (A) Gating mechanics for **Figure 4.10B**, showing FSC, SSC gating; CD8, hCD2 gating; 7AAD read-out **(B)** Graph of apoptosis in reconstituted 13 day FTOCs treated ± 0.5μM DEX for 4 hrs. FTOC disrupted thymocytes were stained with CD8 and hCD2 antibodies, saponin-permeabilised and stained with 7AAD DNA dye. Mean ± SD, n≥3. p-values apply to differences ± gene with or without DEX, as indicated by arrow. Representative expt, n=3.

4.2.10. OP9-DL1 cocultures.

The OP9-DL1 co-culture system was used in parallel with the FTOC system in later experiments to determine the effect of target gene expression upon thymocyte apoptosis. The OP9-DL1 co-culture system lacks the FTOC mechanism for clearing apoptotic cells by macrophage phagocytosis, and therefore should demonstrate increased levels of apoptosis in response to DEX.

Retrovirally infected HPCs were used to seed OP9-DL1 stromal cell co-cultures. 24 hours post infection, 1 x 10^4 HPCs were inoculated into wells of 6-well TC dishes containing OP9-DL1 stromal cells at ≈75% confluence with addition of cytokines (**Figure 4.10**). Co-cultures were split at 8 and 12 days (**Figure 4.11D**) and analysed by flow cytometry (**Figure 4.11A**). A larger proportion of DP cells was seen in Bcl-2-hCD2 and Bcl-XL-hCD2 co-cultures than hCD2 vector control. Tnfaip8-hCD2, Tdag8-hCD2 and Bax-hCD2 co-cultures produced significantly less DP cells than hCD2 vector control.

OP9-DL1 co-cultures containing HPCs transduced with pro-apoptotic target genes demonstrated a loss of $hCD2^+$ cells similar to that seen in FTOC, if less pronounced (**Figure 4.11B and C**). There were successive losses in $hCD2^+$ cells at subsequent time points for pro-apoptotic genes *tdag8* and *tnfaip8*, with the opposite apparent for *bcl-2*.

To determine the degree of apoptosis in thymocytes developed in OP9-DL1 co-cultures, day fifteen day co-cultures were incubated ± 0.5 μM DEX for 12 hrs. Thymocytes were stained with CD8 and hCD2 cell surface markers, and stained with

DRAQ5 DNA dye. Gating was performed as demonstrated in **Figure 4.9A**. Cells were gated for $CD8^+$ (to exclude $CD8^-$, and thus DEX-resistant DN thymocytes), $hCD2^+$ thymocytes. Tdag8-hCD2, Tnfaip8-hCD2, and Bax-hCD2 thymocytes were significantly more susceptible to DEX then hCD2 thymocytes, while Bcl-2-hCD2 and Bcl-XL-hCD2 cells were significantly more resistant (all $p<0.01$) (**Figure 4.11E**).

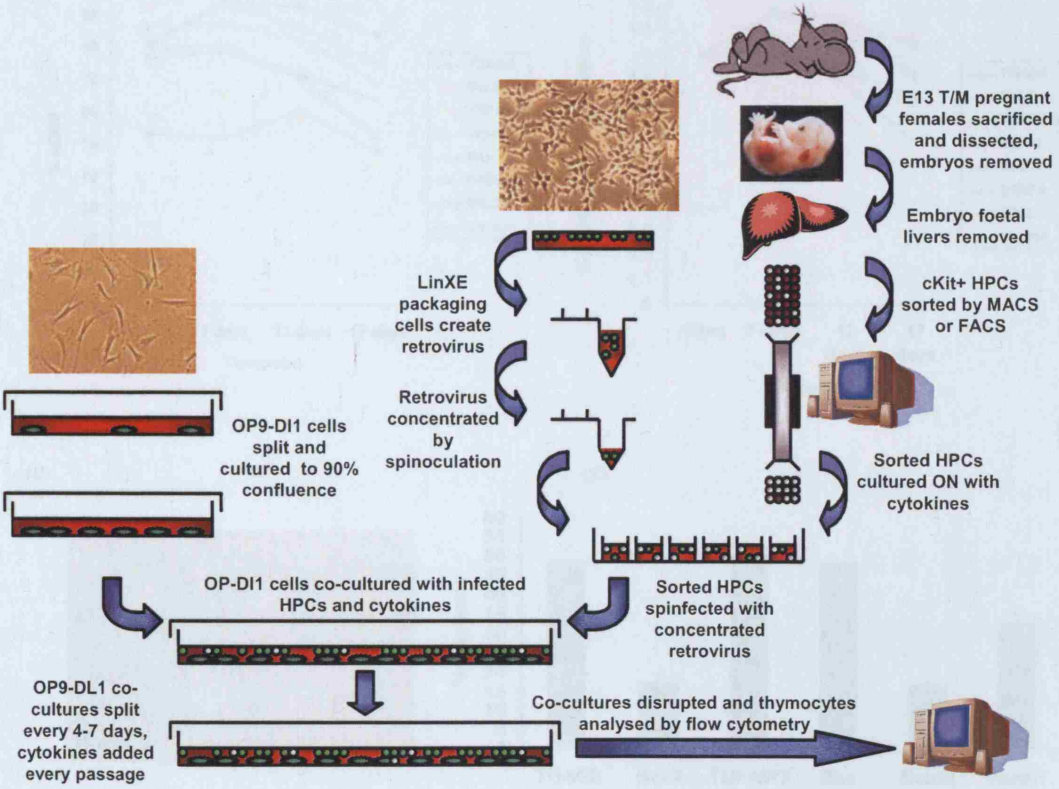

Figure 4.10. OP9-DL1/retrovirus experimental strategy used to transduce primary HPCs and initiate OP9-DL1-thymocyte co-cultures. cKit^{+} HPCs obtained by MACS from E12 or E13 time-mated foetal livers are retrovirally infected with pMSCV retroviral vectors, placed into co-culture with OP9-DL1 bone marrow stromal cells, and cultured to produce DP T cells.

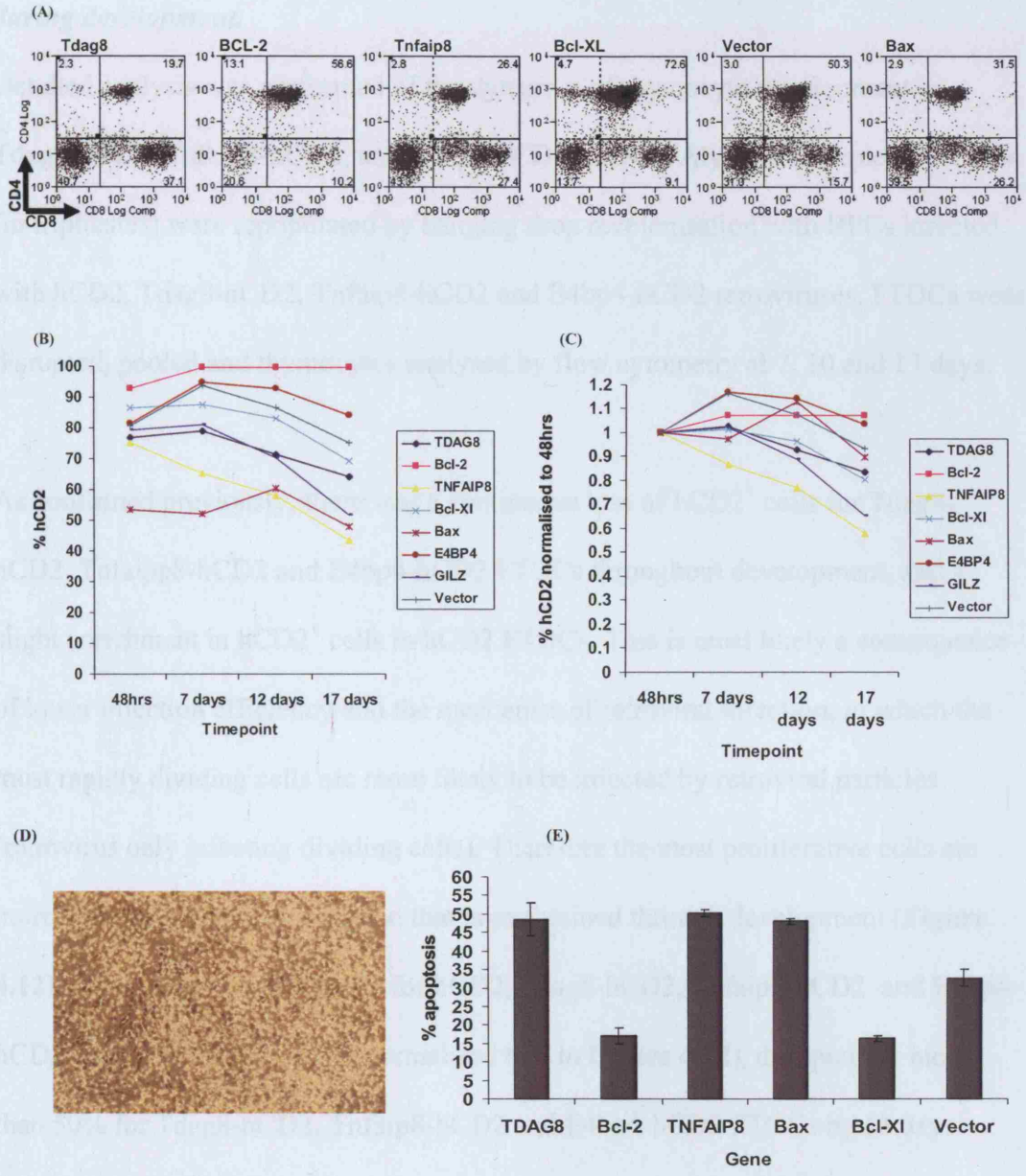

Figure 4.11. Tdag8-hCD2, Tnfaip8-hCD2, and E4bp4-hCD2 thymocytes during development on OP9-DL1-thymocyte co-cultures. (A) Flow cytometry of OP9-DL1 co-culture derived thymocytes at 15 days, stained for CD4 and CD8, gated on live, $hCD2^+$, $CD3^+$ cells. **(B)** Graph of % hCD2 status for Tdag8-hCD2, Tnfaip8-hCD2, Bcl-2-hCD2, Bax-hCD2, Bcl-XL-hCD2 and hCD2 FTOCs at 7, 12 and 17 days of development, as determined by flow cytometry. **(C)** Graph of % hCD2 status normalised to 48 hours post infection, for Tdag8-hCD2, Tnfaip8-hCD2, Bcl-2-hCD2, Bax-hCD2, Bcl-XL-hCD2 and hCD2 FTOCs at 7, 12 and 17 days of development, as determined by flow cytometry. **(D)** Photograph of OP9-DL1 co-culture, 8 days. **(E)** Graph of apoptosis in OP9-DL1 co-culture derived thymocytes treated with 0.5μM DEX for 12 hrs. Error bars mean ± SD.

4.2.11. Detailed analysis of Tdag8-hCD2, Tnfaip8-hCD2, and E4bp4-hCD2 FTOCs during development.

Detailed analysis was performed of the dynamics of thymocyte development in Tdag8-hCD2, Tnfaip8-hCD2, and E4bp4-hCD2 FTOCs. Alymphoid depleted FTOCs (in triplicates) were repopulated by hanging drop recolonisation with HPCs infected with hCD2, Tdag8-hCD2, Tnfaip8-hCD2 and E4bp4-hCD2 retroviruses. FTOCs were disrupted, pooled and thymocytes analysed by flow cytometry at 7, 10 and 13 days.

As confirmed previously, there was a continuous loss of $hCD2^+$ cells for Tdag8-hCD2, Tnfaipp8-hCD2 and E4bp4-hCD2 FTOCs throughout development, and a slight enrichment in $hCD2^+$ cells in hCD2 FTOCs. This is most likely a consequence of lower infection efficiency and the mechanics of retroviral infection, in which the most rapidly dividing cells are more likely to be infected by retroviral particles (retrovirus only infecting dividing cells). Therefore the most proliferative cells are more heavily infected, a condition that is maintained through development (**Figure 4.12**). Initial infection efficiency for hCD2, Tdag8-hCD2, Tnfaip8-hCD2 and E4bp4-hCD2 retroviruses was ≈75% (normalised to 1 in **Figure 4.12**), dropping by more than 50% for Tdag8-hCD2, Tnfaip8-hCD2 and E4bp4-hCD2 FTOCs by 13 days.

Analysis of the CD4, CD8 status (gated for $hCD2^+$ cells) for hCD2, Tdag8-hCD2, Tnfaip-hCD2 and E4bp4-hCD2 FTOCs indicated that DP cells were beginning to appear at 7 days of culture (**Figure 4.13**). The proportion of DP thymocytes increases for all 4 constructs at 10 and 13 days. hCD2 FTOCs generated DP thymocytes with slightly faster kinetics than pro-apoptotic constructs (**Figure 4.13**). This was confirmed by analysis of the CD25, CD44 status (gated for $hCD2^+$ cells) at 7 and 10

days (**Figure 4.14**), which indicated a greater proportion of cells at the DN4 stage of development at 7 days. However there were no significant differences in development at 13 days, either between constructs, or between infected and uninfected cells within FTOCs (data not shown).

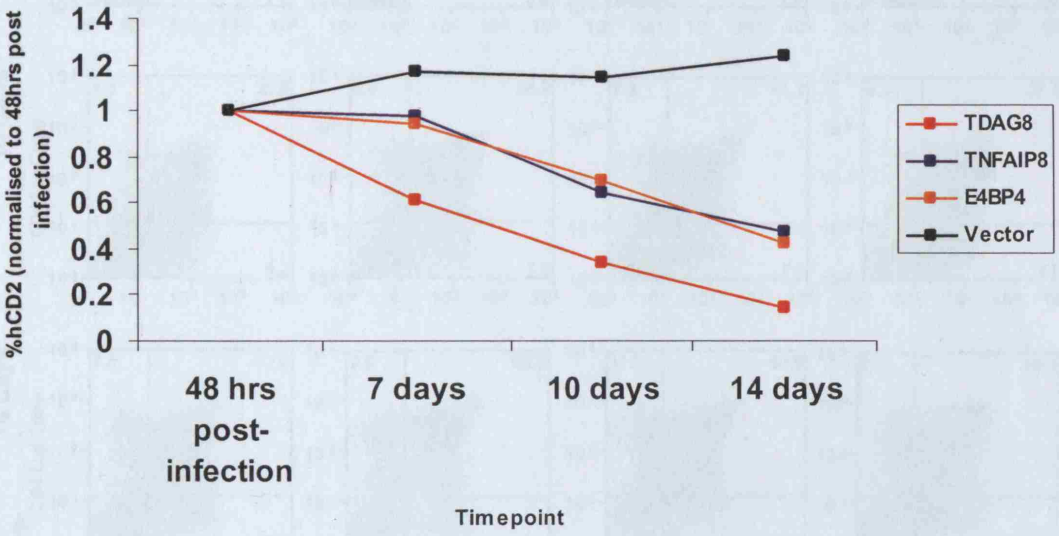

Figure 4.12. Detailed analysis of Tdag8-hCD2, Tnfaip8-hCD2, and E4bp4-hCD2 FTOCs during development – 1 Graph of % hCD2 status for pooled (n=3) Tdag8-hCD2, Tnfaip8-hCD2, and E4bp4-hCD2 FTOCs at 7, 10 and 13 days of development, as determined by flow cytometry.

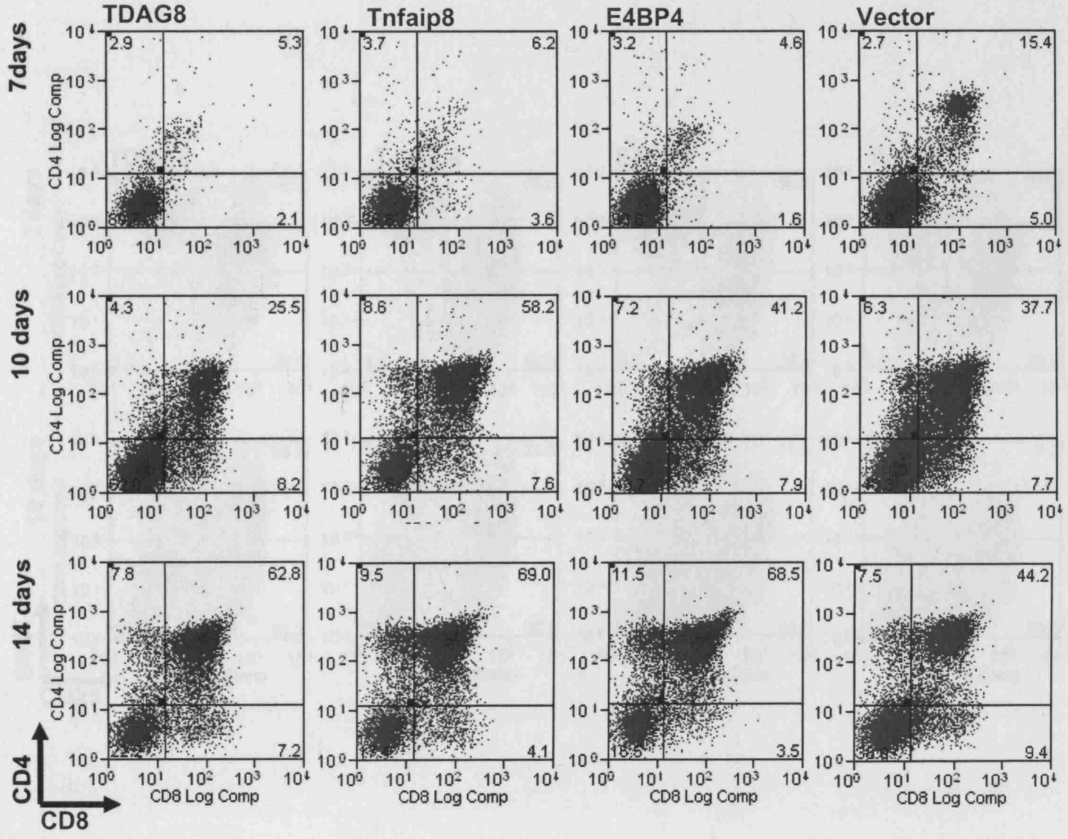

Figure 4.13. Detailed analysis of Tdag8-hCD2, Tnfaip8-hCD2, and E4bp4-hCD2 FTOCs during development – 2 Flow cytometry of Tdag8-hCD2, Tnfaip8-hCD2, and E4bp4-hCD2 FTOCs at 7, 10.5 and 14 days of development. Thymocytes pooled from n=3 FTOCs, stained for CD4 and CD8, gated on $hCD2^+$ cells.

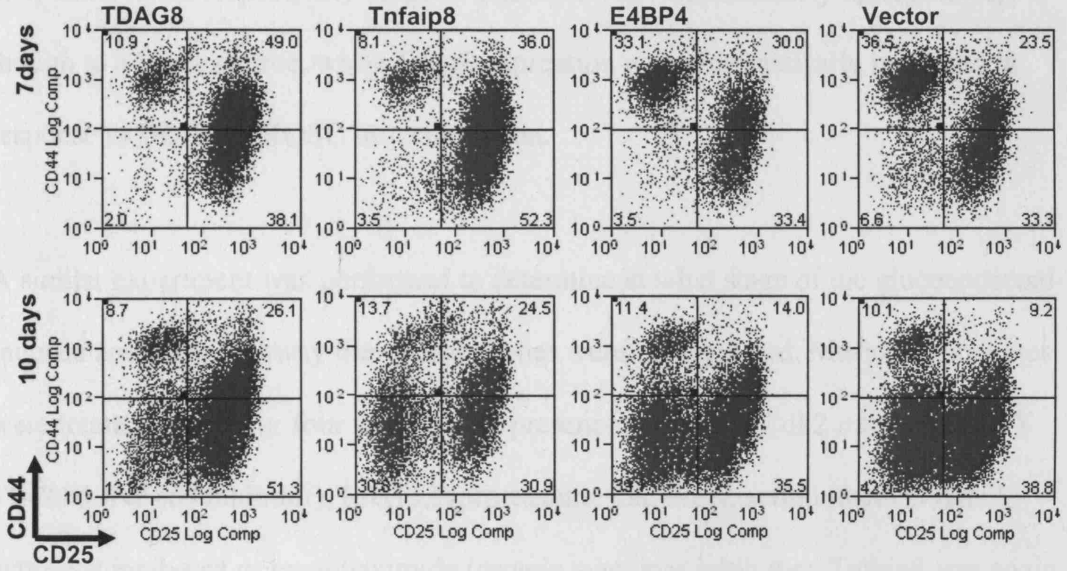

Figure 4.14. Detailed analysis of Tdag8-hCD2, Tnfaip8-hCD2, and E4bp4-hCD2 FTOCs during development – 3 Flow cytometry of Tdag8-hCD2, Tnfaip8-hCD2, and E4bp4-hCD2 FTOCs at 7, 10.5 and 14 days of development. Thymocytes pooled from n=3 FTOCs, stained for CD25 and CD44, gated on $hCD2^+$ cells.

4.2.12. Dynamics of Tdag8, Tnfaip8, and E4bp4 RNA regulation in response to apoptotic stimuli.

Tdag8, *tnfaip8* and *e4bp4* target genes are up-regulated in response to DEX in the presence of ROSC. To further examine the specific nature of this up-regulation, murine thymocytes were treated ± ROSC, ± DEX for 2, 4 and 6 hours. Real-time qPCR on derived cDNA demonstrated that Tnfaip8 is massively up-regulated in response to DEX in conditions of Cdk2 inhibition, 35-fold, 153-fold and 212-fold at 2, 4, and 6 hours respectively (**Figure 4.15A**). E4bp4 was similarly up-regulated, though to a lesser degree, while Tdag8 expression was synergistically increased in response to DEX and ROSC in combination.

A similar experiment was performed to determine at what stage of the glucocorticoid-induced apoptotic pathway these target genes were up-regulated. Murine thymocytes were treated ± DEX for four hours in the presence of ROSC (Cdk2 inhibitor), BAY 11-7085 (NF-κB inhibitor), MG132 (proteasome inhibitor), actinomycin D (RNA synthesis inhibitor) or cycloheximide (protein synthesis inhibitor). Tnfaip8 was again maximally induced in conditions of Cdk2 inhibition, as was E4bp4 (**Figure 4.15B**). Abrogation of thymocyte apoptosis by inhibition of NF-κB signalling with BAY 11-7085 blocked the up-regulation of Tnfaip8 and E4bp4. NF-κB is a nuclear target of GR translocation. When GR is released from HSP90 sequestration in the cytoplasm by GC binding, it translocates to the nucleus and binds to several proteins, AP-1 and NF-κB included (Scheinman, Gualberto et al. 1995). Co-treatment with MG132 did not block up-regulation of E4bp4, but did block Tdag8 up-regulation.

(A)

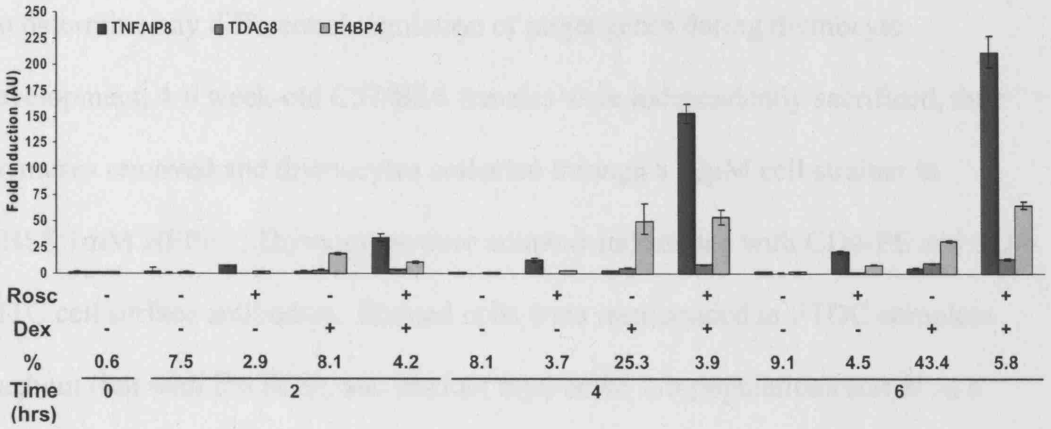

(B)

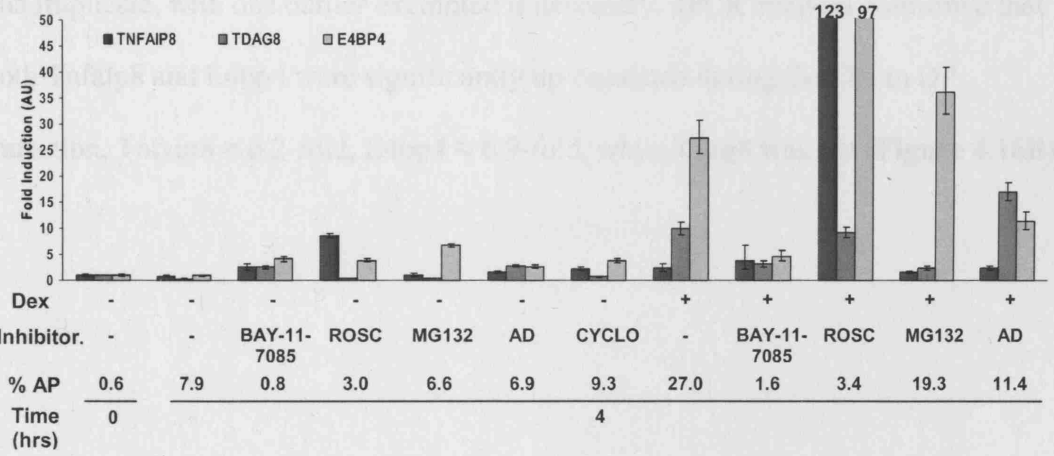

Figure 4.15. Tdag8, Tnfaip8, and E4bp4 are differentially expressed in response to DEX in the presence of different inhibitors. (A) Graph of real-time qPCR of thymocytes treated ± 25μM ROSC, ± 1μM DEX for times stated. qPCR was performed in quadruplicate (with outlier exemption if necessary) on 5ng cDNA, n=2. % AP = apoptosis in parallel samples determined by flow cytometry (7AAD incorporation). **(B)** Real-time qPCR of thymocytes treated ± 1μM DEX, ± 10μM BAY 11-7085, ± 25μM ROSC, ± 30μM MG132, ± 1μM actinomycin D, ± 50μg/ml cycloheximide for times stated. qPCR was performed in quadruplicate (with outlier exemption if necessary) on 5ng cDNA, n=2. % AP = apoptosis in parallel samples determined by flow cytometry (7AAD incorporation).

4.2.13. Tdag8, Tnfaip8, and E4bp4 are differentially expressed in distinct thymocyte sub-populations.

To determine any differential regulation of target genes during thymocyte development, 4-6 week-old C57/BL6 females were independently sacrificed, their thymuses removed and thymocytes collected through a 70μM cell strainer in HBSS:1mM HEPES. Thymocytes were counted and stained with CD4-PE and CD8-FITC cell surface antibodies. Stained cells were resuspended in FTOC complete medium (but with 2% FCS), and distinct thymocyte sub-populations sorted on a Beckton Dickinson FACScalibur cell sorter.

2.5 x 10^5 DN, DP, CD4 SP and CD8 SP cells were collected. RNA was extracted with Trizol and cDNA prepared and quantified. Real-time qPCR was performed in quadruplicate, with one outlier exempted if necessary. qPCR analysis confirmed that both Tnfaip8 and E4bp4 were significantly up-regulated during the DN to DP transition, Tnfaip8 ≈ 6.2-fold, E4bp4 ≈ 6.9-fold, while Tdag8 was not (**Figure 4.16B**).

(A)

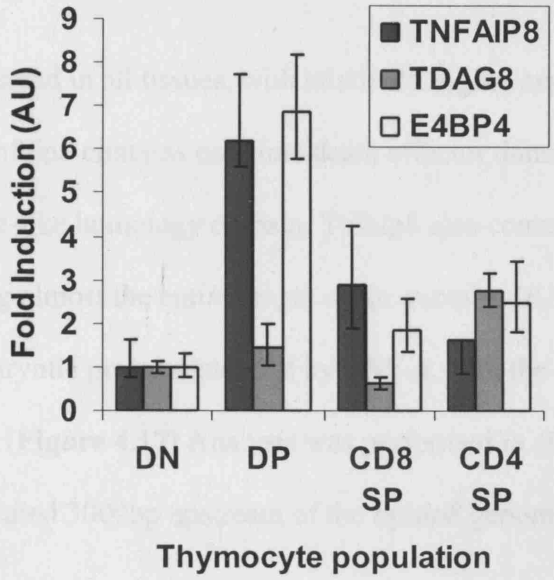

Figure 4.16. Tdag8, Tnfaip8, and E4bp4 are differentially expressed in discrete thymocyte sub-populations. (A) Cell sorts for discrete thymocyte populations, DN, DP, CD4 SP and CD8 SP **(B)** Graph of Real Time qPCR demonstrating differential regulation of Tdag8, Tnfaip8 and E4bp4 during thymocyte development. Normalised to DN levels, qPCR performed in quadruplicate, with outlier exemption.

4.2.14. Tnfaip8 – Structure and Function.

The *Tnfaip8* (human *TNFAIP8*) gene expresses a 198 amino acid, ≈22KD protein (human 188aa, ≈21KD protein) expressed widely in the immune system (Genecard GC05P118719). Aliases for the human form include NDED, GG2-1, MDC-3.13, and SCC-S2. The Tnfaip8 ORF contains a sequence in the amino terminus that bears significant homology to death effector domain II of the cell death regulatory protein, Fas-associated death domain-like interleukin-1b-converting enzyme-inhibitory protein (FLIP) (Kumar, Whiteside et al. 2000).

Tnfaip8 is expressed in all tissues, with relatively higher expression in lymphoid cells. Unlike FLIP, Tnfaip8 contains only one death effector domain and lacks the carboxyl-terminal caspase-like homology domain. Tnfaip8 also contains a PFAM-predicted domain covering almost the entire length of the protein, DUF758, a domain shared by a family of eukaryotic proteins induced by TNF-α, with the nomenclature Tnfaip8-L1, Tnfaip8-L2 etc. (**Figure 4.17**) Analysis was performed *in silico* using Phylofoot, but no GRE was located 3000bp upstream of the *tnfaip8* genomic transcriptional start site.

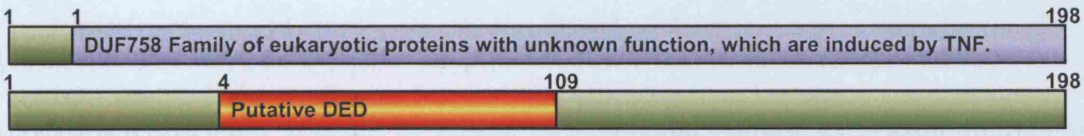

Figure 4.17. Structure of Tnfaip8 protein. 198 amino acid protein, (≈22 KD) expressed relatively highly in lymphoid tissues. Human and mouse forms share 94% homology. TNF- induced, NF-KB induced DED protein. Sequence analysis shows a putative death effector domain II region similar to FLIP, but lacking caspase-like homology domain. Also contains a PFAM-predicted domain covering almost the entire length of the protein, DUF758, a domain shared by a family of eukaryotic proteins induced by TNF-α.

4.2.15. RNA interference knockdown of Tnfaip8 expression.

The FTOC/retrovirus system has been used to investigate candidate genes isolated by our DNA microarray screen. Over-expression of Tnfaip8 in particular has been demonstrated to be pro-apoptotic and deleterious to survival in FTOC. RNAi-mediated knockdown of Tnfaip8 was performed to determine the effect upon thymocyte apoptosis. Short hairpin RNA sequences were generated that were predicted to knockdown RNA expression of Tnfaip8 (**Figure 4.18A**) using the Invitrogen RNAiCentral website. 2 shRNAs were predicted to effectively knock down Tnfaip8 expression (**Figure 4.19B**), showing targeted regions of Tnfaip8 protein.

These shRNAs were cloned into the pENTR™/U6-GW/shRNA entry vector, and knockdown efficiency assayed by testing for beta-galactosidase expression following co-transfection with pSCREEN-iT™/lacZ-DEST-Tnfaip8 fusion expression vectors. Both Tnfaip8 shRNAs achieved knockdown efficiencies of >75% (**Figure 4.19C**). pENTR™/U6-GW/shRNA entry vectors were then recombined with modified (co-expressing hCD2 reporter) pLenti6/BLOCK-iT™-DEST expression vectors in a LR recombination reaction to produce lentiviral expression constructs.

The lentiviral knockdown vectors were used to infect HPCs using a similar protocol to retroviral experiments. Unfortunately, although initial infection efficiency was reasonable, hCD2 expression was not maintained over time (**Figure 4.18B**), the most likely explanation being epigenetic silencing of the U6 promoter. The two shRNA hairpin sequences were therefore re-cloned as components of shRNA^{mir} hairpins in the modified pMSCV-LTRmiR30-PIhCD2 retroviral vector (Dickins, Hemann et al. 2005) (**Figure 4.19A**) (pMSCV-LTRmiR30-PIhCD2-Tnfaip8-1 and pMSCV-

LTRmiR30-PIhCD2-Tnfaip8-2 respectively, hereafter designated as T8-RNAi-1 and T8-RNAi-2). This would drive expression of the shRNA^{mir} hairpins from the MSCV retroviral 5' LTR promoter, a RNA Polymerase II-based promoter system unlike the RNA Polymerase III-based promoter system typically used in lentiviral constructs. This is more similar to cDNA over-expression systems, and much less sensitive to epigenetic silencing. Pol II promoters transcribe endogenous primary microRNA transcripts, and therefore the improved knockdown efficiencies of Polymerase II-vectors is derived from natural mechanisms of RNA-dependent gene inhibition (Dickins, Hemann et al. 2005).

To examine the effect of knocking down Tnfaip8 expression in FTOC, HPCs were infected with RNAi retroviruses (retroviruses expressing shRNA^{mir} hairpins) and again used to repopulate depleted FTOCs in hanging drop recolonisations. FTOCs were cultured for 13 days to investigate the effect of target gene knockdown versus over-expression upon thymocyte development and apoptosis. Constructs and abbreviations are detailed in **Table 4.4**.

Table 4.4. RNAi constructs.

RNAi construct	Knockdown target	Abbreviation
pMSCV-LTRmiR30-PIhCD2-Tnfaip8-1	Tnfaip8	T8-RNAi-1
pMSCV-LTRmiR30-PIhCD2-Tnfaip8-2	Tnfaip8	T8-RNAi-2
pMSCV-LTRmiR30-PIhCD2-BIM^{EL}	Bim isoforms	BIM-RNAi
pMSCV-LTRmiR30-PIhCD2-LUC	Luciferase	LUC-RNAi
pMSCV-LTRmiR30-PIhCD2	none	Vector-RNAi

RNAi FTOCs (FTOCs containing HPCs infected with knockdown constructs) were prepared alongside Bax-hCD2, Bcl-2-hCD2, and Tnfaip8-hCD2 FTOCs. The Bim-RNAi construct was generated using shRNA^{mir} hairpin sequences generated from

shRNAs previously published to knock down Bim expression, and employed as a positive control (Abrams, Robertson et al. 2004). T8-RNAi-1, T8-RNAi-2, BIM-RNAi, and Vector-RNAi FTOCs all maintained expression throughout thymocyte development, showing no evidence of epigenetic silencing. T8-RNAi-1, T8-RNAi-2, BIM-RNAi, and Vector-RNAi demonstrated no loss or enrichment of hCD2 expression during thymocyte development (**Figure 4.19E**).

RNAi FTOCs were prepared as before in replicates of $n \geq 3$, cultured for 13 days and exposed to $\pm$ 0.5μM DEX for 4 hours. Thymocytes were stained with CD8 and hCD2 cell surface antibodies, and stained with DRAQ5 DNA dye. Gating was performed as demonstrated in **Figure 4.9A**. Cells were gated for $CD8^+$ thymocytes (to exclude $CD8^-$, DEX-resistant DN thymocytes), and separated on the basis of hCD2 expression (to separate infected and uninfected cells).

Infected cells in BIM-RNAi FTOCs demonstrated significantly less apoptosis in response to DEX than vector controls ($p<0.001$) (**Figure 4.19F**), as would be expected from knocking down expression of a transcript known to be crucial to glucocorticoid-induced apoptosis (Abrams, Robertson et al. 2004). Both T8-RNAi-1 ($p<0.001$) and T8-RNAi-2 ($p<0.001$) FTOCs demonstrated comparable reductions in apoptosis to vector controls as BIM-RNAi FTOCs.

(A)

Tnfaip RNAi 1 103	Top Strand	5'- CACCGCTACAGATGTCTTCAATTCCCGAAGGAATTGAAGACATCTGTAGC
	Bottom Strand	5'- AAAAGCTACAGATGTCTTCAATTCCTTCGGGAATTGAAGACATCTGTAGC
Tnfaip RNAi 1 480	Top Strand	5'- CACCGCTCCTACACGAGATCATTCACGAATGAATGATCTCGTGTAGGAGC
	Bottom Strand	5'- AAAAGCTCCTACACGAGATCATTCATTCGTGAATGATCTCGTGTAGGAGC

Linker Sense Loop Antisense

(B)

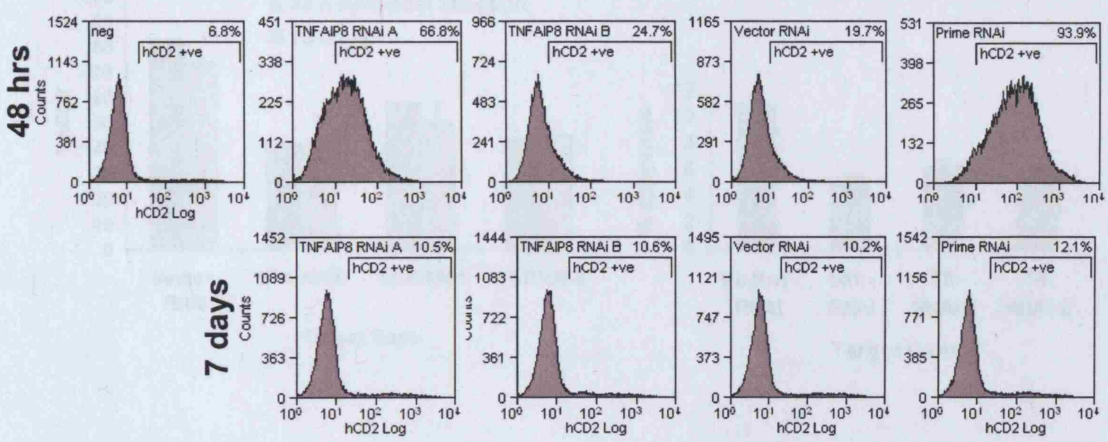

Figure 4.18. **RNAi knockdown of Tnfaip8 expression. (A)** shRNA sequences generated using Invitrogen RNAiCentral predicted to knock down Tnfaip8 **(B)** Flow cytometric analysis of HPCs infected with lentiviral constructs and used to repopulate FTOCs, stained for hCD2, 48 hours post infection and after 7 days culture.

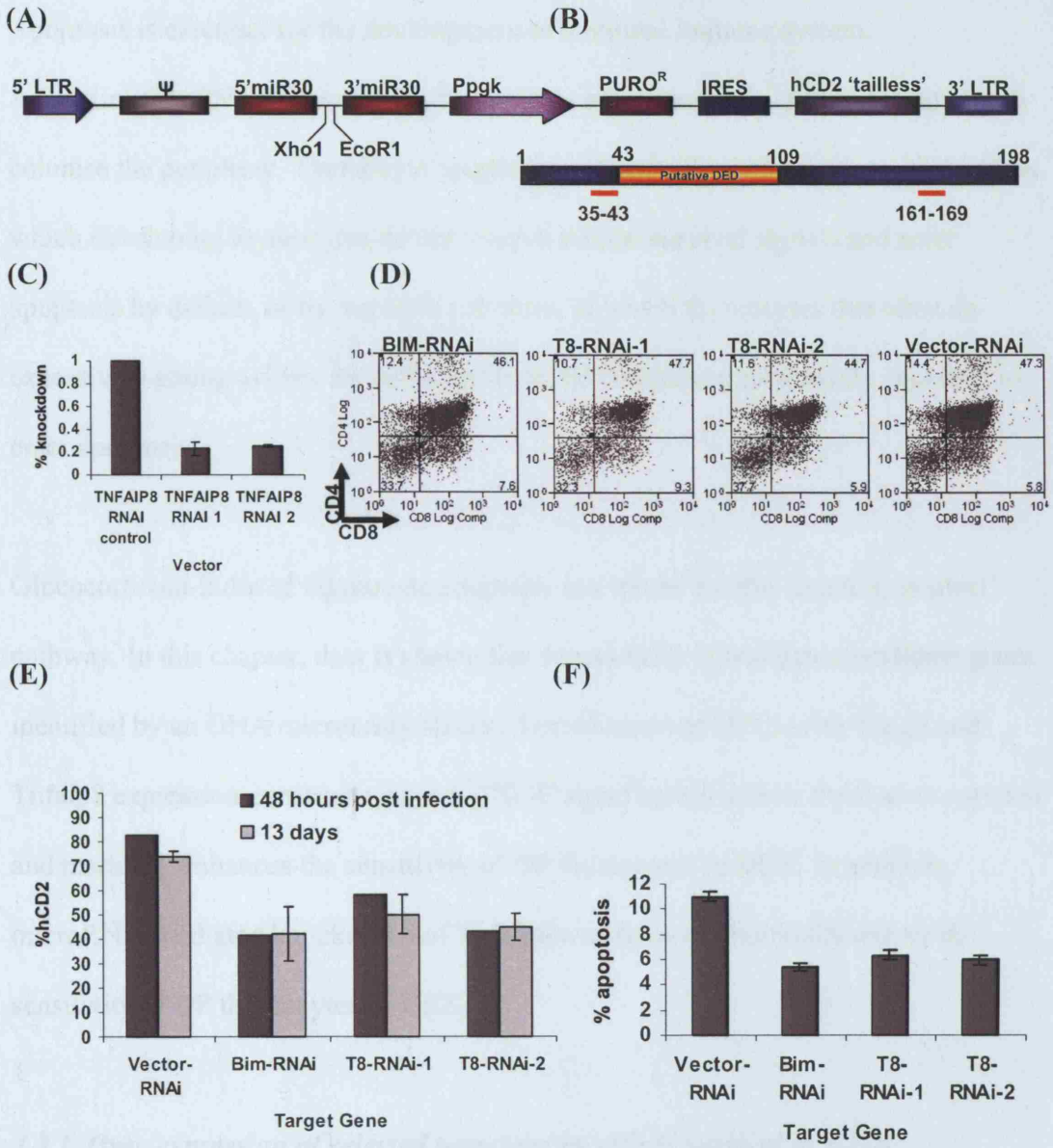

Figure 4.19. RNA interference knockdown of Tnfaip8 expression. (A) Diagram of pMSCV-LTRmiR30-PIhCD2 retroviral vector, microRNAs cloned into Xho1-EcoR1 site **(B)** Diagram of Tnfaip8 protein, illustrating regions of protein against which microRNAs are targeted **(C)** Graph of knockdown levels achieved by microRNAs in LacZ/fusion assay **(D)** Flow cytometry of 13 day T8-RNAi-1, T8-RNAi-2, BIM-RNAi and Vector-RNAi FTOC thymcoytes, stained for CD4 and CD8, gated for $hCD2^+$ infected cells **(E)** Graph of % hCD2 status pre and post FTOC **(F)** Graph of apoptosis in infected cells in reconstituted 13 day FTOCS treated ± 0.5μM DEX for 4 hrs. FTOC thymocytes were stained with CD8 and hCD2 antibodies, and stained with DRAQ5 DNA dye. Mean ± SD, n=3.

4.3. Discussion.

Apoptosis is essential for the development of a normal immune system. Approximately 95% of developing thymocytes enter apoptosis and do not survive to colonise the periphery. Thymocyte apoptosis can occur through 'death by neglect', in which developing thymocytes do not receive critical survival signals and enter apoptosis by default, or by negative selection, in which thymocytes that elicit an excessively strong avidity for self peptide:MHC complexes are actively signalled to enter apoptosis.

Glucocorticoid-induced thymocyte apoptosis is a model for the 'death by neglect' pathway. In this chapter, data is shown that functionally investigates candidate genes identified by an DNA microarray screen. Transduction of HPCs with Tdag8 and Tnfaip8 expression constructs prior to FTOC significantly affects thymocyte survival and markedly enhances the sensitivity of DP thymocytes to DEX. In addition, microRNA-mediated knockdown of Tnfaip8 was shown to markedly reduce the sensitivity of DP thymocytes to DEX.

4.3.1. Over-expression of selected target genes affects survival in FTOC.

Data in this chapter confirmed that over-expression of several target genes, *Tnfaip8*, *Tdag8* and *E4bp4* isolated by an DNA microarray screen adversely affects the survival of infected cells in FTOC. Of 12 genes screened using the FTOC/retrovirus system, one proved antiapoptotic (Dig2), one blocked thymocyte development (Tnfaip3(A20)), one was a confirmed pro-apoptotic member of the *Bcl-2* family (BimEL), while six proved non-functional with respect to cell survival (Fgfr1(L),

Pip49, Mspp1, Lrg-47, Lisch7 and Fkbp51). The three remaining genes were confirmed to affect thymocyte survival.

Tdag8, Tnfaip8, and E4bp4 cells demonstrated a survival disadvantage in FTOC compared to vector and anti-apoptotic controls. During FTOC there was a continuous loss of $hCD2^+$ cells, with the loss more pronounced in DP cells. Bax, a pro-apoptotic member of the *Bcl-2* family, was used as a control. Transgenic over-expression of *Bax* specifically in the T-cell lineage sensitises T cells to apoptotic stimuli (DEX, gamma-irradiation and etoposide) to a similar degree to that seen in FTOC in this chapter (Brady, Salomons et al. 1996; Williams, Norton et al. 1998).

The vector control cells demonstrated no differences in survival, as did cells expressing a non-apoptotic target gene (Mspp1). Bcl-2 cells demonstrated considerable enrichment, consistently achieving over 99% hCD2 levels at 13 days. Continuous over-expression of potentially pro-apoptotic genes during thymocyte development may be placing cells at a survival disadvantage in the competitive FTOC microenvironment. Thymocytes expressing pro-apoptotic target genes may be more sensitive to endogenous glucocorticoids generated by TECs in the FTOC, and may be preferentially deleted during FTOC. This can be contrasted to Bcl-2 FTOCs, where infected cells are almost refractory to DEX-induced apoptosis and are highly competitive in FTOC; almost no uninfected cells remain at 13 days, and infected cells are sequentially enriched for those expressing even higher levels of Bcl-2.

Tdag8 and Tnfaip8 cells also proved at a disadvantage in repopulating depleted FTOCs, both in terms of cell number and relative expansion. Bcl-2 infected HPCs

produced more than 5 times as many thymocytes, and vector control HPCs more than 3 times as many, after 13 days FTOC. However, infected cells demonstrated no significant differences in their ability to develop normally into DP T cells, although a slight delay was evident. Compared to vector control FTOCs, Tdag8, Tnfaip8, and E4bp4 thymocytes appeared to lag slightly behind in development in CD25, CD44 plots, and significantly more vector control DP cells were present at 7 days FTOC. By 14 days these differences had disappeared. This difference may have been due to the pro-apoptotic effect of the target genes in some way slightly slowing but not preventing thymocyte development (of all potential target genes screened, only Tnfaip3(A20) blocked thymocyte development).

Only Bcl-2 and Bcl-XL cells showed significant differences in subset profiles at 13 days, the first being a slight DP enrichment, the second a switch to predominantly CD4 SP mature cells instead of CD8 SP cells. Transgenic over-expression of both pro-apoptotic and anti-apoptotic genes (*Bax and Bcl-2*) has previously been shown not to greatly affect lineage commitment, although anti-apoptotic *Bcl-2* family members have been shown to favour different SP lineages in different systems (Sentman, Shutter et al. 1991; Tao, Teh et al. 1994; Williams, Norton et al. 1998). Both *Bax* and *Bcl-2* have been published to interact with cell cycle genes and affect commitment to cell cycle entry (Brady, Gil-Gomez et al. 1996).

The relative loss of Tnfaip8 and E4bp4 cells in FTOC occurs more strongly after 7 days culture, at which time the more sensitive DP cells are beginning to appear. The loss of Tdag8 cells in FTOC was a more continuous effect, similar to Bax. This could be explained by Tnfaip8 and E4bp4 specifically affecting DP cells, while the pro-

apoptotic effect of Tdag8 acts throughout development. However, both DN and SP T cells are resistant to glucocorticoids (Berki, Palinkas et al. 2002), and therefore should not have been as susceptible to DEX-induced apoptosis.

Endogenous Tnfaip8 and E4bp4 are up-regulated in DP T cells, both more than six-fold, and subsequently down-regulated in SP cells. Tdag8 is only differentially regulated in CD4 SP cells. This suggests a function associated with DP cells, and would suit a hypothesis in which Tnfaip8 and E4bp4 target gene expression correlates with glucocorticoid-induced apoptosis, to which DP thymocytes are especially sensitive.

The up-regulation of Tdag8, Tnfaip8, and E4bp4 in response to DEX was also kinetically regulated. Most strikingly, the up-regulation of Tnfaip8 in response to DEX in conditions of Cdk2 inhibition is very high, peaking at over 200-fold at 6 hours normalised to 0 hour control. This contrasts with DEX alone at 6 hours, where the up-regulation is 5-fold. Our DNA microarray screen was designed to isolate targets of GC engagement upstream of Cdk2 activation. Tnfaip8 up-regulation is maximal when the apoptotic cascade induced by DEX is blockaded at Cdk2 inhibition. This might imply that Tnfaip8 is regulated proximally upstream, and that a large degree of the transient up-regulation is lost upon Cdk2 activation and resultant apoptosis.

Tdag8 and E4bp4 are maximally regulated in conditions of DEX and ROSC administration. Both also demonstrate higher levels of up-regulation in the presence of DEX alone compared to Tnfaip8, which may indicate a more distal (from Cdk2) or

directly genomic regulation. E4bp4 is regulated directly by GR, possessing a GRE in its promoter. Tnfaip8 does not, following *in silico* analysis of 3000bp sequence 5' of the *tnfaip8* transcriptional start site. Tdag8 also lacks a genomic GRE (Malone, Wang et al. 2004). The difference in up-regulation of Tnfaip8 may indicate a lesser mRNA stability (which would also correlate with the loss of Tnfaip8 up-regulation plus DEX minus ROSC), or divergent signalling (glucocorticoid-induced apoptosis is a highly multigenic process, reviewed (Lepine, Sulpice et al. 2005)).

Tnfaip8 has previously been identified as a target for NF-κB signalling, the human form being named NDED (NF-κB inducible Death Effector Domain containing protein) (You, Ouyang et al. 2001). Inhibition of NF-κB signalling by an NF-κB inhibitor BAY 11-7085 (which also completely blocked thymocyte apoptosis), almost completely abrogated Tdag8, Tnfaip8, and E4bp4 up-regulation. This implied that all 3 targets may also be downstream of NF-κB, which is a known protein-protein interaction target of GR nuclear translocation. Again, both Tnfaip8 and E4bp4 were maximally regulated in conditions of Cdk2 inhibition.

4.3.2. Over-expression of selected target genes affects apoptosis in FTOC.

We have confirmed that over-expression of target genes identified in our DNA microarray screen had a negative effect on thymocyte survival in FTOC. However this does not equate to a pro-apoptotic phenotype. Instead, the phenotype could be due to multiple effects, for example influence upon the cell cycle (e.g. *Bax*, which affects cell cycle entry), effects upon TCR rearrangement, or influencing cell survival signalling. Over-expression phenotypes are vulnerable to the artefactual effects that can be produced by the quantity of protein generated by expression from powerful

viral LTR promoters. To address this, apoptosis assays were performed to determine if over-expression of target genes could specifically affect apoptosis caused by an apoptotic stimulus.

Tdag8 and Tnfaip8 both synergised with DEX and markedly enhanced apoptosis, to a similar degree as *Bax*, which has previously been shown to accelerate apoptosis in response to apoptotic stimuli in a transgenic model (Brady, Salomons et al. 1996). *Tdag8* has also been shown to accelerate thymocyte apoptosis in response to Dex in transgenic mice, with transgenic thymocytes also sensitive to exponentially lower doses of DEX (Tosa, Murakami et al. 2003).

The enhancement in apoptosis in Tdag8 and Tnfaip8 cells (but not E4bp4) could be attributed to target gene over-expression. Within FTOCs, infected and uninfected were compared, and levels of apoptosis were greater in infected cells. The enhancement in apoptosis produced statistically significant increases ($p<0.05$) for Tdag8, Tnfaip8 and Bax. This implied that not only was expression of these genes deleterious for survival in FTOC, but expression could specifically enhance DEX-induced apoptosis in DP cells (gating for flow cytometry was manipulated to include only DP cells).The contrast to Bcl-2 FTOCs was also stark, with Bcl-2 FTOCs almost refractory to DEX. However, E4bp4 over-expression was not shown to significantly enhance DEX-induced apoptosis.

The over-expression of Tnfaip8 and Tdag8 could be enhancing apoptosis in a number of ways. Tdag8 is a G-protein-coupled receptor, and it has previously been hypothesised that large quantities of Tdag8 may sensitise cells to a pro-apoptotic

ligand already present. Alternatively, as a receptor, over-expression may produce sufficient quantities of active Tdag8 to induce apoptosis in the absence of exogenous agonist (Malone, Wang et al. 2004). In light of our work, it may be that over-expression of Tdag8 in a multigenic response may act to amplify apoptotic signals, which might then affect the balance of pro-apoptotic and anti-apoptotic *Bcl-2* family members, in much the same way as over-expression of Bax obviously affects the *Bax:Bcl-2* balance.

Tnfaip8 is a NF-κB inducible protein , and therefore downstream of one of the protein-protein interactions known to occur upon GC release from HSP90 sequestration and nuclear translocation (Ivanov and Nikolic-Zugic 1998). Tnfaip8 may be induced as a consequence of NF-κB/GR interaction and act to propagate the glucocorticoid response. When over-expressed, excess Tnfaip8 might sensitise cells to glucocorticoid concentrations to which the infected cell might otherwise be refractory.

Alternatively Tnfaip8 may act directly as a consequence of its putative DED domain, which shows a degree of homology to DEDs found in other DED-containing proteins. Tnfaip8 differs from most other DED-containing proteins however, as Tnfaip8 (You, Ouyang et al. 2001) is anti-apoptotic in response to TNF-α signalling in immortalised cell lines. DED proteins can be either pro-apoptotic or anti-apoptotic according to context. Tnfaip8 expression is also higher in lymphoid cells, suggesting that Tnfaip8 has a role in lymphoid cell death.

4.3.3. Over-expression of selected target genes affects survival and apoptosis in OP9-DL1 co-cultures.

The OP9-DL1 co-cultures system was also used to investigate apoptosis in target gene expressing HPCs. OP9-DL1 bone marrow stromal cells express the Notch ligand Delta-Like 1. This Notch signalling molecule drives development of DP T cells and CD8 SP cells (OP9-DL1 cells only express MHC class I). OP9-DL1 co-culture addressed the macrophage phagocytic clearance of apoptotic cells in FTOC, and removed some of the microenvironment competition effects of FTOC.

Infected HPCS cultured for 7, 12 and 17 days in OP9-DL1 co-culture demonstrated a similar, though less pronounced, loss in $hCD2^+$ infected cells when over-expressing the pro-apoptotic target gene Tnfaip8. It was also determined that over-expression of Bcl-2 and Bcl-XL increased the proportion of DP cells in cultures after 15 days, most likely due to the increased survival capacity of these cells. OP9-DL1 co-culture in our hands is nonetheless far less efficient at generating DP T cells compared to FTOC.

To investigate apoptosis in OP9-DL1 co-culture, fifteen day co-cultures were exposed to 0.5μM DEX for 12 hours. $CD8^+$, $hCD2^+$ infected cells expressing Tdag8, Tnfaip8 and Bax demonstrated higher levels of apoptosis than vector control, while Bcl-2-hCD2 and Bcl-XL-hCD2 cells were significantly more resistant than vector controls (all $p<0.01$). OP9-DL1 co-culture produced similar results to FTOC, demonstrating that HPCs that develop into thymocytes in this system are also more sensitive to DEX when over-expressing pro-apoptotic target genes

The results achieved in OP9-DL1 co-culture are very similar to FTOC. The most reasonable explanation for this is that we used two similar systems to generate DP cells. The DP T cells produced in OP9-DL1 co-culture are phenotypically very similar

to those produced in FTOC (Schmitt and Zuniga-Pflucker 2002), and it is therefore logical that both populations would be similarly sensitive to DEX. The major difference is that apoptotic cells are cleared by phagocytosis in FTOC, which does not occur in OP9-DL1 co-culture, and therefore levels of apoptosis in OP9-DL1 can be induced to much greater levels *in vitro* without needing to address the loss of the population being studied.

4.3.4. RNAi-mediated knockdown of Tnfaip8 affects apoptosis in FTOC.

A significant caveat to over-expression studies is that expressing large, non-physiological amounts of a specific protein from powerful exogenous promoters can produce aberrant phenotypes. We therefore sought to knock down expression of endogenous Tnfaip8 by means of RNA interference. The effect of knocking down Tdag8 expression has already been investigated (Malone, Wang et al. 2004), while *Tdag8*$^{-/-}$ mice exhibit no phenotype with respect to glucocorticoid-induced thymocyte apoptosis (Radu, Cheng et al. 2006).

Two retroviral microRNA constructs were generated that could knockdown expression of endogenous Tnfaip8 by more than 75%, in addition to a microRNA construct targeted against BimEl to act as a positive control. Expression of these constructs throughout thymocyte development had no effect upon the survival of infected cells despite the otherwise pro-apoptotic and anti-survival effect of over-expressing these genes. This might be explained by the mechanics of RNAi-mediated knockdown, which serves only to inhibit the expression of a proportion of the normal level of an endogenous protein, while over-expression studies can generate levels of protein well beyond normal physiological levels.

DP thymocytes expressing shRNA^{mir}s targeted against Tnfaip8 proved significantly more resistant to DEX than vector controls. These thymocyte were also comparably resistant to DEX as DP thymocytes expressing shRNA^{mir}s targeted against BIM isoforms. RNAi-mediated knockdown of BIM isoforms has previously been published to inhibit glucocorticoid-induced apoptosis in lymphoid cells (Abrams, Robertson et al. 2004). Therefore we have demonstrated that RNAi-mediated knockdown of Tnfaip8 is almost as effective at reducing DEX-induced apoptosis as RNAi-mediated knockdown of a *Bcl-2* family member known to be critical to glucocorticoid-induced thymocyte apoptosis. Reduction of the endogenous level of Tnfaip8 may reduce apoptosis in a similar way to knockdown of BIM, by affecting the Bax: Bcl-2 balance in favour of Bcl-2. Alternatively reduction of Tnfaip8 levels may inhibit the multigenic GC-induced apoptotic pathways by reducing the expression of a protein vital for propagating the apoptotic response.

This data strengthens the hypothesis that expression of endogenous Tnfaip8 is critical to glucocorticoid-induced thymocyte apoptosis.

4.3.5. Conclusions.

Data in this chapter demonstrated that target genes (*Tdag8* and *Tnfaip8*) identified by DNA microarray screen were pro-apoptotic and anti-survival in both FTOC and OP9-DL1 co-culture systems, while RNAi-mediated knockdown of Tnfaip8 was demonstrated to be anti-apoptotic. Tnfaip8 has therefore been identified as a novel target of glucocorticoids and potentially critical in thymocyte apoptosis. Further work is required to determine the molecular mechanism of this effect.

Of great interest would be the construction of a full murine knockout model for the *Tnfaip8* gene, to determine the phenotype of complete loss of Tnfaip8 upon thymocyte apoptosis. Mutagenesis assays at the putative DED domain would help to identify whether this region is directly responsible for the pro-apoptotic phenotype. This DNA microarray screen was constructed to identify pro-apoptotic genes upstream of Cdk2 activation. Immunoprecipitation assays could be performed to determine if Tnfaip8 binds directly to any of the known molecules in GC-induced apoptosis besides NF-κB, and to determine any mechanics of interaction with Cdk2.

Understanding the molecular interactions of Tnfaip8 may help shed light on the nature of its activity and potentially highlight a novel candidate for targeting in GC-resistant malignancies.

CHAPTER 5

RESULTS (3)

5.1. Background.

Death by neglect accounts for approximately 90% of thymocyte cell fate. The remaining 5% of cell death (excluding the 5% of cells that are positively selected and survive) is accounted for by negative selection, in which thymocytes exhibiting a TCR with an excessively strong avidity for self peptide:MHC complexes displayed by antigen-presenting cells are signalled to undergo apoptosis (**Introduction**), reviewed in (Sebzda, Mariathasan et al. 1999; Siggs, Makaroff et al. 2006).

The FTOC/retrovirus system described in the previous chapter was used to investigate candidate genes identified by the Affymetrix GeneChip® probe array screen to identify genes differentially regulated during antigen-mediated negative selection. We used a transgenic model in which F5 TCR Rag-$1^{-/-}$ Tap-$1^{-/-}$ thymocytes were exposed to the NP68 cognate antigen *in vivo*, and thymocytes harvested 6 hours following peptide injection. The transgenic thymocytes exposed to NP68 initiated negative selection in response to cognate antigen as thymic APCs processed and displayed peptide (Tarazona, Williams et al. 1998). Candidate genes were identified by DNA microarray analysis.

Confirmed candidate genes were cloned into pMSCV retroviral vectors, over-expressed in developing thymocytes and their effect upon thymocyte development and apoptosis assayed *in vitro*. A diagram of the antigen screen FTOC/retrovirus protocol is shown in figure **5.1**.

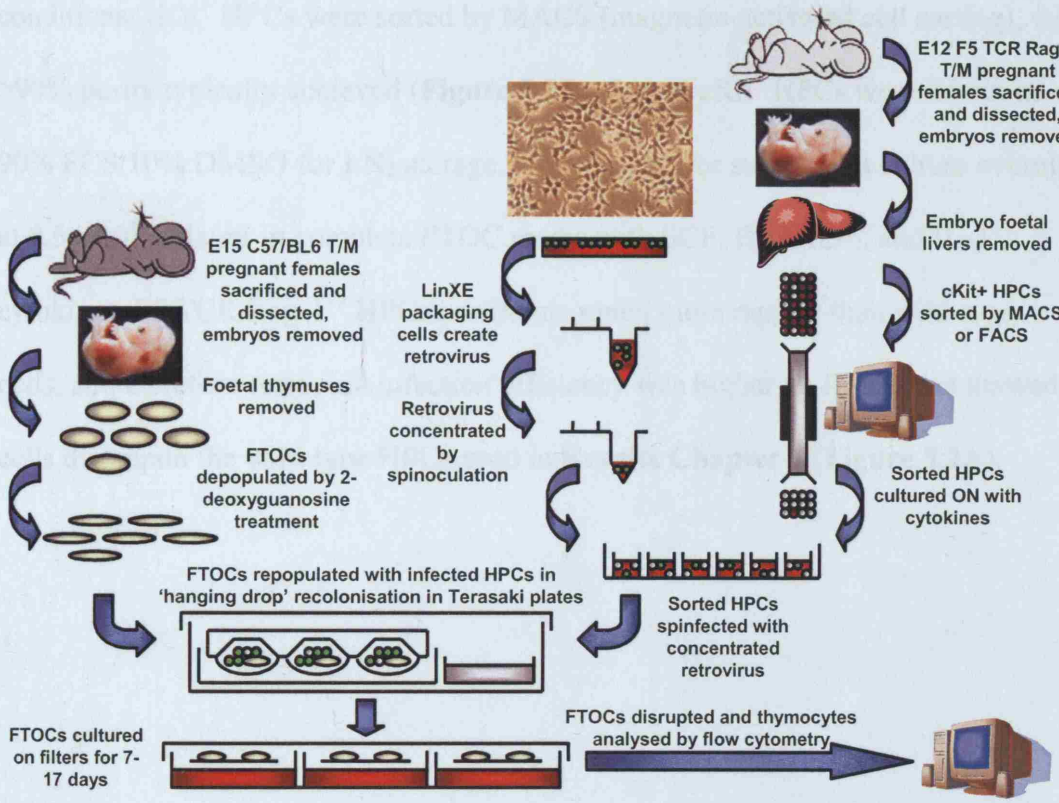

Figure 5.1. FTOC/retrovirus experimental strategy used to transduce primary HPCs and repopulate depleted FTOCs. cKit^{+} HPCs obtained by MACS from E12 F5 TCR Rag$^{-/-}$ time-mated foetal livers are retrovirally infected with pMSCV retroviral vectors, used to repopulate 2dGuo-depleted FTOCs, and cultured to produce DP T cells.

5.2. Results.

5.2.1. MACS sorting of F5 TCR Rag-1$^{-/-}$ murine foetal liver progenitors and concentration of retrovirus.

F5 TCR Rag-1$^{-/-}$ HPCs were obtained by time-mating F5 TCR males to Rag-1$^{-/-}$ (B10/N Rag-1$^{-/-}$-BAL) (NIMR, Mill Hill) females. For several experiments, females were super-ovulated. To obtain HPCs, E12 time-mated pregnant females were sacrificed, embryos removed and the foetal livers dissected out under sterile conditions. cKit^{+} HPCs were sorted by MACS (magnetic-activated cell sorting), with >90% purity typically achieved (**Figure 5.2B**). Sorted cKit^{+} HPCs were frozen in 90% FCS/10% DMSO for LN_2 storage, to be thawed for subsequent culture overnight at 0.5 x 10^6 cells/ml in complete FTOC media with SCF, IL-7, IL-6, and IL-3 cytokines. F5 TCR Rag-1$^{-/-}$ HPCs proliferate much more rapidly than wild-type cells, and therefore retroviral infection efficiency was higher on frozen and thawed cells than upon the wild-type HPCs used in **Results Chapter 2** (**Figure 5.2A**).

(A)

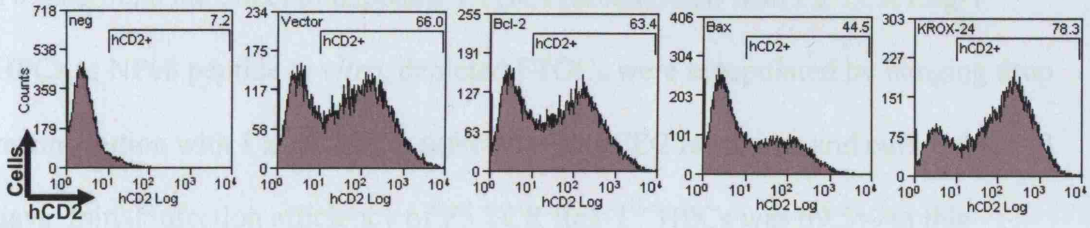

(B)

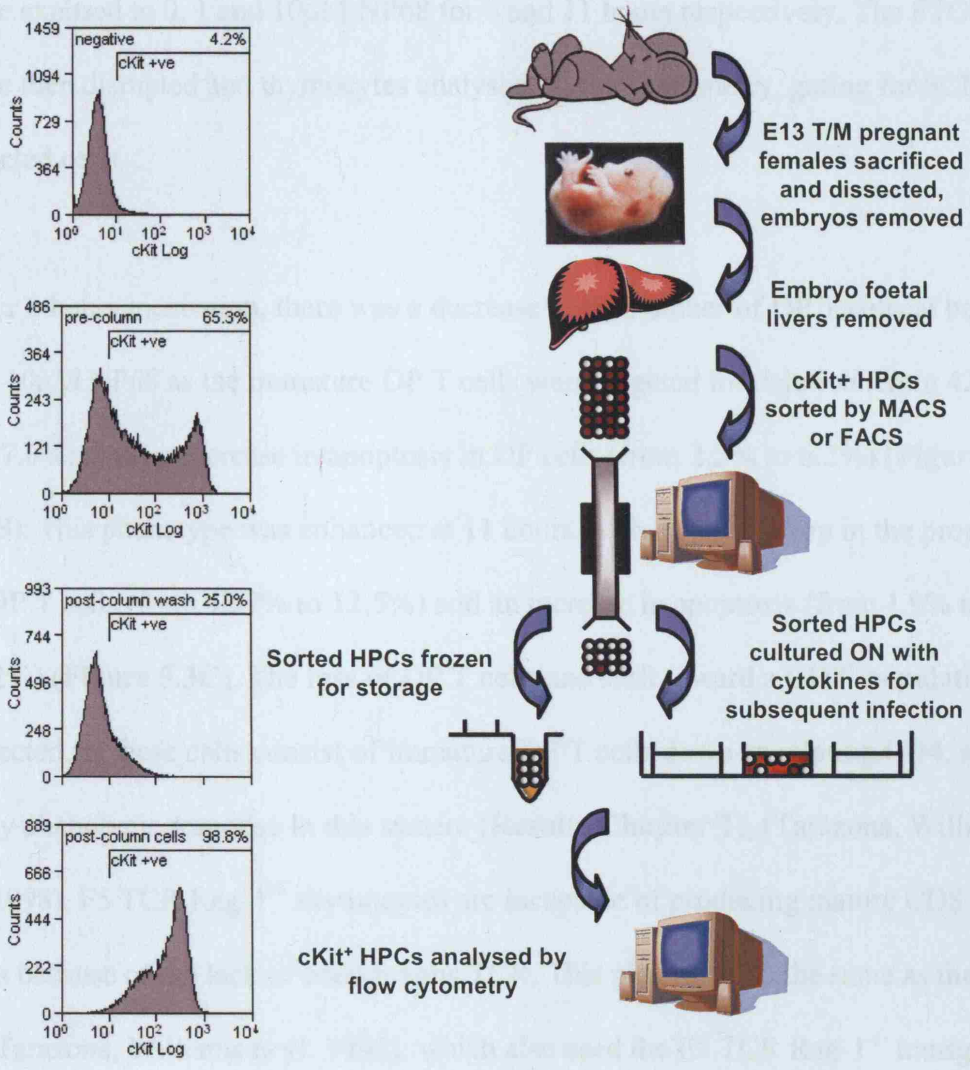

Figure 5.2. MACS sorting and retroviral infection of HPCs. (A) Flow cytometric analysis of HPCs used to repopulate FTOCs, stained for hCD2, 48 hours post infection. Numbers represent hCD2 infection efficiency (%) **(B)** Diagram of MACS sorting protocol. Flow cytometric analysis of F5 TCR Rag-1$^{-/-}$ HPCs during MACS sort, showing samples stained with anti-CD117 (cKit) 2B8 biotin-conjugated antibody, secondary streptavidin-PE.

5.2.2. F5 TCR Rag-1$^{-/-}$ HPCs inFTOCs are sensitive to antigen treatment in vitro.

To determine the effect of exposing FTOCs reconstituted with F5 TCR Rag-1$^{-/-}$ HPCs to NP68 peptide *in vitro*, depleted FTOCs were repopulated by hanging drop reconstitution with 1 x 10^4 HPCs infected with hCD2 retrovirus and cultured for 13 days. Initial infection efficiency of F5 TCR Rag-1$^{-/-}$ HPCs was 69.5% in this experiment (**Figure 5.3A**), representative of two. After 13 days FTOC, triplicates were exposed to 0, 1 and 10μM NP68 for 6 and 11 hours respectively. The FTOCs were then disrupted and thymocytes analysed by flow cytometry, gating for hCD2$^+$ infected cells.

After 6 hours incubation, there was a decrease in the number of DP T cells at both 1 and 10μM NP68 as the immature DP T cells were targeted for deletion (from 42.7% to 27.6%), and an increase in apoptosis in DP cells (from 2.2% to 6.2%) (**Figure 5.3B**). This phenotype was enhanced at 11 hours, with a further drop in the proportion of DP T cells (from 42.7% to 12.5%) and an increase in apoptosis (from 1.9% to 10.2%) (**Figure 5.3C**). The loss of DP T cells and shift toward a CD8$^+$ population is expected, as these cells consist of immature DP T cells down-regulating CD4, an early phenotypic response in this system (**Results Chapter 1**), (Tarazona, Williams et al. 1998). F5 TCR Rag-1$^{-/-}$ thymocytes are incapable of producing mature CD8 SP T cells because of the lack of endogenous TCR. This phenotype is the same as that seen in (Tarazona, Williams et al. 1998), which also used the F5 TCR Rag-1$^{-/-}$ transgenic model to assay the effect of NP68 cognate antigen upon negative selection both *in vivo* and *in vitro*.

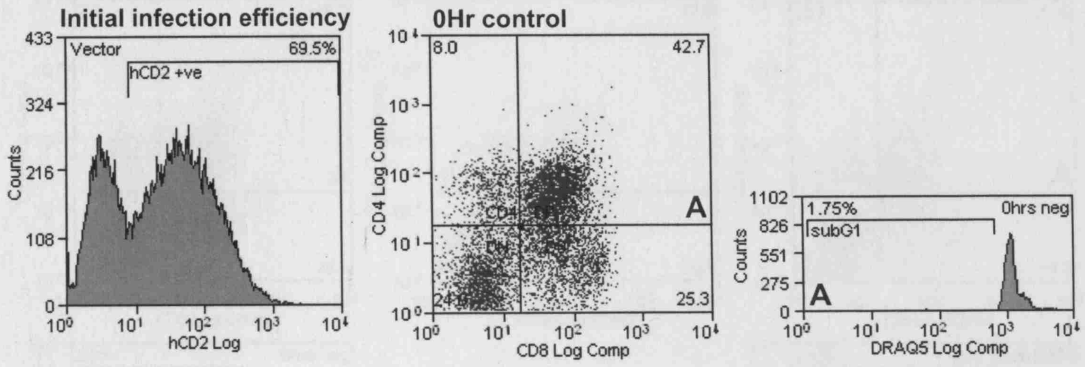

Figure 5.3A. F5 TCR Rag-1$^{-/-}$ HPCs in reconstituted FTOCs are sensitive to NP68 treatment in vitro. Flow cytometric analysis of F5 TCR Rag-1$^{-/-}$ HPCs used to repopulate FTOCs, stained for hCD2, 48 hours post infection. Flow cytometry of 0hr control F5 TCR Rag-1$^{-/-}$ thymocytes at 13 days, stained for CD4 and CD8, gated on live, hCD2^{+} cells. DRAQ5 subG1 quantification of apoptosis in hCD2^{+} cells.

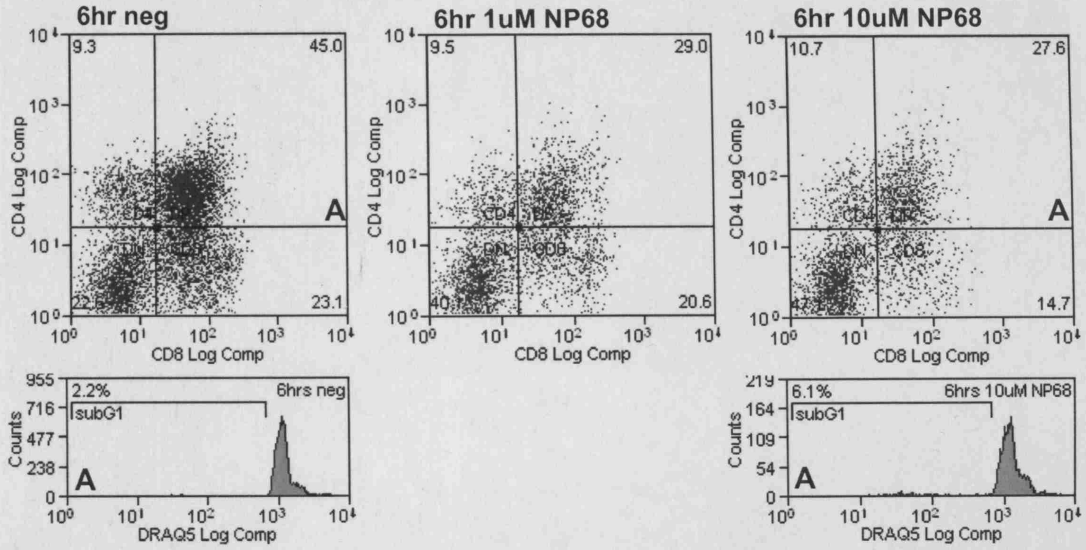

Figure 5.3B. F5 TCR Rag-1$^{-/-}$ HPCs in reconstituted FTOCs are sensitive to NP68 treatment in vitro. Flow cytometry of 6hr F5 TCR Rag-1$^{-/-}$ thymocytes at 13 days, stained for CD4 and CD8, gated on live, hCD2^{+} cells. DRAQ5 subG1 quantification of apoptosis in hCD2^{+} cells.

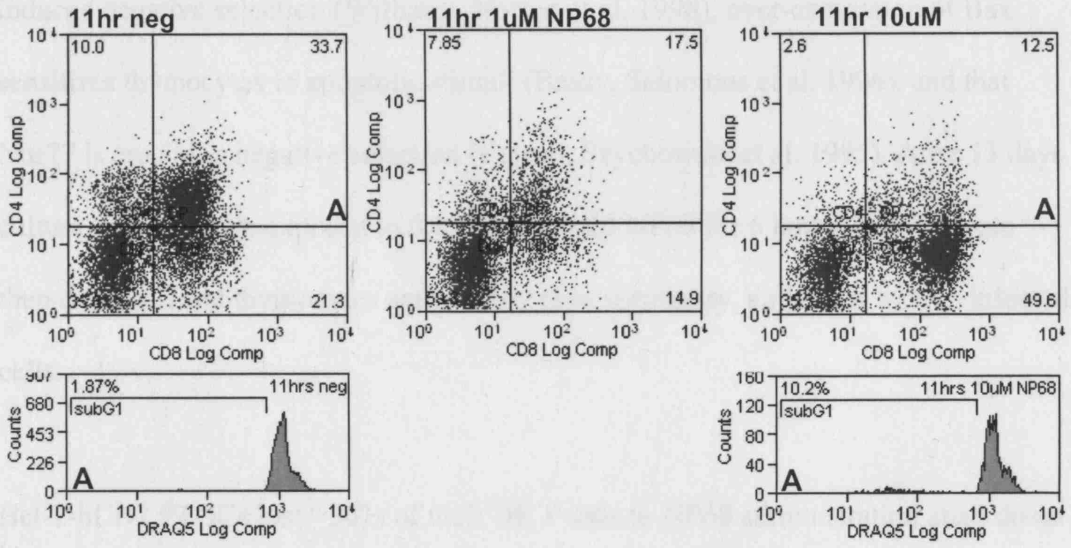

Figure 5.3C. F5 TCR Rag-1$^{-/-}$ HPCs in reconstituted FTOCs are sensitive to NP68 treatment in vitro. Flow cytometry of 11hr F5 TCR Rag-1$^{-/-}$ thymocytes at 13 days, stained for CD4 and CD8, gated on live, hCD2^{+} cells. DRAQ5 subG1 quantification of apoptosis in hCD2^{+} cells.

5.2.3. F5 TCR Rag-1$^{-/-}$ HPCs infected with hCD2, Bcl-2-hCD2, Nur77-hCD2 and Bax-hCD2 retroviruses in reconstituted FTOCs are differentially sensitive to NP68 treatment in vitro.

We wished to establish a system for assessing candidate genes involved in negative selection for their effect upon antigen-mediated deletion. Depleted FTOCs were repopulated by hanging drop recolonisation with 1 x 10^4 HPCs infected with hCD2, Bcl-2-hCD2, Nur77-hCD2 and Bax-hCD2 retroviruses. It has previously been established that over-expression of anti-apoptotic Bcl-2 is protective against antigen-induced negative selection (Williams, Norton et al. 1998), over-expression of Bax sensitizes thymocytes to apoptotic stimuli (Brady, Salomons et al. 1996), and that Nur77 is crucial in negative selection (Calnan, Szychowski et al. 1995). After 13 days culture, FTOCs were exposed to 0,1, 2.5 or 10μM NP68 for 6 hours. FTOCs were then disrupted and thymocytes analysed by flow cytometry, gating for hCD2$^+$ infected cells.

Bcl-2-hCD2 FTOCs lost ≈30% of their DP T cells to NP68 administration at all doses as a proportion of total numbers (**Figure 5.4**). hCD2 FTOCs demonstrated a greater loss in DP T cells, proportionately more than 50% at 10μM NP68. Bax-hCD2 FTOCs demonstrated an even greater loss in DP T cells, more than 80% at 10μM NP68. Nur77-hCD2 FTOCs produced considerably less DP T cells than other constructs, but a proportion greater than 50% were still deleted in response to 10μM NP68. This identified a clear difference in the sensitivity of transduced HPCs to NP68 cognate antigen *in vitro*, dependent on the nature of the over-expressing gene.

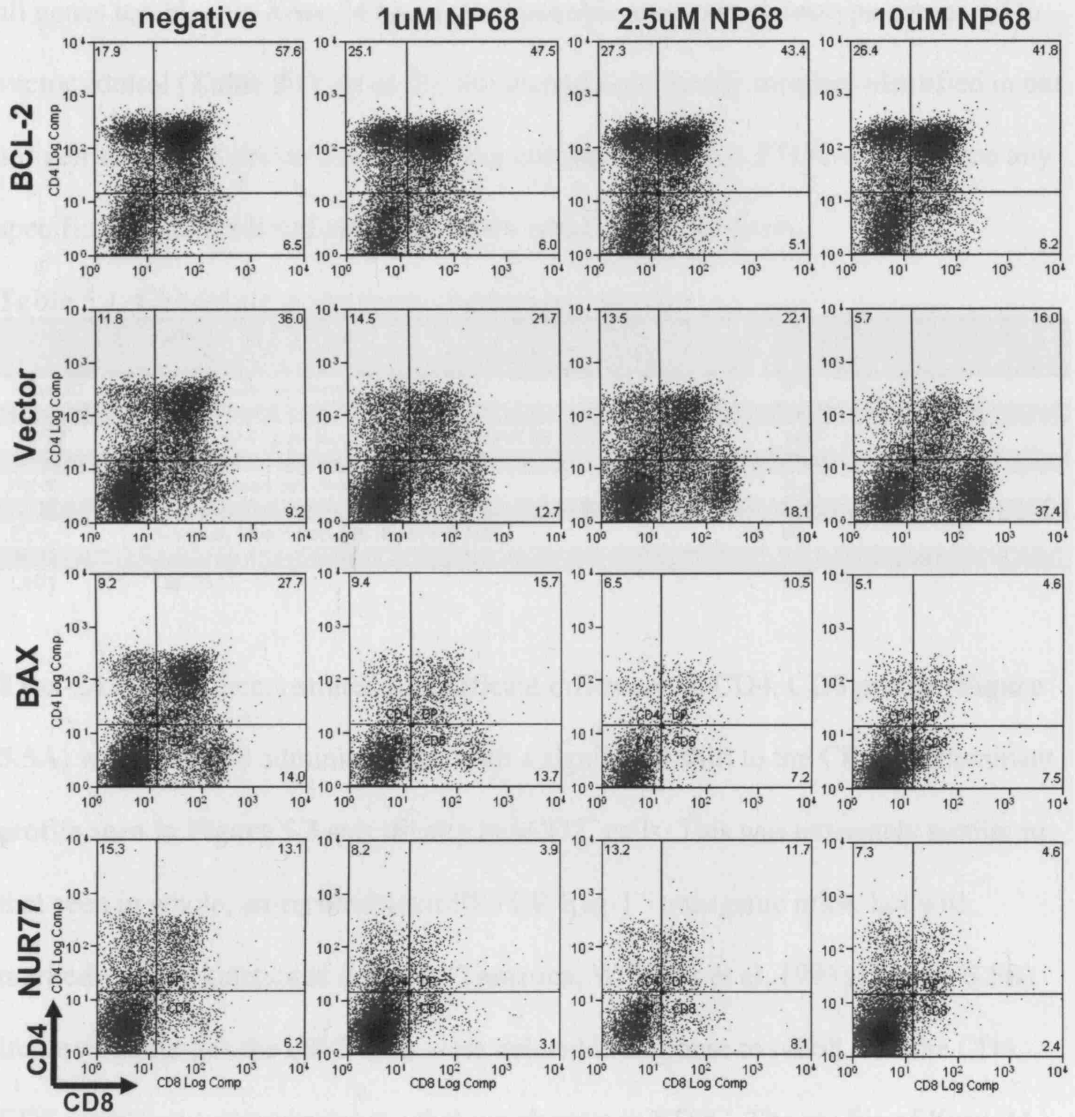

Figure 5.4. F5 TCR Rag-1$^{-/-}$ HPCs infected with hCD2, BCL-2-hCD2, NUR77-hCD2 and BAX-hCD2 retroviruses in reconstituted FTOCs are differentially sensitive to NP68 treatment in vitro. (A) Flow cytometry of F5 TCR Rag-1$^{-/-}$ thymocytes at 13 days, stained for CD4 and CD8. FTOCs were treated with 0, 1, 2.5 and 10μM NP68 for 6 hours.

5.2.4. Krox-24 F5 TCR Rag-1$^{-/-}$ FTOCs are sensitive to NP68 treatment in vitro.

To screen specific candidate genes, depleted FTOCs were repopulated by hanging drop recolonisation with 1 x 10^4 HPCs infected with pMSCV-hCD2 constructs expressing target genes, in an identical manner to that performed in section **5.2.3**. Of all genes tested, only *Krox-24* had a demonstrable apoptotic phenotype compared to vector control (**Table 5.1**). *Krox-20*, the second *Krox* family member identified in our antigen screen did not produce sufficient numbers of cells in FTOC to determine any specific antigen-mediated apoptotic effect within the test system.

Table 5.1. Candidate genes from the antigen screen.

Genes	Description/Function	Pro-apoptotic Phenotype?
Krox-20	Early growth response gene 2	?
Nab2	Ngfi-A binding protein 2	No
Nur77	Mouse N10 gene for a nuclear hormonal binding receptor.	**Yes**
Krox-24	Early growth response gene 1	**Yes**
Pd-1	Programmed cell death 1 gene	No
Nf-Atc	Mus musculus transcription factor NF-ATc isoform a (NF-ATca)	No
E25	putative; Mus musculus (E25) mRNA	No
Bcl-2	Anti-apoptotic member of Bcl-2 family	No, anti-apoptotic
Lef-1	Lef-1S	No

Krox-24 FTOCs demonstrated a significant difference in CD4, CD8 profile (**Figure 5.5A**) without NP68 administration, with a significant shift to the $CD8^+$ predominant profile seen in **Figure 5.3** specifically in $hCD2^+$ cells. This was extremely similar to that seen in whole, un-reconstituted F5 TCR Rag-$1^{-/-}$ transgenic mice, but with markedly faster kinetics of deletion (Tarazona, Williams et al. 1998) (**Figure 5.5B**). In previous studies the DP T cells were deleted in response to NP68, and the CD4, CD8 profiles are very similar to what we observe in FTOC. The profile of Krox-24 FTOCs was exacerbated in response to 10μM NP68 for 6 hours. The number of DP T cells was significantly lower than vector control both with and without NP68 administration. Therefore over-expression of Krox-24 may be having a marked effect upon negative selection and clonal deletion in this system.

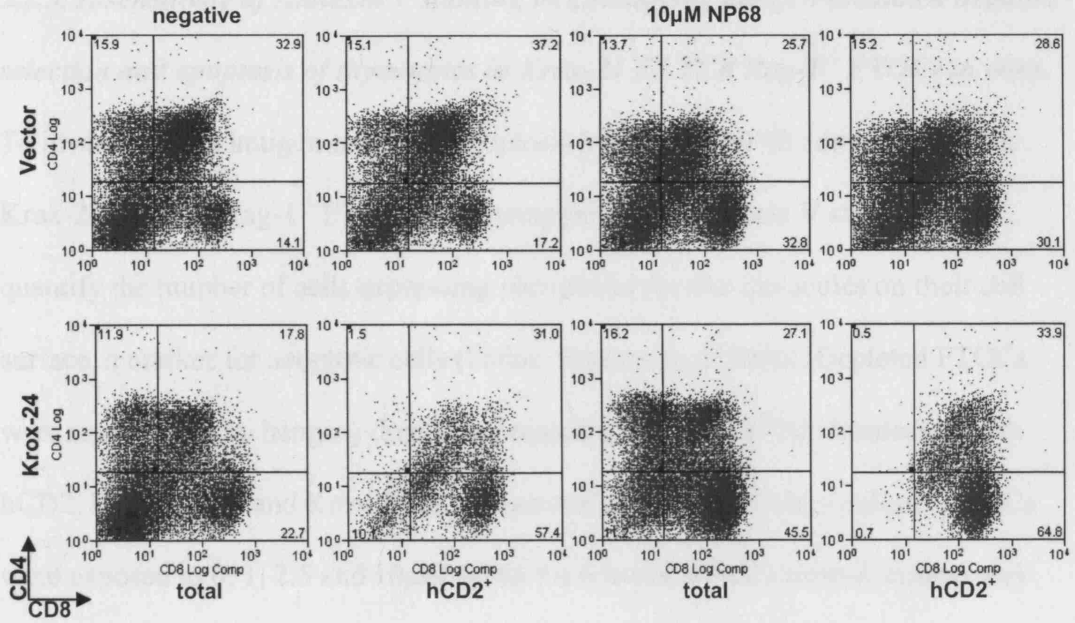

(B)

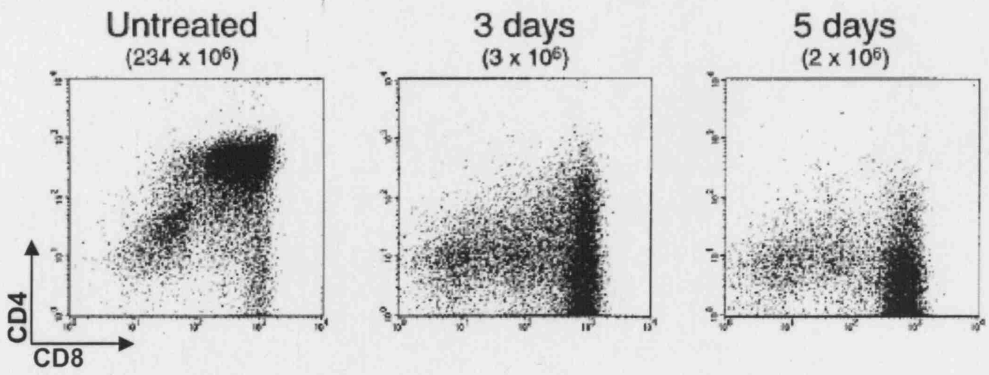

Taken from (Tarazona, Williams et al. 1998).

Figure 5.5. F5 TCR Rag-1$^{-/-}$ HPCs infected with Krox-24-hCD2 retrovirus in reconstituted FTOCs was differentially sensitive to NP68 treatment in vitro. (A) Flow cytometry of F5 TCR Rag-1$^{-/-}$ thymocytes at 13 days, stained for CD4 and CD8. FTOCs were treated with 0 and 10μM NP68 for 6 hours. FC plots show gating for total and hCD2^{+} cells only. **(B)** FC plots, stained for CD4 and CD8, showing deletion of F5 TCR Rag-1$^{-/-}$ thymocytes in transgenic mice over 5 day exposure to IP NP68. **Taken from (Tarazona, Williams et al. 1998).** Numbers represent absolute number of DP thymocytes in each thymus.

5.2.5. Insensitivity of Annexin V staining in quantifying antigen-mediated negative selection and apoptosis of thymocytes in Krox-24 F5 TCR Rag-1$^{-/-}$ FTOCs in vitro.

To investigate the antigen-mediated apoptosis induced by NP68 administration in Krox-24 F5 TCR Rag-1$^{-/-}$ FTOCs, we attempted to use Annexin V staining to quantify the number of cells expressing phosphatidylserine molecules on their cell surface, a marker for apoptotic cells (Fadok, Bratton et al. 2000). Depleted FTOCs were repopulated by hanging drop recolonisation with 1 x 10^4 HPCs infected with hCD2, Bcl-2-hCD2 and Krox-24-hCD2 retroviruses. After 13 days culture, FTOCs were exposed to 0, 1, 2.5 and 10μM NP68 for 6 hours. FTOCs were disrupted and thymocytes analysed by flow cytometry, gating for $CD8^+$ $hCD2^+$ cells. Although there was a trend in that Krox-24-hCD2 cells were more Annexin V^+ than hCD2 and Bcl-2-hCD2 controls, this was not statistically significant (**Figure 5.6**).

(A)

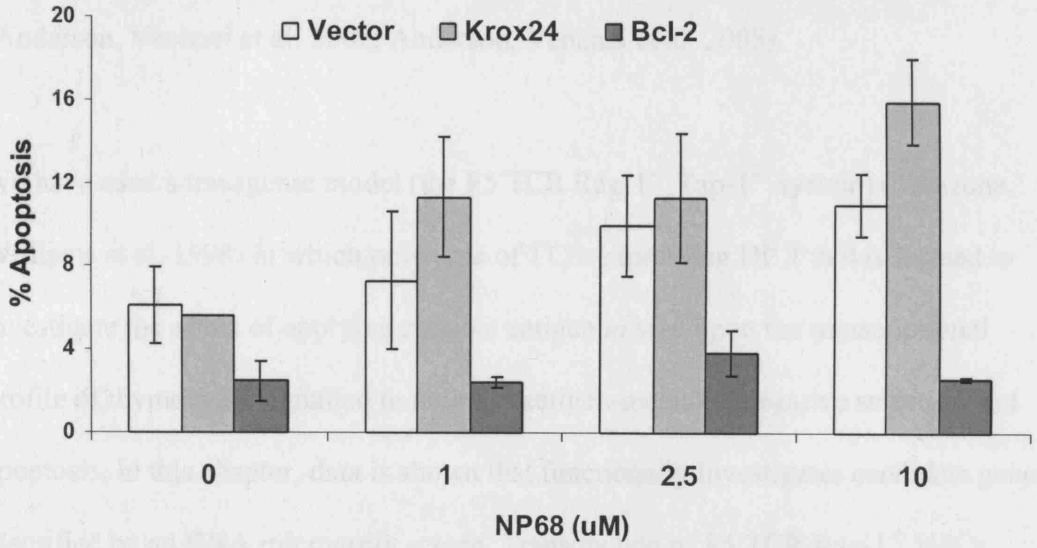

Figure 5.6. Insensitivity of Annexin V staining in quantifying antigen-mediated negative selection and apoptosis of thymocytes in Krox-24 F5 TCR Rag-1-/- ***FTOCs in vitro*** **(A)** Graph of flow cytometry of F5 TCR Rag-$1^{-/-}$ thymocytes at 13 days, stained for CD4, CD8, hCD2 and Annexin V to quantiy apoptotic cells. FTOCs were treated with 0, 1, 2.5 and 10μM NP68 for 6 hours. Mean ± SD, n=3.

5.3. Discussion.

Negative selection, in which thymocytes that elicit an excessively strong avidity for self peptide:MHC complexes are actively signalled to undergo apoptosis, is vital to prevent possible autoimmune reactions. Mutations that affect the efficiency of negative selection can profoundly affect the peripheral T cell repertoire with potentially catastrophic results for the individual. This is made obvious by the phenotype of *AIRE*$^{-/-}$ individuals, who are unable to negatively select a whole repertoire of DP T cells expressing a TCR with an excessive affinity for self-antigen (Anderson, Venanzi et al. 2002; Anderson, Venanzi et al. 2005).

We have used a transgenic model (the F5 TCR Rag-1$^{-/-}$ Tap-1$^{-/-}$ system) (Tarazona, Williams et al. 1998) in which only type of TCR-expressing DP T cell is formed to investigate the effect of applying cognate antigen *in vivo* upon the transcriptional profile of thymocytes signalled to undergo antigen-mediated negative selection and apoptosis. In this chapter, data is shown that functionally investigates candidate genes identified by an DNA microarray screen. Transduction of F5 TCR Rag-1$^{-/-}$ HPCs with retroviruses expressing Nur77, Bax and Bcl-2 prior to FTOC significantly affects thymocyte survival and markedly alters the sensitivity of DP thymocytes to NP68 cognate antigen in FTOC. We have also identified one gene, *Krox-24*, that appears to affect negative selection and apoptosis in FTOCs exposed to NP68 peptide.

5.3.1. Over-expression of Krox-24 affects negative selection in FTOC.

Data in this chapter confirmed that over-expression of Krox-24, identified as a candidate gene in our screen, apparently affects the phenotype of negatively selecting cells in FTOC. Of 9 genes investigated using the FTOC/retrovirus system, one

demonstrated a potential negative selection phenotype, one was a confirmed pro-apoptotic member of the *Nur77* family (Nur77), while five proved non-functional with respect to negative selection. Krox-20 generated too few infected DP T cells to determine any apoptotic phenotype.

Constitutive over-expression of Krox-24 in HPCs in FTOC drives development of a CD4, CD8 profile that is markedly reminiscent of that seen in F5 TCR Rag-$1^{-/-}$ cells in response to NP68 cognate antigen both *in vivo* and *in vitro* (Tarazona, Williams et al. 1998). This profile is enhanced in response to NP68 and is an exaggerated version of that seen in vector control F5 TCR Rag-$1^{-/-}$ cells in response to NP68. The contrast between infected and total cells in Krox-24 FTOCs is also significant, identifying two quite phenotypically distinct populations of cells. The extent of loss of F5 TCR Rag-$1^{-/-}$ DP cells is similar to that seen in Nur77 FTOCs, which generate considerably less DP T cells than vector controls but without demonstrating the $CD8^+$ phenotype. The appearance of the $CD8^+$ population is not a result of positive selection as this is not possible in F5 TCR Rag-$1^{-/-}$ cells because of the lack of endogenous TCR (Spanopoulou, Roman et al. 1994; Tarazona, Williams et al. 1998). This data demonstrates a clear enhancement of the phenotype seen in vector control FTOCs in cells expressing Krox-24, and may be indicative of an enhanced sensitivity to NP68-induced deletion and apoptosis.

We were unable to quantify a statistically significant enhancement of apoptosis in Krox-24 FTOCs with Annexin V staining, although a trend was evident. Krox-24 F5 TCR Rag-$1^{-/-}$ cells were significantly more apoptotic than Bcl-2 controls ($p=0.002$),

but the comparison with vector controls was not significant (p=0.07) at 10μM NP68 for 6 hours.

Krox-20 and *Krox-24*, also termed *Egr-2* and *Egr-1*, are members of the *Egr* family (*Egr-1-4*), three of which are expressed during thymocyte differentiation (Carter, Lefebvre et al. 2007). *In vivo* they are important in pre-TCR signalling and β-selection, but demonstrate considerable functional redundancy between forms. *Krox-24/Egr-1* deficient thymocytes are slightly defective in positive selection but not β-selection (Bettini, Xi et al. 2002).

The mechanism underlying the negative selection phenotype we observed may be that over-expression of Krox-24, which is known to be a downstream target of TCR engagement (Basson, Wilson et al. 2000; Bettini, Xi et al. 2002; Carleton, Haks et al. 2002; Decker, Nehmann et al. 2003; DeRyckere, Mann et al. 2003), might induce a negative selection response even in the absence of TCR engagement, with the phenotype more apparent upon TCR engagement. Negative selection occurs via the Jnk and p38-MapK pathways (Rincon, Whitmarsh et al. 1998), and Krox-24 has been shown to be a downstream target of the Jnk pathway in other systems (Gururajan, Chui et al. 2005; Ke, Gururajan et al. 2006). Krox-24 has also been shown to interact at the protein level with another DNA microarray screen target c-Jun, also part of the Jnk pathway (Levkovitz and Baraban 2002). Therefore over-expression of Krox-24 may result in the initiation of negative selection signalling that would otherwise be signalled by the JNK pathway in response to TCR engagement. This negative selection response might also be sensitised to the effects of TCR signalling when it occurs, as seen in the addition of NP68 in our system.

5.3.2. Current and future work.

In order to further study the effect of Krox-24 upon negative selection and apoptosis in the F5 TCR Rag-$1^{-/-}$ FTOC system, we have generated retroviral $shRNA^{mir}$ knockdown constructs targeting Krox-24, Krox-20, Nur77 and Bim targets. We are currently undertaking FTOC experiments in which expression of these four target genes is knocked down using RNA interference, alongside pro-apoptotic and anti-apoptotic controls. In doing this we hope to ascertain the requirement for expression of Krox-24 (and in parallel Krox-20, and also simultaneous knockdown of both forms) in negative selection in response to NP68 in the F5 TCR Rag-$1^{-/-}$ FTOC system.

CHAPTER 6

CONCLUDING REMARKS

6. Introduction.

6.1. Achievement of project aims.

The aim of this PhD project was to identify novel genes involved in regulating two models of thymocyte apoptosis, the first a model for glucocorticoid-induced thymocyte apoptosis, the second a transgenic model for antigen-mediated negative selection. The first objective was to perform two DNA microarray screens to identify differentially regulated candidate genes. Subsequently an *in vitro* system was to be established to investigate functional expression of candidate genes using retroviral transfer of target genes into primary HPCs and reconstitution of FTOC (and also OP9-DL1 co-culture). Genes shown to have a functional effect in these assays were then to be further investigated in FTOC, with possible further analysis using RNAi-mediated knockdown systems. Data from these DNA microarray screens and functional analyses could then identify potentially novel targets important in thymocyte apoptosis.

6.2. Conclusions.

Two DNA microarray screens were performed on thymocytes, one identifying candidate genes regulated by dexamethasone, and the other identifying candidate genes for involvement in antigen-mediated negative selection. Genes up-regulated by glucocorticoids in conditions of Cdk2 inhibition included Tdag8, E4bp4, Tnfaip8, Mspp1, Fkbp51, Tnfaip3(A20) and BimEL. Several of these targets had been implicated in previous studies (**Results Chapter 1**). Transcripts identified in the F5 TCR $Rag^{-/-}$ $Tap^{-/-}$ transgenic model for negative selection in response to NP68 cognate antigen included Nur77, Krox-20, Krox-24, Nab2, c-Fos and Bcl-2, and again several of these targets had been implicated in previous studies (**Results Chapter 1**). Each of

these genes was shown to be consistently up-regulated in independently derived, GC-treated thymocytes by real-time qPCR analysis, validating these as genuinely regulated genes.

A retroviral transduction/foetal thymic organ culture system was established to investigate the functional effects of over-expressing these genes upon T cell development and apoptosis. The cDNAs of these genes were cloned into a modified pMSCV vector, retroviruses generated and used to infect primary HPCs and then reconstitute depleted FTOCs. Bax, Bcl-2, and Bcl-XL constructs were used as controls. From the glucocorticoid screen, Tdag8, Tnfaip8 and E4bp4 were confirmed to be deleterious in terms of survival in FTOC, while Tdag8 and Tnfaip8 were confirmed to markedly enhance DEX-induced apoptosis in both FTOC and OP9-DL1 co-culture. Tnfaip8 and E4bp4 were also demonstrated to be up-regulated following the DN to DP transition, adding weight to the hypothesis that they might be involved in thymocyte apoptosis *in vitro*. RNAi-mediated knockdown of Tnfaip8 markedly reduced thymocyte apoptosis in response to glucocorticoids, to a similar degree as knocking down BimEL.

The data in Chapters 3 and 4 might suggest a mechanism for Tnfaip8 action. Tnfaip8 as a target of DEX may be one of the initial targets of the GC response, and may be directly induced by NF-κB (You, Ouyang et al. 2001) as a result of its interaction with homodimerized, nuclear GR. Tnfaip8 is also highly regulated upstream of Cdk2 activation and might interact with mitochondrial target genes further downstream (courtesy of the putative DED domain) to promote the executioner stage of apoptosis. Over-expression of Tnfaip8 may sensitise cells to a GC-induced apoptotic stimulus,

while RNAi-mediated knockdown might rob the cell of effective levels of an apoptotic effector gene, thus delaying or reducing the apoptotic response.

The retrovirus/FTOC system was also used to functionally test candidate genes identified in our antigen screen. Krox-24 was demonstrated to affect the sensitivity of retrovirally infected thymocytes to NP68 cognate antigen in the F5 TCR Rag-$1^{-/-}$ FTOC system, rendering them more sensitive in terms of negative selection and clonal deletion than vector control. RNAi-mediated knockdown is currently ongoing to determine if the reduction of Krox-20 and Krox-24 levels abrogates the deletion mediated by cognate antigen *in vitro*.

6.3. Future Work.

6.3.1. Tnfaip8 in glucocorticoid-induced thymocyte apoptosis.

Tnfaip8 has been confirmed as a target gene in DEX-induced thymocyte apoptosis; over-expression sensitises thymocytes to apoptosis, while RNAi-mediated knockdown makes thymocytes more resistant. Further functional analysis needs to be performed to determine the molecular mechanism behind this phenotype.

Constitutive over-expression of Tnfaip8 in HPCs is deleterious to survival and sensitising to DEX-induced apoptosis in FTOC. Inducible expression of Tnfaip8 would be beneficial in controlling the temporal expression of Tnfaip8, with expression switched on specifically in apoptotically sensitive DP cells. Constitutive expression of Tnfaip8, a pro-apoptotic molecule, may select for thymocytes that are more refractory to apoptotic signalling by means of some other aspect of their development, and inducible expression would bypass this potential caveat.

Unfortunately we were unable to demonstrate an effect upon apoptosis when the Tnfaip8 coding region was fused to the ligand binding domain of the tamoxifen sensitive oestrogen receptor (Littlewood, Hancock et al. 1995), which would have made expression dependent upon tamoxifen administration. This method is however inferior to the TET-inducible system (Gossen, Freundlieb et al. 1995), as not all proteins can be successfully fused to the oestrogen receptor while maintaining a tightly regulated, tamoxifen-sensitive degree of expression. Construction of a TET-inducible system for inducibly expressing *tnfaip8* in FTOC would be highly advantageous, but is potentially difficult because of the need to screen TET-inducible clones for inducibility and lack of leaky expression, which is much easier in immortalised cell lines than in primary cultures. A means of bypassing this would be the construction of a *tnfaip8* transgenic line expressing a TET-inducible Tnfaip8 transgene under the regulation of the Lck proximal promoter (Allen, Forbush et al. 1992), targeting expression specifically to T-lymphocyte progenitors. Fully screened inducible Tnfaip8 transgenics could then be used in DNA microarray analysis to identify target genes of *Tnfaip8* expression, with the possible addition of cycloheximide to induce only primary targets in thymocytes treated with apoptotic stimuli.

In addition to an inducible form of expression of Tnfaip8, mutational analysis of the putative DED domain would be advantageous in demonstrating whether this region is responsible for the pro-apoptotic effect of Tnfaip8. Apart from removing the DED domain, comparative analysis with other DED domain family proteins has highlighted 2 regions critical for DED domain–induced apoptosis in other family members

(Kumar, Whiteside et al. 2000). The corresponding amino acids in Tnfaip8 could be altered by site-directed mutagenesis.

RNAi-mediated knockdown of Tnfaip8 reduced the sensitivity of infected thymocytes to DEX. It would be very interesting to examine the phenotype of Tnfaip8 murine knockout mice. This would permit the molecular dissection of the loss of Tnfaip8 upon thymocyte development and apoptosis, by enabling comparison of KO and WT littermate control thymocytes in terms of development and their response to apoptotic stimuli. In comparison, *Tdag8*$^{-/-}$ mice have already been constructed and demonstrated to have no phenotype in terms of development or their response to apoptotic stimuli, but work is currently undergoing to determine if this due to functional redundancy with other family member proteins (Radu, Cheng et al. 2006). We have however already shown that Tnfaip8 is required for GC-induced apoptosis in thymocytes (and therefore not redundant), and therefore the KO mice should demonstrate an interesting phenotype.

6.3.2. Krox-24 in antigen-mediated negative selection.

Krox-24 was demonstrated to apparently affect the sensitivity of infected thymocytes to NP68 cognate antigen in the F5 TCR Rag-1$^{-/-}$ FTOC system, rendering them more sensitive in terms of negative selection than vector control. We are currently undertaking RNAi-mediated knockdown of Krox-24 and Krox-20 levels to determine the effect upon antigen-mediated negative selection in response to NP68.

6.4. Final conclusions.

Tnfaip8 is a pro-apoptotic target gene of glucocorticoids in thymocytes. When over-expressed, Tnfaip8 enhances GC-induced apoptosis in response to DEX, and when knocked down using RNAi, reduces GC-induced apoptosis. *Tnfaip8* is also up-regulated in DP cells. Further examination of the role of *Tnfaip8* in thymocyte apoptosis may help identify other targets in the GC-induced apoptotic cascade, and promote a greater understanding of the genes that initiate the glucocorticoid response. Further examination of the molecular mechanism underlying the pro-apoptotic phenotype of *Tnfaip8* would also prove interesting both in terms of the regulation of thymocyte apoptosis, and in highlighting targets for therapy in GC-resistant malignancies.

REFERENCES

Abrams, M.T., Robertson, N.M., Yoon, K., and Wickstrom, E. 2004. Inhibition of glucocorticoid-induced apoptosis by targeting the major splice variants of BIM mRNA with small interfering RNA and short hairpin RNA. J Biol Chem 279(53): 55809-55817.

Adams, J.M. and Cory, S. 1998. The Bcl-2 protein family: arbiters of cell survival. Science 281(5381): 1322-1326.

Adolfsson, J., Borge, O.J., Bryder, D., Theilgaard-Monch, K., Astrand-Grundstrom, I., Sitnicka, E., Sasaki, Y., and Jacobsen, S.E. 2001. Upregulation of Flt3 expression within the bone marrow Lin(-)Sca1(+)c-kit(+) stem cell compartment is accompanied by loss of self-renewal capacity. Immunity 15(4): 659-669.

Adolfsson, J., Mansson, R., Buza-Vidas, N., Hultquist, A., Liuba, K., Jensen, C.T., Bryder, D., Yang, L., Borge, O.J., Thoren, L.A., Anderson, K., Sitnicka, E., Sasaki, Y., Sigvardsson, M., and Jacobsen, S.E. 2005. Identification of Flt3+ lympho-myeloid stem cells lacking erythro-megakaryocytic potential a revised road map for adult blood lineage commitment. Cell 121(2): 295-306.

Akashi, K., Traver, D., Miyamoto, T., and Weissman, I.L. 2000. A clonogenic common myeloid progenitor that gives rise to all myeloid lineages. Nature 404(6774): 193-197.

Allen, J.M., Forbush, K.A., and Perlmutter, R.M. 1992. Functional dissection of the lck proximal promoter. Mol Cell Biol 12(6): 2758-2768.

Allman, D., Sambandam, A., Kim, S., Miller, J.P., Pagan, A., Well, D., Meraz, A., and Bhandoola, A. 2003. Thymopoiesis independent of common lymphoid progenitors. Nat Immunol 4(2): 168-174.

Anderson, G., Moore, N.C., Owen, J.J., and Jenkinson, E.J. 1996a. Cellular interactions in thymocyte development. Annu Rev Immunol 14: 73-99.

Anderson, K.L., Anderson, G., Michell, R.H., Jenkinson, E.J., and Owen, J.J. 1996b. Intracellular signaling pathways involved in the induction of apoptosis in immature thymic T lymphocytes. J Immunol 156(11): 4083-4091.

Anderson, M.K. 2006. At the crossroads: diverse roles of early thymocyte transcriptional regulators. Immunol Rev 209: 191-211.

Anderson, M.K., Hernandez-Hoyos, G., Dionne, C.J., Arias, A.M., Chen, D., and Rothenberg, E.V. 2002a. Definition of regulatory network elements for T cell development by perturbation analysis with PU.1 and GATA-3. Dev Biol 246(1): 103-121.

Anderson, M.K., Weiss, A.H., Hernandez-Hoyos, G., Dionne, C.J., and Rothenberg, E.V. 2002b. Constitutive expression of PU.1 in fetal hematopoietic progenitors blocks T cell development at the pro-T cell stage. Immunity 16(2): 285-296.

Anderson, M.S., Venanzi, E.S., Chen, Z., Berzins, S.P., Benoist, C., and Mathis, D. 2005. The cellular mechanism of Aire control of T cell tolerance. Immunity 23(2): 227-239.

Anderson, M.S., Venanzi, E.S., Klein, L., Chen, Z., Berzins, S.P., Turley, S.J., von Boehmer, H., Bronson, R., Dierich, A., Benoist, C., and Mathis, D. 2002c. Projection of an immunological self shadow within the thymus by the aire protein. Science 298(5597): 1395-1401.

Ardavin, C., Wu, L., Li, C.L., and Shortman, K. 1993. Thymic dendritic cells and T cells develop simultaneously in the thymus from a common precursor population. Nature 362(6422): 761-763.

Arzt, E., Kovalovsky, D., Igaz, L.M., Costas, M., Plazas, P., Refojo, D., Paez-Pereda, M., Reul, J.M., Stalla, G., and Holsboer, F. 2000. Functional cross-talk among cytokines, T-cell receptor, and glucocorticoid receptor transcriptional activity and action. Ann N Y Acad Sci 917: 672-677.

Asamoto, H. and Mandel, T.E. 1981. Thymus in mice bearing the Steel mutation. Morphologic studies on fetal, neonatal, organ-cultured, and grafted fetal thymus. Lab Invest 45(5): 418-426.

Ashwell, J.D., Lu, F.W., and Vacchio, M.S. 2000. Glucocorticoids in T cell development and function*. Annu Rev Immunol 18: 309-345.

Ayroldi, E., Migliorati, G., Bruscoli, S., Marchetti, C., Zollo, O., Cannarile, L., D'Adamio, F., and Riccardi, C. 2001. Modulation of T-cell activation by the glucocorticoid-induced leucine zipper factor via inhibition of nuclear factor kappaB. Blood 98(3): 743-753.

Baba, Y., Pelayo, R., and Kincade, P.W. 2004. Relationships between hematopoietic stem cells and lymphocyte progenitors. Trends Immunol 25(12): 645-649.

Bain, G., Romanow, W.J., Albers, K., Havran, W.L., and Murre, C. 1999. Positive and negative regulation of V(D)J recombination by the E2A proteins. J Exp Med 189(2): 289-300.

Balciunaite, G., Ceredig, R., and Rolink, A.G. 2005. The earliest subpopulation of mouse thymocytes contains potent T, significant macrophage, and natural killer cell but no B-lymphocyte potential. Blood 105(5): 1930-1936.

Basson, M.A., Wilson, T.J., Legname, G.A., Sarner, N., Tomlinson, P.D., Tybulewicz, V.L., and Zamoyska, R. 2000. Early growth response (Egr)-1 gene induction in the thymus in response to TCR ligation during early steps in positive selection is not required for CD8 lineage commitment. J Immunol 165(5): 2444-2450.

Benlagha, K., Kyin, T., Beavis, A., Teyton, L., and Bendelac, A. 2002. A thymic precursor to the NK T cell lineage. Science 296(5567): 553-555.

Benz, C. and Bleul, C.C. 2005. A multipotent precursor in the thymus maps to the branching point of the T versus B lineage decision. J Exp Med 202(1): 21-31.

Berg, L.J., Pullen, A.M., Fazekas de St Groth, B., Mathis, D., Benoist, C., and Davis, M.M. 1989. Antigen/MHC-specific T cells are preferentially exported from the thymus in the presence of their MHC ligand. Cell 58(6): 1035-1046.

Berki, T., Palinkas, L., Boldizsar, F., and Nemeth, P. 2002. Glucocorticoid (GC) sensitivity and GC receptor expression differ in thymocyte subpopulations. Int Immunol 14(5): 463-469.

Berthet, C., Aleem, E., Coppola, V., Tessarollo, L., and Kaldis, P. 2003. Cdk2 knockout mice are viable. Curr Biol 13(20): 1775-1785.

Berthet, C. and Kaldis, P. 2006. Cdk2 and Cdk4 cooperatively control the expression of Cdc2. Cell Div 1: 10.

Berthet, C., Rodriguez-Galan, M.C., Hodge, D.L., Gooya, J., Pascal, V., Young, H.A., Keller, J., Bosselut, R., and Kaldis, P. 2007. Hematopoiesis and thymic apoptosis are not affected by the loss of Cdk2. Mol Cell Biol.

Bettini, M., Xi, H., Milbrandt, J., and Kersh, G.J. 2002. Thymocyte development in early growth response gene 1-deficient mice. J Immunol 169(4): 1713-1720.

Bhandoola, A. and Sambandam, A. 2006. From stem cell to T cell: one route or many? Nat Rev Immunol 6(2): 117-126.

Bommhardt, U., Scheuring, Y., Bickel, C., Zamoyska, R., and Hunig, T. 2000. MEK activity regulates negative selection of immature CD4+CD8+ thymocytes. J Immunol 164(5): 2326-2337.

Bouillet, P., Purton, J.F., Godfrey, D.I., Zhang, L.C., Coultas, L., Puthalakath, H., Pellegrini, M., Cory, S., Adams, J.M., and Strasser, A. 2002. BH3-only Bcl-2 family member Bim is required for apoptosis of autoreactive thymocytes. Nature 415(6874): 922-926.

Brady, H.J. and Gil-Gomez, G. 1998. Bax. The pro-apoptotic Bcl-2 family member, Bax. Int J Biochem Cell Biol 30(6): 647-650.

-. 1999. The cell cycle and apoptosis. Results Probl Cell Differ 23: 127-144.

Brady, H.J., Gil-Gomez, G., Kirberg, J., and Berns, A.J. 1996a. Bax alpha perturbs T cell development and affects cell cycle entry of T cells. Embo J 15(24): 6991-7001.

Brady, H.J., Salomons, G.S., Bobeldijk, R.C., and Berns, A.J. 1996b. T cells from baxalpha transgenic mice show accelerated apoptosis in response to stimuli but do not show restored DNA damage-induced cell death in the absence of p53. gene product in. Embo J 15(6): 1221-1230.

Brewer, J.A., Kanagawa, O., Sleckman, B.P., and Muglia, L.J. 2002a. Thymocyte apoptosis induced by T cell activation is mediated by glucocorticoids in vivo. J Immunol 169(4): 1837-1843.

Brewer, J.A., Vogt, S.K., Sleckman, B.P., Swat, W., Kanagawa, O., and Muglia, L.J. 2002b. Knock-ins and conditional knockouts: in vivo analysis of glucocorticoid receptor regulation and function. Endocr Res 28(4): 545-550.

Byrd, V.M., Ballard, D.W., Miller, G.G., and Thomas, J.W. 1999. Fibroblast growth factor-1 (FGF-1) enhances IL-2 production and nuclear translocation of NF-kappaB in FGF receptor-bearing Jurkat T cells. J Immunol 162(10): 5853-5859.

Calnan, B.J., Szychowski, S., Chan, F.K., Cado, D., and Winoto, A. 1995. A role for the orphan steroid receptor Nur77 in apoptosis accompanying antigen-induced negative selection. Immunity 3(3): 273-282.

Capone, M., Hockett, R.D., Jr., and Zlotnik, A. 1998. Kinetics of T cell receptor beta, gamma, and delta rearrangements during adult thymic development: T cell receptor rearrangements are present in CD44(+)CD25(+) Pro-T thymocytes. Proc Natl Acad Sci U S A 95(21): 12522-12527.

Carleton, M., Haks, M.C., Smeele, S.A., Jones, A., Belkowski, S.M., Berger, M.A., Linsley, P., Kruisbeek, A.M., and Wiest, D.L. 2002. Early growth response transcription factors are required for development of CD4(-)CD8(-) thymocytes to the CD4(+)CD8(+) stage. J Immunol 168(4): 1649-1658.

Carter, J.H., Lefebvre, J.M., Wiest, D.L., and Tourtellotte, W.G. 2007. Redundant role for early growth response transcriptional regulators in thymocyte differentiation and survival. J Immunol 178(11): 6796-6805.

Ceredig, R., Jenkinson, E.J., MacDonald, H.R., and Owen, J.J. 1982. Development of cytolytic T lymphocyte precursors in organ-cultured mouse embryonic thymus rudiments. J Exp Med 155(2): 617-622.

Champion, S., Imhof, B.A., Savagner, P., and Thiery, J.P. 1986. The embryonic thymus produces chemotactic peptides involved in the homing of hemopoietic precursors. Cell 44(5): 781-790.

Chao, D.T. and Korsmeyer, S.J. 1997. BCL-XL-regulated apoptosis in T cell development. Int Immunol 9(9): 1375-1384.

Chen, D. and Zhang, G. 2001. Enforced expression of the GATA-3 transcription factor affects cell fate decisions in hematopoiesis. Exp Hematol 29(8): 971-980.

Cheng, L.E., Chan, F.K., Cado, D., and Winoto, A. 1997. Functional redundancy of the Nur77 and Nor-1 orphan steroid receptors in T-cell apoptosis. Embo J 16(8): 1865-1875.

Chervenak, R., Dempsey, D., Soloff, R., Wolcott, R.M., and Jennings, S.R. 1993. The expression of CD4 by T cell precursors resident in both the thymus and the bone marrow. J Immunol 151(9): 4486-4493.

Chung, H., Choi, Y.I., Ko, M.G., and Seong, R.H. 2002. Rescuing developing thymocytes from death by neglect. J Biochem Mol Biol 35(1): 7-18.

Cifone, M.G., Migliorati, G., Parroni, R., Marchetti, C., Millimaggi, D., Santoni, A., and Riccardi, C. 1999. Dexamethasone-induced thymocyte apoptosis: apoptotic signal involves the sequential activation of phosphoinositide-specific phospholipase C, acidic sphingomyelinase, and caspases. Blood 93(7): 2282-2296.

Cole, T.J., Myles, K., Purton, J.F., Brereton, P.S., Solomon, N.M., Godfrey, D.I., and Funder, J.W. 2001. GRKO mice express an aberrant dexamethasone-binding glucocorticoid receptor, but are profoundly glucocorticoid resistant. Mol Cell Endocrinol 173(1-2): 193-202.

Cortes, M., Wong, E., Koipally, J., and Georgopoulos, K. 1999. Control of lymphocyte development by the Ikaros gene family. Curr Opin Immunol 11(2): 167-171.

Costas, M., Trapp, T., Pereda, M.P., Sauer, J., Rupprecht, R., Nahmod, V.E., Reul, J.M., Holsboer, F., and Arzt, E. 1996. Molecular and functional evidence for in vitro cytokine enhancement of human and murine target cell sensitivity to glucocorticoids. TNF-alpha priming increases glucocorticoid inhibition of TNF-alpha-induced cytotoxicity/apoptosis. J Clin Invest 98(6): 1409-1416.

Cowell, I.G. 2002. E4BP4/NFIL3, a PAR-related bZIP factor with many roles. Bioessays 24(11): 1023-1029.

Cowell, I.G. and Hurst, H.C. 1994. Transcriptional repression by the human bZIP factor E4BP4: definition of a minimal repression domain. Nucleic Acids Res 22(1): 59-65.

Cowell, I.G., Skinner, A., and Hurst, H.C. 1992. Transcriptional repression by a novel member of the bZIP family of transcription factors. Mol Cell Biol 12(7): 3070-3077.

Crippa, M.P. 2007. Urokinase-type plasminogen activator. Int J Biochem Cell Biol 39(4): 690-694.

Cunningham, N.R., Artim, S.C., Fornadel, C.M., Sellars, M.C., Edmonson, S.G., Scott, G., Albino, F., Mathur, A., and Punt, J.A. 2006. Immature CD4+CD8+ thymocytes and mature T cells regulate Nur77 distinctly in response to TCR stimulation. J Immunol 177(10): 6660-6666.

Cuvillier, O. 2002. Sphingosine in apoptosis signaling. Biochim Biophys Acta 1585(2-3): 153-162.

D'Adamio, F., Zollo, O., Moraca, R., Ayroldi, E., Bruscoli, S., Bartoli, A., Cannarile, L., Migliorati, G., and Riccardi, C. 1997. A new dexamethasone-induced gene of the

leucine zipper family protects T lymphocytes from TCR/CD3-activated cell death. Immunity 7(6): 803-812.

Dahl, R. and Simon, M.C. 2003. The importance of PU.1 concentration in hematopoietic lineage commitment and maturation. Blood Cells Mol Dis 31(2): 229-233.

De Azevedo, W.F., Leclerc, S., Meijer, L., Havlicek, L., Strnad, M., and Kim, S.H. 1997. Inhibition of cyclin-dependent kinases by purine analogues: crystal structure of human cdk2 complexed with roscovitine. Eur J Biochem 243(1-2): 518-526.

De Bosscher, K., Schmitz, M.L., Vanden Berghe, W., Plaisance, S., Fiers, W., and Haegeman, G. 1997. Glucocorticoid-mediated repression of nuclear factor-kappaB-dependent transcription involves direct interference with transactivation. Proc Natl Acad Sci U S A 94(25): 13504-13509.

De Bosscher, K., Vanden Berghe, W., and Haegeman, G. 2003. The interplay between the glucocorticoid receptor and nuclear factor-kappaB or activator protein-1: molecular mechanisms for gene repression. Endocr Rev 24(4): 488-522.

Decker, E.L., Nehmann, N., Kampen, E., Eibel, H., Zipfel, P.F., and Skerka, C. 2003. Early growth response proteins (EGR) and nuclear factors of activated T cells (NFAT) form heterodimers and regulate proinflammatory cytokine gene expression. Nucleic Acids Res 31(3): 911-921.

Deftos, M.L., He, Y.W., Ojala, E.W., and Bevan, M.J. 1998. Correlating notch signaling with thymocyte maturation. Immunity 9(6): 777-786.

DeKoter, R.P., Lee, H.J., and Singh, H. 2002. PU.1 regulates expression of the interleukin-7 receptor in lymphoid progenitors. Immunity 16(2): 297-309.

Delfino, D.V., Agostini, M., Spinicelli, S., Vito, P., and Riccardi, C. 2004. Decrease of Bcl-xL and augmentation of thymocyte apoptosis in GILZ overexpressing transgenic mice. Blood 104(13): 4134-4141.

Denny, M.F., Patai, B., and Straus, D.B. 2000. Differential T-cell antigen receptor signaling mediated by the Src family kinases Lck and Fyn. Mol Cell Biol 20(4): 1426-1435.

Dequiedt, F., Kasler, H., Fischle, W., Kiermer, V., Weinstein, M., Herndier, B.G., and Verdin, E. 2003. HDAC7, a thymus-specific class II histone deacetylase, regulates Nur77 transcription and TCR-mediated apoptosis. Immunity 18(5): 687-698.

Dequiedt, F., Van Lint, J., Lecomte, E., Van Duppen, V., Seufferlein, T., Vandenheede, J.R., Wattiez, R., and Kettmann, R. 2005. Phosphorylation of histone deacetylase 7 by protein kinase D mediates T cell receptor-induced Nur77 expression and apoptosis. J Exp Med 201(5): 793-804.

Derbinski, J., Gabler, J., Brors, B., Tierling, S., Jonnakuty, S., Hergenhahn, M., Peltonen, L., Walter, J., and Kyewski, B. 2005. Promiscuous gene expression in thymic epithelial cells is regulated at multiple levels. J Exp Med 202(1): 33-45.

Derbinski, J., Schulte, A., Kyewski, B., and Klein, L. 2001. Promiscuous gene expression in medullary thymic epithelial cells mirrors the peripheral self. Nat Immunol 2(11): 1032-1039.

Deroo, B.J. and Archer, T.K. 2001. Glucocorticoid receptor activation of the I kappa B alpha promoter within chromatin. Mol Biol Cell 12(11): 3365-3374.

DeRyckere, D., Mann, D.L., and DeGregori, J. 2003. Characterization of transcriptional regulation during negative selection in vivo. J Immunol 171(2): 802-811.

Diamond, R.A., Ward, S.B., Owada-Makabe, K., Wang, H., and Rothenberg, E.V. 1997. Different developmental arrest points in RAG-2 -/- and SCID thymocytes on two genetic backgrounds: developmental choices and cell death mechanisms before TCR gene rearrangement. J Immunol 158(9): 4052-4064.

Dickins, R.A., Hemann, M.T., Zilfou, J.T., Simpson, D.R., Ibarra, I., Hannon, G.J., and Lowe, S.W. 2005. Probing tumor phenotypes using stable and regulated synthetic microRNA precursors. Nat Genet 37(11): 1289-1295.

Distelhorst, C.W. 2002. Recent insights into the mechanism of glucocorticosteroid-induced apoptosis. Cell Death Differ 9(1): 6-19.

Erlacher, M., Knoflach, M., Stec, I.E., Bock, G., Wick, G., and Wiegers, G.J. 2005. TCR signaling inhibits glucocorticoid-induced apoptosis in murine thymocytes depending on the stage of development. Eur J Immunol 35(11): 3287-3296.

Fadok, V.A., Bratton, D.L., Rose, D.M., Pearson, A., Ezekewitz, R.A., and Henson, P.M. 2000. A receptor for phosphatidylserine-specific clearance of apoptotic cells. Nature 405(6782): 85-90.

Falk, I., Nerz, G., Haidl, I., Krotkova, A., and Eichmann, K. 2001. Immature thymocytes that fail to express TCRbeta and/or TCRgamma delta proteins die by apoptotic cell death in the CD44(-)CD25(-) (DN4) subset. Eur J Immunol 31(11): 3308-3317.

Fehling, H.J. and von Boehmer, H. 1997. Early alpha beta T cell development in the thymus of normal and genetically altered mice. Curr Opin Immunol 9(2): 263-275.

Fowlkes, B.J. and Robey, E.A. 2002. A reassessment of the effect of activated Notch1 on CD4 and CD8 T cell development. J Immunol 169(4): 1817-1821.

Frankfurt, O. and Rosen, S.T. 2004. Mechanisms of glucocorticoid-induced apoptosis in hematologic malignancies: updates. Curr Opin Oncol 16(6): 553-563.

Gallegos, A.M. and Bevan, M.J. 2004. Central tolerance to tissue-specific antigens mediated by direct and indirect antigen presentation. J Exp Med 200(8): 1039-1049.

Georgopoulos, K. 2002. Haematopoietic cell-fate decisions, chromatin regulation and ikaros. Nat Rev Immunol 2(3): 162-174.

Gil-Gomez, G., Berns, A., and Brady, H.J. 1998. A link between cell cycle and cell death: Bax and Bcl-2 modulate Cdk2 activation during thymocyte apoptosis. Embo J 17(24): 7209-7218.

Gil-Gomez, G. and Brady, H.J. 1998. Transgenic mice in apoptosis research. Apoptosis 3(4): 215-228.

Gil, D., Schrum, A.G., Alarcon, B., and Palmer, E. 2005. T cell receptor engagement by peptide-MHC ligands induces a conformational change in the CD3 complex of thymocytes. J Exp Med 201(4): 517-522.

Godfrey, D.I., Kennedy, J., Mombaerts, P., Tonegawa, S., and Zlotnik, A. 1994. Onset of TCR-beta gene rearrangement and role of TCR-beta expression during CD3-CD4-CD8- thymocyte differentiation. J Immunol 152(10): 4783-4792.

Godfrey, D.I., Kennedy, J., Suda, T., and Zlotnik, A. 1993. A developmental pathway involving four phenotypically and functionally distinct subsets of CD3-CD4-CD8- triple-negative adult mouse thymocytes defined by CD44 and CD25 expression. J Immunol 150(10): 4244-4252.

Godfrey, D.I., Zlotnik, A., and Suda, T. 1992. Phenotypic and functional characterization of c-kit expression during intrathymic T cell development. J Immunol 149(7): 2281-2285.

Gossen, M., Freundlieb, S., Bender, G., Muller, G., Hillen, W., and Bujard, H. 1995. Transcriptional activation by tetracyclines in mammalian cells. Science 268(5218): 1766-1769.

Gotter, J., Brors, B., Hergenhahn, M., and Kyewski, B. 2004. Medullary epithelial cells of the human thymus express a highly diverse selection of tissue-specific genes colocalized in chromosomal clusters. J Exp Med 199(2): 155-166.

Granes, F., Roig, M.B., Brady, H.J., and Gil-Gomez, G. 2004. Cdk2 activation acts upstream of the mitochondrion during glucocorticoid induced thymocyte apoptosis. Eur J Immunol 34(10): 2781-2790.

Gratiot-Deans, J., Merino, R., Nunez, G., and Turka, L.A. 1994. Bcl-2 expression during T-cell development: early loss and late return occur at specific stages of commitment to differentiation and survival. Proc Natl Acad Sci U S A 91(22): 10685-10689.

Grez, M., Akgun, E., Hilberg, F., and Ostertag, W. 1990. Embryonic stem cell virus, a recombinant murine retrovirus with expression in embryonic stem cells. Proc Natl Acad Sci U S A 87(23): 9202-9206.

Groves, T., Parsons, M., Miyamoto, N.G., and Guidos, C.J. 1997. TCR engagement of CD4+CD8+ thymocytes in vitro induces early aspects of positive selection, but not apoptosis. J Immunol 158(1): 65-75.

Groves, T., Smiley, P., Cooke, M.P., Forbush, K., Perlmutter, R.M., and Guidos, C.J. 1996. Fyn can partially substitute for Lck in T lymphocyte development. Immunity 5(5): 417-428.

Guidos, C.J., Williams, C.J., Wu, G.E., Paige, C.J., and Danska, J.S. 1995. Development of CD4+CD8+ thymocytes in RAG-deficient mice through a T cell receptor beta chain-independent pathway. J Exp Med 181(3): 1187-1195.

Guo, J., Hawwari, A., Li, H., Sun, Z., Mahanta, S.K., Littman, D.R., Krangel, M.S., and He, Y.W. 2002. Regulation of the TCRalpha repertoire by the survival window of CD4(+)CD8(+) thymocytes. Nat Immunol 3(5): 469-476.

Gururajan, M., Chui, R., Karuppannan, A.K., Ke, J., Jennings, C.D., and Bondada, S. 2005. c-Jun N-terminal kinase (JNK) is required for survival and proliferation of B-lymphoma cells. Blood 106(4): 1382-1391.

Hakem, A., Sasaki, T., Kozieradzki, I., and Penninger, J.M. 1999. The cyclin-dependent kinase Cdk2 regulates thymocyte apoptosis. J Exp Med 189(6): 957-968.

Hakem, R., Hakem, A., Duncan, G.S., Henderson, J.T., Woo, M., Soengas, M.S., Elia, A., de la Pompa, J.L., Kagi, D., Khoo, W., Potter, J., Yoshida, R., Kaufman, S.A., Lowe, S.W., Penninger, J.M., and Mak, T.W. 1998. Differential requirement for caspase 9 in apoptotic pathways in vivo. Cell 94(3): 339-352.

Han, H., Tanigaki, K., Yamamoto, N., Kuroda, K., Yoshimoto, M., Nakahata, T., Ikuta, K., and Honjo, T. 2002. Inducible gene knockout of transcription factor recombination signal binding protein-J reveals its essential role in T versus B lineage decision. Int Immunol 14(6): 637-645.

Han, J., Flemington, C., Houghton, A.B., Gu, Z., Zambetti, G.P., Lutz, R.J., Zhu, L., and Chittenden, T. 2001. Expression of bbc3, a pro-apoptotic BH3-only gene, is regulated by diverse cell death and survival signals. Proc Natl Acad Sci U S A 98(20): 11318-11323.

Hare, K.J., Jenkinson, E.J., and Anderson, G. 1999. In vitro models of T cell development. Semin Immunol 11(1): 3-12.

Harker, N., Naito, T., Cortes, M., Hostert, A., Hirschberg, S., Tolaini, M., Roderick, K., Georgopoulos, K., and Kioussis, D. 2002. The CD8alpha gene locus is regulated by the Ikaros family of proteins. Mol Cell 10(6): 1403-1415.

Hashimoto, Y., Montecino-Rodriguez, E., Leathers, H., Stephan, R.P., and Dorshkind, K. 2002. B-cell development in the thymus is limited by inhibitory signals from the thymic microenvironment. Blood 100(10): 3504-3511.

Hawley, R.G., Lieu, F.H., Fong, A.Z., and Hawley, T.S. 1994. Versatile retroviral vectors for potential use in gene therapy. Gene Ther 1(2): 136-138.

Heck, S., Bender, K., Kullmann, M., Gottlicher, M., Herrlich, P., and Cato, A.C. 1997. I kappaB alpha-independent downregulation of NF-kappaB activity by glucocorticoid receptor. Embo J 16(15): 4698-4707.

Heemskerk, M.H., Blom, B., Nolan, G., Stegmann, A.P., Bakker, A.Q., Weijer, K., Res, P.C., and Spits, H. 1997. Inhibition of T cell and promotion of natural killer cell development by the dominant negative helix loop helix factor Id3. J Exp Med 186(9): 1597-1602.

Heinzel, K., Benz, C., Martins, V.C., Haidl, I.D., and Bleul, C.C. 2007. Bone marrow-derived hemopoietic precursors commit to the T cell lineage only after arrival in the thymic microenvironment. J Immunol 178(2): 858-868.

Hendriks, R.W., Nawijn, M.C., Engel, J.D., van Doorninck, H., Grosveld, F., and Karis, A. 1999. Expression of the transcription factor GATA-3 is required for the development of the earliest T cell progenitors and correlates with stages of cellular proliferation in the thymus. Eur J Immunol 29(6): 1912-1918.

Herold, M.J., McPherson, K.G., and Reichardt, H.M. 2006. Glucocorticoids in T cell apoptosis and function. Cell Mol Life Sci 63(1): 60-72.

Hockenbery, D.M., Zutter, M., Hickey, W., Nahm, M., and Korsmeyer, S.J. 1991. BCL2 protein is topographically restricted in tissues characterized by apoptotic cell death. Proc Natl Acad Sci U S A 88(16): 6961-6965.

Howie, S.E., Harrison, D.J., and Wyllie, A.H. 1994. Lymphocyte apoptosis--mechanisms and implications in disease. Immunol Rev 142: 141-156.

Hozumi, K., Abe, N., Chiba, S., Hirai, H., and Habu, S. 2003. Active form of Notch members can enforce T lymphopoiesis on lymphoid progenitors in the monolayer culture specific for B cell development. J Immunol 170(10): 4973-4979.

Hsu, Y.T., Wolter, K.G., and Youle, R.J. 1997. Cytosol-to-membrane redistribution of Bax and Bcl-X(L) during apoptosis. Proc Natl Acad Sci U S A 94(8): 3668-3672.

Huang, E.Y., Gallegos, A.M., Richards, S.M., Lehar, S.M., and Bevan, M.J. 2003. Surface expression of Notch1 on thymocytes: correlation with the double-negative to double-positive transition. J Immunol 171(5): 2296-2304.

Huesmann, M., Scott, B., Kisielow, P., and von Boehmer, H. 1991. Kinetics and efficacy of positive selection in the thymus of normal and T cell receptor transgenic mice. Cell 66(3): 533-540.

Huseby, E.S., White, J., Crawford, F., Vass, T., Becker, D., Pinilla, C., Marrack, P., and Kappler, J.W. 2005. How the T cell repertoire becomes peptide and MHC specific. Cell 122(2): 247-260.

Igarashi, H., Gregory, S.C., Yokota, T., Sakaguchi, N., and Kincade, P.W. 2002. Transcription from the RAG1 locus marks the earliest lymphocyte progenitors in bone marrow. Immunity 17(2): 117-130.

Ikuta, K. and Weissman, I.L. 1992. Evidence that hematopoietic stem cells express mouse c-kit but do not depend on steel factor for their generation. Proc Natl Acad Sci U S A 89(4): 1502-1506.

Ioannidis, V., Beermann, F., Clevers, H., and Held, W. 2001. The beta-catenin--TCF-1 pathway ensures CD4(+)CD8(+) thymocyte survival. Nat Immunol 2(8): 691-697.

Ishida, Y., Agata, Y., Shibahara, K., and Honjo, T. 1992. Induced expression of PD-1, a novel member of the immunoglobulin gene superfamily, upon programmed cell death. Embo J 11(11): 3887-3895.

Ismaili, J., Antica, M., and Wu, L. 1996. CD4 and CD8 expression and T cell antigen receptor gene rearrangement in early intrathymic precursor cells. Eur J Immunol 26(4): 731-737.

Ivanov, V., Merkenschlager, M., and Ceredig, R. 1993. Antioxidant treatment of thymic organ cultures decreases NF-kappa B and TCF1(alpha) transcription factor activities and inhibits alpha beta T cell development. J Immunol 151(9): 4694-4704.

Ivanov, V.N. and Nikolic-Zugic, J. 1998. Biochemical and kinetic characterization of the glucocorticoid-induced apoptosis of immature CD4+CD8+ thymocytes. Int Immunol 10(12): 1807-1817.

Jacobsen, S.E. 2007. Biological and molecular evidence for existence of lymphoid-primed multipotent progenitors. Ann N Y Acad Sci.

Jenkinson, E.J., Franchi, L.L., Kingston, R., and Owen, J.J. 1982. Effect of deoxyguanosine on lymphopoiesis in the developing thymus rudiment in vitro: application in the production of chimeric thymus rudiments. Eur J Immunol 12(7): 583-587.

Jenkinson, E.J., Kingston, R., Smith, C.A., Williams, G.T., and Owen, J.J. 1989. Antigen-induced apoptosis in developing T cells: a mechanism for negative selection of the T cell receptor repertoire. Eur J Immunol 19(11): 2175-2177.

Jenkinson, E.J. and Owen, J.J. 1990. T-cell differentiation in thymus organ cultures. Semin Immunol 2(1): 51-58.

Jonat, C., Rahmsdorf, H.J., Park, K.K., Cato, A.C., Gebel, S., Ponta, H., and Herrlich, P. 1990. Antitumor promotion and antiinflammation: down-modulation of AP-1 (Fos/Jun) activity by glucocorticoid hormone. Cell 62(6): 1189-1204.

Junghans, D., Chauvet, S., Buhler, E., Dudley, K., Sykes, T., and Henderson, C.E. 2004. The CES-2-related transcription factor E4BP4 is an intrinsic regulator of motoneuron growth and survival. Development 131(18): 4425-4434.

Kamarck, M.E. and Gottlieb, P.D. 1977. Expression of thymocyte surface alloantigens in the fetal mouse thymus in vivo and in organ culture. J Immunol 119(2): 407-415.

Kappler, J.W., Roehm, N., and Marrack, P. 1987. T cell tolerance by clonal elimination in the thymus. Cell 49(2): 273-280.

Kappler, J.W., Staerz, U., White, J., and Marrack, P.C. 1988. Self-tolerance eliminates T cells specific for Mls-modified products of the major histocompatibility complex. Nature 332(6159): 35-40.

Kawamoto, H., Ohmura, K., Fujimoto, S., Lu, M., Ikawa, T., and Katsura, Y. 2003. Extensive proliferation of T cell lineage-restricted progenitors in the thymus: an essential process for clonal expression of diverse T cell receptor beta chains. Eur J Immunol 33(3): 606-615.

Kaye, J., Hsu, M.L., Sauron, M.E., Jameson, S.C., Gascoigne, N.R., and Hedrick, S.M. 1989. Selective development of CD4+ T cells in transgenic mice expressing a class II MHC-restricted antigen receptor. Nature 341(6244): 746-749.

Ke, J., Gururajan, M., Kumar, A., Simmons, A., Turcios, L., Chelvarajan, R.L., Cohen, D.M., Wiest, D.L., Monroe, J.G., and Bondada, S. 2006. The role of MAPKs in B cell receptor-induced down-regulation of Egr-1 in immature B lymphoma cells. J Biol Chem 281(52): 39806-39818.

Kee, B.L., Bain, G., and Murre, C. 2002. IL-7Ralpha and E47: independent pathways required for development of multipotent lymphoid progenitors. Embo J 21(1-2): 103-113.

Kerr, J.F., Wyllie, A.H., and Currie, A.R. 1972. Apoptosis: a basic biological phenomenon with wide-ranging implications in tissue kinetics. Br J Cancer 26(4): 239-257.

King, L.B., Vacchio, M.S., Dixon, K., Hunziker, R., Margulies, D.H., and Ashwell, J.D. 1995. A targeted glucocorticoid receptor antisense transgene increases thymocyte apoptosis and alters thymocyte development. Immunity 3(5): 647-656.

Kingston, R., Jenkinson, E.J., and Owen, J.J. 1985. A single stem cell can recolonize an embryonic thymus, producing phenotypically distinct T-cell populations. Nature 317(6040): 811-813.

Kisielow, P., Bluthmann, H., Staerz, U.D., Steinmetz, M., and von Boehmer, H. 1988. Tolerance in T-cell-receptor transgenic mice involves deletion of nonmature CD4+8+ thymocytes. Nature 333(6175): 742-746.

Klein-Hessling, S., Jha, M.K., Santner-Nanan, B., Berberich-Siebelt, F., Baumruker, T., Schimpl, A., and Serfling, E. 2003. Protein kinase A regulates GATA-3-dependent activation of IL-5 gene expression in Th2 cells. J Immunol 170(6): 2956-2961.

Ko, M., Jang, J., Ahn, J., Lee, K., Chung, H., Jeon, S.H., and Seong, R.H. 2004. T cell receptor signaling inhibits glucocorticoid-induced apoptosis by repressing the SRG3 expression via Ras activation. J Biol Chem 279(21): 21903-21915.

Kondo, M., Wagers, A.J., Manz, M.G., Prohaska, S.S., Scherer, D.C., Beilhack, G.F., Shizuru, J.A., and Weissman, I.L. 2003. Biology of hematopoietic stem cells and progenitors: implications for clinical application. Annu Rev Immunol 21: 759-806.

Kondo, M., Weissman, I.L., and Akashi, K. 1997. Identification of clonogenic common lymphoid progenitors in mouse bone marrow. Cell 91(5): 661-672.

Kuida, K., Haydar, T.F., Kuan, C.Y., Gu, Y., Taya, C., Karasuyama, H., Su, M.S., Rakic, P., and Flavell, R.A. 1998. Reduced apoptosis and cytochrome c-mediated caspase activation in mice lacking caspase 9. Cell 94(3): 325-337.

Kumar, D., Whiteside, T.L., and Kasid, U. 2000. Identification of a novel tumor necrosis factor-alpha-inducible gene, SCC-S2, containing the consensus sequence of a death effector domain of fas-associated death domain-like interleukin- 1beta-converting enzyme-inhibitory protein. J Biol Chem 275(4): 2973-2978.

Kurebayashi, S., Ueda, E., Sakaue, M., Patel, D.D., Medvedev, A., Zhang, F., and Jetten, A.M. 2000. Retinoid-related orphan receptor gamma (RORgamma) is essential for lymphoid organogenesis and controls apoptosis during thymopoiesis. Proc Natl Acad Sci U S A 97(18): 10132-10137.

Kyewski, B. and Derbinski, J. 2004. Self-representation in the thymus: an extended view. Nat Rev Immunol 4(9): 688-698.

La Motte-Mohs, R.N., Herer, E., and Zuniga-Pflucker, J.C. 2005. Induction of T-cell development from human cord blood hematopoietic stem cells by Delta-like 1 in vitro. Blood 105(4): 1431-1439.

Lai, C.K. and Ting, L.P. 1999. Transcriptional repression of human hepatitis B virus genes by a bZIP family member, E4BP4. J Virol 73(4): 3197-3209.

Lechner, O., Wiegers, G.J., Oliveira-Dos-Santos, A.J., Dietrich, H., Recheis, H., Waterman, M., Boyd, R., and Wick, G. 2000. Glucocorticoid production in the murine thymus. Eur J Immunol 30(2): 337-346.

Lee, C.K., Kim, J.K., Kim, Y., Lee, M.K., Kim, K., Kang, J.K., Hofmeister, R., Durum, S.K., and Han, S.S. 2001a. Generation of macrophages from early T progenitors in vitro. J Immunol 166(10): 5964-5969.

Lee, E.G., Boone, D.L., Chai, S., Libby, S.L., Chien, M., Lodolce, J.P., and Ma, A. 2000. Failure to regulate TNF-induced NF-kappaB and cell death responses in A20-deficient mice. Science 289(5488): 2350-2354.

Lee, G.R., Fields, P.E., and Flavell, R.A. 2001b. Regulation of IL-4 gene expression by distal regulatory elements and GATA-3 at the chromatin level. Immunity 14(4): 447-459.

Lee, S.L., Wesselschmidt, R.L., Linette, G.P., Kanagawa, O., Russell, J.H., and Milbrandt, J. 1995. Unimpaired thymic and peripheral T cell death in mice lacking the nuclear receptor NGFI-B (Nur77). Science 269(5223): 532-535.

Lensch, M.W. and Daley, G.Q. 2004. Origins of mammalian hematopoiesis: in vivo paradigms and in vitro models. Curr Top Dev Biol 60: 127-196.

Lepine, S., Lakatos, B., Courageot, M.P., Le Stunff, H., Sulpice, J.C., and Giraud, F. 2004. Sphingosine contributes to glucocorticoid-induced apoptosis of thymocytes independently of the mitochondrial pathway. J Immunol 173(6): 3783-3790.

Lepine, S., Sulpice, J.C., and Giraud, F. 2005. Signaling pathways involved in glucocorticoid-induced apoptosis of thymocytes. Crit Rev Immunol 25(4): 263-288.

Letai, A., Bassik, M.C., Walensky, L.D., Sorcinelli, M.D., Weiler, S., and Korsmeyer, S.J. 2002. Distinct BH3 domains either sensitize or activate mitochondrial apoptosis, serving as prototype cancer therapeutics. Cancer Cell 2(3): 183-192.

Levkovitz, Y. and Baraban, J.M. 2002. A dominant negative Egr inhibitor blocks nerve growth factor-induced neurite outgrowth by suppressing c-Jun activation: role of an Egr/c-Jun complex. J Neurosci 22(10): 3845-3854.

Li, H., Kolluri, S.K., Gu, J., Dawson, M.I., Cao, X., Hobbs, P.D., Lin, B., Chen, G., Lu, J., Lin, F., Xie, Z., Fontana, J.A., Reed, J.C., and Zhang, X. 2000. Cytochrome c release and apoptosis induced by mitochondrial targeting of nuclear orphan receptor TR3. Science 289(5482): 1159-1164.

Liblau, R.S., Tisch, R., Shokat, K., Yang, X., Dumont, N., Goodnow, C.C., and McDevitt, H.O. 1996. Intravenous injection of soluble antigen induces thymic and peripheral T-cells apoptosis. Proc Natl Acad Sci U S A 93(7): 3031-3036.

Lin, B., Kolluri, S.K., Lin, F., Liu, W., Han, Y.H., Cao, X., Dawson, M.I., Reed, J.C., and Zhang, X.K. 2004. Conversion of Bcl-2 from protector to killer by interaction with nuclear orphan receptor Nur77/TR3. Cell 116(4): 527-540.

Linette, G.P., Grusby, M.J., Hedrick, S.M., Hansen, T.H., Glimcher, L.H., and Korsmeyer, S.J. 1994. Bcl-2 is upregulated at the CD4+ CD8+ stage during positive selection and promotes thymocyte differentiation at several control points. Immunity 1(3): 197-205.

Littlewood, T.D., Hancock, D.C., Danielian, P.S., Parker, M.G., and Evan, G.I. 1995. A modified oestrogen receptor ligand-binding domain as an improved switch for the regulation of heterologous proteins. Nucleic Acids Res 23(10): 1686-1690.

Liu, Z.G., Smith, S.W., McLaughlin, K.A., Schwartz, L.M., and Osborne, B.A. 1994. Apoptotic signals delivered through the T-cell receptor of a T-cell hybrid require the immediate-early gene nur77. Nature 367(6460): 281-284.

Livak, F., Tourigny, M., Schatz, D.G., and Petrie, H.T. 1999. Characterization of TCR gene rearrangements during adult murine T cell development. J Immunol 162(5): 2575-2580.

Luisi, B.F., Xu, W.X., Otwinowski, Z., Freedman, L.P., Yamamoto, K.R., and Sigler, P.B. 1991. Crystallographic analysis of the interaction of the glucocorticoid receptor with DNA. Nature 352(6335): 497-505.

Ma, A., Pena, J.C., Chang, B., Margosian, E., Davidson, L., Alt, F.W., and Thompson, C.B. 1995. Bclx regulates the survival of double-positive thymocytes. Proc Natl Acad Sci U S A 92(11): 4763-4767.

Malone, M.H., Wang, Z., and Distelhorst, C.W. 2004. The glucocorticoid-induced gene tdag8 encodes a pro-apoptotic G protein-coupled receptor whose activation promotes glucocorticoid-induced apoptosis. J Biol Chem 279(51): 52850-52859.

Mamalaki, C., Elliott, J., Norton, T., Yannoutsos, N., Townsend, A.R., Chandler, P., Simpson, E., and Kioussis, D. 1993. Positive and negative selection in transgenic mice expressing a T-cell receptor specific for influenza nucleoprotein and endogenous superantigen. Dev Immunol 3(3): 159-174.

Mamalaki, C., Norton, T., Tanaka, Y., Townsend, A.R., Chandler, P., Simpson, E., and Kioussis, D. 1992. Thymic depletion and peripheral activation of class I major histocompatibility complex-restricted T cells by soluble peptide in T-cell receptor transgenic mice. Proc Natl Acad Sci U S A 89(23): 11342-11346.

Manning, J.S., Hackett, A.J., and Darby, N.B., Jr. 1971. Effect of polycations on sensitivity of BALD-3T3 cells to murine leukemia and sarcoma virus infectivity. Appl Microbiol 22(6): 1162-1163.

Martin, S. and Bevan, M.J. 1997. Antigen-specific and nonspecific deletion of immature cortical thymocytes caused by antigen injection. Eur J Immunol 27(10): 2726-2736.

Masuda, K., Itoi, M., Amagai, T., Minato, N., Katsura, Y., and Kawamoto, H. 2005. Thymic anlage is colonized by progenitors restricted to T, NK, and dendritic cell lineages. J Immunol 174(5): 2525-2532.

Matsuzaki, Y., Gyotoku, J., Ogawa, M., Nishikawa, S., Katsura, Y., Gachelin, G., and Nakauchi, H. 1993. Characterization of c-kit positive intrathymic stem cells that are restricted to lymphoid differentiation. J Exp Med 178(4): 1283-1292.

McCarty, N., Paust, S., Ikizawa, K., Dan, I., Li, X., and Cantor, H. 2005. Signaling by the kinase MINK is essential in the negative selection of autoreactive thymocytes. Nat Immunol 6(1): 65-72.

McColl, K.S., He, H., Zhong, H., Whitacre, C.M., Berger, N.A., and Distelhorst, C.W. 1998. Apoptosis induction by the glucocorticoid hormone dexamethasone and the calcium-ATPase inhibitor thapsigargin involves Bc1-2 regulated caspase activation. Mol Cell Endocrinol 139(1-2): 229-238.

McConkey, D.J., Nicotera, P., Hartzell, P., Bellomo, G., Wyllie, A.H., and Orrenius, S. 1989. Glucocorticoids activate a suicide process in thymocytes through an elevation of cytosolic Ca2+ concentration. Arch Biochem Biophys 269(1): 365-370.

McKercher, S.R., Torbett, B.E., Anderson, K.L., Henkel, G.W., Vestal, D.J., Baribault, H., Klemsz, M., Feeney, A.J., Wu, G.E., Paige, C.J., and Maki, R.A. 1996. Targeted disruption of the PU.1 gene results in multiple hematopoietic abnormalities. Embo J 15(20): 5647-5658.

Meijer, L., Borgne, A., Mulner, O., Chong, J.P., Blow, J.J., Inagaki, N., Inagaki, M., Delcros, J.G., and Moulinoux, J.P. 1997. Biochemical and cellular effects of roscovitine, a potent and selective inhibitor of the cyclin-dependent kinases cdc2, cdk2 and cdk5. Eur J Biochem 243(1-2): 527-536.

Melton, E., Sarner, N., Torkar, M., van der Merwe, P.A., Russell, J.Q., Budd, R.C., Mamalaki, C., Tolaini, M., Kioussis, D., and Zamoyska, R. 1996. Transgene-encoded human CD2 acts in a dominant negative fashion to modify thymocyte selection signals in mice. Eur J Immunol 26(12): 2952-2963.

Memon, S.A., Moreno, M.B., Petrak, D., and Zacharchuk, C.M. 1995. Bcl-2 blocks glucocorticoid- but not Fas- or activation-induced apoptosis in a T cell hybridoma. J Immunol 155(10): 4644-4652.

Miller, A.D. and Rosman, G.J. 1989. Improved retroviral vectors for gene transfer and expression. Biotechniques 7(9): 980-982, 984-986, 989-990.

Miller, J.F. and Osoba, D. 1967. Current concepts of the immunological function of the thymus. Physiol Rev 47(3): 437-520.

Milne, C.D., Fleming, H.E., Zhang, Y., and Paige, C.J. 2004. Mechanisms of selection mediated by interleukin-7, the preBCR, and hemokinin-1 during B-cell development. Immunol Rev 197: 75-88.

Mitsui, S., Yamaguchi, S., Matsuo, T., Ishida, Y., and Okamura, H. 2001. Antagonistic role of E4BP4 and PAR proteins in the circadian oscillatory mechanism. Genes Dev 15(8): 995-1006.

Miyazaki, T. and Lemonnier, F.A. 1998. Modulation of thymic selection by expression of an immediate-early gene, early growth response 1 (Egr-1). J Exp Med 188(4): 715-723.

Mohapatra, S., Agrawal, D., and Pledger, W.J. 2001. p27Kip1 regulates T cell proliferation. J Biol Chem 276(24): 21976-21983.

Mok, C.L., Gil-Gomez, G., Williams, O., Coles, M., Taga, S., Tolaini, M., Norton, T., Kioussis, D., and Brady, H.J. 1999. Bad can act as a key regulator of T cell apoptosis and T cell development. J Exp Med 189(3): 575-586.

Montecino-Rodriguez, E., Johnson, A., and Dorshkind, K. 1996. Thymic stromal cells can support B cell differentiation from intrathymic precursors. J Immunol 156(3): 963-967.

Moore, M.A. and Metcalf, D. 1970. Ontogeny of the haemopoietic system: yolk sac origin of in vivo and in vitro colony forming cells in the developing mouse embryo. Br J Haematol 18(3): 279-296.

Moore, N.C., Anderson, G., Williams, G.T., Owen, J.J., and Jenkinson, E.J. 1994. Developmental regulation of bcl-2 expression in the thymus. Immunology 81(1): 115-119.

Moore, T.A. and Zlotnik, A. 1995. T-cell lineage commitment and cytokine responses of thymic progenitors. Blood 86(5): 1850-1860.

Morrow, M., Horton, S., Kioussis, D., Brady, H.J., and Williams, O. 2004. TEL-AML1 promotes development of specific hematopoietic lineages consistent with preleukemic activity. Blood 103(10): 3890-3896.

Murphy, K.M., Heimberger, A.B., and Loh, D.Y. 1990. Induction by antigen of intrathymic apoptosis of CD4+CD8+TCRlo thymocytes in vivo. Science 250(4988): 1720-1723.

Nakano, T., Kodama, H., and Honjo, T. 1994. Generation of lymphohematopoietic cells from embryonic stem cells in culture. Science 265(5175): 1098-1101.

Nawijn, M.C., Ferreira, R., Dingjan, G.M., Kahre, O., Drabek, D., Karis, A., Grosveld, F., and Hendriks, R.W. 2001. Enforced expression of GATA-3 during T cell development inhibits maturation of CD8 single-positive cells and induces thymic lymphoma in transgenic mice. J Immunol 167(2): 715-723.

Neilson, J.R., Winslow, M.M., Hur, E.M., and Crabtree, G.R. 2004. Calcineurin B1 is essential for positive but not negative selection during thymocyte development. Immunity 20(3): 255-266.

Nichogiannopoulou, A., Trevisan, M., Neben, S., Friedrich, C., and Georgopoulos, K. 1999. Defects in hemopoietic stem cell activity in Ikaros mutant mice. J Exp Med 190(9): 1201-1214.

Nishimura, M., Fukushima-Nakase, Y., Fujita, Y., Nakao, M., Toda, S., Kitamura, N., Abe, T., and Okuda, T. 2004. VWRPY motif-dependent and -independent roles of AML1/Runx1 transcription factor in murine hematopoietic development. Blood 103(2): 562-570.

Nocentini, G., Giunchi, L., Ronchetti, S., Krausz, L.T., Bartoli, A., Moraca, R., Migliorati, G., and Riccardi, C. 1997. A new member of the tumor necrosis factor/nerve growth factor receptor family inhibits T cell receptor-induced apoptosis. Proc Natl Acad Sci U S A 94(12): 6216-6221.

O'Connor, L., Strasser, A., O'Reilly, L.A., Hausmann, G., Adams, J.M., Cory, S., and Huang, D.C. 1998. Bim: a novel member of the Bcl-2 family that promotes apoptosis. Embo J 17(2): 384-395.

O'Doherty, U., Swiggard, W.J., and Malim, M.H. 2000. Human immunodeficiency virus type 1 spinoculation enhances infection through virus binding. J Virol 74(21): 10074-10080.

Owen, J.J. and Jenkinson, E.J. 1992. Apoptosis and T-cell repertoire selection in the thymus. Ann N Y Acad Sci 663: 305-310.

Owen, J.J., Owen, M.J., Williams, G.T., Kingston, R., and Jenkinson, E.J. 1988. The effects of anti-CD3 antibodies on the development of T-cell receptor alpha beta + lymphocytes in embryonic thymus organ cultures. Immunology 63(4): 639-642.

Owen, J.J. and Ritter, M.A. 1969. Tissue interaction in the development of thymus lymphocytes. J Exp Med 129(2): 431-442.

Pai, S.Y., Truitt, M.L., Ting, C.N., Leiden, J.M., Glimcher, L.H., and Ho, I.C. 2003. Critical roles for transcription factor GATA-3 in thymocyte development. Immunity 19(6): 863-875.

Palmer, E. 2003. Negative selection--clearing out the bad apples from the T-cell repertoire. Nat Rev Immunol 3(5): 383-391.

Papathanasiou, P., Perkins, A.C., Cobb, B.S., Ferrini, R., Sridharan, R., Hoyne, G.F., Nelms, K.A., Smale, S.T., and Goodnow, C.C. 2003. Widespread failure of hematolymphoid differentiation caused by a recessive niche-filling allele of the Ikaros transcription factor. Immunity 19(1): 131-144.

Pazirandeh, A., Jondal, M., and Okret, S. 2005. Conditional expression of a glucocorticoid receptor transgene in thymocytes reveals a role for thymic-derived glucocorticoids in thymopoiesis in vivo. Endocrinology 146(6): 2501-2507.

Pazirandeh, A., Xue, Y., Prestegaard, T., Jondal, M., and Okret, S. 2002. Effects of altered glucocorticoid sensitivity in the T cell lineage on thymocyte and T cell homeostasis. Faseb J 16(7): 727-729.

Pelayo, R., Welner, R., Perry, S.S., Huang, J., Baba, Y., Yokota, T., and Kincade, P.W. 2005. Lymphoid progenitors and primary routes to becoming cells of the immune system. Curr Opin Immunol 17(2): 100-107.

Pennington, D.J., Silva-Santos, B., Silberzahn, T., Escorcio-Correia, M., Woodward, M.J., Roberts, S.J., Smith, A.L., Dyson, P.J., and Hayday, A.C. 2006. Early events in the thymus affect the balance of effector and regulatory T cells. Nature 444(7122): 1073-1077.

Persons, D.A., Allay, J.A., Allay, E.R., Smeyne, R.J., Ashmun, R.A., Sorrentino, B.P., and Nienhuis, A.W. 1997. Retroviral-mediated transfer of the green fluorescent protein gene into murine hematopoietic cells facilitates scoring and selection of

transduced progenitors in vitro and identification of genetically modified cells in vivo. Blood 90(5): 1777-1786.

Petit, P.X., Lecoeur, H., Zorn, E., Dauguet, C., Mignotte, B., and Gougeon, M.L. 1995. Alterations in mitochondrial structure and function are early events of dexamethasone-induced thymocyte apoptosis. J Cell Biol 130(1): 157-167.

Porritt, H.E., Rumfelt, L.L., Tabrizifard, S., Schmitt, T.M., Zuniga-Pflucker, J.C., and Petrie, H.T. 2004. Heterogeneity among DN1 prothymocytes reveals multiple progenitors with different capacities to generate T cell and non-T cell lineages. Immunity 20(6): 735-745.

Pruett, S.B. and Padgett, E.L. 2004. Thymus-derived glucocorticoids are insufficient for normal thymus homeostasis in the adult mouse. BMC Immunol 5(1): 24.

Pui, J.C., Allman, D., Xu, L., DeRocco, S., Karnell, F.G., Bakkour, S., Lee, J.Y., Kadesch, T., Hardy, R.R., Aster, J.C., and Pear, W.S. 1999. Notch1 expression in early lymphopoiesis influences B versus T lineage determination. Immunity 11(3): 299-308.

Purton, J.F., Boyd, R.L., Cole, T.J., and Godfrey, D.I. 2000. Intrathymic T cell development and selection proceeds normally in the absence of glucocorticoid receptor signaling. Immunity 13(2): 179-186.

Purton, J.F., Zhan, Y., Liddicoat, D.R., Hardy, C.L., Lew, A.M., Cole, T.J., and Godfrey, D.I. 2002. Glucocorticoid receptor deficient thymic and peripheral T cells develop normally in adult mice. Eur J Immunol 32(12): 3546-3555.

Radtke, F., Wilson, A., Stark, G., Bauer, M., van Meerwijk, J., MacDonald, H.R., and Aguet, M. 1999. Deficient T cell fate specification in mice with an induced inactivation of Notch1. Immunity 10(5): 547-558.

Radu, C.G., Cheng, D., Nijagal, A., Riedinger, M., McLaughlin, J., Yang, L.V., Johnson, J., and Witte, O.N. 2006. Normal immune development and glucocorticoid-induced thymocyte apoptosis in mice deficient for the T-cell death-associated gene 8 receptor. Mol Cell Biol 26(2): 668-677.

Rammensee, H.G. and Bevan, M.J. 1984. Evidence from in vitro studies that tolerance to self antigens is MHC-restricted. Nature 308(5961): 741-744.

Ranganath, S. and Murphy, K.M. 2001. Structure and specificity of GATA proteins in Th2 development. Mol Cell Biol 21(8): 2716-2725.

Rathmell, J.C., Lindstèn, T., Zong, W.X., Cinalli, R.M., and Thompson, C.B. 2002. Deficiency in Bak and Bax perturbs thymic selection and lymphoid homeostasis. Nat Immunol 3(10): 932-939.

Ray, R.J., Paige, C.J., Furlonger, C., Lyman, S.D., and Rottapel, R. 1996. Flt3 ligand supports the differentiation of early B cell progenitors in the presence of interleukin-11 and interleukin-7. Eur J Immunol 26(7): 1504-1510.

Refojo, D., Liberman, A.C., Giacomini, D., Carbia Nagashima, A., Graciarena, M., Echenique, C., Paez Pereda, M., Stalla, G., Holsboer, F., and Arzt, E. 2003. Integrating systemic information at the molecular level: cross-talk between steroid receptors and cytokine signaling on different target cells. Ann N Y Acad Sci 992: 196-204.

Reichardt, H.M., Kaestner, K.H., Tuckermann, J., Kretz, O., Wessely, O., Bock, R., Gass, P., Schmid, W., Herrlich, P., Angel, P., and Schutz, G. 1998. DNA binding of the glucocorticoid receptor is not essential for survival. Cell 93(4): 531-541.

Reichardt, H.M., Tuckermann, J.P., Gottlicher, M., Vujic, M., Weih, F., Angel, P., Herrlich, P., and Schutz, G. 2001. Repression of inflammatory responses in the absence of DNA binding by the glucocorticoid receptor. Embo J 20(24): 7168-7173.

Reichardt, H.M., Umland, T., Bauer, A., Kretz, O., and Schutz, G. 2000. Mice with an increased glucocorticoid receptor gene dosage show enhanced resistance to stress and endotoxic shock. Mol Cell Biol 20(23): 9009-9017.

Reynolds, P.D., Ruan, Y., Smith, D.F., and Scammell, J.G. 1999. Glucocorticoid resistance in the squirrel monkey is associated with overexpression of the immunophilin FKBP51. J Clin Endocrinol Metab 84(2): 663-669.

Rincon, M., Whitmarsh, A., Yang, D.D., Weiss, L., Derijard, B., Jayaraj, P., Davis, R.J., and Flavell, R.A. 1998. The JNK pathway regulates the In vivo deletion of immature CD4(+)CD8(+) thymocytes. J Exp Med 188(10): 1817-1830.

Rothenberg, E.V. and Taghon, T. 2005. Molecular genetics of T cell development. Annu Rev Immunol 23: 601-649.

Rouse, R.V. and Weissman, I.L. 1982. The principal cells in the thymus expressing MHC antigens are epithelial. Adv Exp Med Biol 149: 401-405.

Rudolph, B., Hueber, A.O., and Evan, G.I. 2000. Reversible activation of c-Myc in thymocytes enhances positive selection and induces proliferation and apoptosis in vitro. Oncogene 19(15): 1891-1900.

Sacedon, R., Vicente, A., Varas, A., Morale, M.C., Barden, N., Marchetti, B., and Zapata, A.G. 1999. Partial blockade of T-cell differentiation during ontogeny and marked alterations of the thymic microenvironment in transgenic mice with impaired glucocorticoid receptor function. J Neuroimmunol 98(2): 157-167.

Sakaguchi, N., Takahashi, T., Hata, H., Nomura, T., Tagami, T., Yamazaki, S., Sakihama, T., Matsutani, T., Negishi, I., Nakatsuru, S., and Sakaguchi, S. 2003. Altered thymic T-cell selection due to a mutation of the ZAP-70 gene causes autoimmune arthritis in mice. Nature 426(6965): 454-460.

Samir, A.A., Ropolo, A., Grasso, D., Tomasini, R., Dagorn, J.C., Dusetti, N., Iovanna, J.L., and Vaccaro, M.I. 2000. Cloning and expression of the mouse PIP49 (Pancreatitis Induced Protein 49) mRNA which encodes a new putative

transmembrane protein activated in the pancreas with acute pancreatitis. Mol Cell Biol Res Commun 4(3): 188-193.

Scheinman, R.I., Gualberto, A., Jewell, C.M., Cidlowski, J.A., and Baldwin, A.S., Jr. 1995. Characterization of mechanisms involved in transrepression of NF-kappa B by activated glucocorticoid receptors. Mol Cell Biol 15(2): 943-953.

Schmid, I., Hausner, M.A., Cole, S.W., Uittenbogaart, C.H., Giorgi, J.V., and Jamieson, B.D. 2001. Simultaneous flow cytometric measurement of viability and lymphocyte subset proliferation. J Immunol Methods 247(1-2): 175-186.

Schmidt, S., Rainer, J., Ploner, C., Presul, E., Riml, S., and Kofler, R. 2004. Glucocorticoid-induced apoptosis and glucocorticoid resistance: molecular mechanisms and clinical relevance. Cell Death Differ 11 Suppl 1: S45-55.

Schmitt, T.M., de Pooter, R.F., Gronski, M.A., Cho, S.K., Ohashi, P.S., and Zuniga-Pflucker, J.C. 2004. Induction of T cell development and establishment of T cell competence from embryonic stem cells differentiated in vitro. Nat Immunol 5(4): 410-417.

Schmitt, T.M. and Zuniga-Pflucker, J.C. 2002. Induction of T cell development from hematopoietic progenitor cells by delta-like-1 in vitro. Immunity 17(6): 749-756.

Scollay, R.G., Butcher, E.C., and Weissman, I.L. 1980. Thymus cell migration. Quantitative aspects of cellular traffic from the thymus to the periphery in mice. Eur J Immunol 10(3): 210-218.

Screpanti, I., Morrone, S., Meco, D., Santoni, A., Gulino, A., Paolini, R., Crisanti, A., Mathieson, B.J., and Frati, L. 1989. Steroid sensitivity of thymocyte subpopulations during intrathymic differentiation. Effects of 17 beta-estradiol and dexamethasone on subsets expressing T cell antigen receptor or IL-2 receptor. J Immunol 142(10): 3378-3383.

Sebzda, E., Mariathasan, S., Ohteki, T., Jones, R., Bachmann, M.F., and Ohashi, P.S. 1999. Selection of the T cell repertoire. Annu Rev Immunol 17: 829-874.

Sentman, C.L., Shutter, J.R., Hockenbery, D., Kanagawa, O., and Korsmeyer, S.J. 1991. bcl-2 inhibits multiple forms of apoptosis but not negative selection in thymocytes. Cell 67(5): 879-888.

Sha, W.C., Nelson, C.A., Newberry, R.D., Kranz, D.M., Russell, J.H., and Loh, D.Y. 1988a. Positive and negative selection of an antigen receptor on T cells in transgenic mice. Nature 336(6194): 73-76.

-. 1988b. Selective expression of an antigen receptor on CD8-bearing T lymphocytes in transgenic mice. Nature 335(6187): 271-274.

Shen, H.Q., Lu, M., Ikawa, T., Masuda, K., Ohmura, K., Minato, N., Katsura, Y., and Kawamoto, H. 2003. T/NK bipotent progenitors in the thymus retain the potential to generate dendritic cells. J Immunol 171(7): 3401-3406.

Shimizu, C., Kawamoto, H., Yamashita, M., Kimura, M., Kondou, E., Kaneko, Y., Okada, S., Tokuhisa, T., Yokoyama, M., Taniguchi, M., Katsura, Y., and Nakayama, T. 2001. Progression of T cell lineage restriction in the earliest subpopulation of murine adult thymus visualized by the expression of lck proximal promoter activity. Int Immunol 13(1): 105-117.

Shinkai, Y., Koyasu, S., Nakayama, K., Murphy, K.M., Loh, D.Y., Reinherz, E.L., and Alt, F.W. 1993. Restoration of T cell development in RAG-2-deficient mice by functional TCR transgenes. Science 259(5096): 822-825.

Shockett, P.E., Zhou, S., Hong, X., and Schatz, D.G. 2004. Partial reconstitution of V(D)J rearrangement and lymphocyte development in RAG-deficient mice expressing inducible, tetracycline-regulated RAG transgenes. Mol Immunol 40(11): 813-829.

Shortman, K., Vremec, D., Corcoran, L.M., Georgopoulos, K., Lucas, K., and Wu, L. 1998. The linkage between T-cell and dendritic cell development in the mouse thymus. Immunol Rev 165: 39-46.

Siegel, R.M., Katsumata, M., Miyashita, T., Louie, D.C., Greene, M.I., and Reed, J.C. 1992. Inhibition of thymocyte apoptosis and negative antigenic selection in bcl-2 transgenic mice. Proc Natl Acad Sci U S A 89(15): 7003-7007.

Siggs, O.M., Makaroff, L.E., and Liston, A. 2006. The why and how of thymocyte negative selection. Curr Opin Immunol 18(2): 175-183.

Spangrude, G.J., Heimfeld, S., and Weissman, I.L. 1988. Purification and characterization of mouse hematopoietic stem cells. Science 241(4861): 58-62.

Spanopoulou, E., Roman, C.A., Corcoran, L.M., Schlissel, M.S., Silver, D.P., Nemazee, D., Nussenzweig, M.C., Shinton, S.A., Hardy, R.R., and Baltimore, D. 1994. Functional immunoglobulin transgenes guide ordered B-cell differentiation in Rag-1-deficient mice. Genes Dev 8(9): 1030-1042.

Sprent, J. 1993. Lifespans of naive, memory and effector lymphocytes. Curr Opin Immunol 5(3): 433-438.

Sprent, J. and Tough, D.F. 1994. Lymphocyte life-span and memory. Science 265(5177): 1395-1400.

Sprent, J. and Webb, S.R. 1987. Function and specificity of T cell subsets in the mouse. Adv Immunol 41: 39-133.

Stoecklin, E., Wissler, M., Moriggl, R., and Groner, B. 1997. Specific DNA binding of Stat5, but not of glucocorticoid receptor, is required for their functional cooperation in the regulation of gene transcription. Mol Cell Biol 17(11): 6708-6716.

Strasser, A., Harris, A.W., and Cory, S. 1991. bcl-2 transgene inhibits T cell death and perturbs thymic self-censorship. Cell 67(5): 889-899.

Strasser, A., Harris, A.W., von Boehmer, H., and Cory, S. 1994. Positive and negative selection of T cells in T-cell receptor transgenic mice expressing a bcl-2 transgene. Proc Natl Acad Sci U S A 91(4): 1376-1380.

Sugawara, T., Moriguchi, T., Nishida, E., and Takahama, Y. 1998. Differential roles of ERK and p38 MAP kinase pathways in positive and negative selection of T lymphocytes. Immunity 9(4): 565-574.

Sun, Z., Unutmaz, D., Zou, Y.R., Sunshine, M.J., Pierani, A., Brenner-Morton, S., Mebius, R.E., and Littman, D.R. 2000. Requirement for RORgamma in thymocyte survival and lymphoid organ development. Science 288(5475): 2369-2373.

Suniara, R.K., Jenkinson, E.J., and Owen, J.J. 1999. Studies on the phenotype of migrant thymic stem cells. Eur J Immunol 29(1): 75-80.

Taghon, T.N., David, E.S., Zuniga-Pflucker, J.C., and Rothenberg, E.V. 2005. Delayed, asynchronous, and reversible T-lineage specification induced by Notch/Delta signaling. Genes Dev 19(8): 965-978.

Takahama, Y. 2006. Journey through the thymus: stromal guides for T-cell development and selection. Nat Rev Immunol 6(2): 127-135.

Taniuchi, I., Osato, M., Egawa, T., Sunshine, M.J., Bae, S.C., Komori, T., Ito, Y., and Littman, D.R. 2002. Differential requirements for Runx proteins in CD4 repression and epigenetic silencing during T lymphocyte development. Cell 111(5): 621-633.

Tao, W., Teh, S.J., Melhado, I., Jirik, F., Korsmeyer, S.J., and Teh, H.S. 1994. The T cell receptor repertoire of CD4-8+ thymocytes is altered by overexpression of the BCL-2 protooncogene in the thymus. J Exp Med 179(1): 145-153.

Tarazona, R., Williams, O., Moskophidis, D., Smyth, L.A., Tanaka, Y., Murdjeva, M., Wack, A., Mamalaki, C., and Kioussis, D. 1998. Susceptibility and resistance to antigen-induced apoptosis in the thymus of transgenic mice. J Immunol 160(11): 5397-5403.

Teh, H.S., Kisielow, P., Scott, B., Kishi, H., Uematsu, Y., Bluthmann, H., and von Boehmer, H. 1988. Thymic major histocompatibility complex antigens and the alpha beta T-cell receptor determine the CD4/CD8 phenotype of T cells. Nature 335(6187): 229-233.

Thien, C.B., Blystad, F.D., Zhan, Y., Lew, A.M., Voigt, V., Andoniou, C.E., and Langdon, W.Y. 2005. Loss of c-Cbl RING finger function results in high-intensity TCR signaling and thymic deletion. Embo J 24(21): 3807-3819.

Ting, C.N., Olson, M.C., Barton, K.P., and Leiden, J.M. 1996. Transcription factor GATA-3 is required for development of the T-cell lineage. Nature 384(6608): 474-478.

Tonomura, N., McLaughlin, K., Grimm, L., Goldsby, R.A., and Osborne, B.A. 2003. Glucocorticoid-induced apoptosis of thymocytes: requirement of proteasome-dependent mitochondrial activity. J Immunol 170(5): 2469-2478.

Tosa, N., Murakami, M., Jia, W.Y., Yokoyama, M., Masunaga, T., Iwabuchi, C., Inobe, M., Iwabuchi, K., Miyazaki, T., Onoe, K., Iwata, M., and Uede, T. 2003. Critical function of T cell death-associated gene 8 in glucocorticoid-induced thymocyte apoptosis. Int Immunol 15(6): 741-749.

Tough, D.F. and Sprent, J. 1995. Life span of naive and memory T cells. Stem Cells 13(3): 242-249.

Tourne, S., van Santen, H.M., van Roon, M., Berns, A., Benoist, C., Mathis, D., and Ploegh, H. 1996. Biosynthesis of major histocompatibility complex molecules and generation of T cells in Ii TAP1 double-mutant mice. Proc Natl Acad Sci U S A 93(4): 1464-1469.

Townsend, A.R., Rothbard, J., Gotch, F.M., Bahadur, G., Wraith, D., and McMichael, A.J. 2006. The epitopes of influenza nucleoprotein recognized by cytotoxic T lymphocytes can be defined with short synthetic peptides. 1986. J Immunol 176(9): 5141-5150.

Tracey, W.D. and Speck, N.A. 2000. Potential roles for RUNX1 and its orthologs in determining hematopoietic cell fate. Semin Cell Dev Biol 11(5): 337-342.

Urban, J.A. and Winandy, S. 2004. Ikaros null mice display defects in T cell selection and CD4 versus CD8 lineage decisions. J Immunol 173(7): 4470-4478.

van den Brandt, J., Luhder, F., McPherson, K.G., de Graaf, K.L., Tischner, D., Wiehr, S., Herrmann, T., Weissert, R., Gold, R., and Reichardt, H.M. 2007. Enhanced glucocorticoid receptor signaling in T cells impacts thymocyte apoptosis and adaptive immune responses. Am J Pathol 170(3): 1041-1053.

van Oers, N.S., Lowin-Kropf, B., Finlay, D., Connolly, K., and Weiss, A. 1996. alpha beta T cell development is abolished in mice lacking both Lck and Fyn protein tyrosine kinases. Immunity 5(5): 429-436.

Veis, D.J., Sorenson, C.M., Shutter, J.R., and Korsmeyer, S.J. 1993. Bcl-2-deficient mice demonstrate fulminant lymphoid apoptosis, polycystic kidneys, and hypopigmented hair. Cell 75(2): 229-240.

Verhasselt, B., De Smedt, M., Verhelst, R., Naessens, E., and Plum, J. 1998. Retrovirally transduced CD34++ human cord blood cells generate T cells expressing high levels of the retroviral encoded green fluorescent protein marker in vitro. Blood 91(2): 431-440.

von Freeden-Jeffry, U., Vieira, P., Lucian, L.A., McNeil, T., Burdach, S.E., and Murray, R. 1995. Lymphopenia in interleukin (IL)-7 gene-deleted mice identifies IL-7 as a nonredundant cytokine. J Exp Med 181(4): 1519-1526.

Wallace, A.D., Wheeler, T.T., and Young, D.A. 1997. Inducibility of E4BP4 suggests a novel mechanism of negative gene regulation by glucocorticoids. Biochem Biophys Res Commun 232(2): 403-406.

Wang, J.C., Derynck, M.K., Nonaka, D.F., Khodabakhsh, D.B., Haqq, C., and Yamamoto, K.R. 2004. Chromatin immunoprecipitation (ChIP) scanning identifies primary glucocorticoid receptor target genes. Proc Natl Acad Sci U S A 101(44): 15603-15608.

Wang, Z., Malone, M.H., He, H., McColl, K.S., and Distelhorst, C.W. 2003a. Microarray analysis uncovers the induction of the proapoptotic BH3-only protein Bim in multiple models of glucocorticoid-induced apoptosis. J Biol Chem 278(26): 23861-23867.

Wang, Z., Malone, M.H., Thomenius, M.J., Zhong, F., Xu, F., and Distelhorst, C.W. 2003b. Dexamethasone-induced gene 2 (dig2) is a novel pro-survival stress gene induced rapidly by diverse apoptotic signals. J Biol Chem 278(29): 27053-27058.

Wang, Z., Rong, Y.P., Malone, M.H., Davis, M.C., Zhong, F., and Distelhorst, C.W. 2006. Thioredoxin-interacting protein (txnip) is a glucocorticoid-regulated primary response gene involved in mediating glucocorticoid-induced apoptosis. Oncogene 25(13): 1903-1913.

Wiegers, G.J., Knoflach, M., Bock, G., Niederegger, H., Dietrich, H., Falus, A., Boyd, R., and Wick, G. 2001. CD4(+)CD8(+)TCR(low) thymocytes express low levels of glucocorticoid receptors while being sensitive to glucocorticoid-induced apoptosis. Eur J Immunol 31(8): 2293-2301.

Wilkinson, B., Owen, J.J., and Jenkinson, E.J. 1999. Factors regulating stem cell recruitment to the fetal thymus. J Immunol 162(7): 3873-3881.

Williams, G.T., Kingston, R., Owen, M.J., Jenkinson, E.J., and Owen, J.J. 1986. A single micromanipulated stem cell gives rise to multiple T-cell receptor gene rearrangements in the thymus in vitro. Nature 324(6092): 63-64.

Williams, N.S., Klem, J., Puzanov, I.J., Sivakumar, P.V., Bennett, M., and Kumar, V. 1999. Differentiation of NK1.1+, Ly49+ NK cells from flt3+ multipotent marrow progenitor cells. J Immunol 163(5): 2648-2656.

Williams, N.S., Moore, T.A., Schatzle, J.D., Puzanov, I.J., Sivakumar, P.V., Zlotnik, A., Bennett, M., and Kumar, V. 1997. Generation of lytic natural killer 1.1+, Ly-49- cells from multipotential murine bone marrow progenitors in a stroma-free culture: definition of cytokine requirements and developmental intermediates. J Exp Med 186(9): 1609-1614.

Williams, O. and Brady, H.J. 2001. The role of molecules that mediate apoptosis in T-cell selection. Trends Immunol 22(2): 107-111.

Williams, O., Gil-Gomez, G., Norton, T., Kioussis, D., and Brady, H.J. 2000. Activation of Cdk2 is a requirement for antigen-mediated thymic negative selection. Eur J Immunol 30(2): 709-713.

Williams, O., Mok, C.L., Norton, T., Harker, N., Kioussis, D., and Brady, H.J. 2001. Elevated Bcl-2 is not a causal event in the positive selection of T cells. Eur J Immunol 31(6): 1876-1882.

Williams, O., Norton, T., Halligey, M., Kioussis, D., and Brady, H.J. 1998. The action of Bax and bcl-2 on T cell selection. J Exp Med 188(6): 1125-1133.

Wilson, A., MacDonald, H.R., and Radtke, F. 2001. Notch 1-deficient common lymphoid precursors adopt a B cell fate in the thymus. J Exp Med 194(7): 1003-1012.

Winandy, S., Wu, L., Wang, J.H., and Georgopoulos, K. 1999. Pre-T cell receptor (TCR) and TCR-controlled checkpoints in T cell differentiation are set by Ikaros. J Exp Med 190(8): 1039-1048.

Wisniewska, M., Stanczyk, M., Grzelakowska-Sztabert, B., and Kaminska, B. 1997. Nuclear factor of activated T cells (NFAT) is a possible target for dexamethasone in thymocyte apoptosis. Cell Biol Int 21(3): 127-132.

Wolfer, A., Wilson, A., Nemir, M., MacDonald, H.R., and Radtke, F. 2002. Inactivation of Notch1 impairs VDJbeta rearrangement and allows pre-TCR-independent survival of early alpha beta Lineage Thymocytes. Immunity 16(6): 869-879.

Wolter, K.G., Hsu, Y.T., Smith, C.L., Nechushtan, A., Xi, X.G., and Youle, R.J. 1997. Movement of Bax from the cytosol to mitochondria during apoptosis. J Cell Biol 139(5): 1281-1292.

Woolf, E., Xiao, C., Fainaru, O., Lotem, J., Rosen, D., Negreanu, V., Bernstein, Y., Goldenberg, D., Brenner, O., Berke, G., Levanon, D., and Groner, Y. 2003. Runx3 and Runx1 are required for CD8 T cell development during thymopoiesis. Proc Natl Acad Sci U S A 100(13): 7731-7736.

Woronicz, J.D., Calnan, B., Ngo, V., and Winoto, A. 1994. Requirement for the orphan steroid receptor Nur77 in apoptosis of T-cell hybridomas. Nature 367(6460): 277-281.

Wu, L., Scollay, R., Egerton, M., Pearse, M., Spangrude, G.J., and Shortman, K. 1991. CD4 expressed on earliest T-lineage precursor cells in the adult murine thymus. Nature 349(6304): 71-74.

Wurch, A., Biro, J., Potocnik, A.J., Falk, I., Mossmann, H., and Eichmann, K. 1998. Requirement of CD3 complex-associated signaling functions for expression of rearranged T cell receptor beta VDJ genes in early thymic development. J Exp Med 188(9): 1669-1678.

Wyllie, A.H. 1980. Glucocorticoid-induced thymocyte apoptosis is associated with endogenous endonuclease activation. Nature 284(5756): 555-556.

Wyllie, A.H., Morris, R.G., Smith, A.L., and Dunlop, D. 1984. Chromatin cleavage in apoptosis: association with condensed chromatin morphology and dependence on macromolecular synthesis. J Pathol 142(1): 67-77.

Yamasaki, S. and Saito, T. 2007. Molecular basis for pre-TCR-mediated autonomous signaling. Trends Immunol 28(1): 39-43.

Yang-Yen, H.F. 2006. Mcl-1: a highly regulated cell death and survival controller. J Biomed Sci 13(2): 201-204.

Yeung, J., O'Sullivan, E., Hubank, M., and Brady, H.J. 2004. E4BP4 expression is regulated by the t(17;19)-associated oncoprotein E2A-HLF in pro-B cells. Br J Haematol 125(5): 560-567.

Yoshida, H., Nishina, H., Takimoto, H., Marengere, L.E., Wakeham, A.C., Bouchard, D., Kong, Y.Y., Ohteki, T., Shahinian, A., Bachmann, M., Ohashi, P.S., Penninger, J.M., Crabtree, G.R., and Mak, T.W. 1998. The transcription factor NF-ATc1 regulates lymphocyte proliferation and Th2 cytokine production. Immunity 8(1): 115-124.

You, Z., Ouyang, H., Lopatin, D., Polver, P.J., and Wang, C.Y. 2001. Nuclear factor-kappa B-inducible death effector domain-containing protein suppresses tumor necrosis factor-mediated apoptosis by inhibiting caspase-8 activity. J Biol Chem 276(28): 26398-26404.

Yu, J., Baron, V., Mercola, D., Mustelin, T., and Adamson, E.D. 2007. A network of p73, p53 and Egr1 is required for efficient apoptosis in tumor cells. Cell Death Differ 14(3): 640.

Zamoyska, R., Basson, A., Filby, A., Legname, G., Lovatt, M., and Seddon, B. 2003. The influence of the src-family kinases, Lck and Fyn, on T cell differentiation, survival and activation. Immunol Rev 191: 107-118.

Zhang, J., Gong, Y., Shao, X., Zhang, R., Xu, W., Chu, Y., Wang, Y., and Xiong, S. 2007. Asynchronism of thymocyte development in vivo and in vitro. DNA Cell Biol 26(1): 19-27.

Zhang, J., Mikecz, K., Finnegan, A., and Glant, T.T. 2000. Spontaneous thymocyte apoptosis is regulated by a mitochondrion-mediated signaling pathway. J Immunol 165(6): 2970-2974.

Zhang, W., Zhang, J., Kornuc, M., Kwan, K., Frank, R., and Nimer, S.D. 1995. Molecular cloning and characterization of NF-IL3A, a transcriptional activator of the human interleukin-3 promoter. Mol Cell Biol 15(11): 6055-6063.

Zhao, Y., Tan, J., Zhuang, L., Jiang, X., Liu, E.T., and Yu, Q. 2005. Inhibitors of histone deacetylases target the Rb-E2F1 pathway for apoptosis induction through

activation of proapoptotic protein Bim. Proc Natl Acad Sci U S A 102(44): 16090-16095.

Zhou, T., Cheng, J., Yang, P., Wang, Z., Liu, C., Su, X., Bluethmann, H., and Mountz, J.D. 1996. Inhibition of Nur77/Nurr1 leads to inefficient clonal deletion of self-reactive T cells. J Exp Med 183(4): 1879-1892.

Zilberman, Y., Yefenof, E., Katzav, S., Dorogin, A., Rosenheimer-Goudsmid, N., and Guy, R. 1999. Apoptosis of thymic lymphoma clones by thymic epithelial cells: a putative model for 'death by neglect'. Immunol Lett 67(2): 95-104.

Zilberman, Y., Zafrir, E., Ovadia, H., Yefenof, E., Guy, R., and Sionov, R.V. 2004. The glucocorticoid receptor mediates the thymic epithelial cell-induced apoptosis of CD4+8+ thymic lymphoma cells. Cell Immunol 227(1): 12-23.

Zong, W.X., Lindsten, T., Ross, A.J., MacGregor, G.R., and Thompson, C.B. 2001. BH3-only proteins that bind pro-survival Bcl-2 family members fail to induce apoptosis in the absence of Bax and Bak. Genes Dev 15(12): 1481-1486.

APPENDICES

Table A.1. Genes up-regulated by DEX in the presence of ROSC.

	Probe set ID	Gene Title	Gene Symbol	Description	P-value	Fold change	Chromosomal Location	UniGene ID	Representative Public ID
1	*92780_f_at*	*Mammary gland RCB-0526 Jyg-MC(A) cDNA, RIKEN full-length enriched library, clone:G830022P11 product:unclassifiable, full insert sequence*		*Mammary tumor virus locus 43*	*0.001179*	*87.721 (83.847 to 92.419)*		*422812*	*M90535 NCBI*
2	*93928_f_at*	*hypothetical protein LOC624610*	*LOC624610*		*0.04528*	*25.25 (19.269 to 34.599)*	*4 B1*		*AF043689 NCBI*
3	*102663_at*	*plasminogen activator, urokinase receptor*	*Plaur*	*M.musculus muPAR1 mRNA.*	*0.001179*	*24.745 (23.936 to 25.323)*	*7 A3*	*1359*	*X62700 NCBI*
4	*102955_at*	*nuclear factor, interleukin 3, regulated*	*Nfil3*	*Mus musculus NFIL3/E4BP4 transcription factor mRNA, complete cds.*	***0.04354***	***21.17 (14.468 to 26.46)***	*13 B1|13 32.0 cM*	*136604*	*U83148 NCBI*
5	92925_at	CCAAT/enhancer binding protein (C/EBP), beta	Cebpb	Mouse alpha-1-acid glycoprotein (AGP/EBP) mRNA, complete cds.		**18.154 (9.792 to 28.171)**	2 H3|2 95.5 cM		M61007 NCBI
6	96553_at	G-protein coupled receptor 65	Gpr65	putative G protein-coupled receptor; Mus musculus putative G protein-coupled receptor TDAG8 (TDAG8) mRNA, complete cds.		**16.609 (6.518 to 28.918)**	12 E	378924	U39827 NCBI
7	*97509_f_at*	*fibroblast growth factor receptor 1*	*Fgfr1*	*FGFR1(L); similar to mouse FGFR-1 encoded by GenBank Accession Number M28998 and to human FGFR-1 encoded by GenBank Accession Numbers M34187 and M34188; Mus musculus fibroblast growth factor receptor-1 mRNA, long isoform precursor, complete cds.*	***0.04141***	***14.174 (10.57 to 17.964)***	*8 A2|8 10.0 cM*	*265716*	*U22324 NCBI*
8	*160246_at*	*tumor necrosis factor, alpha-induced protein 8*	*Tnfaip8*	*UI-M-AO0-ach-a-08-0-UI.s1 NIH_BMAP_MPG Mus musculus cDNA clone UI-M-AO0-ach-a-08-0-UI 3', mRNA sequence.*	***0.01814***	***7.994 (7.125 to 8.821)***	*18 D1*	*27740*	*AI839109 NCBI*
9	93316_at	oxysterol binding protein-like 1A	Osbpl1a	putative; Mus musculus mRNA for oxysterol-binding protein, complete cds.		**7.871 (5.492 to 12.02)**	18 A2	259470	AB017026 NCBI
10	*101805_f_at*	*nuclear factor, interleukin 3, regulated*	*Nfil3*	*similar to human transcriptional repressor E4BP4, PIR Accession Number S18995; belongs to CREB-ATF subfamily of bZIP family of transcription factors; Mus musculus strain BALB/c transcription factor E4BP4 mRNA, partial cds.*	***0.04141***	***7.861 (5.593 to 9.11)***	*13 B1|13 32.0 cM*	*136604*	*U89411 NCBI*
11	103460_at	DNA-damage-inducible transcript 4	Ddit4	UI-M-BG0-ahz-g-03-0-UI.s1 NIH_BMAP_MSC Mus musculus cDNA clone UI-M-BG0-ahz-g-03-0-UI 3', mRNA sequence.		**7.292 (4.224 to 9.064)**	10 B3	21697	AI849939 NCBI
12	*92356_at*	*protein tyrosine phosphatase, non-receptor type 22 (lymphoid)*	*Ptpn22*	*Mouse protein tyrosine phosphatase (70zpep) mRNA, complete cds.*	***0.04141***	***7.26 (5.942 to 8.64)***	*3 F3*	*395*	*M90388 NCBI*
13	*160904_at*	*RIKEN cDNA B230317C12 gene*	*B230317C12Rik*	*UI-M-AH0-acy-c-05-0-UI.s1 NIH_BMAP_MCE Mus musculus cDNA clone UI-M-AH0-acy-c-05-0-UI 3', mRNA sequence.*	***0.04141***	***7.161 (6.049 to 9.074)***	*2 A3*	*279863*	*AI841484 NCBI*
14	94501_at	sphingosine-1-phosphate phosphatase 1	Sgpp1	UI-M-AI0-aaq-b-10-0-UI.s1 NIH_BMAP_MBS Mus musculus cDNA clone UI-M-AI0-aaq-b-10-0-UI 3', mRNA sequence.		**6.89 (3.306 to 10.533)**	12 C3	280199	AI835784 NCBI
15	*160547_s_at*	*thioredoxin interacting protein*	*Txnip*	*UI-M-AO0-ach-d-06-0-UI.s1 NIH_BMAP_MPG Mus musculus cDNA clone UI-M-AO0-ach-d-06-0-UI 3', mRNA sequence.*	***0.0346***	***6.647 (5.47 to 7.546)***	*3 47.1 cM*	*410189*	*AI839138 NCBI*
16	97409_at	immunity-related GTPase family, M	Irgm	related to GTP-binding proteins; Mus musculus G-protein-like LRG-47 mRNA, complete cds.		**6.275 (2.712 to 8.304)**	11 B1.2	29938	U19119 NCBI
17	97349_at	FERM domain containing 6	Frmd6	vu99g08.r1 Stratagene mouse skin (#937313) Mus musculus cDNA clone IMAGE:1210334 5', mRNA sequence.		**6.093 (3.097 to 9.299)**	12 C3	2962	AA727410 NCBI
18	*99452_at*	*lipolysis stimulated lipoprotein receptor*	*Lsr*	*liver-specific gene; Mus musculus B6CBA Lisch7 mRNA, partial cds.*	***0.04141***	***5.981 (4.509 to 6.98)***	*7 B1*	*4067*	*U49507 NCBI*
19	*92778_i_at*	*Coronin, actin binding protein 2A*	*Coro2a*	*M.musculus membrane glycoprotein gene.*	***0.04528***	***5.921 (4.564 to 7.666)***	*4 B1*	*384420*	*Z22552 NCBI*
20	104058_at	coiled-coil domain containing 128	Ccdc128	UI-M-BH1-ama-d-09-0-UI.s1 NIH_BMAP_M_S2 Mus musculus cDNA clone UI-M-BH1-ama-d-09-0-UI 3', mRNA sequence.		**5.796 (3.938 to 8.334)**	17 E4	271817	AW047528 NCBI
21	*95024_at*	*ubiquitin specific peptidase 18*	*Usp18*	*UI-M-BH1-alo-a-12-0-UI.s1 NIH_BMAP_M_S2 Mus musculus cDNA clone UI-M-BH1-alo-a-12-0-UI 3', mRNA sequence.*		***5.733 (3.994 to 7.14)***	*6 F|6 56.0 cM*	*326911*	*AW047653 NCBI*
22	103891_i_at	elongation factor RNA polymerase II 2	Ell2	ue51h10.r1 Soares_mammary_gland_NMLMG Mus musculus cDNA clone IMAGE:1494691 5', mRNA sequence.		**5.665 (3.783 to 8.076)**	13 C1	21288	AI197161 NCBI
23	*103599_at*	*transformed mouse 3T3 cell double minute 1*	*Mdm1*	*Source: Mouse nuclear protein (mdm-1a) mRNA, complete cds.*	***0.04657***	***5.238 (4.334 to 6.587)***	*10 C1-C3|10 67.0 cM*	*101191*	*M20824 NCBI*
24	103264_at	myotubularin related protein 1	Mtmr1	Mus musculus myotubularin related protein 1 (Mtmr1) mRNA, complete cds.		**5.155 (2.01 to 7.384)**	X A7.2	219672	AF073997 NCBI
25	*93360_at*	*phosphomannomutase 1*	*Pmm1*	*similar to yeast Sec53p; Mus musculus phosphomannomutase Sec53p homolog mRNA, complete cds.*	***0.04354***	***4.63 (3.527 to 5.705)***	*15 E1*	*18939*	*AF007267 NCBI*
26	102293_at	IKAROS family zinc finger 1	Ikzf1	Mouse Ikaros DNA binding protein (Ikaros) mRNA, complete cds.		**4.582 (1.666 to 6.938)**	11 A1|11 6.0 cM	103545	L03547 NCBI
27	*104670_at*	*DENN/MADD domain containing 4C*	*Dennd4c*	*uj34a01.x1 Sugano mouse kidney mkia Mus musculus cDNA clone IMAGE:1921800 3', mRNA sequence.*	***0.01814***	***4.484 (4.223 to 4.619)***	*4 C4*	*273718*	*AI315698 NCBI*

Genes italicised indicate those that have passed the Benjamini-Hochberg false discovery rate procedure.

Table A.1. Genes up-regulated by DEX in the presence of ROSC.

	Probe set ID	Gene Title	Gene Symbol	Description	P-value	Fold change	Chromosomal Location	UniGene ID	Representative Public ID
28	160236_at	SLAIN motif family, member 1	Slain1	UI-M-AI0-aap-g-03-0-UI.s1 NIH_BMAP_MBS Mus musculus cDNA clone UI-M-AI0-aap-g-03-0-UI 3', mRNA sequence.		**4.425 (2.457 to 5.709)**	14 E2.3	27548	AI835624 NCBI
29	*98923_at*	*RNA terminal phosphate cyclase-like 1*	*Rcl1*	*UI-M-BH0-aiu-d-07-0-UI.s1 NIH_BMAP_M_S1 Mus musculus cDNA clone UI-M-BH0-aiu-d-07-0-UI 3', mRNA sequence.*	***0.04354***	***4.327 (3.251 to 5.066)***	*19 C1*	*28630*	*AI852608 NCBI*
30	99419_g_at	BCL2-like 11 (apoptosis facilitator)	Bcl2l11	pro-apoptotic BH3-containing Bcl-2 family member; Mus musculus BimEL mRNA, complete cds.		**4.278 (2.006 to 5.499)**	2 F3-G1	141083	AF032459 NCBI
31	160273_at	zinc finger protein 36, C3H type-like 2	Zfp36l2	vw64d05.s1 Soares_mammary_gland_NMLMG Mus musculus cDNA clone IMAGE:1248585 3', mRNA sequence.		**4.259 (2.995 to 5.595)**	17 E4	259321	AA960603 NCBI
32	98440_at	leukotriene B4 12-hydroxydehydrogenase	Ltb4dh	vm60d08.r1 Stratagene mouse Tcell 937311 Mus musculus cDNA clone IMAGE:1002639 5' similar to TR:E212316 E212316 NADP DEPENDENT LEUKOTREINE B4 12-HYDROXYDEHYDROGENASE. ;, mRNA sequence.		**4.234 (2.793 to 5.702)**	4 C1	34497	AA596710 NCBI
33	*94297_at*	*FK506 binding protein 5*	*Fkbp5*	*T-cell specific immunophilin that inhibits calcineurin; Mus musculus immunophilin FKBP51 mRNA, complete cds.*	***0.04354***	***4.133 (3.261 to 5.127)***	*17 A3.3|17 13.0 cM*	*276405*	*U16959 NCBI*
34	99392_at	tumor necrosis factor, alpha-induced protein 3	Tnfaip3	Mus musculus zinc finger protein A20 (murine A20) mRNA, complete cds.		**4.085 (2.039 to 6.664)**	10 A3|10 13.0 cM	116683	U19463 NCBI
35	*95057_at*	*homocysteine-inducible, endoplasmic reticulum stress-inducible, ubiquitin-like domain member 1*	*Herpud1*	*UI-M-AK1-aey-e-10-0-UI.s1 NIH_BMAP_MHY_N Mus musculus cDNA clone UI-M-AK1-aey-e-10-0-UI 3', mRNA sequence.*	***0.03171***	***4.077 (3.629 to 4.413)***	*8 C5*	*29151*	*AI846938 NCBI*
36	99033_at	inositol 1,3,4-triphosphate 5/6 kinase	Itpk1	UI-M-AK0-adc-g-01-0-UI.s1 NIH_BMAP_MHY Mus musculus cDNA clone UI-M-AK0-adc-g-01-0-UI 3', mRNA sequence.		**4.028 (2.806 to 4.865)**	12 E	347546	AI837130 NCBI
37	96650_at	AU RNA binding protein/enoyl-coenzyme A hydratase	Auh	UI-M-AK0-adj-f-11-0-UI.s1 NIH_BMAP_MHY Mus musculus cDNA clone UI-M-AK0-adj-f-11-0-UI 3', mRNA sequence.		**3.917 (2.674 to 5.518)**	13 A5-B1	252034	AI837724 NCBI
38	*101560_at*	*embigin*	*Emb*	*UI-M-BH1-anw-f-04-0-UI.s1 NIH_BMAP_M_S2 Mus musculus cDNA clone UI-M-BH1-anw-f-04-0-UI 3', mRNA sequence.*	***0.03171***	***3.882 (3.546 to 4.191)***	*13 D2.3*	*274926*	*AW061330 NCBI*
39	*101457_at*	*Janus kinase 2*	*Jak2*	*Mouse protein-tyrosine kinase (Jak2) mRNA, complete cds.*	***0.04141***	***3.795 (3.027 to 4.434)***	*19 C1|19 24.0 cM*	*275839*	*L16956 NCBI*
40	*103064_at*	*checkpoint kinase 1 homolog (S. pombe)*	*Chek1*	*similar to S.pombe CHK1 protein kinase; checkpoint kinase; Mus musculus checkpoint kinase Chk1 (Chk1) mRNA, complete cds.*	***0.04141***	***3.777 (3.249 to 4.349)***	*9 A5.3*	*16753*	*AF016583 NCBI*
41	*92443_i_at*	*zinc finger protein 1*	*Zfp1*	*Zfp-1 protein (AA 1-424); M.musculus mRNA for Zpf-1 zinc finger protein.*	***0.04899***	***3.668 (2.828 to 4.585)***	*8 E1|8 57.0 cM*	*4184*	*X16493 NCBI*
42	*99019_at*	*P450 (cytochrome) oxidoreductase*	*Por*	*Mouse mRNA for NADPH-cytochrome P450 oxidoreductase, complete cds.*	***0.04354***	***3.664 (2.775 to 4.269)***	*5 G2|5 75.0 cM*	*3863*	*D17571 NCBI*
43	*96130_at*	*STE20-like kinase (yeast)*	*Slk*	*vw13g10.r1 Soares_thymus_2NbMT Mus musculus cDNA clone IMAGE:1243746 5', mRNA sequence.*	***0.04141***	***3.618 (3.146 to 4.309)***	*19 D2*	*391941*	*AA822531 NCBI*
44	104598_at	dual specificity phosphatase 1	Dusp1	Mouse mRNA for a growth factor-inducible immediate early gene (3CH134).		**3.614 (2.792 to 4.911)**	17 A2-C|17 13.0 cM	239041	X61940 NCBI
45	*98589_at*	*adipose differentiation related protein*	*Adfp*	*Mouse adipose differentiation related protein (ADFP) mRNA, complete cds.*	***0.04141***	***3.561 (2.916 to 4.206)***	*4 C4|4 38.9 cM*	*381*	*M93275 NCBI*
46	*160285_at*	*DEAH (Asp-Glu-Ala-His) box polypeptide 40*	*Dhx40*	*UI-M-AJ1-ahd-e-07-0-UI.s1 NIH_BMAP_MOB_N Mus musculus cDNA clone UI-M-AJ1-ahd-e-07-0-UI 3', mRNA sequence.*	***0.04354***	***3.532 (2.714 to 4.156)***	*11 C*	*260627*	*AI848996 NCBI*
47	104735_at	potassium channel tetramerisation domain containing 12	Kctd12	UI-M-AN1-afg-a-10-0-UI.s1 NIH_BMAP_MBG_N Mus musculus cDNA clone UI-M-AN1-afg-a-10-0-UI 3', mRNA sequence.		**3.518 (2.758 to 4.871)**	14 E2.3	246466	AI842065 NCBI
48	*160419_r_at*	*Phosphoglycerate dehydrogenase like 1*	*Phgdhl1*	*ud06c09.r1 Soares_NMPu Mus musculus cDNA clone IMAGE:1434352 5', mRNA sequence.*	***0.04528***	***3.344 (2.583 to 3.937)***	*14 E5*	*393408*	*AA866869 NCBI*
49	*104141_at*	*DNA segment, Chr 15, Wayne State University 75, expressed*	*D15Wsu75e*	*UI-M-BG1-aig-f-01-0-UI.s1 NIH_BMAP_MSC_N Mus musculus cDNA clone UI-M-BG1-aig-f-01-0-UI 3', mRNA sequence.*	***0.03171***	***3.209 (3.075 to 3.442)***	*15 E1|15 46.7 cM*	*432072*	*AI850401 NCBI*
50	*160673_at*	*cDNA sequence BC020002*	*BC020002*	*vf04g08.y1 Knowles Solter mouse blastocyst B3 Mus musculus cDNA clone IMAGE:834782 5' similar to SW:YBK4_YEAST P38164 HYPOTHETICAL 104.7 KD PROTEIN IN PKC1-RTG3 INTERGENIC REGION. ;, mRNA sequence.*	***0.04141***	***3.178 (2.824 to 3.572)***	*6 A1*	*257151*	*AI596544 NCBI*
51	*100988_at*	*BCL2-like 11 (apoptosis facilitator)*	*Bcl2l11*	*vp15a12.r1 Soares_mammary_gland_NbMMG Mus musculus cDNA clone IMAGE:1068670 5', mRNA sequence.*	***0.04141***	***3.178 (2.599 to 3.534)***	*2 F3-G1*	*141083*	*AA796690 NCBI*
52	*98122_at*	*LIM domain only 4*	*Lmo4*	*Mus musculus LIM domain transcription factor LMO4 mRNA, complete cds.*	***0.03171***	***3.165 (2.942 to 3.316)***	*3 H2|3 73.1 cM*	*29187*	*AF074600 NCBI*
53	*92444_f_at*	*zinc finger protein 1*	*Zfp1*	*Zfp-1 protein (AA 1-424); M.musculus mRNA for Zpf-1 zinc finger protein.*	***0.04354***	***3.142 (2.555 to 3.727)***	*8 E1|8 57.0 cM*	*4184*	*X16493 NCBI*
54	*94387_at*	*spermatogenesis associated 5*	*Spata5*	*Mus musculus SPAF (SPAF) mRNA, partial cds.*	***0.04354***	***3.095 (2.501 to 3.594)***	*3 B*	*172679*	*AF016544 NCBI*
55	101369_at	zinc finger protein 213	Zfp213	mc20c01.y1 Soares mouse p3NMF19.5 Mus musculus cDNA clone IMAGE:349056 5', mRNA sequence.		**3.076 (2.11 to 4.382)**	17 A3.3	268582	AI391071 NCBI
56	*102351_at*	*carboxypeptidase A3, mast cell*	*Cpa3*	*carboxypeptidase A precursor; Mouse mast cell carboxypeptidase A mRNA, complete cds.*	***0.04141***	***3.07 (2.886 to 3.438)***	*3 A2|3 13.2 cM*	*1135*	*J05118 NCBI*
57	97844_at	regulator of G-protein signaling 2	Rgs2	contains an RGS domain; expressed in a wide variety of tissues; Mus musculus G protein signaling regulator RGS2 (rgs2) mRNA, complete cds.		**3.056 (1.313 to 4.253)**	1 F|1 78.0 cM	28262	U67187 NCBI

Genes italicised indicate those that have passed the Benjamini-Hochberg false discovery rate procedure.

Table A.1. Genes up-regulated by DEX in the presence of ROSC.

	Probe set ID	Gene Title	Gene Symbol	Description	P-value	Fold change	Chromosomal Location	UniGene ID	Representative Public ID
58	*161147_f_at*			*AV221100 RIKEN full-length enriched, 14, 17 days embryo head Mus musculus cDNA clone 3230402O16 3', mRNA sequence.*	***0.04141***	***3.045 (2.586 to 3.315)***			*AV221100 NCBI*
59	101437_at	STE20-like kinase (yeast)	Slk	mSLK; Mus musculus serine/threonine protein kinase mRNA, complete cds.		**3.025 (2.105 to 4.358)**	19 D2	281011	AF039574 NCBI
60	*95577_at*	*expressed sequence AI314180*	*AI314180*	*UI-M-BH1-and-e-07-0-UI.s1 NIH_BMAP_M_S2 Mus musculus cDNA clone UI-M-BH1-and-e-07-0-UI 3', mRNA sequence.*	***0.04141***	***3.014 (2.661 to 3.34)***	*4 B3*	*234801*	*AW049625 NCBI*
61	99866_at	RNA binding motif, single stranded interacting protein 1	Rbms1	vt02g03.x1 Barstead mouse myotubes MPLRB5 Mus musculus cDNA clone IMAGE:1161940 3', mRNA sequence.		**2.989 (2.307 to 3.717)**	2 C3	259667	AI642417 NCBI
62	*94439_at*	*oxysterol binding protein-like 11*	*Osbpl11*	*UI-M-BH2.1-apq-h-10-0-UI.s1 NIH_BMAP_M_S3.1 Mus musculus cDNA clone UI-M-BH2.1-apq-h-10-0-UI 3', mRNA sequence.*	***0.04141***	***2.965 (2.691 to 3.395)***	*16 B3*	*26564*	*AW124363 NCBI*
63	162438_f_at	DNA segment, Chr 15, Wayne State University 75, expressed	D15Wsu75e	AV345874 RIKEN full-length enriched, adult male olfactory bulb Mus musculus cDNA clone 6430564D04 3', mRNA sequence.		**2.892 (2.343 to 3.57)**	15 E1|15 46.7 cM	432072	AV345874 NCBI
64	*97890_at*	*serum/glucocorticoid regulated kinase*	*Sgk*	*UI-M-BH1-akw-d-06-0-UI.s1 NIH_BMAP_M_S2 Mus musculus cDNA clone UI-M-BH1-akw-d-06-0-UI 3', mRNA sequence.*	***0.04141***	***2.874 (2.605 to 3.142)***	*10 A3*	*28405*	*AW046181 NCBI*
65	99030_at	interleukin 7 receptor	Il7r	interleukin-7 receptor precursor; Mouse interleukin-7 receptor (IL-7) mRNA, complete cds.		**2.853 (2.313 to 3.665)**	15 A1|15 4.6 cM	389	M29697 NCBI
66	*96348_at*	*patatin-like phospholipase domain containing 2*	*Pnpla2*	*UI-M-BH2.3-aok-d-10-0-UI.s1 NIH_BMAP_M_S3.3 Mus musculus cDNA clone UI-M-BH2.3-aok-d-10-0-UI 3', mRNA sequence.*	***0.04547***	***2.827 (2.527 to 3.42)***	*7 F5*	*29998*	*AW121217 NCBI*
67	103443_at	absent in melanoma 1	Aim1	vu58c09.r1 Soares_mammary_gland_NbMMG Mus musculus cDNA clone IMAGE:1195600 5', mRNA sequence.		**2.818 (2.225 to 3.313)**	10 B2|10 29.0 cM	292082	AA711704 NCBI
68	*161132_at*	*sciellin*	*Scel*	*vv01c09.r1 Stratagene mouse skin (#937313) Mus musculus cDNA clone IMAGE:1210384 5', mRNA sequence.*	***0.04141***	***2.815 (2.693 to 3.041)***	*14 E*	*244003*	*AA727482 NCBI*
69	*160840_at*	*Rho guanine nucleotide exchange factor (GEF) 3*	*Arhgef3*	*UI-M-BH0-ajq-c-11-0-UI.s1 NIH_BMAP_M_S1 Mus musculus cDNA clone UI-M-BH0-ajq-c-11-0-UI 3', mRNA sequence.*	***0.04354***	***2.802 (2.416 to 3.276)***	*14 A3|14 9.0 cM*	*248606*	*AI853706 NCBI*
70	160379_at	erythrocyte protein band 4.1	Epb4.1	ORF1; ORF2; Mus musculus protein 4.1 mRNA, 5' end of ORF1, 3' end of ORF2, and 23 exons.		**2.765 (2.273 to 3.509)**	4 D2.3	30038	L00919 NCBI
71	*160858_at*	*RIKEN cDNA 2310061C15 gene*	*2310061C15Rik*	*UI-M-BH1-alc-a-11-0-UI.s1 NIH_BMAP_M_S2 Mus musculus cDNA clone UI-M-BH1-alc-a-11-0-UI 3', mRNA sequence.*	***0.04528***	***2.739 (2.319 to 3.248)***	*8 E1*	*4011*	*AW045976 NCBI*
72	94787_at	AU RNA binding protein/enoyl-coenzyme A hydratase	Auh	vy95e11.r1 Soares_mammary_gland_NbMMG Mus musculus cDNA clone IMAGE:1313996 5', mRNA sequence.		**2.737 (2.17 to 3.798)**	13 A5-B1		AA914517 NCBI
73	*99810_at*	*glutathione peroxidase 2*	*Gpx2*	*M.musculus DNA for Gpx2 pseudogene.*	***0.04141***	***2.724 (2.52 to 3.069)***	*12 C3|12 36.0 cM*	*371561*	*X91864 NCBI*
74	98859_at	acid phosphatase 5, tartrate resistant	Acp5	Mus musculus (clone lambda-MG5.3) acid phosphatase type 5 gene, complete cds.		**2.691 (1.813 to 4.18)**	9 A3|9 6.0 cM	46354	M99054 NCBI
75	100597_at	glycogenin	Gyg	UI-M-BH1-ani-g-03-0-UI.s1 NIH_BMAP_M_S2 Mus musculus cDNA clone UI-M-BH1-ani-g-03-0-UI 3', mRNA sequence.		**2.684 (1.896 to 3.565)**	3 A2|3 12.5 cM	6375	AW049730 NCBI
76	*104087_at*	*DNA segment, Chr 10, ERATO Doi 641, expressed*	*D10Ertd641e*	*UI-M-AM0-adq-c-01-0-UI.s1 NIH_BMAP_MAM Mus musculus cDNA clone UI-M-AM0-adq-c-01-0-UI 3', mRNA sequence.*	***0.04657***	***2.644 (2.298 to 3.151)***	*10 B4|10 30.0 cM*	*21793*	*AI840598 NCBI*
77	93144_at	DIP2 disco-interacting protein 2 homolog B (Drosophila)	Dip2b	UI-M-BH0-ake-c-05-0-UI.s1 NIH_BMAP_M_S1 Mus musculus cDNA clone UI-M-BH0-ake-c-05-0-UI 3', mRNA sequence.		**2.641 (1.744 to 3.505)**	15 F1	243658	AI854602 NCBI
78	*102744_at*	*T-cell receptor gamma chain*	*Tcrg*	*gamma-subunit; Murine mRNA for T-cell gamma gene.*	***0.04141***	***2.631 (2.468 to 2.754)***	*13 10.0 cM*	*211738*	*X00697 NCBI*
79	*92480_f_at*	*zinc finger protein 53*	*Zfp53*	*KRAB (Kruppel-associated box)-containing zinc-finger protein; Mus musculus mRNA for KRAB-containing zinc-finger protein KRAZ1, complete cds.*	***0.04528***	***2.619 (2.244 to 3.059)***	*17 A3.2|17 9.9 cM*	*42140*	*AB024004 NCBI*
80	104750_at	interferon gamma inducible protein 47	Ifi47	protein is predicted; Mus musculus predicted GTP binding protein (IRG-47) mRNA, complete cds.		**2.619 (2.029 to 3.149)**	11 B1.2	24769	M63630 NCBI
81	93203_f_at	forkhead box N2	Foxn2	um17a12.x1 Sugano mouse kidney mkia Mus musculus cDNA clone IMAGE:2192542 3', mRNA sequence.		**2.618 (1.9 to 3.308)**	17 E5	112824	AW107463 NCBI
82	103892_r_at	elongation factor RNA polymerase II 2	Ell2	ue51h10.r1 Soares_mammary_gland_NMLMG Mus musculus cDNA clone IMAGE:1494691 5', mRNA sequence.		**2.615 (1.984 to 3.266)**	13 C1	21288	AI197161 NCBI
83	162477_r_at	signal recognition particle 14	Srp14	AV096879 Mus musculus C57BL/6J ES cell Mus musculus cDNA clone 2410022H05, mRNA sequence.		**2.611 (1.521 to 3.675)**	2 E5	363404	AV096879 NCBI
84	95571_at	solute carrier family 30 (zinc transporter), member 4	Slc30a4	zinc transporter; Mus musculus zinc transporter (ZnT4) gene, fragment 4, and partial cds.		**2.555 (1.487 to 3.905)**	2 E5|2 69.0 cM	27801	AF004100 NCBI
85	*94027_at*	*8 cells embryo 8 cells cDNA, RIKEN full-length enriched library, clone:E860019P17 product:unclassifiable, full insert sequence*		*vp70h06.r1 Knowles Solter mouse blastocyst B3 Mus musculus cDNA clone IMAGE:1082075 5', mRNA sequence.*	***0.04141***	***2.548 (2.357 to 2.73)***		*309265*	*AA815831 NCBI*
86	160579_at	mannosidase 1, alpha	Man1a	ub01f03.r1 Soares_mammary_gland_NbMMG Mus musculus cDNA clone IMAGE:1365725 5', mRNA sequence.		**2.544 (1.492 to 3.519)**	10 B3	117294	AI021125 NCBI

Genes italicised indicate those that have passed the Benjamini-Hochberg false discovery rate procedure.

Table A.1. Genes up-regulated by DEX in the presence of ROSC.

	Probe set ID	Gene Title	Gene Symbol	Description	P-value	Fold change	Chromosomal Location	UniGene ID	Representative Public ID
87	93468_at	AF4/FMR2 family, member 1	Aff1	Mus musculus proto-oncogene AF4 mRNA, complete cds.		**2.523 (1.727 to 3.45)**	5 E|5 56.0 cM	6949	AF074266 NCBI
88	102384_at	SWI/SNF related, matrix associated, actin dependent regulator of chromatin, subfamily a, member 2	Smarca2	UI-M-AO1-aem-g-04-0-UI.s1 NIH_BMAP_MPG_N Mus musculus cDNA clone UI-M-AO1-aem-g-04-0-UI 3', mRNA sequence.		**2.461 (1.615 to 3.444)**	19 C1|19 17.0 cM	313303	AI842968 NCBI
89	*94028_f_at*	*8 cells embryo 8 cells cDNA, RIKEN full-length enriched library, clone:E860019P17 product:unclassifiable, full insert sequence*		*vn72g05.y1 Knowles Solter mouse blastocyst B1 Mus musculus cDNA clone IMAGE:1037528 5' similar to SW:ENV_SMSAV P03384 P15E PROTEIN ;, mRNA sequence.*	***0.04141***	***2.46 (2.288 to 2.683)***		*393605*	*AI642245 NCBI*
90	103683_at	dihydroorotate dehydrogenase	Dhodh	oxidoreductase; flavoprotein; DHOdehase; mitochondrial inner membrane protein; Mus musculus dihydroorotate dehydrogenase mRNA, complete cds; nuclear gene for mitochondrial product.		**2.46 (1.676 to 3.75)**	8 D3	23894	AF029667 NCBI
91	*96031_r_at*	*F-box and leucine-rich repeat protein 5*	*Fbxl5*	*up29c03.x1 NCI_CGAP_Mam2 Mus musculus cDNA clone IMAGE:2655748 3', mRNA sequence.*	***0.04354***	***2.459 (2.181 to 2.764)***	*5 B3*	*25794*	*AW259411 NCBI*
92	161723_at	WD repeat and FYVE domain containing 2	Wdfy2	AV264147 RIKEN full-length enriched, adult male testis (DH10B) Mus musculus cDNA clone 4930443O22 3', mRNA sequence.		**2.445 (1.633 to 3.397)**	14 D1	392194	AV264147 NCBI
93	96519_at	pyridoxal (pyridoxine, vitamin B6) kinase	Pdxk	ms02d10.x1 Stratagene mouse embryonic carcinoma (#937317) Mus musculus cDNA clone IMAGE:605779 3' similar to TR:O35331 O35331 PYRIDOXAL KINASE ;, mRNA sequence.		**2.439 (1.832 to 3.588)**	10 C1|10 42.1 cM	206159	AI450876 NCBI
94	104228_at	Predicted gene, EG668701	EG668701	vm88h05.r1 Knowles Solter mouse blastocyst B1 Mus musculus cDNA clone IMAGE:1005369 5', mRNA sequence.		**2.434 (1.56 to 2.92)**	12 A1.3	352240	AA607237 NCBI
95	96862_at	RIKEN cDNA 1110002B05 gene	1110002B05Rik	UI-M-AM1-aga-d-04-0-UI.s2 NIH_BMAP_MAM_N Mus musculus cDNA clone UI-M-AM1-aga-d-04-0-UI 3', mRNA sequence.		**2.427 (2.035 to 3.121)**	12 C1	292775	AI848584 NCBI
96	*100489_at*	*phosphodiesterase 7A*	*Pde7a*	*cyclic nucleotide phosphodiesterase of the PDE7 family, specific for cAMP as substrate; Mus musculus cyclic nucleotide phosphodiesterase PDE7A2 (MMPDE7A) mRNA, complete cds.*	***0.04528***	***2.424 (2.23 to 2.795)***	*3 A2|3 7.0 cM*	*296814*	*U68171 NCBI*
97	160580_at	mannosidase 1, alpha	Man1a	Mus musculus BALB/c mannosyl-oligosaccharide alpha-1,2-mannosidase mRNA, complete cds.		**2.404 (1.616 to 3.361)**	10 B3	117294	U04299 NCBI
98	97255_at	CUG triplet repeat, RNA binding protein 2	Cugbp2	UI-M-BH1-anw-e-02-0-UI.s1 NIH_BMAP_M_S2 Mus musculus cDNA clone UI-M-BH1-anw-e-02-0-UI 3', mRNA sequence.		**2.329 (1.576 to 2.948)**	2 A2-A3	398543	AW061318 NCBI
99	92368_at	receptor (calcitonin) activity modifying protein 3	Ramp3	Source: Mus musculus mRNA for receptor activity modifying protein 3 (Ramp3 gene).		**2.311 (1.848 to 3.012)**	11 A1|11 2.1 cM	39884	AJ250491 NCBI
100	103451_at	PTK2 protein tyrosine kinase 2 beta	Ptk2b	UI-M-AQ0-aaf-e-10-0-UI.s1 NIH_BMAP_MHI Mus musculus cDNA clone UI-M-AQ0-aaf-e-10-0-UI 3', mRNA sequence.		**2.31 (1.796 to 2.774)**	14 D1|14 28.0 cM	21613	AI835159 NCBI
101	100151_at	serine incorporator 3	Serinc3	overexpressed in testicular tumors; Mus musculus mRNA, complete cds.		**2.277 (1.878 to 2.796)**	2 H3	218473	L29441 NCBI
102	*93528_s_at*	*Kruppel-like factor 9*	*Klf9*	*UI-M-AH1-agp-g-10-0-UI.s1 NIH_BMAP_MCE_N Mus musculus cDNA clone UI-M-AH1-agp-g-10-0-UI 3', mRNA sequence.*	***0.04141***	***2.258 (2.176 to 2.351)***	*19 C1*	*291595*	*AI848050 NCBI*
103	160625_f_at	methyltransferase like 8	Mettl8	mj24a07.r1 Soares mouse embryo NbME13.5 14.5 Mus musculus cDNA clone IMAGE:477012 5', mRNA sequence.		**2.239 (2.048 to 2.584)**	2 C2	282641	AA048058 NCBI
104	104320_at	pyridoxal (pyridoxine, vitamin B6) kinase	Pdxk	UI-M-AN0-acl-d-07-0-UI.s1 NIH_BMAP_MBG Mus musculus cDNA clone UI-M-AN0-acl-d-07-0-UI 3', mRNA sequence.		**2.21 (1.147 to 3)**	10 C1|10 42.1 cM	206159	AI841777 NCBI
105	161974_r_at	RIKEN cDNA 2810417H13 gene	2810417H13Rik	AV372058 RIKEN full-length enriched, adult male colon Mus musculus cDNA clone 9030425J09 3', mRNA sequence.		**2.204 (1.43 to 2.855)**	9 C	351273	AV372058 NCBI
106	96529_at	AP1 gamma subunit binding protein 1	Ap1gbp1	UI-M-BH2.2-aoo-d-12-0-UI.s1 NIH_BMAP_M_S3.2 Mus musculus cDNA clone UI-M-BH2.2-aoo-d-12-0-UI 3', mRNA sequence.		**2.197 (1.623 to 2.591)**	11 C	82680	AW122059 NCBI
107	103537_at	eukaryotic translation initiation factor 2 alpha kinase 3	Eif2ak3	Mus musculus type-I transmembrane ER-resident serine/threonine kinase PERK mRNA, complete cds.		**2.196 (1.114 to 2.833)**	6 C1	247167	AF076681 NCBI
108	102695_at	T-cell receptor gamma, constant region	Tcrg-C	TCR C gamma 2; TCR J gamma 2; TCR V gamma 1.2; V gamma pseudogene fragment; TCR V gamma 1.1; TCR J gamma 4; TCR C gamma 4; Mus musculus T cell receptor gamma locus, TCR gamma 2 and gamma 4 gene clusters.		**2.191 (1.888 to 2.344)**	13 A2	210785	AF021335 NCBI
109	93892_at	CUG triplet repeat, RNA binding protein 2	Cugbp2	Mus musculus mRNA for elav-type RNA-binding protein.		**2.183 (1.893 to 2.713)**	2 A2-A3	398543	Y18298 NCBI
110	*160934_s_at*	*SH3-domain GRB2-like (endophilin) interacting protein 1*	*Sgip1*	*Murine (DBA/2) mRNA fragment for gag related peptide.*	***0.04354***	***2.173 (2.13 to 2.238)***	*4 C6*	*425962*	*X05546 NCBI*
111	94736_at	lysosomal trafficking regulator	Lyst	beige; Mus musculus beige (bg) mRNA, partial cds.		**2.172 (1.371 to 2.621)**	13 A1|13 7.0 cM	342337	U52461 NCBI
112	96189_at	zinc finger, CCHC domain containing 10	Zcchc10	UI-M-BH1-akw-d-10-0-UI.s1 NIH_BMAP_M_S2 Mus musculus cDNA clone UI-M-BH1-akw-d-10-0-UI 3', mRNA sequence.		**2.168 (1.338 to 3.065)**	11 B1.3|11 28.5 cM	288072	AW046184 NCBI

Genes italicised indicate those that have passed the Benjamini-Hochberg false discovery rate procedure.

Table A.1. Genes up-regulated by DEX in the presence of ROSC.

	Probe set ID	Gene Title	Gene Symbol	Description	P-value	Fold change	Chromosomal Location	UniGene ID	Representative Public ID
113	100293_at	CD59b antigen	Cd59b	vb01d09.r1 Soares mouse NML Mus musculus cDNA clone IMAGE:747665 5' similar to TR:G1199655 G1199655 CD59 PROTEIN PRECURSOR. ;, mRNA sequence.		**2.154 (1.828 to 2.497)**	2 E2	359026	AA268823 NCBI
114	100464_at	RIKEN cDNA 3110043O21 gene	3110043O21Rik	UI-M-AM0-adq-a-06-0-UI.s1 NIH_BMAP_MAM Mus musculus cDNA clone UI-M-AM0-adq-a-06-0-UI 3', mRNA sequence.		**2.149 (1.614 to 2.725)**	4 A5	331544	AI840585 NCBI
115	*98911_at*	*Janus kinase 1*	*Jak1*	*UI-M-AL0-abs-b-09-0-UI.s1 NIH_BMAP_MCO Mus musculus cDNA clone UI-M-AL0-abs-b-09-0-UI 3', mRNA sequence.*	***0.04602***	***2.136 (1.949 to 2.251)***	*4 C6|4 46.3 cM*	*289657*	*AI837528 NCBI*
116	96183_at	forkhead box P1	Foxp1	UI-M-BH2.1-apb-b-02-0-UI.s1 NIH_BMAP_M_S3.1 Mus musculus cDNA clone UI-M-BH2.1-apb-b-02-0-UI 3', mRNA sequence.		**2.131 (1.891 to 2.347)**	6 E1	234965	AW122985 NCBI
117	161706_f_at	laminin, gamma 1	Lamc1	AV244043 RIKEN full-length enriched, 0 day neonate head Mus musculus cDNA clone 4831427F22 3' similar to J02930 Mouse laminin B2 chain mRNA, mRNA sequence.		**2.128 (1.804 to 2.619)**	1 G3|1 81.1 cM	1249	AV244043 NCBI
118	95564_at	coiled-coil domain containing 117	Ccdc117	uc41d02.r1 Soares_mammary_gland_NMLMG Mus musculus cDNA clone IMAGE:1400547 5', mRNA sequence.		**2.089 (1.951 to 2.365)**	11 A1	210403	AI117859 NCBI
119	95123_at	RIKEN cDNA 4930566A11 gene	4930566A11Rik	UI-M-AL1-ahi-a-08-0-UI.s1 NIH_BMAP_MCO_N Mus musculus cDNA clone UI-M-AL1-ahi-a-08-0-UI 3', mRNA sequence.		**2.089 (1.324 to 2.543)**	8 D3	180410	AI844003 NCBI
120	98577_f_at					**2.083 (1.483 to 2.733)**			Y12713 NCBI
121	102152_f_at	similar to Ig heavy chain V region M167 precursor	LOC632502	Ig H-chain V-region; Mouse Ig germline H-chain gene V-region (subfamily T15), exons 1 and 2.		**2.066 (1.675 to 2.706)**			M16724 NCBI
122	92644_s_at	myeloblastosis oncogene	Myb	Mouse myb proto-oncogene mRNA encoding 71 kd myb protein, complete cds.		**2.04 (1.624 to 2.531)**	10 A3|10 16.0 cM	52109	M12848 NCBI
123	104415_at	Adult male corpora quadrigemina cDNA, RIKEN full-length enriched library, clone:B230341P20 product:inferred: forkhead box P1, full insert sequence		ud05d05.r1 Soares_NMPu Mus musculus cDNA clone IMAGE:1434249 5', mRNA sequence.		**2.011 (1.737 to 2.224)**		392884	AA833293 NCBI
124	93013_at	inhibitor of DNA binding 2	Id2	3' region; Mus musculus helix-loop-helix protein Id2 gene, 3' region.		**2.001 (1.468 to 2.706)**	12 B|12 7.0 cM	34871	AF077861 NCBI
125	96238_at	RAB11a, member RAS oncogene family	Rab11a	UI-M-BH0-aiv-g-11-0-UI.s1 NIH_BMAP_M_S1 Mus musculus cDNA clone UI-M-BH0-aiv-g-11-0-UI 3', mRNA sequence.		**2 (1.661 to 2.31)**	9 C	1387	AI853996 NCBI
126	161537_f_at	tripeptidyl peptidase II	Tpp2	AV236858 RIKEN full-length enriched, 10 day neonate skin Mus musculus cDNA clone 4732416D17 3' similar to X81323 M.musculus mRNA for tripeptidyl peptidase II, mRNA sequence.		**1.996 (1.246 to 2.613)**	1 C1.1|1 27.0 cM	401675	AV236858 NCBI
127	95366_at			cold shock domain		**1.99 (1.881 to 2.143)**			L35599 NCBI
128	98554_at	N-myc downstream regulated gene 3	Ndrg3	Mus musculus mRNA for Ndr1 related protein Ndr3, complete cds.		**1.974 (1.248 to 2.368)**	2 H1	279256	AB033922 NCBI
129	97975_at	nuclear factor of activated T-cells, cytoplasmic, calcineurin-dependent 3	Nfatc3	Mouse mRNA for NFATx, complete cds.		**1.966 (1.548 to 2.388)**	8 D|8 51.0 cM	383185	D85612 NCBI
130	93187_at	tripartite motif protein 47	Trim47	UI-M-BH1-akk-e-03-0-UI.s1 NIH_BMAP_M_S2 Mus musculus cDNA clone UI-M-BH1-akk-e-03-0-UI 3', mRNA sequence.		**1.964 (1.721 to 2.12)**	11 E2	347770	AW048347 NCBI
131	97118_at	RIKEN cDNA A630007B06 gene	A630007B06Rik	uf03d06.x1 Sugano mouse liver mlia Mus musculus cDNA clone IMAGE:1499531 3', mRNA sequence.		**1.959 (1.62 to 2.339)**	19 D2	131555	AI159700 NCBI
132	93619_at	period homolog 1 (Drosophila)	Per1	circadian pacemaker protein; Mus musculus Rigui mRNA, complete cds.		**1.953 (1.284 to 2.31)**	11 B	7373	AF022992 NCBI
133	103362_at	prostaglandin E receptor 4 (subtype EP4)	Ptger4	Mouse mRNA for prostaglandin E receptor EP2 subtype, complete cds.		**1.94 (1.515 to 2.758)**	15 A1|15 6.4 cM	18509	D13458 NCBI
134	95998_at	Phosphodiesterase 4B, cAMP specific	Pde4b	C79930 Mouse 3.5-dpc blastocyst cDNA Mus musculus cDNA clone J0073H08 3', mRNA sequence.		**1.94 (1.178 to 2.444)**	4 C6|4 46.8 cM	20181	C79930 NCBI
135	100462_at	ADP-ribosylation factor 6	Arf6	Mouse mRNA for ARF6, complete cds.		**1.938 (1.607 to 2.331)**	12 C2	27308	D87903 NCBI
136	104091_at	tetraspanin 9	Tspan9	UI-M-BH2.2-aox-e-09-0-UI.s1 NIH_BMAP_M_S3.2 Mus musculus cDNA clone UI-M-BH2.2-aox-e-09-0-UI 3', mRNA sequence.		**1.932 (1.195 to 2.357)**	6 F3	21814	AW122563 NCBI
137	161656_r_at	protein C	Proc	AV103587 Mus musculus liver C57BL/6J 13-day embryo Mus musculus cDNA clone 2500004D08, mRNA sequence.		**1.927 (1.621 to 2.211)**	18 B3	2786	AV103587 NCBI
138	100516_at	choline kinase alpha	Chka	alternative splicing; Mus musculus Chetk-alpha gene for choline/ethanolamine kinase-alpha, exon 9, 10, 11 and complete cds.		**1.926 (1.653 to 2.127)**	19 A|19 3.0 cM	225505	AB030621 NCBI
139	99445_at	solute carrier family 44, member 2	Slc44a2	UI-M-BH1-alp-g-12-0-UI.s1 NIH_BMAP_M_S2 Mus musculus cDNA clone UI-M-BH1-alp-g-12-0-UI 3', mRNA sequence.		**1.906 (1.704 to 2.135)**	9 A3	148425	AW047012 NCBI
140	100012_at	lysosomal-associated protein transmembrane 5	Laptm5	ORFA; ORFB; Mus musculus retinoic acid-inducible E3 protein mRNA, complete cds.		**1.904 (1.467 to 2.156)**	4 D2.3	271868	U29539 NCBI
141	92542_at	DNA segment, Chr 4, Wayne State University 53, expressed	D4Wsu53e	UI-M-AH1-agw-a-06-0-UI.s1 NIH_BMAP_MCE_N Mus musculus cDNA clone UI-M-AH1-agw-a-06-0-UI 3', mRNA sequence.		**1.903 (1.513 to 2.33)**	4 D3|4 65.7 cM	331964	AI849035 NCBI

Genes italicised indicate those that have passed the Benjamini-Hochberg false discovery rate procedure.

Table A.1. Genes up-regulated by DEX in the presence of ROSC.

	Probe set ID	Gene Title	Gene Symbol	Description	P-value	Fold change	Chromosomal Location	UniGene ID	Representative Public ID
142	161819_f_at	lysosomal-associated protein transmembrane 5	Laptm5	AV356071 RIKEN full-length enriched, adult male adrenal gland Mus musculus cDNA clone 7330423G02 3' similar to U29539 Mus musculus retinoic acid-inducible E3 protein mRNA, mRNA sequence.		**1.898 (1.658 to 2.212)**	4 D2.3	271868	AV356071 NCBI
143	102198_at	potassium intermediate/small conductance calcium-activated channel, subfamily N, member 4	Kcnn4	Mus musculus intermediate conductance potassium channel mIK1 mRNA, complete cds.		**1.895 (1.633 to 2.081)**	7 A3	9911	AF042487 NCBI
144	93410_at	WNK lysine deficient protein kinase 2	Wnk2	UI-M-BH2.3-aoa-e-01-0-UI.s1 NIH_BMAP_M_S3.3 Mus musculus cDNA clone UI-M-BH2.3-aoa-e-01-0-UI 3', mRNA sequence.		**1.892 (1.567 to 2.502)**	13 B1	342723	AW120840 NCBI
145	94637_at	sema domain, immunoglobulin domain (Ig), transmembrane domain (TM) and short cytoplasmic domain, (semaphorin) 4B	Sema4b	M.musculus mRNA for semaphorin C.		**1.888 (1.51 to 2.155)**		275909	X85992 NCBI
146	93530_at	Integrin alpha FG-GAP repeat containing 1	Itfg1	UI-M-AP1-agi-f-08-0-UI.s1 NIH_BMAP_MST_N Mus musculus cDNA clone UI-M-AP1-agi-f-08-0-UI 3', mRNA sequence.		**1.886 (1.535 to 2.108)**	8 C4|8 39.0 cM	334685	AI842807 NCBI
147	95650_at	NHP2 non-histone chromosome protein 2-like 1 (S. cerevisiae)	Nhp2l1	sperm-specific protein; proposed as a candidate for the development of contraceptive vaccine; FA-1; Mus musculus fertilization antigen-1 mRNA, complete cds.		**1.882 (1.505 to 2.221)**	15 E1|15 48.0 cM	390130	U95114 NCBI
148	104314_r_at	RIKEN cDNA 1110032A03 gene	1110032A03Rik	UI-M-BH0-ajx-f-05-0-UI.s1 NIH_BMAP_M_S1 Mus musculus cDNA clone UI-M-BH0-ajx-f-05-0-UI 3', mRNA sequence.		**1.878 (1.651 to 2.326)**	9 B	171374	AI851206 NCBI
149	94550_at	sorting nexin 1	Snx1	UI-M-BH2.2-aom-a-06-0-UI.s1 NIH_BMAP_M_S3.2 Mus musculus cDNA clone UI-M-BH2.2-aom-a-06-0-UI 3', mRNA sequence.		**1.874 (1.66 to 2.248)**		271891	AW121324 NCBI
150	103359_at	methyltransferase like 8	Mettl8	UI-M-BH0-ajw-g-04-0-UI.s1 NIH_BMAP_M_S1 Mus musculus cDNA clone UI-M-BH0-ajw-g-04-0-UI 3', mRNA sequence.		**1.874 (1.637 to 2.169)**	2 C2	282641	AI854144 NCBI
151	162379_r_at			AV245272 RIKEN full-length enriched, 0 day neonate head Mus musculus cDNA clone 4831437K04 3' similar to X56397 Mouse mRNA for vimentin, mRNA sequence.		**1.871 (1.712 to 1.991)**			AV245272 NCBI
152	93088_at	beta-2 microglobulin	B2m	beta2-microglobulin precursor (aa -20 to 99); Mouse mRNA for beta2-microglobulin.		**1.866 (1.65 to 2.139)**	2 F1-F3|2 69.0 cM	163	X01838 NCBI
153	104633_at	disabled homolog 2 (Drosophila)	Dab2	UI-M-BH2.3-aqc-a-07-0-UI.s1 NIH_BMAP_M_S3.3 Mus musculus cDNA clone UI-M-BH2.3-aqc-a-07-0-UI 3', mRNA sequence.		**1.865 (1.772 to 1.913)**	15 6.7 cM	240830	AW123921 NCBI
154	98415_at	cytokine receptor-like factor 3	Crlf3	Mus musculus cytokine receptor related protein 4 (Cytor4) mRNA, complete cds.		**1.864 (1.673 to 2.1)**	11 B5|11 47.21 cM	272093	AF046060 NCBI
155	93293_at	calmodulin 2	Calm2	Mus musculus calmodulin synthesis (CaM) cDNA, complete cds.		**1.862 (1.579 to 2.258)**	17 E4	329243	M27844 NCBI
156	101404_at	coiled-coil domain containing 115	Ccdc115	UI-M-BH0-ajq-b-06-0-UI.s1 NIH_BMAP_M_S1 Mus musculus cDNA clone UI-M-BH0-ajq-b-06-0-UI 3', mRNA sequence.		**1.847 (1.464 to 2.536)**	1 B	379170	AI853654 NCBI
157	97958_at	protein kinase C binding protein 1	Prkcbp1	UI-M-BH2.2-aow-a-02-0-UI.s1 NIH_BMAP_M_S3.2 Mus musculus cDNA clone UI-M-BH2.2-aow-a-02-0-UI 3', mRNA sequence.		**1.84 (1.595 to 2.111)**	2 H3	227598	AW122355 NCBI
158	93496_at	ELOVL family member 5, elongation of long chain fatty acids (yeast)	Elovl5	UI-M-BH0-aja-h-11-0-UI.s1 NIH_BMAP_M_S1 Mus musculus cDNA clone UI-M-BH0-aja-h-11-0-UI 3', mRNA sequence.		**1.837 (1.634 to 2.027)**	9 E1	430736	AI852098 NCBI
159	92694_at	chitinase 3-like 3	Chi3l3	Mus musculus secretory protein precursor (Ym1) mRNA, complete cds.		**1.83 (1.461 to 2.313)**	3 F2.3|3 50.5 cM	387173	M94584 NCBI
160	96945_at	synaptosomal-associated protein 23	Snap23	SNAP-25 related protein; Mus musculus syndet mRNA, complete cds.		**1.826 (1.617 to 2.015)**	2 E5|2 61.8 cM	245715	U73143 NCBI
161	103564_at	UV radiation resistance associated gene	Uvrag	ub26f01.r1 Soares_thymus_2NbMT Mus musculus cDNA clone IMAGE:1378873 5', mRNA sequence.		**1.825 (1.702 to 1.925)**	7 E1	323072	AI020259 NCBI
162	95318_at	zinc finger protein 105	Zfp105	Mus musculus zinc finger protein 105 (Zfp105) mRNA, complete cds.		**1.825 (1.408 to 2.508)**	9 F4|9 72.0 cM	290595	AF045565 NCBI
163	103625_at	AFG3(ATPase family gene 3)-like 1 (yeast)	Afg3l1	vw25a08.r1 Soares_mammary_gland_NbMMG Mus musculus cDNA clone IMAGE:1244822 5', mRNA sequence.		**1.818 (1.304 to 2.447)**	8 E2	287475	AA797556 NCBI
164	94815_at	2,3-bisphosphoglycerate mutase	Bpgm	2,3-bisphosphoglycerate mutase (AA 1 - 259); Murine mRNA for 2,3-bisphosphoglycerate mutase (BPGM; EC 5.4.2.4).		**1.817 (1.381 to 2.25)**	6 B1	282863	X13586 NCBI
165	99823_r_at	DNA segment, Chr 18, ERATO Doi 232, expressed	D18Ertd232e	C79676 Mouse 3.5-dpc blastocyst cDNA Mus musculus cDNA clone J0070C12 3', mRNA sequence.		**1.816 (1.746 to 1.906)**	18 9.0 cM		C79676 NCBI
166	100742_at	expressed sequence AA409749	AA409749	EST01534 Mouse 7.5 dpc embryo ectoplacental cone cDNA library Mus musculus cDNA clone C0011A07 3', mRNA sequence.		**1.815 (1.413 to 2.199)**			AA409749 NCBI
167	160617_at	Kruppel-like factor 13	Klf13	UI-M-BH2.2-aql-f-08-0-UI.s1 NIH_BMAP_M_S3.2 Mus musculus cDNA clone UI-M-BH2.2-aql-f-08-0-UI 3', mRNA sequence.		**1.811 (1.683 to 1.937)**	7 C	240473	AW125783 NCBI
168	93568_i_at	hypothetical protein LOC544988	LOC544988	UI-M-BH0-ajy-d-09-0-UI.s1 NIH_BMAP_M_S1 Mus musculus cDNA clone UI-M-BH0-ajy-d-09-0-UI 3', mRNA sequence.		**1.81 (1.49 to 2.287)**	14 A1	432066	AI853444 NCBI

Genes italicised indicate those that have passed the Benjamini-Hochberg false discovery rate procedure.

Table A.1. Genes up-regulated by DEX in the presence of ROSC.

	Probe set ID	Gene Title	Gene Symbol	Description	P-value	Fold change	Chromosomal Location	UniGene ID	Representative Public ID
169	103029_at	programmed cell death 4	Pdcd4	Mouse mRNA for Topoisomerase-inhibitor suppressed, complete cds.		**1.809 (1.564 to 1.944)**	19 D2|19 20.0 cM	1605	D86344 NCBI
170	99916_at	protein kinase C, eta	Prkch	Mouse mRNA for nPKC-eta.		**1.808 (1.322 to 2.166)**	12 C3-D1	341677	D90242 NCBI
171	98852_at	sal-like 3 (Drosophila)	Sall3	transcription factor; M.musculus mRNA for spalt transcription factor.		**1.803 (1.455 to 2.382)**	18 E3	215917	X97581 NCBI
172	95800_s_at	zinc finger protein, autosomal	Zfa	M.musculus Zfa gene.		**1.802 (1.147 to 2.275)**	10 B3|10 27.5 cM	390269	X53250 NCBI
173	96753_at	B-cell CLL/lymphoma 7C	Bcl7c	member of BCL7 gene family; M.musculus BCL7C mRNA.		**1.788 (1.361 to 2.221)**	7 F4	89667	Y11905 NCBI
174	95914_at	death inducer-obliterator 1	Dido1	mt29b12.r1 Soares mouse 3NbMS Mus musculus cDNA clone IMAGE:622463 5', mRNA sequence.		**1.783 (1.191 to 2.239)**	2 H4	253836	AA177382 NCBI
175	103028_at	IL2-inducible T-cell kinase	Itk	putative; Mus musculus tlk mRNA for tyrosine kinase, complete cds.		**1.783 (1.163 to 2.204)**	11 B1.1|11 22.0 cM	339927	D14042 NCBI
176	95022_at	A kinase (PRKA) anchor protein (gravin) 12	Akap12	Src Suppressed C Kinase Substrate; Mus musculus mRNA for SSeCKS, complete cds.		**1.778 (1.6 to 2.087)**	10 A1	27481	AB020886 NCBI
177	99500_at	solute carrier family 12, member 2	Slc12a2	Mus musculus putative basolateral Na-K-2Cl cotransporter mRNA, complete cds.		**1.773 (1.357 to 2.192)**	18 D3|18 32.0 cM	399997	U13174 NCBI
178	102841_at	similar to ubiquitin A-52 residue ribosomal protein fusion product 1	LOC668206	vn25g06.r1 Knowles Solter mouse blastocyst B1 Mus musculus cDNA clone IMAGE:1022266 5' similar to gb:M26880 UBIQUITIN (HUMAN); gb:X51703 Mouse mRNA for ubiquitin (MOUSE);, mRNA sequence.		**1.765 (1.384 to 2.272)**	11 B2	14707	AA623483 NCBI
179	160731_at	RAB25, member RAS oncogene family	Rab25	mj98f09.y1 Soares mouse p3NMF19.5 Mus musculus cDNA clone IMAGE:484169 5' similar to SW:RB25_RABIT P46629 RAS-RELATED PROTEIN RAB-25. ;, mRNA sequence.		**1.759 (1.506 to 2.1)**	3 E3-F1	26994	AI893677 NCBI
180	96564_at	heat shock protein 8	Hspa8			**1.757 (1.526 to 2.141)**	9 A5.1|9 24.0 cM	432164	X54401 NCBI
181	98999_at	adenylosuccinate lyase 1	Adsl	vm86b01.r1 Knowles Solter mouse blastocyst B1 Mus musculus cDNA clone IMAGE:1005097 5' similar to gb:U20225 Mus musculus adenylosuccinate lyase (MOUSE);, mRNA sequence.		**1.747 (1.348 to 1.949)**	15 E1|15 46.0 cM	38151	AA606587 NCBI
182	104149_at	nuclear factor of kappa light chain gene enhancer in B-cells inhibitor, alpha	Nfkbia	ub75b05.x1 Soares_mammary_gland_NMLMG Mus musculus cDNA clone IMAGE:1383537 3' similar to gb:M69043 MAJOR HISTOCOMPATIBILITY COMPLEX ENHANCER-BINDING PROTEIN (HUMAN);, mRNA sequence.		**1.741 (1.591 to 1.908)**	12 C1-C3	170515	AI642048 NCBI
183	103242_at	adaptor protein complex AP-1, gamma 1 subunit	Ap1g1	UI-M-BH2.1-apm-h-06-0-UI.s1 NIH_BMAP_M_S3.1 Mus musculus cDNA clone UI-M-BH2.1-apm-h-06-0-UI 3', mRNA sequence.		**1.736 (1.409 to 2.155)**	8 D3|8 53.0 cM	37210	AW123834 NCBI
184	96669_at	RIKEN cDNA 2400003C14 gene	2400003C14Rik	UI-M-BH2.1-apb-a-02-0-UI.s1 NIH_BMAP_M_S3.1 Mus musculus cDNA clone UI-M-BH2.1-apb-a-02-0-UI 3', mRNA sequence.		**1.735 (1.225 to 2.077)**	8 D3	290036	AW122973 NCBI
185	95752_at	Shwachman-Bodian-Diamond syndrome homolog (human)	Sbds	UI-M-AP0-abm-a-02-0-UI.s1 NIH_BMAP_MST Mus musculus cDNA clone UI-M-AP0-abm-a-02-0-UI 3', mRNA sequence.		**1.729 (1.526 to 1.868)**	5 G1.3	280484	AI837369 NCBI
186	96839_at	RIKEN cDNA 1110014N23 gene	1110014N23Rik	mc55g05.x1 Soares mouse embryo NbME13.5 14.5 Mus musculus cDNA clone IMAGE:352472 3', mRNA sequence.		**1.722 (1.331 to 2.114)**	19 A	227361	AI415446 NCBI
187	100965_at	cytochrome c oxidase, subunit VIIIc	Cox8c	ml56c11.r1 Stratagene mouse testis (#937308) Mus musculus cDNA clone IMAGE:516020 5', mRNA sequence.		**1.717 (1.417 to 1.89)**	12 E	660	AA108893 NCBI
188	101631_at	SRY-box containing gene 11	Sox11	putative transcription factor; Mus musculus SOX11 (Sox11) mRNA, complete cds.		**1.716 (1.527 to 1.883)**	12 A3	41702	AF009414 NCBI
189	101554_at	nuclear factor of kappa light chain gene enhancer in B-cells inhibitor, alpha	Nfkbia	Mus musculus I kappa B alpha gene, exons 2-6, partial cds.		**1.713 (1.556 to 1.922)**	12 C1-C3	170515	U57524 NCBI
190	97083_at	eukaryotic translation initiation factor 2, subunit 2 (beta)	Eif2s2	vm78h03.r1 Knowles Solter mouse blastocyst B1 Mus musculus cDNA clone IMAGE:1004405 5' similar to gb:M29536 TRANSLATIONAL INITIATION FACTOR 2 BETA SUBUNIT (HUMAN);, mRNA sequence.		**1.706 (1.454 to 1.909)**	2 H1|2 90.0 cM	377134	AA600468 NCBI
191	95622_at	kelch domain containing 2	Klhdc2	UI-M-BH2.1-app-h-01-0-UI.s1 NIH_BMAP_M_S3.1 Mus musculus cDNA clone UI-M-BH2.1-app-h-01-0-UI 3', mRNA sequence.		**1.701 (1.159 to 2.056)**	12 C3|12 30.0 cM	234368	AW123907 NCBI
192	98299_s_at	schlafen 3, schlafen 4	Slfn3, Slfn4	mSLFN3; Mus musculus schlafen3 (Slfn3) mRNA, complete cds.		**1.7 (1.617 to 1.791)**	11 C	290922	AF099974 NCBI
193	98535_at	catechol-O-methyltransferase	Comt	Mus musculus catechol-O-methyltransferase (Comt) mRNA, complete cds.		**1.697 (1.576 to 1.861)**	16 A3|16 11.2 cM	100940	AF076156 NCBI
194	95428_at	IMP4, U3 small nucleolar ribonucleoprotein, homolog (yeast)	Imp4	vr07b11.r1 Knowles Solter mouse blastocyst B3 Mus musculus cDNA clone IMAGE:1111101 5', mRNA sequence.		**1.693 (1.56 to 1.887)**	1 B|1 17.0 cM	291745	AA688761 NCBI
195	101658_f_at	histocompatibility 2, Q region locus 8	H2-Q8	Mouse Q8/9d gene.		**1.686 (1.336 to 2.037)**	17 B1|17 19.2 cM		D90146 NCBI
196	93235_at	expressed sequence BB128963	BB128963	ub24c02.r1 Soares_thymus_2NbMT Mus musculus cDNA clone IMAGE:1378658 5', mRNA sequence.		**1.684 (1.412 to 2.103)**	7 C	214959	AI020029 NCBI

Genes italicised indicate those that have passed the Benjamini-Hochberg false discovery rate procedure.

Table A.1. Genes up-regulated by DEX in the presence of ROSC.

	Probe set ID	Gene Title	Gene Symbol	Description	P-value	Fold change	Chromosomal Location	UniGene ID	Representative Public ID
197	94467_at	CCAAT/enhancer binding protein zeta	Cebpz	putative CCAAT binding factor 2; alternatively spliced transcript mCBF2; Mus musculus putative CCAAT binding factor 2 (mCBF) mRNA, alternatively spliced transcript mCBF2, complete cds.		**1.681 (1.136 to 2.03)**	17 E3	24169	U19892 NCBI
198	102745_at	T-cell receptor gamma chain	Tcrg	T cell receptor C-gamma-7.1; Mouse T cell receptor C-gamma-7.1 mRNA, 3' end.		**1.673 (1.441 to 1.947)**	13 10.0 cM		M18858 NCBI
199	103685_at	Transcribed locus		UI-M-AK0-adh-d-11-0-UI.s1 NIH_BMAP_MHY Mus musculus cDNA clone UI-M-AK0-adh-d-11-0-UI 3', mRNA sequence.		**1.671 (1.419 to 1.994)**		23897	AI839232 NCBI
200	95754_at	membrane-bound transcription factor peptidase, site 1	Mbtps1	UI-M-AL0-abx-c-12-0-UI.s1 NIH_BMAP_MCO Mus musculus cDNA clone UI-M-AL0-abx-c-12-0-UI 3', mRNA sequence.		**1.67 (1.514 to 1.788)**	8 E1	206934	AI838216 NCBI
201	96025_g_at	S-adenosylhomocysteine hydrolase	Ahcy	copper binding protein; Mus musculus (clone C7/B9) S-adenosyl homocysteine hydrolase (ahcy) mRNA, complete cds.		**1.668 (1.378 to 2.077)**	2 H1|2 89.0 cM	330692	L32836 NCBI
202	98903_at	Mitochondrial ribosomal protein L14	Mrpl14	mc68e12.r1 Soares mouse embryo NbME13.5 14.5 Mus musculus cDNA clone IMAGE:353710 5' similar to WP:F45E12.4 CE02740 ;, mRNA sequence.		**1.665 (1.269 to 1.995)**	17 B3	379158	W41966 NCBI
203	102818_at	Xlr-related, meiosis regulated	Xmr	M.musculus XMR mRNA.		**1.662 (1.478 to 1.878)**	X A2	429937	X72697 NCBI
204	161767_r_at	mitochondrial ribosomal protein S18A	Mrps18a	AV339603 RIKEN full-length enriched, adult male olfactory bulb Mus musculus cDNA clone 6430509H22 3', mRNA sequence.		**1.657 (1.527 to 1.724)**	17 B3	287443	AV339603 NCBI
205	96506_at	anaplastic lymphoma kinase	Alk	Mouse mRNA for tyrosine kinase, complete cds.		**1.657 (1.323 to 1.951)**	17 E1.3|17 50.0 cM	311854	D83002 NCBI
206	104179_at	expressed sequence AI788669	AI788669	uk47h11.x1 Sugano mouse kidney mkia Mus musculus cDNA clone IMAGE:1972197 3', mRNA sequence.		**1.657 (1.2 to 1.934)**		364779	AI788669 NCBI
207	103096_at	zinc finger protein 259	Zfp259	Mus musculus zinc finger protein (ZPR1) mRNA, complete cds.		**1.655 (1.595 to 1.74)**	9 A5.2	17519	U41287 NCBI
208	97482_at	calcium binding protein 39-like	Cab39l	vw43b11.r1 Soares_mammary_gland_NbMMG Mus musculus cDNA clone IMAGE:1246557 5', mRNA sequence.		**1.653 (1.174 to 1.958)**	14 C3	179091	AA832565 NCBI
209	102306_at	heparan sulfate 2-O-sulfotransferase 1	Hs2st1	Mus musculus heparan sulfate 2-sulfotransferase (Hs2st) mRNA, complete cds.		**1.645 (1.424 to 2.045)**	3 H2	12863	AF060178 NCBI
210	95468_at	EGL nine homolog 1 (C. elegans)	Egln1	UI-M-BG1-aie-b-01-0-UI.s1 NIH_BMAP_MSC_N Mus musculus cDNA clone UI-M-BG1-aie-b-01-0-UI 3', mRNA sequence.		**1.641 (1.262 to 2.1)**	8 E2	140619	AI850202 NCBI
211	94225_at	autophagy-related 5 (yeast)	Atg5	UI-M-AL1-ahr-f-03-0-UI.s1 NIH_BMAP_MCO_N Mus musculus cDNA clone UI-M-AL1-ahr-f-03-0-UI 3', mRNA sequence.		**1.639 (1.246 to 2.038)**	10 B2|10 26.0 cM	22264	AI844679 NCBI
212	101106_at	GTPase activating protein (SH3 domain) binding protein 2	G3bp2	UI-M-BH0-air-a-07-0-UI.s1 NIH_BMAP_M_S1 Mus musculus cDNA clone UI-M-BH0-air-a-07-0-UI 3', mRNA sequence.		**1.635 (1.429 to 1.742)**	5 E2	290530	AI853331 NCBI
213	98533_at	cytochrome b-5	Cyb5	UI-M-BH0-aka-d-08-0-UI.s1 NIH_BMAP_M_S1 Mus musculus cDNA clone UI-M-BH0-aka-d-08-0-UI 3', mRNA sequence.		**1.633 (1.489 to 1.823)**	18 E4|18 55.0 cM	31018	AI854779 NCBI
214	102009_at	cytoplasmic FMR1 interacting protein 2	Cyfip2	UI-M-AQ0-aab-c-12-0-UI.s1 NIH_BMAP_MHI Mus musculus cDNA clone UI-M-AQ0-aab-c-12-0-UI 3', mRNA sequence.		**1.626 (1.259 to 1.927)**	11 B1.2	154358	AI835274 NCBI
215	97521_at	argininosuccinate synthetase 1	Ass1	argininosuccinate synthetase (EC 6.3.4.5); Mouse argininosuccinate synthetase (Ass) mRNA, complete cds.		**1.625 (1.476 to 1.764)**	2 B|2 20.0 cM	3217	M31690 NCBI
216	101295_s_at	chloride channel, nucleotide-sensitive, 1A	Clns1a	Mus musculus chloride channel regulator Icln (Icln) pseudogene.		**1.62 (1.402 to 1.813)**	7 E3|7 50.0 cM	21482	U72059 NCBI
217	93620_at	RNA polymerase 1-4	Rpo1-4	Mus musculus RNA polymerase I largest subunit (RPA1) mRNA, complete cds.		**1.617 (1.394 to 2.033)**	6 C1|6 31.2 cM	135581	AF000938 NCBI
218	93503_at	secreted frizzled-related protein 2	Sfrp2	Mus musculus secreted frizzled related protein sFRP-2 (Sfrp2) mRNA, complete cds.		**1.617 (1.333 to 1.949)**	3 F1|3 38.5 cM	19155	U88567 NCBI
219	94699_at	IAP promoted placental gene	Ipp	Mouse MIPP mRNA for a placenta-expressed gene.		**1.617 (1.253 to 2.032)**	4 D1|4 51.4 cM	1350	X58523 NCBI
220	100991_at	integrin beta 1 binding protein 1	Itgb1bp1	UI-M-BH0-ajk-d-01-0-UI.s1 NIH_BMAP_M_S1 Mus musculus cDNA clone UI-M-BH0-ajk-d-01-0-UI 3', mRNA sequence.		**1.614 (1.164 to 1.922)**	12 A1.3	273333	AI852849 NCBI
221	95702_at	STT3, subunit of the oligosaccharyltransferase complex, homolog B (S. cerevisiae)	Stt3b	uc43c04.x1 Soares_mammary_gland_NMLMG Mus musculus cDNA clone IMAGE:1400742 3', mRNA sequence.		**1.613 (1.407 to 1.962)**	9 F3	296158	AI461803 NCBI
222	104699_at	phosphoinositide-3-kinase, class 3	Pik3c3	UI-M-AP1-agm-d-10-0-UI.s1 NIH_BMAP_MST_N Mus musculus cDNA clone UI-M-AP1-agm-d-10-0-UI 3', mRNA sequence.		**1.609 (1.384 to 1.847)**	18 B1	194127	AI847699 NCBI
223	102794_at	chemokine (C-X-C motif) receptor 4	Cxcr4	Mus musculus lcr-1 gene.		**1.607 (1.363 to 1.827)**	1 E4|1 67.4 cM	1401	Z80112 NCBI
224	103734_at	Abelson helper integration site	Ahi1	ua66e10.r1 Soares_thymus_2NbMT Mus musculus cDNA clone IMAGE:1362474 5', mRNA sequence.		**1.605 (1.475 to 1.695)**	10 A3|10 16.0 cM	253280	AA985771 NCBI
225	160210_at	RIKEN cDNA 4930539H15 gene	4930539H15Rik	Mus musculus ldlBp (LDLB) mRNA, complete cds.		**1.604 (1.319 to 1.889)**			AF109377 NCBI
226	98778_at	septin 11	40787	UI-M-AL0-abs-d-04-0-UI.s1 NIH_BMAP_MCO Mus musculus cDNA clone UI-M-AL0-abs-d-04-0-UI 3', mRNA sequence.		**1.603 (1.518 to 1.689)**	5 E3|5 52.0 cM	428571	AI837543 NCBI
227	99025_at	DEAD (Asp-Glu-Ala-Asp) box polypeptide 19a	Ddx19a	putative; RNA-dependent ATPase; Mouse RNA helicase and RNA-dependent ATPase from the DEAD box family mRNA, complete cds.		**1.603 (1.401 to 1.79)**	8 D3	287901	L25125 NCBI

Genes italicised indicate those that have passed the Benjamini-Hochberg false discovery rate procedure.

Table A.1. Genes up-regulated by DEX in the presence of ROSC.

	Probe set ID	Gene Title	Gene Symbol	Description	P-value	Fold change	Chromosomal Location	UniGene ID	Representative Public ID
228	160302_at	RIKEN cDNA 1200003C05 gene	1200003C05Rik	UI-M-BH1-ali-g-11-0-UI.s1 NIH_BMAP_M_S2 Mus musculus cDNA clone UI-M-BH1-ali-g-11-0-UI 3', mRNA sequence.		**1.603 (1.397 to 1.778)**	12 C3	278477	AW046391 NCBI
229	93842_at	death-associated protein	Dap	ui53d07.y1 Sugano mouse liver mlia Mus musculus cDNA clone IMAGE:1886125 5' similar to SW:DAP1_HUMAN P51397 DEATH-ASSOCIATED PROTEIN 1 ;, mRNA sequence.		**1.602 (1.544 to 1.698)**	15 B2	222867	AI196645 NCBI
230	103733_at	RIKEN cDNA 2900006A08 gene	2900006A08Rik	ua67e08.r1 Soares_thymus_2NbMT Mus musculus cDNA clone IMAGE:1362566 5', mRNA sequence.		**1.602 (1.305 to 1.796)**		24343	AI006698 NCBI
231	95722_at	glutaredoxin	Glrx	Mus musculus mRNA for glutaredoxin, complete cds.		**1.602 (1.2 to 1.884)**	13 C1|13 44.0 cM	25844	AB013137 NCBI
232	160801_at	PQ loop repeat containing 1	Pqlc1	UI-M-BH1-anp-b-03-0-UI.s1 NIH_BMAP_M_S2 Mus musculus cDNA clone UI-M-BH1-anp-b-03-0-UI 3', mRNA sequence.		**1.6 (1.433 to 1.755)**	18 E3	29247	AW061073 NCBI
233	104256_at	pleckstrin homology, Sec7 and coiled-coil domains, binding protein	Pscdbp	ub73a05.r1 Soares_mammary_gland_NMLMG Mus musculus cDNA clone IMAGE:1383344 5', mRNA sequence.		**1.599 (1.439 to 1.691)**	2 C1.1	273905	AI120844 NCBI
234	99824_at			C79764 Mouse 3.5-dpc blastocyst cDNA Mus musculus cDNA clone J0071E12 3', mRNA sequence.		**1.598 (1.422 to 1.767)**			C79764 NCBI
235	161050_at	10 days neonate cerebellum cDNA, RIKEN full-length enriched library, clone:6530415D11 product:unclassifiable, full insert sequence		vo06h07.x1 Stratagene mouse skin (#937313) Mus musculus cDNA clone IMAGE:1040701 3', mRNA sequence.		**1.597 (1.513 to 1.678)**		383529	AI504506 NCBI
236	104259_at	chromobox homolog 5 (Drosophila HP1a)	Cbx5	chromo domain and chromo shadow domain; M.musculus mRNA for HP1 alpha protein.		**1.593 (1.508 to 1.698)**	15 F3	262059	X99641 NCBI
237	100618_f_at	solute carrier family 25 (mitochondrial carrier, adenine nucleotide translocator), member 5	Slc25a5	mj83h01.r1 Soares mouse p3NMF19.5 Mus musculus cDNA clone IMAGE:482737 5' similar to gb:J02683 ADP,ATP CARRIER PROTEIN, FIBROBLAST ISOFORM (HUMAN); gb:X70847 M.musculus mRNA for adenine nucleotide translocase (MOUSE);, mRNA sequence.		**1.593 (1.258 to 1.945)**	X A4|X 12.7 cM	389141	AA062013 NCBI
238	94285_at	histocompatibility 2, class II antigen E beta	H2-Eb1	Mouse mRNA for I-E(beta-b) gene.		**1.591 (1.478 to 1.687)**	17 B1|17 18.66 cM	22564	X00958 NCBI
239	103815_at	peroxisomal biogenesis factor 11b	Pex11b	UI-M-BH0-aje-g-04-0-UI.s1 NIH_BMAP_M_S1 Mus musculus cDNA clone UI-M-BH0-aje-g-04-0-UI 3', mRNA sequence.		**1.59 (1.468 to 1.727)**	3 F2.1	20901	AI852311 NCBI
240	95285_at			uc48c08.r1 Soares_thymus_2NbMT Mus musculus cDNA clone IMAGE:1428878 5', mRNA sequence.		**1.59 (1.16 to 1.818)**			AI153315 NCBI
241	92367_at	Scl/Tal1 interrupting locus	Stil	Mus musculus Sil mRNA, complete cds.		**1.587 (1.506 to 1.636)**	4 D1	3988	U36778 NCBI
242	160699_at	cell division cycle associated 5	Cdca5	uc56g02.r1 Soares_thymus_2NbMT Mus musculus cDNA clone IMAGE:1429682 5', mRNA sequence.		**1.583 (1.445 to 1.736)**	19 A	23526	AI877184 NCBI
243	94332_at	E26 avian leukemia oncogene 1, 5' domain	Ets1	ub97f03.r1 Soares_mammary_gland_NbMMG Mus musculus cDNA clone IMAGE:1396445 5', mRNA sequence.		**1.58 (1.448 to 1.825)**	9 A4|9 15.0 cM	292415	AI882555 NCBI
244	95305_at	RIKEN cDNA A630098A13 gene	A630098A13Rik	vv40d02.r1 Soares_thymus_2NbMT Mus musculus cDNA clone IMAGE:1224867 5' similar to SW:TVA1_HUMAN P04436 T-CELL RECEPTOR ALPHA CHAIN PRECURSOR V REGION ;, mRNA sequence.		**1.58 (1.35 to 1.871)**	14 C2		AA756275 NCBI
245	96026_at	S-adenosylhomocysteine hydrolase	Ahcy	uc80h10.x1 Sugano mouse kidney mkia Mus musculus cDNA clone IMAGE:1432003 3' similar to gb:L32836 Mus musculus (MOUSE);, mRNA sequence.		**1.58 (1.259 to 1.787)**	2 H1|2 89.0 cM	371964	AA987153 NCBI
246	161596_f_at	A kinase (PRKA) anchor protein 8	Akap8	AV292740 RIKEN full-length enriched, 6 days neonate head Mus musculus cDNA clone 5430428E04 3' similar to U01914 Rattus norvegicus AKAP95 mRNA, mRNA sequence.		**1.577 (1.414 to 1.801)**	17 B2	328945	AV292740 NCBI
247	101458_at	wee 1 homolog (S. pombe)	Wee1	Mouse mRNA for wee1 kinase.		**1.574 (1.348 to 1.745)**	7 E3	287173	D30743 NCBI
248	93455_s_at	bone morphogenetic protein 4	Bmp4	M.musculus mRNA for bone morphogenetic protein 4 (BMP-4).		**1.573 (1.318 to 1.85)**	14 C1|14 15.0 cM	6813	X56848 NCBI
249	98509_at	cDNA sequence BC002199	BC002199	UI-M-AM1-afw-e-03-0-UI.s1 NIH_BMAP_MAM_N Mus musculus cDNA clone UI-M-AM1-afw-e-03-0-UI 3', mRNA sequence.		**1.57 (1.443 to 1.66)**	3 G2 _	403486	AI834979 NCBI
250	160775_at	tubby like protein 4	Tulp4	UI-M-AM1-aga-e-01-0-UI.s2 NIH_BMAP_MAM_N Mus musculus cDNA clone UI-M-AM1-aga-e-01-0-UI 3', mRNA sequence.		**1.57 (1.25 to 1.829)**	17 A1|17 3.2 cM	28251	AI848591 NCBI
251	102346_at	excision repair cross-complementing rodent repair deficiency, complementation group 3	Ercc3	ul21h12.x1 Sugano mouse embryo mewa Mus musculus cDNA clone IMAGE:2088263 3' similar to gb:M31899 DNA-REPAIR PROTEIN COMPLEMENTING XP-B CELLS (HUMAN);, mRNA sequence.		**1.568 (1.264 to 1.747)**	18 B3	282335	AI747755 NCBI
252	94889_at	vesicle-associated membrane protein, associated protein A	Vapa	UI-M-BH2.3-aok-f-05-0-UI.s1 NIH_BMAP_M_S3.3 Mus musculus cDNA clone UI-M-BH2.3-aok-f-05-0-UI 3', mRNA sequence.		**1.564 (1.485 to 1.617)**	17 E1.2	391032	AW121235 NCBI

Genes italicised indicate those that have passed the Benjamini-Hochberg false discovery rate procedure.

Table A.1. Genes up-regulated by DEX in the presence of ROSC.

	Probe set ID	Gene Title	Gene Symbol	Description	P-value	Fold change	Chromosomal Location	UniGene ID	Representative Public ID
253	96761_at	solute carrier family 44, member 4	Slc44a4	Intron-exon boundaries defined in relation to human cDNA in L03411.; complement factor B; Intron-exon boundaries defined in relation to cDNA in M57890; complement factor C2; Intron-exon boundaries defined in relation to cDNA in M57891; Zn finger; This new gene is defined in relation to ESTs AA793840 and AA119175; This CDS could be the 5' end of G9A. Intron-exon boundaries are defined in relation to ESTs AA284078, AA934369, AA822514, AA017911 and AA152958. The latter three ESTs match to exons at the beginning of G9A, starting at 52332-52413. It is puzzling that the ESTs are all in the opposite orientation from what one would expect for the 5' end of a gene.; Intron-exon boundaries defined in relation to human cDNA in X69838.; unknown; Possible new gene. Inron-exon boundaries defined in relation to ESTs AA245579, SS04F08, AA612666, AA630850, and C77015. By blast x, this gene is simliar to the conceptual translation of C. elegans cDNA CEESE93F. The splice acceptor for the exon from 72746-72838 is 'GG' rather than 'AG.' The sequence is clear in this region. Therefore this is possibly a pseudogene; lysosomal sialidase; Intron-exon boundaries defined in relation to mouse cDNA in U93702; heat shock protein; This is hsp70.1 found in M35021; heat shock protein; This is the hsp70 gene found in M76613; heat shock protein 70; This is HSC70t, found in L27086; possible small nuclear ribonuclear protein; Intron-exon boundaries defined in relation to EST AA036320. Also see genomic sequence in U85207; valyl tRNA synthetase; Intron-exon boundaries defined in relation to human cDNA in X59303; Mus musculus MHC class III region RD gene, partial cds; Bf, C2, G9A, NG22, G9, HSP70, HSP70, HSC70t, and smRNP genes, complete cds; G7A gene, partial cds; and unknown genes.		**1.564 (1.378 to 1.788)**	17 B2	183126	AF109906 NCBI
254	96024_at	S-adenosylhomocysteine hydrolase	Ahcy	copper binding protein; Mus musculus (clone C7/B9) S-adenosyl homocysteine hydrolase (ahcy) mRNA, complete cds.		**1.563 (1.307 to 1.888)**	2 H1|2 89.0 cM	371964	L32836 NCBI
255	100890_at	chromatin assembly factor 1, subunit B (p60)	Chaf1b	uh16b06.r1 Barstead mouse testis MPLRB11 Mus musculus cDNA clone IMAGE:1745555 5' similar to TR:Q99548 Q99548 M-PHASE PHOSPHOPROTEIN 7 ;, mRNA sequence.		**1.562 (1.478 to 1.709)**	16 C4|16 67.4 cM	274222	AI173038 NCBI
256	161348_r_at	PDZ and LIM domain 1 (elfin)	Pdlim1	AV149007 Mus musculus C57BL/6J 10-11 day embryo Mus musculus cDNA clone 2810482M10, mRNA sequence.		**1.562 (1.179 to 1.785)**	19 D1	5567	AV149007 NCBI
257	103427_at	F-box and leucine-rich repeat protein 3	Fbxl3	UI-M-BH2.1-apg-e-07-0-UI.s1 NIH_BMAP_M_S3.1 Mus musculus cDNA clone UI-M-BH2.1-apg-e-07-0-UI 3', mRNA sequence.		**1.561 (1.312 to 1.93)**	14 E2.2	214746	AW123223 NCBI
258	92375_at	activating signal cointegrator 1 complex subunit 1	Ascc1	ul29a03.y1 Sugano mouse kidney mkia Mus musculus cDNA clone IMAGE:2099692 5', mRNA sequence.		**1.557 (1.373 to 1.715)**	10 B4	155839	AW211207 NCBI
259	103211_at	WD repeat and FYVE domain containing 2	Wdfy2	UI-M-BH0-aiu-a-02-0-UI.s1 NIH_BMAP_M_S1 Mus musculus cDNA clone UI-M-BH0-aiu-a-02-0-UI 3', mRNA sequence.		**1.554 (1.499 to 1.625)**	14 D1	392194	AI852574 NCBI
260	97536_at	WD and tetratricopeptide repeats 1	Wdtc1	UI-M-BH1-ald-e-10-0-UI.s1 NIH_BMAP_M_S2 Mus musculus cDNA clone UI-M-BH1-ald-e-10-0-UI 3', mRNA sequence.		**1.554 (1.429 to 1.783)**	4 D2.3	226576	AW046650 NCBI
261	96738_at	a disintegrin and metallopeptidase domain 9 (meltrin gamma)	Adam9	Method: conceptual translation supplied by author; Mus musculus metalloprotease/disintegrin/cysteine rich protein precursor (MDC9) cDNA, complete cds.		**1.553 (1.371 to 1.759)**	8 A2|8 8.0 cM	28908	U41765 NCBI
262	95683_g_at	damage specific DNA binding protein 1	Ddb1	homolog of Human xeroderma pigmentosum group E UV-damaged DNA binding factor; Mus musculus mRNA for XPE UV-damaged DNA binding factor, complete cds.		**1.551 (1.507 to 1.633)**	19 centromere|19 5.0 cM	289915	AB026432 NCBI
263	162006_r_at	inner membrane protein, mitochondrial	Immt	AV334115 RIKEN full-length enriched, adult male medulla oblongata Mus musculus cDNA clone 6330554F06 3' similar to D21092 Human mRNA for motor protein, mRNA sequence.		**1.548 (1.189 to 1.797)**	6 C3	235123	AV334115 NCBI
264	100948_at	progressive ankylosis	Ank	UI-M-BH1-amr-h-10-0-UI.s1 NIH_BMAP_M_S2 Mus musculus cDNA clone UI-M-BH1-amr-h-10-0-UI 3', mRNA sequence.		**1.547 (1.306 to 1.824)**	15 B1|15 14.4 cM	265264	AW049351 NCBI
265	94003_at	WNK lysine deficient protein kinase 1	Wnk1	UI-M-AP1-agf-d-06-0-UI.s2 NIH_BMAP_MST_N Mus musculus cDNA clone UI-M-AP1-agf-d-06-0-UI 3', mRNA sequence.		**1.546 (1.233 to 1.709)**	6 F1	333349	AI848510 NCBI
266	93267_at	RNA binding motif protein 39	Rbm39	vs04a06.r1 Barstead mouse irradiated colon MPLRB7 Mus musculus cDNA clone IMAGE:1137202 5' similar to TR:Q14498 Q14498 SPLICING FACTOR. [1] ;, mRNA sequence.		**1.544 (1.479 to 1.658)**	2 H1	392436	AA688834 NCBI
267	95986_at	SCO-spondin	Sspo	C79529 Mouse 3.5-dpc blastocyst cDNA Mus musculus cDNA clone J0067F08 3' similar to B.taurus mRNA for SCO-spondin protein, mRNA sequence.		**1.541 (1.335 to 1.662)**	6 B2.3	25039	C79529 NCBI

Genes italicised indicate those that have passed the Benjamini-Hochberg false discovery rate procedure.

Table A.1. Genes up-regulated by DEX in the presence of ROSC.

	Probe set ID	Gene Title	Gene Symbol	Description	P-value	Fold change	Chromosomal Location	UniGene ID	Representative Public ID
268	103013_at	upstream transcription factor 2	Usf2	M.musculus USF2 gene (exons 1-7).		**1.541 (1.301 to 1.838)**	7 A2-B1|7 11.0 cM	322453	X77602 NCBI
269	97894_at	valyl-tRNA synthetase 2	Vars2	heat shock protein; Hsc70t, found in L27086; small ribonuclear protein; Intron-exon boundaries defined in relation to EST AA036320 and also by genomic sequence in U85207; valyl-tRNA synthetase; intron-exon boundaries defined in relation to human cDNA in X59303; the eighteenth coding exon has a 'GC' rather than 'GT' splice donor; the sequence in this region is clear; hypothetical protein; This gene is predicted by Genscan; exons 4 and 6 match EST AA133560; the middle of the conceptual translation (exons 6-11) contain similarity to C. elegans hemicentin by blastx; 3' end defined by ESTs C89323 and AA466842; unknown; Intron-exon boundaries defined in relation to mouse EST AA182356; Intron-exon boundaries defined in relation to human cDNA in AF034759; nuclear chloride ion channel protein; Intron-exon boundaries defined in relation to human cDNA in U93205; Intron-exon boundaries defined in relation to mouse cDNA in AF004106; unknown; Intron-exon boundaries defined in relation to ESTs AA930440, AA500454 and AI151937; unknown; Intron-exon boundaries defined in relation to EST AA794551; unknown; Intron-exon boundaries defined in relation to ESTs AA915231, AA037323, AA323699, T09123, AA111907, AA319071, AA799016, AA499771, AI131864,and AA168164. This gene has blastx similarity to a hypothetical protein from C. elegans; Mus musculus major histocompatibility locus class III regions Hsc70t gene, partial cds; smRNP, G7A, NG23, MutS homolog, CLCP, NG24, NG25, and NG26 genes, complete cds; and unknown genes.		**1.539 (1.311 to 1.671)**	17 B1|17 19.02 cM	28420	AF109905 NCBI
270	100992_at	polyhomeotic-like 1 (Drosophila)	Phc1	similar to Drosophila melanogaster polyhomeotic gene; contains a single zinc finger and a conserved alpha helical domain at the C-terminus; Mus musculus nuclear transcriptional repressor Mph1 mRNA, complete cds.		**1.539 (1.285 to 1.723)**	6 F3|6 57.0 cM	6822	U63386 NCBI
271	103363_at	taube nuss	Tbn	uo45c03.x2 NCI_CGAP_Lu29 Mus musculus cDNA clone IMAGE:2645476 3', mRNA sequence.		**1.538 (1.329 to 1.841)**	17 C	275901	AW214244 NCBI
272	93996_at	cytochrome P450, family 2, subfamily e, polypeptide 1	Cyp2e1	URF; Mouse mRNA fragment for repetitive element B2.		**1.536 (1.358 to 1.694)**	7 F5|7 68.4 cM	21758	X01026 NCBI
273	97259_at	cAMP-regulated phosphoprotein 19	Arpp19	Mus musculus mRNA for cAMP-regulated phosphoprotein (ARPP-19).		**1.534 (1.425 to 1.661)**	9 E1	247837	AJ005983 NCBI
274	92956_at	Notch gene homolog 3 (Drosophila)	Notch3	M.musculus mRNA for Notch 3.		**1.532 (1.465 to 1.575)**	17 B1|17 20.0 cM	4945	X74760 NCBI
275	92468_at	ankyrin repeat domain 49	Ankrd49	similar to human fetal globin inducing factor; Mus musculus fetal globin inducing factor mRNA, complete cds.		**1.532 (1.296 to 1.687)**	9 A3	272618	AF028722 NCBI
276	104077_at	L antigen family, member 3	Lage3	UI-M-BH2.3-aoj-f-11-0-UI.s1 NIH_BMAP_M_S3.3 Mus musculus cDNA clone UI-M-BH2.3-aoj-f-11-0-UI 3', mRNA sequence.		**1.529 (1.45 to 1.572)**	X A6	21705	AW121992 NCBI
277	98951_at	transcription factor 25 (basic helix-loop-helix)	Tcf25	RIKEN cDNA 1100001J13 gene		**1.527 (1.415 to 1.728)**	8 E1|8 67.0 cM	178818	AI843258 NCBI
278	160288_at	microtubule-associated protein 1 light chain 3 beta	Map1lc3b	UI-M-AM0-adv-a-01-0-UI.s1 NIH_BMAP_MAM Mus musculus cDNA clone UI-M-AM0-adv-a-01-0-UI 3', mRNA sequence.		**1.524 (1.444 to 1.643)**	8 E1	28357	AI841311 NCBI
279	161410_r_at			AV313844 RIKEN full-length enriched, adult male thymus Mus musculus cDNA clone 5830413I01 3' similar to M92933 Mouse lymphocyte common antigen (Ly5) mRNA, mRNA sequence.		**1.524 (1.193 to 1.72)**			AV313844 NCBI
280	100701_r_at	nuclear receptor subfamily 5, group A, member 1	Nr5a1	Ad4BP; SF-1; Mouse mRNA for ELP3, complete cds.		**1.522 (1.371 to 1.715)**	2 B|2 23.5 cM	31387	AB000490 NCBI
281	101625_at	K+ voltage-gated channel, subfamily S, 2	Kcns2	Mus musculus potassium channel alpha subunit (Kv9.2) mRNA, complete cds.		**1.518 (1.372 to 1.66)**	15 B3.1	71045	AF008574 NCBI
282	95893_at	B lymphoid kinase	Blk	mu61b04.r1 Soares mouse lymph node NbMLN Mus musculus cDNA clone IMAGE:643855 5', mRNA sequence.		**1.517 (1.223 to 1.673)**	14 D1|14 28.0 cM	3962	AA204265 NCBI
283	98943_at	replication protein A2	Rpa2	Mus musculus mRNA for 30-kDa subunit of replication protein A, complete cds.		**1.516 (1.349 to 1.634)**	4 D2.3	2870	D00812 NCBI
284	101226_at	SH3 domain containing ring finger 1	Sh3rf1	C77776 Mouse 3.5-dpc blastocyst cDNA Mus musculus cDNA clone J0037D08 3', mRNA sequence.		**1.516 (1.285 to 1.796)**	8 B3.1	27949	C77776 NCBI
285	95339_r_at	matrix metallopeptidase 12	Mmp12	Mus musculus macrophage metalloelastase mRNA, complete cds.		**1.513 (1.391 to 1.756)**	9 A1|9 1.0 cM	2055	M82831 NCBI
286	100552_at	interferon gamma receptor 1	Ifngr1	interferon-gamma receptor precursor; Mouse interferon-gamma receptor mRNA, complete cds.		**1.513 (1.282 to 1.718)**	10 A3|10 15.0 cM	549	M28233 NCBI
287	101447_at	adenomatosis polyposis coli	Apc	putative; Mouse APC mRNA, complete cds.		**1.511 (1.296 to 1.804)**	18 B1|18 15.0 cM	384171	M88127 NCBI
288	95635_g_at	RIKEN cDNA 0610010K14 gene	0610010K14Rik	UI-M-AP1-agk-e-09-0-UI.s1 NIH_BMAP_MST_N Mus musculus cDNA clone UI-M-AP1-agk-e-09-0-UI 3', mRNA sequence.		**1.51 (1.413 to 1.628)**	11 B3	39265	AI848107 NCBI

Genes italicised indicate those that have passed the Benjamini-Hochberg false discovery rate procedure.

Table A.1. Genes up-regulated by DEX in the presence of ROSC.

	Probe set ID	Gene Title	Gene Symbol	Description	P-value	Fold change	Chromosomal Location	UniGene ID	Representative Public ID
289	93080_at	Bernardinelli-Seip congenital lipodystrophy 2 homolog (human)	Bscl2	Mus musculus Gng3lg mRNA, complete cds.		**1.509 (1.37 to 1.602)**	19 A|19 4.0 cM	345134	AF069954 NCBI
290	102914_s_at	B-cell leukemia/lymphoma 2 related protein A1a	Bcl2a1a	Mus musculus hematopoietic-specific early-response A1-b protein (A1b) gene, exon 2, and complete cds.		**1.507 (1.444 to 1.58)**	9 E3.1|9 50.0 cM	378888	U23778 NCBI
291	99668_at	bridging integrator 1	Bin1	BRAMP2; Mus musculus brain amphiphysin 2 mRNA, complete cds.		**1.5 (1.42 to 1.601)**	18 B1|18 14.0 cM	4383	U86405 NCBI
292	103098_at	brain-specific angiogenesis inhibitor 1-associated protein 2	Baiap2	UI-M-BH1-akt-c-06-0-UI.s1 NIH_BMAP_M_S2 Mus musculus cDNA clone UI-M-BH1-akt-c-06-0-UI 3', mRNA sequence.		**1.488 (1.425 to 1.556)**	11 E2	197534	AW045765 NCBI
293	161257_r_at	sorting nexin 17	Snx17	AV321519 RIKEN full-length enriched, 13 days embryo male testis Mus musculus cDNA clone 6030435C06 3', mRNA sequence.		**1.481 (1.351 to 1.557)**	5 B1	6118	AV321519 NCBI
294	98298_at	dihydropyrimidinase-like 2	Dpysl2	M.musculus mRNA for Ulip2 protein.		**1.472 (1.392 to 1.523)**	14 D1|14 28.2 cM	352648	Y10339 NCBI
295	101595_at	RAN binding protein 9	Ranbp9	C78787 Mouse 3.5-dpc blastocyst cDNA Mus musculus cDNA clone J0055A07 3' similar to Mesocricetus auratus alpha-cardiac myosin heavy chain gene, mRNA, mRNA sequence.		**1.472 (1.296 to 1.583)**	13 A4	148781	C78787 NCBI
296	102986_at	myogenic differentiation 1	Myod1	Mouse myoblast D1 (MyoD1) mRNA, complete cds.		**1.47 (1.298 to 1.591)**	7 B3|7 23.5 cM	1526	M18779 NCBI
297	161446_r_at	HtrA serine peptidase 2	Htra2	AV353694 RIKEN full-length enriched, 2 days neonate sympathetic ganglion Mus musculus cDNA clone 7120411F16 3', mRNA sequence.		**1.462 (1.409 to 1.523)**	6 C3|6 34.75 cM	21880	AV353694 NCBI
298	101618_r_at	P53-variant (p53)		Mus musculus p53-variant (p53) mRNA, partial cds.		**1.462 (1.357 to 1.661)**		423008	U59758 NCBI
299	98800_at	solute carrier family 23 (nucleobase transporters), member 3	Slc23a3	presumed nucleobase permease; Description: yolk sac permease-like molecule 1 form 1; Description: Yolk sac permease-like molecule 1 form 2; presumed secreted form of YSPL-1; Description: yolk sac permease-like molecule 1 form 3; presumed intracellular, short form of YSPL-1; Description: Yolk sac permease-like molecule 1 form 4; Mus musculus yolk sac permease-like molecule 1 (YSPL-1) mRNA, complete cds.		**1.446 (1.321 to 1.59)**	1 C3	68157	U25739 NCBI
300	92916_at	synaptotagmin III	Syt3	Mus musculus mRNA for synaptotagumin III, complete cds.		**1.433 (1.349 to 1.496)**	7 B3|7 23.0 cM	4824	D45858 NCBI
301	161633_r_at			AV003177 Mus musculus C57BL/6J kidney Mus musculus cDNA clone 0610025F08, mRNA sequence.		**1.432 (1.392 to 1.477)**			AV003177 NCBI

Genes italicised indicate those that have passed the Benjamini-Hochberg false discovery rate procedure.

Table A.2. Genes down-regulated by DEX in the presence of ROSC.

	Probe set ID	Gene Title	Gene Symbol	Description	Fold change	Chromosomal Location	UniGene ID	Representative Public ID
1	102921_s_at	Fas (TNF receptor superfamily member)	Fas	NGF/TNF-receptor-related protein; Mus musculus Fas antigen mRNA, complete cds.	**0.251 (0.155 to 0.439)**	19 C1|19 23.0 cM	1626	M83649 NCBI
2	102282_g_at	CD antigen 27	Cd27	Mus musculus CD27 antigen (Cd27) mRNA.	**0.299 (0.186 to 0.499)**	6 F3|6 60.35 cM	367714	L24495 NCBI
3	92832_at	suppressor of cytokine signaling 1	Socs1	Mus musculus suppressor of cytokine signalling-1 (SOCS-1) mRNA, complete cds.	**0.327 (0.24 to 0.427)**	16 A1|16 3.4 cM	130	U88325 NCBI
4	102940_at	lymphotoxin B	Ltb	bp 1-11 were derived from genomic sequence; Mus musculus lymphotoxin-beta mRNA, complete cds.	**0.334 (0.139 to 0.52)**	17 B1|17 19.06 cM	1715	U16985 NCBI
5	99027_at	Bcl2-like 1	Bcl2l1	Mus musculus Bcl-xL mRNA, complete cds.	**0.348 (0.271 to 0.456)**	2 H1|2 87.5 cM	238213	L35049 NCBI
6	93285_at	dual specificity phosphatase 6	Dusp6	UI-M-AQ1-adx-c-06-0-UI.s1 NIH_BMAP_MHI_N Mus musculus cDNA clone UI-M-AQ1-adx-c-06-0-UI 3', mRNA sequence.	**0.354 (0.335 to 0.365)**	10 C3	1791	AI845584 NCBI
7	102123_at	Lysosomal acid lipase 1	Lip1	M.musculus (C57 Black/6X CBA) LAL mRNA for lysosomal acid lipase.	**0.358 (0.343 to 0.384)**	19 C1	157545	Z31689 NCBI
8	100011_at	Kruppel-like factor 3 (basic)	Klf3	UI-M-BH0-ain-f-03-0-UI.s1 NIH_BMAP_M_S1 Mus musculus cDNA clone UI-M-BH0-ain-f-03-0-UI 3', mRNA sequence.	**0.372 (0.224 to 0.48)**	5 C3.1	319499	AI851658 NCBI
9	94835_f_at	tubulin, beta 2a	Tubb2a	beta-tubulin; Mouse beta-tubulin gene M-beta-2, 3' end.	**0.372 (0.316 to 0.406)**	13 A3.3|13 16.0 cM	434383	M28739 NCBI
10	94345_at	interleukin 6 signal transducer	Il6st	UI-M-AK1-aer-e-08-0-UI.s1 NIH_BMAP_MHY_N Mus musculus cDNA clone UI-M-AK1-aer-e-08-0-UI 3', mRNA sequence.	**0.393 (0.275 to 0.592)**	13 D2.2|13 67.0 cM	4364	AI843709 NCBI
11	103259_at	growth factor independent 1	Gfi1	zinc finger protein; Mus musculus growth factor independence (Gfi1) mRNA, complete cds.	**0.395 (0.198 to 0.715)**	5 F|5 56.0 cM	2078	U58972 NCBI
12	96865_at	myristoylated alanine rich protein kinase C substrate	Marcks	putative; Mouse myristoylated alanine-rich C-kinase substrate (MARCKS) mRNA, complete cds.	**0.408 (0.19 to 0.817)**	10 B1|10 22.0 cM	30059	M60474 NCBI
13	101014_at	interferon (alpha and beta) receptor 2	Ifnar2	M.musculus mRNA for type I interferon receptor, IFNaR2b.	**0.413 (0.223 to 0.573)**	16 C3.3|16 63.1 cM	6834	Y09864 NCBI
14	95665_at	SEC14-like 1 (S. cerevisiae)	Sec14l1	UI-M-BH0-aja-g-04-0-UI.s1 NIH_BMAP_M_S1 Mus musculus cDNA clone UI-M-BH0-aja-g-04-0-UI 3', mRNA sequence.	**0.414 (0.297 to 0.56)**	11 E2	272312	AI852087 NCBI
15	104372_at	abhydrolase domain containing 8	Abhd8	UI-M-AP0-abg-e-08-0-UI.s2 NIH_BMAP_MST Mus musculus cDNA clone UI-M-AP0-abg-e-08-0-UI 3', mRNA sequence.	**0.434 (0.339 to 0.59)**	8 C1	276383	AI836883 NCBI
16	161788_f_at	endothelial differentiation sphingolipid G-protein-coupled receptor 1	Edg1	AV347228 RIKEN full-length enriched, adult male olfactory bulb Mus musculus cDNA clone 6430594J09 3', mRNA sequence.	**0.436 (0.362 to 0.493)**	3 G1	982	AV347228 NCBI
17	160462_f_at	tubulin, beta 3	Tubb3	UI-M-BH1-ans-b-12-0-UI.s1 NIH_BMAP_M_S2 Mus musculus cDNA clone UI-M-BH1-ans-b-12-0-UI 3', mRNA sequence.	**0.438 (0.349 to 0.561)**	8 E1	40068	AW050256 NCBI
18	160829_at	pleckstrin homology-like domain, family A, member 1	Phlda1	Mus musculus TDAG51 (TDAG51) mRNA, complete cds.	**0.439 (0.35 to 0.581)**	10 D1	3117	U44088 NCBI
19	96096_f_at	hydroxysteroid dehydrogenase like 2	Hsdl2	uk39c03.x1 Sugano mouse kidney mkia Mus musculus cDNA clone IMAGE:1971364 3' similar to SW:DHB4_HUMAN P51659 ESTRADIOL 17 BETA-DEHYDROGENASE 4 ;, mRNA sequence.	**0.439 (0.376 to 0.501)**	4 C1	272905	AI648018 NCBI
20	97497_at	Notch gene homolog 1 (Drosophila)	Notch1	homologue of Drosophila neurogenic gene Notch; M.musculus notch-1 mRNA.	**0.441 (0.391 to 0.488)**	2 A3|2 15.0 cM	290610	Z11886 NCBI
21	103970_at	AT rich interactive domain 3B (Bright like)	Arid3b	Mus musculus bright and dead ringer gene product homologous protein Bdp mRNA, complete cds.	**0.442 (0.366 to 0.49)**	9 C	425588	AF116847 NCBI
22	96623_at	UDP-glucose ceramide glucosyltransferase	Ugcg	UI-M-BH0-ajh-b-06-0-UI.s1 NIH_BMAP_M_S1 Mus musculus cDNA clone UI-M-BH0-ajh-b-06-0-UI 3', mRNA sequence.	**0.444 (0.357 to 0.514)**	4 B3|4 32.0 cM	198803	AI853172 NCBI
23	AFFX-MurFAS_at	Fas (TNF receptor superfamily member)	Fas	NGF/TNF-receptor-related protein; Mus musculus Fas antigen mRNA, complete cds.	**0.446 (0.375 to 0.54)**	19 C1|19 23.0 cM	1626	M83649 NCBI
24	96752_at	intercellular adhesion molecule	Icam1	Mouse intercellular adhesion molecule 1 (ICAM-1) gene, exons 6 and 7 and complete cds.	**0.448 (0.228 to 0.596)**	9 A3|9 7.0 cM	427576	M90551 NCBI
25	103946_at	proline-serine-threonine phosphatase-interacting protein 1	Pstpip1	similar to S. pombe Cdc15p, a protein associated with formation of the cleavage furrow during cytokinesis; actin interacting protein with C-terminal SH3 domain; PSTPIP; Mus musculus PEST phosphatase interacting protein mRNA, complete cds.	**0.461 (0.268 to 0.645)**	9 C	2534	U87814 NCBI
26	102978_at	RIKEN cDNA A430104N18 gene	A430104N18Rik	ub02f03.r1 Soares_mammary_gland_NbMMG Mus musculus cDNA clone IMAGE:1365821 5', mRNA sequence.	**0.464 (0.34 to 0.561)**		372207	AI021175 NCBI
27	104645_at	Kruppel-like factor 7 (ubiquitous)	Klf7	UI-M-BH0-ajq-d-05-0-UI.s1 NIH_BMAP_M_S1 Mus musculus cDNA clone UI-M-BH0-ajq-d-05-0-UI 3', mRNA sequence.	**0.469 (0.32 to 0.593)**	1 C1-C3	29466	AI853712 NCBI
28	102711_at	regulator of G-protein signaling 14	Rgs14	Mus musculus rap1/rap2 interacting protein mRNA, complete cds.	**0.471 (0.361 to 0.646)**	13 B1|13 32.0 cM	1426	U85055 NCBI

Genes italicised indicate those that have passed the Benjamini-Hochberg false discovery rate procedure.

Table A.2. Genes down-regulated by DEX in the presence of ROSC.

	Probe set ID	Gene Title	Gene Symbol	Description	Fold change	Chromosomal Location	UniGene ID	Representative Public ID
29	102871_at	Eph receptor B6	Ephb6	putative; Mus musculus MEP mRNA, complete cds.	**0.48 (0.294 to 0.737)**	6 B2.1	271976	L77867 NCBI
30	93372_at	acidic (leucine-rich) nuclear phosphoprotein 32 family, member A	Anp32a	LANP; PHAPI; I1-PP2A; Mus musculus acidic nuclear phosphoprotein pp32 mRNA, complete cds.	**0.485 (0.323 to 0.598)**	9 B|9 36.0 cM	269088	U73478 NCBI
31	92653_at	RIKEN cDNA D530037H12 gene	D530037H12Rik	vg38e09.x1 Soares_mammary_gland_NbMMG Mus musculus cDNA clone IMAGE:863656 3', mRNA sequence.	**0.485 (0.409 to 0.53)**			AI482432 NCBI
32	162410_s_at	CD8 antigen, beta chain 1	Cd8b1	AV316162 RIKEN full-length enriched, adult male thymus Mus musculus cDNA clone 5830434K21 3' similar to M19504 Mouse T-cell differentiation antigen (Ly-3) mRNA, mRNA sequence.	**0.485 (0.424 to 0.581)**	6 C1|6 30.5 cM		AV316162 NCBI
33	160359_at	RIKEN cDNA 1190002H23 gene	1190002H23Rik	UI-M-BG1-aic-e-02-0-UI.s1 NIH_BMAP_MSC_N Mus musculus cDNA clone UI-M-BG1-aic-e-02-0-UI 3', mRNA sequence.	**0.494 (0.286 to 0.764)**	14 D3	29811	AI854358 NCBI
34	92564_at	leucine rich repeat (in FLII) interacting protein 1	Lrrfip1	ul59a06.x1 Sugano mouse kidney mkia Mus musculus cDNA clone IMAGE:2123314 3', mRNA sequence.	**0.494 (0.357 to 0.62)**	1 D	45039	AI891475 NCBI
35	95758_at	stearoyl-Coenzyme A desaturase 2	Scd2	stearoyl-CoA desaturase 2; Mouse stearoyl-CoA desaturase (SCD2) mRNA, complete cds.	**0.504 (0.45 to 0.574)**	19 C3|19 43.0 cM		M26270 NCBI
36	94369_at	glucosamine-phosphate N-acetyltransferase 1	Gnpnat1	UI-M-BH2.1-apb-f-07-0-UI.s1 NIH_BMAP_M_S3.1 Mus musculus cDNA clone UI-M-BH2.1-apb-f-07-0-UI 3', mRNA sequence.	**0.51 (0.393 to 0.695)**	14 C1		AW123026 NCBI
37	96871_at	RIKEN cDNA 2310042G06 gene	2310042G06Rik	UI-M-AL1-ahp-a-08-0-UI.s1 NIH_BMAP_MCO_N Mus musculus cDNA clone UI-M-AL1-ahp-a-08-0-UI 3', mRNA sequence.	**0.51 (0.451 to 0.584)**	2 H4	182294	AI844355 NCBI
38	95599_at	ST3 beta-galactoside alpha-2,3-sialyltransferase 4	St3gal4	'Mouse Gal-beta-(1-3/1-4)-GlcNAc-alpha-2, 3-sialyltransferase ST-4'; Mouse mRNA for alpha-2,3-sialyltransferase, complete cds.	**0.51 (0.478 to 0.555)**	9 A5.3	275973	D28941 NCBI
39	94420_f_at	cryptochrome 1 (photolyase-like)	Cry1	Mus musculus mRNA for photolyase/blue-light receptor homolog, complete cds.	**0.512 (0.4 to 0.619)**	10 C|10 46.0 cM	26237	AB000777 NCBI
40	101475_at	B lymphoma Mo-MLV insertion region 1	Bmi1	minor transcript; Mouse zinc finger protein (bmi-1) gene, complete cds.	**0.513 (0.299 to 0.709)**	2 A3|2 9.0 cM	289584	M64068 NCBI
41	103596_at	diacylglycerol kinase, alpha	Dgka	alpha-DGK; Mus musculus alpha diacylglycerol kinase mRNA, complete cds.	**0.515 (0.379 to 0.73)**	10 D3|10 71.0 cM	291235	AF085219 NCBI
42	100010_at	Kruppel-like factor 3 (basic)	Klf3	Mus musculus CACCC-box binding protein BKLF mRNA, complete cds.	**0.515 (0.512 to 0.518)**	5 C3.1	319499	U36340 NCBI
43	103696_r_at	RIKEN cDNA C330007P06 gene	C330007P06Rik	UI-M-BH1-amh-h-04-0-UI.s1 NIH_BMAP_M_S2 Mus musculus cDNA clone UI-M-BH1-amh-h-04-0-UI 3', mRNA sequence.	**0.516 (0.494 to 0.539)**	X A3.2	290704	AW047329 NCBI
44	100902_at	RIKEN cDNA 2610019F03 gene	2610019F03Rik	UI-M-AN1-aff-h-05-0-UI.s1 NIH_BMAP_MBG_N Mus musculus cDNA clone UI-M-AN1-aff-h-05-0-UI 3', mRNA sequence.	**0.52 (0.48 to 0.549)**	8 A1.1	5727	AI846549 NCBI
45	99503_at	PTC7 protein phosphatase homolog (S. cerevisiae)	Pptc7	UI-M-BH1-alh-c-10-0-UI.s1 NIH_BMAP_M_S2 Mus musculus cDNA clone UI-M-BH1-alh-c-10-0-UI 3', mRNA sequence.	**0.527 (0.41 to 0.678)**	5 F		AW045204 NCBI
46	93637_at	CD5 antigen	Cd5	precursor; Mouse lymphocyte differentiation antigen Ly-1 mRNA, complete cds.	**0.528 (0.418 to 0.704)**	19 A|19 5.0 cM	779	M15177 NCBI
47	100928_at	fibulin 2	Fbln2	M.musculus mRNA for fibulin-2.	**0.529 (0.472 to 0.58)**	6 D-E|6 37.2 cM	249146	X75285 NCBI
48	99451_at	RIKEN cDNA C230093N12 gene	C230093N12Rik	UI-M-BH1-ann-d-01-0-UI.s1 NIH_BMAP_M_S2 Mus musculus cDNA clone UI-M-BH1-ann-d-01-0-UI 3', mRNA sequence.	**0.538 (0.452 to 0.624)**	2 B	4065	AW060510 NCBI
49	95418_at	RAS-like, family 11, member B	Rasl11b	UI-M-AJ1-ahb-d-09-0-UI.s1 NIH_BMAP_MOB_N Mus musculus cDNA clone UI-M-AJ1-ahb-d-09-0-UI 3', mRNA sequence.	**0.541 (0.462 to 0.623)**	5 D	293316	AI848851 NCBI
50	101848_g_at	nuclear antigen Sp100	Sp100	nuclear dot gene; Mus musculus Sp100 gene, exon 8 and partial cds.	**0.544 (0.404 to 0.688)**	1 C5|1 50.0 cM	290906	AF040242 NCBI
51	95701_at	CXXC finger 5	Cxxc5	UI-M-BH2.1-apn-f-11-0-UI.s1 NIH_BMAP_M_S3.1 Mus musculus cDNA clone UI-M-BH2.1-apn-f-11-0-UI 3', mRNA sequence.	**0.548 (0.397 to 0.628)**	18 B3	94560	AW124069 NCBI
52	103574_at	actin-binding LIM protein 1	Ablim1	UI-M-AP0-abn-h-07-0-UI.s1 NIH_BMAP_MST Mus musculus cDNA clone UI-M-AP0-abn-h-07-0-UI 3', mRNA sequence.	**0.548 (0.432 to 0.623)**	19 D2|19 53.0 cM	217161	AI841606 NCBI
53	92262_at	zinc finger matrin type 3	Zmat3	Mus musculus p53-inducible zinc finger protein (Wig-1) mRNA, complete cds.	**0.553 (0.447 to 0.617)**	3 B	35705	AF012923 NCBI
54	104315_at	Rho GTPase activating protein 1	Arhgap1	UI-M-AO1-ael-f-02-0-UI.s1 NIH_BMAP_MPG_N Mus musculus cDNA clone UI-M-AO1-ael-f-02-0-UI 3', mRNA sequence.	**0.559 (0.525 to 0.581)**	2 E1	22413	AI846773 NCBI
55	102383_at	RIKEN cDNA 5730593F17 gene	5730593F17Rik	UI-M-BH1-amo-h-10-0-UI.s1 NIH_BMAP_M_S2 Mus musculus cDNA clone UI-M-BH1-amo-h-10-0-UI 3', mRNA sequence.	**0.56 (0.504 to 0.649)**	11 D	262113	AW048977 NCBI
56	93319_at	RAS p21 protein activator 3	Rasa3	Mus musculus GTPase-activating protein GAPIII mRNA, complete cds.	**0.562 (0.461 to 0.686)**	8 A1.1	18517	U20238 NCBI
57	98624_at	RNA binding motif protein 38	Rbm38	M.musculus seb4 mRNA.	**0.562 (0.483 to 0.61)**	2 H3	3865	X75316 NCBI

Genes italicised indicate those that have passed the Benjamini-Hochberg false discovery rate procedure.

Table A.2. Genes down-regulated by DEX in the presence of ROSC.

	Probe set ID	Gene Title	Gene Symbol	Description	Fold change	Chromosomal Location	UniGene ID	Representative Public ID
58	99080_at	coiled-coil domain containing 6	Ccdc6	UI-M-BH0-aju-g-05-0-UI.s1 NIH_BMAP_M_S1 Mus musculus cDNA clone UI-M-BH0-aju-g-05-0-UI 3', mRNA sequence.	**0.567 (0.505 to 0.632)**	10 B5.3	281741	AI853930 NCBI
59	96095_i_at	hydroxysteroid dehydrogenase like 2	Hsdl2	uk39c03.x1 Sugano mouse kidney mkia Mus musculus cDNA clone IMAGE:1971364 3' similar to SW:DHB4_HUMAN P51659 ESTRADIOL 17 BETA-DEHYDROGENASE 4 ;, mRNA sequence.	**0.569 (0.507 to 0.686)**	4 C1	272905	AI648018 NCBI
60	103065_at	solute carrier family 20, member 1	Slc20a1	Murine Glvr-1 mRNA, complete cds.	**0.579 (0.529 to 0.638)**	2 F1|2 73.0 cM	272675	M73696 NCBI
61	97967_at	plexin D1	Plxnd1	vx18h07.r1 Soares_thymus_2NbMT Mus musculus cDNA clone IMAGE:1264861 5', mRNA sequence.	**0.589 (0.559 to 0.649)**	6 E3	3085	AA881438 NCBI
62	95716_at	3-monooxygenase/tryptophan 5-monooxygenase activation protein, gamma polypeptide	Ywhag	UI-M-BH2.1-apx-b-01-0-UI.s1 NIH_BMAP_M_S3.1 Mus musculus cDNA clone UI-M-BH2.1-apx-b-01-0-UI 3', mRNA sequence.	**0.591 (0.561 to 0.638)**	5 G2	233813	AW125041 NCBI

Genes italicised indicate those that have passed the Benjamini-Hochberg false discovery rate procedure.

Table A.3. Genes up-regulated by NP68 cognate antigen in F5 TCR Rag-1$^{-/-}$ Tap-1$^{-/-}$ transgenic mice.

	Probe set ID	Gene Title	Gene Symbol	Description	Fold change	Chromosomal Location	UniGene ID	Representative Public ID
1	*101587_at*	*epoxide hydrolase 1, microsomal*	*Ephx1*	*Allele: b; Mus musculus microsomal expoxide hydrolase (Eph1) mRNA, allele b, complete cds.*	*80.2920413*	*1 H4|1 98.5 cM*	*9075*	*U89491*
2	*102661_at*	*early growth response 2*	*Egr2*	*zinc finger protein A; zinc finger protein B; Mouse zinc finger protein (krox-20) gene, exon 2.*	*70.26385631*	*10 B5|10 35.0 cM*	*290421*	*M24377*
3	*100962_at*	*Ngfi-A binding protein 2*	*Nab2*	*represses transcription mediated by NGFI-A/Egr-1 and Krox20; similar to NAB1 protein sequence; transcriptional co-repressor; Mus musculus NGFI-A binding protein 2 (NAB2) mRNA, complete cds.*	*55.7838096*	*10 D3|10 70.0 cM*	*336898*	*U47543*
4	*102371_at*	*nuclear receptor subfamily 4, group A, member 1*	*Nr4a1*	*Mouse N10 gene for a nuclear hormonal binding receptor.*	*40.54992302*	*15 F*	*119*	*X16995*
5	*98579_at*	*early growth response 1*	*Egr1*	*Mus musculus zinc finger protein (Krox-24) gene, exon 2.*	*24.42272725*	*18 C/D|18 16.0 cM*	*181959*	*M28845*
6	*160901_at*	*FBJ osteosarcoma oncogene*	*Fos*	*Mouse c-fos oncogene.*	*24.05096348*	*12 D2|12 40.0 cM*	*246513*	*V00727*
7	*103560_at*	*LysM, putative peptidoglycan-binding, domain containing 2*	*Lysmd2*	*UI-M-BH2.1-ape-d-04-0-UI.s1 NIH_BMAP_M_S3.1 Mus musculus cDNA clone UI-M-BH2.1-ape-d-04-0-UI 3', mRNA sequence.*	*23.879658*	*9 D*	*19119*	*AW124401*
8	*93637_at*	*CD5 antigen*	*Cd5*	*precursor; Mouse lymphocyte differentiation antigen Ly-1 mRNA, complete cds.*	*23.04372369*	*19 A|19 5.0 cM*	*779*	*M15177*
9	161666_f_at	growth arrest and DNA-damage-inducible 45 beta	Gadd45b	AV138783 Mus musculus C57BL/6J 10-11 day embryo Mus musculus cDNA clone 2810046L02, mRNA sequence.	22.73874092	10 C1|10 60.5 cM	1360	AV138783
10	*98836_at*	*programmed cell death 1*	*Pdcd1*	*M.musculus PD-1 mRNA.*	*15.06922656*	*1 D*	*5024*	*X67914*
11	*102209_at*	*nuclear factor of activated T-cells, cytoplasmic, calcineurin-dependent 1*	*Nfatc1*	*Mus musculus transcription factor NF-ATc isoform a (NF-ATca) mRNA, complete cds.*	*12.07189415*	*18 E4|18 54.0 cM*	*329560*	*AF087434*
12	*93915_at*	*POU domain, class 2, associating factor 1*	*Pou2af1*	*POU domain, class 2, associating factor 1*	*12.00437714*	*9 A5.3*	*897*	*Z54283*
13	104445_at	RIKEN cDNA 4631408O11 gene	4631408O11Rik	UI-M-BH1-alm-d-07-0-UI.s1 NIH_BMAP_M_S2 Mus musculus cDNA clone UI-M-BH1-alm-d-07-0-UI 3', mRNA sequence.	11.33650486		2935	AW046694
14	*95373_at*	*CD2 antigen*	*Cd2*	*precursor (-22 to -1); Murine mRNA for T11 protein.*	*10.74588323*	*3 F2.2|3 48.2 cM*	*22842*	*X06143*
15	*95673_s_at*	*brain abundant, membrane attached signal protein 1*	*Basp1*	*UI-M-BH2.1-apr-b-09-0-UI.s1 NIH_BMAP_M_S3.1 Mus musculus cDNA clone UI-M-BH2.1-apr-b-09-0-UI 3', mRNA sequence.*	*10.5852837*	*15 B1*	*29586*	*AW124113*
16	93511_at	integral membrane protein 2A	Itm2a	putative; Mus musculus (E25) mRNA, complete cds.	9.868450032	X A2-A3	193	L38971
17	92758_at	dual specificity phosphatase 2	Dusp2	Source: Mus musculus domesticus 129 tyrosine-threonine dual specificity phosphatase PAC-1 gene, complete cds.	7.881777013	2 F1	4729	U09268
18	*92975_at*	*SH3-domain binding protein 2*	*Sh3bp2*	*PH domain, aa 25-133; SH2, aa 453-555; SH3 binding site, aa 201-210; putative; Mouse SH3 binding protein 3BP2 mRNA, complete cds.*	*7.675971445*	*5 B2*	*5012*	*L14543*
19	98868_at	B-cell leukemia/lymphoma 2	Bcl2	bcl2-alpha; Mus musculus bcl-2 alpha gene, exon 2.	7.645360262	1 E2.1|1 59.8 cM	257460	L31532
20	92534_at	GTP binding protein (gene overexpressed in skeletal muscle)	Gem	Mus musculus Gem GTPase (gem) mRNA, complete cds.	6.912092602	4 A1|4 2.6 cM	247486	U10551
21	*98282_at*	*inducible T-cell co-stimulator*	*Icos*	*Mus musculus mRNA for activation-inducible lymphocyte immunomediatory molecule AILIM, complete cds.*	*6.744154778*	*1 C2|1 32.0 cM*	*42044*	*AB023132*
22	*160629_at*	*regulator of G-protein signalling 10*	*Rgs10*	*UI-M-AI1-afr-f-03-0-UI.s1 NIH_BMAP_MBS_N Mus musculus cDNA clone UI-M-AI1-afr-f-03-0-UI 3', mRNA sequence.*	*6.63850231*	*7 F3*	*18635*	*AI847399*
23	102272_at	CD160 antigen	Cd160	similar to human natural killer cell BY55; Mus musculus natural killer cell BY55 precursor, mRNA, complete cds.	6.485392263	3 F2.1	34693	AF060982
24	103629_g_at	lymphoid enhancer binding factor 1	Lef1	Mouse mRNA for LEF-1S, complete cds.	6.086040106	3 G3|3 61.6 cM	255219	D16503
25	161765_f_at	regulator of G-protein signalling 10	Rgs10	AV335997 RIKEN full-length enriched, adult male medulla oblongata Mus musculus cDNA clone 6330579C12 3', mRNA sequence.	6.008065407	7 F3	18635	AV335997
26	102362_i_at	Jun-B oncogene	Junb	Mus musculus transcription factor junB (junB) gene, 5' region and complete cds.	5.993565701	8 C2-D1|8 38.6 cM	1167	U20735
27	*99109_at*	*immediate early response 2*	*Ier2*	*Mouse growth factor-inducible protein (pip92) mRNA, complete cds.*	*5.834417906*	*8 C3|8 38.4 cM*	*399*	*M59821*
28	96596_at	N-myc downstream regulated gene 1	Ndrg1	differentially repressed by testosterone and dihydrotestosterone; Mus musculus TDD5 mRNA, complete cds.	5.778821475	15 D2	30837	U52073
29	*99916_at*	*protein kinase C, eta*	*Prkch*	*Mouse mRNA for nPKC-eta.*	*5.368793767*	*12 C3-D1*	*341677*	*D90242*
30	*94278_at*	*lymphocyte cytosolic protein 1*	*Lcp1*	*Mouse mRNA for 65-kDa macrophage cytosolic protein, complete cds.*	*5.289561186*	*14 D3|14 42.0 cM*	*153911*	*D37837*
31	160464_s_at	N-myc downstream regulated-like	Ndrl	Mus musculus cytoplasmic protein Ndr1 (Ndr1) mRNA, complete cds.	5.239062162	15 D2		U60593
32	93869_s_at	B-cell leukemia/lymphoma 2 related protein A1a	Bcl2a1a	Mus musculus hematopoietic-specific early-response A1-d protein (A1d) gene, exon 2, and complete cds.	4.933908757	9 E3.1|9 50.0 cM	378888	U23781
33	97834_g_at	phosphofructokinase, platelet	Pfkp	UI-M-BH0-ajg-h-01-0-UI.s1 NIH_BMAP_M_S1 Mus musculus cDNA clone UI-M-BH0-ajg-h-01-0-UI 3', mRNA sequence.	4.838037598	13 A1	273874	AI853802
34	98869_g_at	B-cell leukemia/lymphoma 2	Bcl2	bcl2-alpha; Mus musculus bcl-2 alpha gene, exon 2.	4.734601164	1 E2.1|1 59.8 cM	257460	L31532

Genes italicised indicate those that have passed the Benjamini-Hochberg false discovery rate procedure.

Table A.3. Genes up-regulated by NP68 cognate antigen in F5 TCR Rag-1$^{-/-}$ Tap-1$^{-/-}$ transgenic mice.

	Probe set ID	Gene Title	Gene Symbol	Description	Fold change	Chromosomal Location	UniGene ID	Representative Public ID
35	97796_at	cofactor required for Sp1 transcriptional activation, subunit 2	Crsp2	similar to human EXLM1 gene; Mus musculus gene, complete cds, similar to EXLM1.	4.684658746	X A1.1	17616	AB019029
36	95733_at	solute carrier family 29 (nucleoside transporters), member 1	Slc29a1	UI-M-AO0-aby-a-05-0-UI.s1 NIH_BMAP_MPG Mus musculus cDNA clone UI-M-AO0-aby-a-05-0-UI 3', mRNA sequence.	4.453102386	17 C	29744	AI838274
37	*97833_at*	*phosphofructokinase, platelet*	*Pfkp*	*UI-M-BH0-ajg-h-01-0-UI.s1 NIH_BMAP_M_S1 Mus musculus cDNA clone UI-M-BH0-ajg-h-01-0-UI 3', mRNA sequence.*	*4.426045673*	*13 A1*	*273874*	*AI853802*
38	*92203_s_at*	*CD6 antigen*	*Cd6*	*Mus musculus T cell surface glycoprotein CD6 mRNA, complete cds.*	*4.299402604*	*19 A|19 5.0 cM*	*290897*	*U37543*
39	92204_at	CD6 antigen	Cd6	Mus musculus mscd6 precursor (Cd6) mRNA, complete cds.	4.15336851	19 A|19 5.0 cM	290897	U12434
40	95102_at	scotin gene	Scotin	UI-M-BH2.1-apm-a-08-0-UI.s1 NIH_BMAP_M_S3.1 Mus musculus cDNA clone UI-M-BH2.1-apm-a-08-0-UI 3', mRNA sequence.	4.070119685	9 F2	196533	AW123754
41	*103628_at*			*Mouse mRNA for LEF-1S, complete cds.*	*3.909334639*			*D16503*
42	93694_at	period homolog 2 (Drosophila)	Per2	Rigui2; Mus musculus circadian clock protein (Per2) mRNA, complete cds.	3.833767608	1 C5	218141	AF036893
43	94995_at	RIKEN cDNA A030007L17 gene	A030007L17Rik	UI-M-BG1-aic-b-07-0-UI.s1 NIH_BMAP_MSC_N Mus musculus cDNA clone UI-M-BG1-aic-b-07-0-UI 3', mRNA sequence.	3.823475199	6 B3	294708	AI854331
44	94939_at	CD53 antigen	Cd53	M.musculus mRNA for cell surface glycoprotein CD53.	3.80401724	3 F2.3|3 50.5 cM	316861	X97227
45	103091_at	avian reticuloendotheliosis viral (v-rel) oncogene related B	Relb	transcription factor; Mouse transcription factor relB mRNA, complete cds.	3.779647084	7 A3|7 4.0 cM	1741	M83380
46	*95542_at*	*tropomyosin 4*	*Tpm4*	*UI-M-AI0-aat-c-09-0-UI.s1 NIH_BMAP_MBS Mus musculus cDNA clone UI-M-AI0-aat-c-09-0-UI 3', mRNA sequence.*	*3.753754739*	*8 B3.3*	*295124*	*AI835858*
47	*95931_at*	*Cofactor required for Sp1 transcriptional activation, subunit 2*	*Crsp2*	*uj27g06.x1 Sugano mouse kidney mkia Mus musculus cDNA clone IMAGE:1921210 3', mRNA sequence.*	*3.751433644*	*X A1.1*	*17616*	*AI314706*
48	93025_at	Nedd4 family interacting protein 1	Ndfip1	UI-M-AQ0-aab-b-03-0-UI.s1 NIH_BMAP_MHI Mus musculus cDNA clone UI-M-AQ0-aab-b-03-0-UI 3', mRNA sequence.	3.635710903	18 B3	102496	AI835257
49	103443_at	absent in melanoma 1	Aim1	vu58c09.r1 Soares_mammary_gland_NbMMG Mus musculus cDNA clone IMAGE:1195600 5', mRNA sequence.	3.597693012	10 B2|10 29.0 cM	292082	AA711704
50	101851_at	Cd200 antigen	Cd200	Mus musculus MRC OX-2 antigen homolog gene, exons 2-5, and complete cds.	3.532109209	16 A1|16 29.0 cM	245851	AF029215
51	*160150_f_at*	*calponin 3, acidic*	*Cnn3*	*UI-M-BH2.2-aqj-h-02-0-UI.s1 NIH_BMAP_M_S3.2 Mus musculus cDNA clone UI-M-BH2.2-aqj-h-02-0-UI 3', mRNA sequence.*	*3.463478989*	*3 G1*	*275555*	*AW125626*
52	95518_at	RIKEN cDNA 1810015C04 gene	1810015C04Rik	UI-M-BH2.1-apa-d-07-0-UI.s1 NIH_BMAP_M_S3.1 Mus musculus cDNA clone UI-M-BH2.1-apa-d-07-0-UI 3', mRNA sequence.	3.330351957	15 B1	25311	AW122893
53	99489_at	heat shock protein 4 like	Hspa4l	mRNA expression is increased during hyperosmolar NaCl stress; similar to heat shock protein: SwissProt Accession Number P34932; Mus musculus osmotic stress protein 94 (Osp94) mRNA, complete cds.	3.31860945	3 B	39330	U23921
54	*98905_at*	*septin 7*	*39326*	*Mus musculus CDC10 gene, promoter, exon 1 and joined CDS.*	*3.31385644*	*9 A4*	*270259*	*AJ223782*
55	94369_at	glucosamine-phosphate N-acetyltransferase 1	Gnpnat1	UI-M-BH2.1-apb-f-07-0-UI.s1 NIH_BMAP_M_S3.1 Mus musculus cDNA clone UI-M-BH2.1-apb-f-07-0-UI 3', mRNA sequence.	3.288980526	14 C1		AW123026
56	*103362_at*	*prostaglandin E receptor 4 (subtype EP4)*	*Ptger4*	*Mouse mRNA for prostaglandin E receptor EP2 subtype, complete cds.*	*3.277886706*	*15 A1|15 6.4 cM*	*18509*	*D13458*
57	96344_at	enolase 3, beta muscle	Eno3	beta-enolase subunit; M.musculus gene for beta-enolase.	3.240822394	11 B4|11 42.0 cM	251322	X61600
58	160137_at	UDP-GlcNAc:betaGal beta-1,3-N-acetylglucosaminyltransferase 2	B3gnt2	um76d02.x1 Sugano mouse kidney mkia Mus musculus cDNA clone IMAGE:2301123 3', mRNA sequence.	3.051773572	11 A3.2|11 12.0 cM	258094	AW260308
59	93212_at	protein tyrosine phosphatase-like A domain containing 1	Ptplad1	Mus musculus partial mRNA for B-IND1 protein (B-ind1 gene).	2.965927601	9 D	308180	Z97207
60	96186_at	low-density lipoprotein receptor-related protein 10	Lrp10	UI-M-AO0-acb-c-08-0-UI.s1 NIH_BMAP_MPG Mus musculus cDNA clone UI-M-AO0-acb-c-08-0-UI 3', mRNA sequence.	2.953036161	14 C2	28465	AI839286
61	94063_at	sema domain, immunoglobulin domain (Ig), transmembrane domain (TM) and short cytoplasmic domain, (semaphorin) 4A	Sema4a	M.musculus mRNA for semaphorin B.	2.938667562	3 F1		X85991
62	*100048_at*	*RAS-related protein-1a*	*Rap1a*	*UI-M-BH1-ani-c-01-0-UI.s1 NIH_BMAP_M_S2 Mus musculus cDNA clone UI-M-BH1-ani-c-01-0-UI 3', mRNA sequence.*	*2.906106526*	*3 F2.2|3 48.5 cM 7 B3*	*430611*	*AW049685*
63	98059_s_at	lamin A	Lmna		2.900805808	3 F1|3 42.6 cM	243014	D49733
64	*95622_at*	*kelch domain containing 2*	*Klhdc2*	*UI-M-BH2.1-app-h-01-0-UI.s1 NIH_BMAP_M_S3.1 Mus musculus cDNA clone UI-M-BH2.1-app-h-01-0-UI 3', mRNA sequence.*	*2.879529315*	*12 C3|12 30.0 cM*	*234368*	*AW123907*
65	*104256_at*	*pleckstrin homology, Sec7 and coiled-coil domains, binding protein*	*Pscdbp*	*ub73a05.r1 Soares_mammary_gland_NMLMG Mus musculus cDNA clone IMAGE:1383344 5', mRNA sequence.*	*2.867155254*	*2 C1.1*	*273905*	*AI120844*

Genes italicised indicate those that have passed the Benjamini-Hochberg false discovery rate procedure.

Table A.3. Genes up-regulated by NP68 cognate antigen in F5 TCR Rag-1$^{-/-}$ Tap-1$^{-/-}$ transgenic mice.

	Probe set ID	Gene Title	Gene Symbol	Description	Fold change	Chromosomal Location	UniGene ID	Representative Public ID
66	92614_at	inhibitor of DNA binding 3	Id3	Mouse helix-loop-helix protein (Id related) mRNA, complete cds.	2.855665021	4 D3|4 66.0 cM	110	M60523
67	98988_at	nuclear factor of kappa light polypeptide gene enhancer in B-cells inhibitor, zeta	Nfkbiz	vo32e09.r1 Barstead mouse irradiated colon MPLRB7 Mus musculus cDNA clone IMAGE:1051624 5', mRNA sequence.	2.840756209	16 C1.2-C1.3	247272	AA614971
68	93942_at	inositol polyphosphate-1-phosphatase	Inpp1	Mus musculus inositol polyphosphate 1-phosphatase mRNA, complete cds.	2.79451791	1 C1.1|1 27.1 cM	917	U27295
69	102281_at	CD antigen 27	Cd27	Mus musculus CD27 antigen (Cd27) mRNA.	2.784394557	6 F3|6 60.35 cM	367714	L24495
70	*97309_at*	*suppression of tumorigenicity 13*	*St13*	*uo41a02.x1 NCI_CGAP_Lu29 Mus musculus cDNA clone IMAGE:2645066 3', mRNA sequence.*	*2.730771024*	*15 E2*	*180337*	*AW214164*
71	102090_f_at	SET and MYND domain containing 5	Smyd5	UI-M-AL0-abo-d-04-0-UI.s1 NIH_BMAP_MCO Mus musculus cDNA clone UI-M-AL0-abo-d-04-0-UI 3', mRNA sequence.	2.725525729	6 C3|6 35.61 cM	219946	AI841710
72	93324_at	zinc finger protein 36, C3H type-like 1	Zfp36l1	Mouse TIS11 primary response gene, complete cds.	2.722736958	12 C3	235132	M58566
73	*104257_g_at*	*pleckstrin homology, Sec7 and coiled-coil domains, binding protein*	*Pscdbp*	*ub73a05.r1 Soares_mammary_gland_NMLMG Mus musculus cDNA clone IMAGE:1383344 5', mRNA sequence.*	*2.718353781*	*2 C1.1*	*273905*	*AI120844*
74	*94345_at*	*interleukin 6 signal transducer*	*Il6st*	*UI-M-AK1-aer-e-08-0-UI.s1 NIH_BMAP_MHY_N Mus musculus cDNA clone UI-M-AK1-aer-e-08-0-UI 3', mRNA sequence.*	*2.717522996*	*13 D2.2|13 67.0 cM*	*4364*	*AI843709*
75	93092_at	histocompatibility 2, class II, locus DMa	H2-DMa		2.656682201	17 B1|17 18.56 cM	16373	U35323
76	*94004_at*	*calponin 2*	*Cnn2*	*M.musculus h2-calponin cDNA.*	*2.646258909*	*10 C1*	*157770*	*Z19543*
77	*93619_at*	*period homolog 1 (Drosophila)*	*Per1*	*circadian pacemaker protein; Mus musculus Rigui mRNA, complete cds.*	*2.532975706*	*11 B*	*7373*	*AF022992*
78	100133_at	Fyn proto-oncogene	Fyn	p59fyn; Mouse fyn proto-oncogene encoding p59fyn, complete cds.	2.505461466	10 B1|10 25.0 cM	4848	M27266
79	96276_r_at	transmembrane 9 superfamily member 3	Tm9sf3	UI-M-AQ1-adz-a-05-0-UI.s1 NIH_BMAP_MHI_N Mus musculus cDNA clone UI-M-AQ1-adz-a-05-0-UI 3', mRNA sequence.	2.478989078	19 C3	246440	AI843327
80	93962_at	RAS-related protein-1a	Rap1a	UI-M-AH1-agv-b-04-0-UI.s1 NIH_BMAP_MCE_N Mus musculus cDNA clone UI-M-AH1-agv-b-04-0-UI 3', mRNA sequence.	2.467166485	3 F2.2|3 48.5 cM	365961	AI848598
81	100924_at	GATA binding protein 3	Gata3	Mouse mRNA for GATA-3 transcription factor.	2.458301521	2 A1|2 7.0 cM	313866	X55123
82	*92220_s_at*	*bridging integrator 1*	*Bin1*	*amphiphysin-like protein; Method: conceptual translation supplied by author; Mus musculus SH3P9 mRNA, complete cds.*	*2.456413322*	*18 B1|18 14.0 cM*	*4383*	*U60884*
83	*99133_at*	*solute carrier family 3 (activators of dibasic and neutral amino acid transport), member 2*	*Slc3a2*	*4F2 heavy chain (AA 1-526); Murine mRNA for 4F2 antigen heavy chain.*	*2.454476545*	*19 A|19 0.0 cM*	*4114*	*X14309*
84	93285_at	dual specificity phosphatase 6	Dusp6	UI-M-AQ1-adx-c-06-0-UI.s1 NIH_BMAP_MHI_N Mus musculus cDNA clone UI-M-AQ1-adx-c-06-0-UI 3', mRNA sequence.	2.392211963	10 C3	1791	AI845584
85	104730_at	midasin homolog (yeast)	Mdn1	UI-M-BH1-akl-d-04-0-UI.s1 NIH_BMAP_M_S2 Mus musculus cDNA clone UI-M-BH1-akl-d-04-0-UI 3', mRNA sequence.	2.382966055	4 A5	24627	AW046889
86	94341_at	jumonji, AT rich interactive domain 2	Jarid2	Mouse mRNA for jumonji protein.	2.375719527	13 A5|13 27.0 cM	25059	D31967
87	97310_at	suppression of tumorigenicity 13	St13	UI-M-BH2.1-apq-d-11-0-UI.s1 NIH_BMAP_M_S3.1 Mus musculus cDNA clone UI-M-BH2.1-apq-d-11-0-UI 3', mRNA sequence.	2.367076555	15 E2	180337	AW124318
88	103614_at	nuclear factor of kappa light polypeptide gene enhancer in B-cells 2, p49/p100	Nfkb2	UI-M-BH1-aln-a-06-0-UI.s1 NIH_BMAP_M_S2 Mus musculus cDNA clone UI-M-BH1-aln-a-06-0-UI 3', mRNA sequence.	2.365731494	19 C3-D2|19 45.75 cM	102365	AW047899
89	*95543_at*	*tropomyosin 4*	*Tpm4*	*UI-M-AK1-aeq-g-04-0-UI.s1 NIH_BMAP_MHY_N Mus musculus cDNA clone UI-M-AK1-aeq-g-04-0-UI 3', mRNA sequence.*	*2.362924679*	*8 B3.3*	*295124*	*AI843046*
90	160353_i_at	MAP kinase-activated protein kinase 2	Mapkapk2	M. musculus mRNA for MAP kinase-activated protein kinase 2.	2.33772097	1 E4	221235	X76850
91	*160393_at*	*ethanolamine kinase 1*	*Etnk1*	*UI-M-BH0-ajh-g-12-0-UI.s1 NIH_BMAP_M_S1 Mus musculus cDNA clone UI-M-BH0-ajh-g-12-0-UI 3', mRNA sequence.*	*2.30066267*	*6 G3|6 74.0 cM*	*272548*	*AI853226*
92	98594_at	RIKEN cDNA 1190002N15 gene	1190002N15Rik	UI-M-BH2.2-aqm-a-02-0-UI.s1 NIH_BMAP_M_S3.2 Mus musculus cDNA clone UI-M-BH2.2-aqm-a-02-0-UI 3', mRNA sequence.	2.287818102	9 E3.3	258746	AW125453
93	*95721_at*	*MAP kinase-activated protein kinase 2*	*Mapkapk2*	*UI-M-BH2.3-any-a-09-0-UI.s1 NIH_BMAP_M_S3.3 Mus musculus cDNA clone UI-M-BH2.3-any-a-09-0-UI 3', mRNA sequence.*	*2.269296504*	*1 E4*	*221235*	*AW120722*
94	*92484_at*	*human immunodeficiency virus type I enhancer binding protein 2*	*Hivep2*	*Mus musculus mRNA for myc-intron-binding protein-1.*	*2.25573749*		*42157*	*Y15907*
95	*97319_at*	*Ras-related associated with diabetes*	*Rrad*	*Mus musculus Ras-like GTP-binding protein Rad mRNA, complete cds.*	*2.245521926*	*8 D3*	*29467*	*AF084466*
96	93842_at	death-associated protein	Dap	ui53d07.y1 Sugano mouse liver mlia Mus musculus cDNA clone IMAGE:1886125 5' similar to SW:DAP1_HUMAN P51397 DEATH-ASSOCIATED PROTEIN 1 ;, mRNA sequence.	2.226582125	15 B2	222867	AI196645
97	98427_s_at	nuclear factor of kappa light chain gene enhancer in B-cells 1, p105	Nfkb1	Mouse transcription factor NF-kappa-B DNA binding subunit mRNA, complete cds.	2.226317682	3 G3|3 68.9 cM	256765	M57999
98	97974_at	zinc finger protein, multitype 1	Zfpm1	friend of GATA-1; zinc finger protein; Mus musculus friend of GATA-1 (FOG) mRNA, complete cds.	2.215393845	8 E1	390068	AF006492

Genes italicised indicate those that have passed the Benjamini-Hochberg false discovery rate procedure.

Table A.3. Genes up-regulated by NP68 cognate antigen in F5 TCR Rag-1$^{-/-}$ Tap-1$^{-/-}$ transgenic mice.

	Probe set ID	Gene Title	Gene Symbol	Description	Fold change	Chromosomal Location	UniGene ID	Representative Public ID
99	*92949_at*	*protein kinase C and casein kinase substrate in neurons 1*	*Pacsin1*	*M.musculus pacsin gene.*	*2.214151505*		*4926*	*X85124*
100	102959_at	transducin-like enhancer of split 4, homolog of Drosophila E(spl)	Tle4	putative transcriptional co-repressor; similar to transducin-like enhancer proteins; Mus musculus groucho-related gene 4 protein (Grg4) mRNA, partial cds.	2.210748917	19 A|19 7.0 cM	103638	U61363
101	*99855_at*	*similar to mitogen activated protein kinase kinase kinase 5*	*LOC675366*	*ASK1; Mus musculus mRNA for apoptosis signal-regulating kinase 1, complete cds.*	*2.210697285*			*AB006787*
102	102848_f_at	RIKEN cDNA 2610524H06 gene	2610524H06Rik	UI-M-AM0-adp-h-10-0-UI.s1 NIH_BMAP_MAM Mus musculus cDNA clone UI-M-AM0-adp-h-10-0-UI 3', mRNA sequence.	2.192859326	5 F		AI840577
103	103098_at	brain-specific angiogenesis inhibitor 1-associated protein 2	Baiap2	UI-M-BH1-akt-c-06-0-UI.s1 NIH_BMAP_M_S2 Mus musculus cDNA clone UI-M-BH1-akt-c-06-0-UI 3', mRNA sequence.	2.187231513	11 E2	197534	AW045765
104	94408_at	Ngfi-A binding protein 1	Nab1	Mus musculus transcriptional repressor (NAB1) NAB1 mRNA, complete cds.	2.166725638	1 C1.1|1 27.0 cM	25903	U47008
105	99620_at	splicing factor proline/glutamine rich (polypyrimidine tract binding protein associated)	Sfpq	UI-M-BH1-ann-g-04-0-UI.s1 NIH_BMAP_M_S2 Mus musculus cDNA clone UI-M-BH1-ann-g-04-0-UI 3', mRNA sequence.	2.098606466	4 D2.2|4 57.6 cM	257276	AW060546
106	104154_at	transformation related protein 53	Trp53	Amino acid no.191 leusine (L) in wild-type mouse P53 is substituted to arginine (R).; Mus musculus mutant p53 mRNA, complete cds.	2.093041842	11 B2-C|11 39.0 cM	222	AB021961
107	102282_g_at	CD antigen 27	Cd27	Mus musculus CD27 antigen (Cd27) mRNA.	2.064185594	6 F3|6 60.35 cM	367714	L24495
108	98129_at	thymosin, beta 10	Tmsb10	UI-M-BH0-aiw-g-02-0-UI.s1 NIH_BMAP_M_S1 Mus musculus cDNA clone UI-M-BH0-aiw-g-02-0-UI 3', mRNA sequence.	2.019382586	6 C1|7	3532	AI852553
109	102796_at	nucleoplasmin 3	Npm3	parental gene to the pseudogene Npm3-ps1: GenBank Accession Number U67172; Mus musculus nucleophosmin/nucleoplasmin-3 (Npm3) mRNA, complete cds.	1.953518431	19 C3|19 45.0 cM	1406	U64450

Genes italicised indicate those that have passed the Benjamini-Hochberg false discovery rate procedure.

Table A.4. Genes down-regulated by NP68 cognate antigen in F5 TCR Rag-1$^{-/-}$ Tap-1$^{-/-}$ transgenic mice.

	Probe set ID	Gene Title	Gene Symbol	Description	Fold change	Chromosomal Location	UniGene ID	Representative Public ID
1	93683_at	recombination activating gene 1	Rag1	recombination activating protein; Mouse recombination activating protein (RAG-1) mRNA, complete cds.	0.027494432	2 E2|2 56.0 cM	828	M29475
2	101163_at	recombination activating gene 2	Rag2	Mus musculus RAG-2 protein (RAG-2) mRNA, complete cds.	0.037772925	2 E2|2 56.0 cM	4988	M64796
3	*102397_at*	*core-binding factor, runt domain, alpha subunit 2, translocated to, 3 homolog (human)*	*Cbfa2t3h*	*Mus musculus ETO/MTG8-related protein ETO-2 mRNA, complete cds.*	*0.074067808*		*194339*	*AF038029*
4	*102692_s_at*	*histocompatibility 2, T region locus 18*	*H2-T18*	*Mouse mRNA for TL antigen, complete cds.*	*0.07890813*	*17 19.78 cM*		*D86082*
5	*98354_at*	*pre T-cell antigen receptor alpha*	*Ptcra*	*aa 31 (Cys) potentially involved in intramolecular disulphide linkage; aa 91 (Cys) potentially involved in intramolecular disulphide linkage; aa 139 (Cys) potentially involved in intermolecular disulphide linkage to TCR-beta chain; aa 51-54 and aa 101-104 are potential N-linked glycosylation sites; Mus musculus pre-T cell receptor alpha-type chain precursor mRNA, complete cds.*	*0.08392641*	*17 D-E1*	*215173*	*U16958*
6	*162206_f_at*	*suppressor of cytokine signaling 3*	*Socs3*	*AV374868 RIKEN full-length enriched, adult male cecum Mus musculus cDNA clone 9130017A09 3' similar to U88328 Mus musculus suppressor of cytokine signalling-3 (SOCS-3) mRNA, mRNA sequence.*	*0.10155657*	*11 E2*	*3468*	*AV374868*
7	*94246_at*	*E26 avian leukemia oncogene 2, 3' domain*	*Ets2*	*ets2 protein; Mouse erythroblastosis virus oncogene homolog 2 (ets-2) mRNA, complete cds.*	*0.102001658*	*16 C3-qter|16 69.6 cM*	*290207*	*J04103*
8	93484_at	GRAM domain containing 3	Gramd3	UI-M-BH1-anw-d-01-0-UI.s1 NIH_BMAP_M_S2 Mus musculus cDNA clone UI-M-BH1-anw-d-01-0-UI 3', mRNA sequence.	0.135329021	18 D2	24356	AW061306
9	*162410_s_at*	*CD8 antigen, beta chain 1*	*Cd8b1*	*AV316162 RIKEN full-length enriched, adult male thymus Mus musculus cDNA clone 5830434K21 3' similar to M19504 Mouse T-cell differentiation antigen (Ly-3) mRNA, mRNA sequence.*	*0.139364259*	*6 C1|6 30.5 cM*		*AV316162*
10	101699_at	per-hexamer repeat gene 2	Phxr2	ORF (AA 1 - 65); Mouse period repetitive mRNA (lambda Sp28).	0.150353036	10 C3	432036	X12808
11	101470_at	WD repeat domain 78	Wdr78	UI-M-BH0-ajv-c-08-0-UI.s1 NIH_BMAP_M_S1 Mus musculus cDNA clone UI-M-BH0-ajv-c-08-0-UI 3', mRNA sequence.	0.151335149	4 C6	374877	AI851014
12	99637_at	procollagen, type XV	Col15a1	Mus musculus type XV collagen mRNA, complete cds.	0.153905569	4 B1-B3	233547	AF011450
13	*96712_at*	*SPARC related modular calcium binding 1*	*Smoc1*	*UI-M-AP1-agf-d-04-0-UI.s2 NIH_BMAP_MST_N Mus musculus cDNA clone UI-M-AP1-agf-d-04-0-UI 3', mRNA sequence.*	*0.156445029*	*12 D1*	*273295*	*AI848508*
14	92185_at	ADP-ribosylation factor-like 4C	Arl4c	UI-M-AP1-agl-g-02-0-UI.s1 NIH_BMAP_MST_N Mus musculus cDNA clone UI-M-AP1-agl-g-02-0-UI 3', mRNA sequence.	0.184044267	1 D	27968	AI846023
15	103961_s_at	deoxynucleotidyltransferase, terminal	Dntt	M.musculus mRNA for terminal deoxynucleotidyltransferase.	0.195832833	19 C3|19 39.5 cM	25620	X68670
16	104014_at	hemochromatosis	Hfe	Hemochromatosis	0.197097651	13 A2-A4|13 15.0 cM	2681	Y12650
17	102203_at	placental protein 11 related	Pp11r	Mus musculus T cell-specific protein (Tcl-30) mRNA, complete cds.	0.203079235	15 F1|15 56.8 cM	1001	M95545
18	160413_at	neuron specific gene family member 2	Nsg2	Mus musculus p19 mRNA, complete cds.	0.2064935	11 A4	3304	U17259
19	161409_f_at	deoxynucleotidyltransferase, terminal	Dntt	AV312871 RIKEN full-length enriched, adult male thymus Mus musculus cDNA clone 5830406G23 3' similar to X68670 M.musculus mRNA for terminal deoxynucleotidyltransferase, mRNA sequence.	0.209585376	19 C3|19 39.5 cM	25620	AV312871
20	103971_at	purinergic receptor P2X, ligand-gated ion channel, 1	P2rx1	M.musculus mRNA for ATP receptor.	0.210824922	11 B4|11 40.0 cM	25722	X84896
21	*104745_at*	*ADP-ribosylation factor-like 6 interacting protein 2*	*Arl6ip2*	*vv48a12.r1 Soares_thymus_2NbMT Mus musculus cDNA clone IMAGE:1225630 5', mRNA sequence.*	*0.222616078*	*17 E3*	*175403*	*AA763874*
22	103480_at	CD4 antigen	Cd4	precursor; brain allele; Mouse T-cell differentiation antigen CD4 (L3T4) gene, exons 8-10.	0.226386483	6 F2|6 60.18 cM	2209	M17080
23	99813_g_at	calpain 3	Capn3	M.musculus mRNA for skeletal muscle-specific calpain.	0.228542925	2 E5|2 67.2 cM	38851	X92523
24	94977_at	inositol 1,4,5-triphosphate receptor 1	Itpr1	P400 protein; Mouse cerebellum mRNA for P400 protein.	0.23407998	6 E1-E2|6 48.0 cM	227912	X15373
25	*92472_f_at*	*schlafen 2*	*Slfn2*	*mSLFN2; Mus musculus schlafen2 (Slfn2) mRNA, complete cds.*	*0.23537603*	*11 C|11 48.0 cM*	*278689*	*AF099973*
26	101410_at	claudin 4	Cldn4	Mus musculus mCPE-R mRNA for CPE-receptor, complete cds.	0.236887513	5 G2|5 75.0 cM	7339	AB000713
27	*100928_at*	*fibulin 2*	*Fbln2*	*M.musculus mRNA for fibulin-2.*	*0.241046237*	*6 D-E|6 37.2 cM*	*249146*	*X75285*
28	*92471_i_at*	*schlafen 2*	*Slfn2*	*mSLFN2; Mus musculus schlafen2 (Slfn2) mRNA, complete cds.*	*0.251061189*	*11 C|11 48.0 cM*	*278689*	*AF099973*
29	*97967_at*	*plexin D1*	*Plxnd1*	*vx18h07.r1 Soares_thymus_2NbMT Mus musculus cDNA clone IMAGE:1264861 5', mRNA sequence.*	*0.252302803*	*6 E3*	*3085*	*AA881438*
30	*95016_at*	*neuropilin 1*	*Nrp1*	*Mouse mRNA for neuropilin, complete cds.*	*0.252921783*	*8 E|8 73.0 cM*	*271745*	*D50086*
31	*97908_at*	*required for meiotic nuclear division 5 homolog A (S. cerevisiae)*	*Rmnd5a*	*UI-M-BH2.3-anz-b-10-0-UI.s1 NIH_BMAP_M_S3.3 Mus musculus cDNA clone UI-M-BH2.3-anz-b-10-0-UI 3', mRNA sequence.*	*0.26261113*	*6 C1*	*28474*	*AW120676*
32	*96976_f_at*	*histocompatibility 2, T region locus 18*	*H2-T18*	*MHC T11 class I antigen (30 AA) (84 is 2nd base in codon); Protein sequence is in conflict with the conceptual translation; Mouse T11 class I MHC gene (exon 5).*	*0.267529432*	*17 19.78 cM*		*X16217*
33	*103931_at*	*G protein-coupled receptor 162*	*Gpr162*		*0.268181517*	*6 F2|6 60.18 cM*	*2514*	*AC002397*

Genes italicised indicate those that have passed the Benjamini-Hochberg false discovery rate procedure.

Table A.4. Genes down-regulated by NP68 cognate antigen in F5 TCR Rag-1$^{-/-}$ Tap-1$^{-/-}$ transgenic mice.

	Probe set ID	Gene Title	Gene Symbol	Description	Fold change	Chromosomal Location	UniGene ID	Representative Public ID
34	*99951_at*	*RAR-related orphan receptor gamma*	*Rorc*	*The cDNA for mouse ROR gamma is deposited in GenBank Accession Number U43508; Mus musculus nuclear orphan receptor RORgamma (RORC) gene, exon 11 and complete cds.*	*0.269368457*	*3 F2*	*4372*	*AF019660*
35	95355_at	angiotensin II, type I receptor-associated protein	Agtrap	EST02385 Mouse 7.5 dpc embryo ectoplacental cone cDNA library Mus musculus cDNA clone C0021B10 3', mRNA sequence.	0.270773798	4 E1|4 76.4 cM	46247	AA407794
36	*93865_s_at*	*histocompatibility 2, T region locus 10*	*H2-T10*	*MHC H2-TL-T10-129; Mouse MHC class I H2-TL-T10-129 mRNA (b haplotype), complete cds.*	*0.276621676*	*17 B1|17 19.96 cM*		*M35244*
37	*92685_at*	*thromboxane A2 receptor*	*Tbxa2r*	*TXA2 receptor; Mus musculus mRNA for thromboxane A2 receptor, complete cds.*	*0.281100776*	*10 C1|10 43.0 cM*	*4545*	*D10849*
38	101384_at	degenerative spermatocyte homolog 2 (Drosophila), lipid desaturase	Degs2	UI-M-BH0-aiz-c-09-0-UI.s1 NIH_BMAP_M_S1 Mus musculus cDNA clone UI-M-BH0-aiz-c-09-0-UI 3', mRNA sequence.	0.282073777	12 F1		AI852933
39	160547_s_at	thioredoxin interacting protein	Txnip	UI-M-AO0-ach-d-06-0-UI.s1 NIH_BMAP_MPG Mus musculus cDNA clone UI-M-AO0-ach-d-06-0-UI 3', mRNA sequence.	0.28804545	3 47.1 cM	410189	AI839138
40	*96713_at*	*3'-phosphoadenosine 5'-phosphosulfate synthase 2*	*Papss2*	*bifunctional enzyme; Mus musculus ATP sulfurylase/APS kinase 2 mRNA, complete cds.*	*0.289595988*	*19 C1|19 32.0 cM*	*203916*	*AF052453*
41	94354_at	ATP-binding cassette, sub-family A (ABC1), member 1	Abca1	UI-M-AO1-aek-d-04-0-UI.s1 NIH_BMAP_MPG_N Mus musculus cDNA clone UI-M-AO1-aek-d-04-0-UI 3', mRNA sequence.	0.289783098	4 A5-B3|4 23.1 cM	277376	AI845514
42	93853_at	DnaJ (Hsp40) homolog, subfamily B, member 4	Dnajb4	vv48f08.r1 Soares_thymus_2NbMT Mus musculus cDNA clone IMAGE:1225671 5' similar to SW:DNJ1_HUMAN P25685 DNAJ PROTEIN HOMOLOG 1 ;, mRNA sequence.	0.293672425	3 H3	46746	AA763918
43	104299_at	zinc finger, DHHC domain containing 14	Zdhhc14	UI-M-AM1-afy-f-05-0-UI.s1 NIH_BMAP_MAM_N Mus musculus cDNA clone UI-M-AM1-afy-f-05-0-UI 3', mRNA sequence.	0.294567387	17 A1	399660	AI842472
44	161885_f_at	GRAM domain containing 3	Gramd3	AV370153 RIKEN full-length enriched, adult male colon Mus musculus cDNA clone 9030209D18 3', mRNA sequence.	0.295970536	18 D2	24356	AV370153
45	*103685_at*	*Transcribed locus*		*UI-M-AK0-adh-d-11-0-UI.s1 NIH_BMAP_MHY Mus musculus cDNA clone UI-M-AK0-adh-d-11-0-UI 3', mRNA sequence.*	*0.299140511*		*23897*	*AI839232*
46	101433_at	major histocompatibility complex, class I-related	Mr1	MHC class I related gene 1 isoform E; MHC class I related protein 1 isoform E; Mus musculus MHC class I related protein 1 isoform E (MR1E) pseudogene mRNA, complete sequence.	0.30113754	1 H1	7580	AF010452
47	94956_at	DiGeorge syndrome critical region gene 6	Dgcr6	similar to Drosophila gonadal protein; Mus musculus Dgcr6 protein (Dgcr6) mRNA, partial cds.	0.302009957	16 B2|16 10.71 cM	27155	AF021031
48	102039_at	general transcription factor II H, polypeptide 4	Gtf2h4	UI-M-BH0-ajt-f-06-0-UI.s1 NIH_BMAP_M_S1 Mus musculus cDNA clone UI-M-BH0-ajt-f-06-0-UI 3', mRNA sequence.	0.309135592	17 B1	10182	AI850881
49	*101876_s_at*	*histocompatibility 2, T region locus 10*	*H2-T10*	*MHC H2-TL-T17-c; Mouse MHC class I H2-TL-T17-c mRNA (d haplotype), complete cds.*	*0.312545377*	*17 B1|17 19.96 cM*		*M35247*
50	102975_at	CD8 antigen, alpha chain	Cd8a	Lyt2a; Mus musculus CD8 mRNA, Lyt2a allele, complete cds.	0.317593338	6 C|6 30.5 cM	1858	U34881
51	93311_at	CDC-like kinase 3	Clk3	SR protein kinase; Mus musculus cdc2/CDC28-like protein kinase 3 (Clk3) mRNA, complete cds.	0.31922683	9 C	25720	AF033565
53	*103278_at*	*peptidyl arginine deiminase, type IV*	*Padi4*	*Mus musculus mRNA for peptidylarginine deiminase type IV, complete cds.*	*0.33311381*	*4 E1|4 71.0 cM*	*250358*	*AB013850*
54	103036_at	X-ray repair complementing defective repair in Chinese hamster cells 6	Xrcc6	Mus musculus murine p70 Ku lupus autoantigen mRNA, 3' end.	0.33468476	15 E-F|15 47.5 cM	288809	M38700
55	*93895_s_at*	*inositol 1,4,5-triphosphate receptor 1*	*Itpr1*	*putative; Mus musculus PCD-6 mRNA.*	*0.341538451*	*6 E1-E2|6 48.0 cM*	*227912*	*M21530*
56	98071_f_at	deoxycytidine kinase	Dck	M.musculus mRNA for Deoxycytidine kinase.	0.342979906		298892	X77731
57	*100961_at*	*potassium voltage-gated channel, subfamily H (eag-related), member 2*	*Kcnh2*	*similar to HERG; Ether-a-go-go-related protein; cardiac specific isoform; Ether-a-go-go-related protein; Mus musculus potassium channel isoforms Merg1a, Merg1a', and Merg1b (Merg1) gene, exons 3-15 and complete cds.*	*0.347592788*	*5 A3|5 12.0 cM*	*6539*	*AF012871*
58	99024_at	Max dimerization protein 4	Mxd4	Mus musculus Max-interacting transcriptional repressor (Mad4) mRNA, complete cds.	0.348766769	5 B2|5 20.0 cM	259260	U32395
59	92956_at	Notch gene homolog 3 (Drosophila)	Notch3	M.musculus mRNA for Notch 3.	0.348769139	17 B1|17 20.0 cM	4945	X74760
60	98072_r_at	deoxycytidine kinase	Dck	M.musculus mRNA for Deoxycytidine kinase.	0.348958193		298892	X77731
61	101442_f_at	inositol 1,4,5-triphosphate receptor 2	Itpr2	Mus musculus inositol trisphosphate receptor type 2 (Itpr2) gene, partial cds.	0.350307293	6 G3|6 73.0 cM	7800	AF031127
62	*99812_at*	*calpain 3*	*Capn3*	*M.musculus mRNA for skeletal muscle-specific calpain.*	*0.351421369*	*2 E5|2 67.2 cM*	*38851*	*X92523*
63	160793_at	POU domain, class 6, transcription factor 1	Pou6f1	UI-M-BH0-akf-h-09-0-UI.s1 NIH_BMAP_M_S1 Mus musculus cDNA clone UI-M-BH0-akf-h-09-0-UI 3', mRNA sequence.	0.360030493	15 F1|15 56.6 cM	28825	AI851313
64	*95022_at*	*A kinase (PRKA) anchor protein (gravin) 12*	*Akap12*	*Src Suppressed C Kinase Substrate; Mus musculus mRNA for SSeCKS, complete cds.*	*0.36132534*	*10 A1*	*27481*	*AB020886*
65	95688_at	degenerative spermatocyte homolog 1 (Drosophila)	Degs1	transmembrane protein; Mus musculus mRNA for Mdes transmembrane protein.	0.367582325	1 H5	29648	Y08460
66	*104660_at*	*suppression inducing transmembrane adaptor 1*	*Sit1*	*Mus musculus mRNA for SIT protein.*	*0.369965296*	*4 B1*	*31775*	*AJ236881*

Genes italicised indicate those that have passed the Benjamini-Hochberg false discovery rate procedure.

Table A.4. Genes down-regulated by NP68 cognate antigen in F5 TCR Rag-1$^{-/-}$ Tap-1$^{-/-}$ transgenic mice.

	Probe set ID	Gene Title	Gene Symbol	Description	Fold change	Chromosomal Location	UniGene ID	Representative Public ID
67	102745_at	T-cell receptor gamma chain	Tcrg	T cell receptor C-gamma-7.1; Mouse T cell receptor C-gamma-7.1 mRNA, 3' end.	0.372485776	13 10.0 cM		M18858
68	99027_at	Bcl2-like 1	Bcl2l1	Mus musculus Bcl-xL mRNA, complete cds.	0.372661907	2 H1|2 87.5 cM	238213	L35049
69	94835_f_at	tubulin, beta 2a	Tubb2a	beta-tubulin; Mouse beta-tubulin gene M-beta-2, 3' end.	0.380757693	13 A3.3|13 16.0 cM	434383	M28739
70	102029_at	interleukin 16	Il16	Mus musculus IL-16 precursor, mRNA, complete cds.	0.382304127	7 D2-D3|7 41.2 cM	10137	AF017111
71	*160597_at*	*DNA segment, Chr 1, ERATO Doi 622, expressed*	*D1Ertd622e*	*UI-M-BH1-all-e-01-0-UI.s1 NIH_BMAP_M_S2 Mus musculus cDNA clone UI-M-BH1-all-e-01-0-UI 3', mRNA sequence.*	*0.38347965*	*1 D|1 60.2 cM*	*12309*	*AW047450*
72	160965_at	RAS p21 protein activator 4	Rasa4	mr24e06.r1 Soares mouse 3NbMS Mus musculus cDNA clone IMAGE:598402 5', mRNA sequence.	0.385404161	5 G2	290655	AA163960
73	97688_at	POZ (BTB) and AT hook containing zinc finger 1	Patz1	mu21f07.x1 Soares_thymus_2NbMT Mus musculus cDNA clone IMAGE:640069 3', mRNA sequence.	0.39000267	11 A1	275563	AI666506
74	93319_at	RAS p21 protein activator 3	Rasa3	Mus musculus GTPase-activating protein GAPIII mRNA, complete cds.	0.390566555	8 A1.1	18517	U20238
75	160359_at	RIKEN cDNA 1190002H23 gene	1190002H23Rik	UI-M-BG1-aic-e-02-0-UI.s1 NIH_BMAP_MSC_N Mus musculus cDNA clone UI-M-BG1-aic-e-02-0-UI 3', mRNA sequence.	0.390756295	14 D3	29811	AI854358
76	94899_at	expressed sequence AA536749	AA536749	Mus musculus p116Rip mRNA, complete cds.	0.392966027	11 B1.3	2402	U73200
77	*99146_at*	*syntaxin 6*	*Stx6*	*UI-M-BH2.1-apq-h-02-0-UI.s1 NIH_BMAP_M_S3.1 Mus musculus cDNA clone UI-M-BH2.1-apq-h-02-0-UI 3', mRNA sequence.*	*0.403768812*	*1 G3*	*66264*	*AW124355*
78	160841_at	D site albumin promoter binding protein	Dbp	UI-M-BH1-ame-a-08-0-UI.s1 NIH_BMAP_M_S2 Mus musculus cDNA clone UI-M-BH1-ame-a-08-0-UI 3', mRNA sequence.	0.410472478	7 B3|7 23.0 cM	378235	AW047343
79	161012_at	CD79B antigen	Cd79b	B-cell-specific glycoprotein precursor; Mouse B-cell-specific glycoprotein (B29) mRNA, complete cds.	0.410733895	11 E1|11 65.0 cM	2987	J03857
80	161076_at	cDNA sequence BC023882	BC023882	ub62c01.x1 Soares_mammary_gland_NMLMG Mus musculus cDNA clone IMAGE:1382304 3', mRNA sequence.	0.410756871	5 B2|5 20.0 cM	319286	AI462312
81	*95511_at*	*integrin alpha 6*	*Itga6*	*M.musculus mRNA for integrin alpha6 subunit.*	*0.411460116*	*2 C2|2 38.0 cM*	*225096*	*X69902*
82	*98981_s_at*	*transcription factor 12*	*Tcf12*	*M.musculus ALF1 mRNA.*	*0.413360909*	*9 D|9 42.0 cM*	*171615*	*X64840*
83	95693_at	isocitrate dehydrogenase 2 (NADP+), mitochondrial	Idh2	Mus musculus isocitrate dehydrogenase mRNA, complete cds.	0.4149393	7 D2|7 41.0 cM	246432	U51167
84	*103504_at*	*single-stranded DNA binding protein 2*	*Ssbp2*	*UI-M-AK0-adc-d-11-0-UI.s1 NIH_BMAP_MHY Mus musculus cDNA clone UI-M-AK0-adc-d-11-0-UI 3', mRNA sequence.*	*0.417379726*	*13 C3*	*343095*	*AI837107*
85	102995_s_at	granzyme A	Gzma	preserine protease; Mouse T cell-specific serine protease mRNA, complete cds.	0.417499285	13 D|13 64.0 cM	15510	M13226
86	*100902_at*	*RIKEN cDNA 2610019F03 gene*	*2610019F03Rik*	*UI-M-AN1-aff-h-05-0-UI.s1 NIH_BMAP_MBG_N Mus musculus cDNA clone UI-M-AN1-aff-h-05-0-UI 3', mRNA sequence.*	*0.418873768*	*8 A1.1*	*5727*	*AI846549*
87	160921_at	acyl-CoA synthetase short-chain family member 1	Acss1	UI-M-BH2.2-aqk-g-07-0-UI.s1 NIH_BMAP_M_S3.2 Mus musculus cDNA clone UI-M-BH2.2-aqk-g-07-0-UI 3', mRNA sequence.	0.42009882	2 G3	7044	AW125884
88	*103539_at*	*cytoplasmic tyrosine kinase, Dscr28C related (Drosophila)*	*Tec*	*Mouse mRNA for protein-tyrosine kinase, tec type I.*	*0.42657963*	*5 C3.2|5 41.0 cM*	*319581*	*X55663*
89	95457_at	inositol monophosphatase domain containing 1	Impad1	UI-M-BH0-ajz-e-09-0-UI.s1 NIH_BMAP_M_S1 Mus musculus cDNA clone UI-M-BH0-ajz-e-09-0-UI 3', mRNA sequence.	0.427607995	4 A1	369779	AI854214
90	*94821_at*	*X-box binding protein 1*	*Xbp1*	*UI-M-BH2.1-app-e-07-0-UI.s1 NIH_BMAP_M_S3.1 Mus musculus cDNA clone UI-M-BH2.1-app-e-07-0-UI 3', mRNA sequence.*	*0.429273059*	*11 A1|11 3.0 cM*	*434371*	*AW123880*
91	99511_at	protein kinase C, beta 1	Prkcb1	protein kinase C beta-II (AA 1-673); Mouse mRNA for protein kinase C beta-II.	0.433304	7 F2|7 60.0 cM	207496	X53532
92	102994_at	signal transducer and activator of transcription 4	Stat4	Mus musculus signal transducer and activator of transcription (Stat4) mRNA, complete cds.	0.433389291	1 C1.1|1 25.9 cM	1550	U06923
93	103800_at	ATP-binding cassette, sub-family C (CFTR/MRP), member 5	Abcc5	Mus musculus MRP5 mRNA, complete cds.	0.434943512	16 A3|16 14.0 cM	20845	AB019003
94	93985_at	TCDD-inducible poly(ADP-ribose) polymerase	Tiparp	UI-M-BH2.3-aoa-g-07-0-UI.s1 NIH_BMAP_M_S3.3 Mus musculus cDNA clone UI-M-BH2.3-aoa-g-07-0-UI 3', mRNA sequence.	0.435065396	3 E1	246398	AW120868
95	103282_at	RAS, guanyl releasing protein 2	Rasgrp2	Mus musculus calcium- and diacylglycerol-regulated guanine nucleotide exchange factor I (CalDAG-GEFI) mRNA, complete cds.	0.437051344		77017	U78171
96	*92595_r_at*	*ferrochelatase*	*Fech*	*Mus musculus ferrochelatase mRNA, complete cds.*	*0.437714658*	*18 E1|18 39.0 cM*	*1070*	*M61215*
97	94439_at	oxysterol binding protein-like 11	Osbpl11	UI-M-BH2.1-apq-h-10-0-UI.s1 NIH_BMAP_M_S3.1 Mus musculus cDNA clone UI-M-BH2.1-apq-h-10-0-UI 3', mRNA sequence.	0.438781718	16 B3	26564	AW124363
98	*94415_at*	*BTB and CNC homology 1*	*Bach1*	*vt42e01.r1 Barstead mouse proximal colon MPLRB6 Mus musculus cDNA clone IMAGE:1165752 5', mRNA sequence.*	*0.441278134*	*16 C3.3*	*26147*	*AA710439*
99	97525_at	glycerol kinase	Gyk	ATP:glycerol 3-phosphotransferase; Mus musculus glycerol kinase (Gyk) mRNA, complete cds.	0.443002311	X C-D|X 33.0 cM	246682	U48403
100	98632_at	adenosine deaminase	Ada	adenosine deaminase (EC 3.5.4.4); Mouse adenosine deaminase mRNA, complete cds.	0.443639117	2 H3|2 94.0 cM	388	M10319

Genes italicised indicate those that have passed the Benjamini-Hochberg false discovery rate procedure.

Table A.4. Genes down-regulated by NP68 cognate antigen in F5 TCR Rag-1$^{-/-}$ Tap-1$^{-/-}$ transgenic mice.

	Probe set ID	Gene Title	Gene Symbol	Description	Fold change	Chromosomal Location	UniGene ID	Representative Public ID
101	93486_at	solute carrier family 27 (fatty acid transporter), member 1	Slc27a1	integral plasma membrane protein; Mus musculus fatty acid transport protein (FATP) mRNA, complete cds.	0.44444547	8 B3.3	38165	U15976
102	98483_at	calcium channel, voltage-dependent, beta 3 subunit	Cacnb3	Mus musculus partial b3 gene for alpha3 subunit of L-type Ca2+ channel, exon 1 and joined CDS.	0.448341113	15 F1|15 59.8 cM	3544	X94404
103	AFFX-MurFAS_at	Fas (TNF receptor superfamily member)	Fas	NGF/TNF-receptor-related protein; Mus musculus Fas antigen mRNA, complete cds.	0.449759272	19 C1|19 23.0 cM	1626	M83649
104	*97312_at*	*CD164 antigen*	*Cd164*	*Mus musculus mRNA for MGC-24v, complete cds.*	*0.449766518*	*10 B2|10 25.0 cM*	*269815*	*AB014464*
105	104065_at	ER degradation enhancer, mannosidase alpha-like 1	Edem1	uo68g01.x1 NCI_CGAP_Mam1 Mus musculus cDNA clone IMAGE:2647728 3' similar to TR:Q92611 Q92611 MYELOBLAST KIAA0212. ;, mRNA sequence.	0.450559255		21596	AW212878
106	160078_at	protein phosphatase 1, regulatory (inhibitor) subunit 14B	Ppp1r14b	phospholipase C3 neighbouring protein; M.musculus mRNA for PNG protein.	0.456369014	19 A	140	X97490
107	95063_at	cell division cycle associated 7	Cdca7	vo03b06.x1 Stratagene mouse skin (#937313) Mus musculus cDNA clone IMAGE:1040339 3', mRNA sequence.	0.458208078	2 C3	270676	AI606257
108	*93206_g_at*	*adenosine deaminase*	*Ada*	*adenosine deaminase (EC3.5.4.4); Mouse ADA gene encoding adenosine deaminase, promoter region.*	*0.46756581*	*2 H3|2 94.0 cM*	*388*	*M14167*
109	92561_at	ectonucleoside triphosphate diphosphohydrolase 5	Entpd5	Mus musculus mRNA for nucleoside diphosphatase (ER-UDPase gene).	0.468466402	12 E|12 39.0 cM	10211	AJ238636
110	161038_at	phosphoribosyl pyrophosphate synthetase 2	Prps2	mp75e10.r1 Soares_thymus_2NbMT Mus musculus cDNA clone IMAGE:575082 5' similar to gb:Y00971_ma1 RIBOSE-PHOSPHATE PYROPHOSPHOKINASE II (HUMAN);, mRNA sequence.	0.47789023	X 72.0 cM	272955	AA120675
111	160783_at	DNA segment, Chr 14, ERATO Doi 436, expressed	D14Ertd436e	UI-M-BH2.1-apd-c-06-0-UI.s1 NIH_BMAP_M_S3.1 Mus musculus cDNA clone UI-M-BH2.1-apd-c-06-0-UI 3', mRNA sequence.	0.478622652	14 C1|14 18.2 cM	287279	AW123154
112	160612_at	ATP-binding cassette, sub-family G (WHITE), member 1	Abcg1	M.musculus ABC8 mRNA for ABC transporter.	0.478873088	17 A2-B	427613	Z48745
113	94736_at	lysosomal trafficking regulator	Lyst	beige; Mus musculus beige (bg) mRNA, partial cds.	0.479641311	13 A1|13 7.0 cM	342337	U52461
114	98472_at	histocompatibility 2, T region locus 23	H2-T23	Murine gene 37 for pot. membrane bound protein.	0.480369831	17 B1|17 19.73 cM		Y00629
115	102383_at	RIKEN cDNA 5730593F17 gene	5730593F17Rik	UI-M-BH1-amo-h-10-0-UI.s1 NIH_BMAP_M_S2 Mus musculus cDNA clone UI-M-BH1-amo-h-10-0-UI 3', mRNA sequence.	0.480897957	11 D	262113	AW048977
116	*160138_at*	*Max interacting protein 1*	*Mxi1*	*This protein form of mouse Mxi strongly suppresses c-Myc cotransformation activity and interacts with mammalian homolog of yeast Sin3 through the 'repressive domain'.; Mus musculus Mxi-SR protein gene, complete cds.*	*0.503130009*	*19 D|19 49.5 cM*	*2154*	*L38822*
117	103488_at	selectin, platelet (p-selectin) ligand	Selpl	M.musculus mRNA for P-selectin glycoprotein ligand 1.	0.503325052	5 F|5 64.0 cM	332590	X91144
118	103422_at	CD1d1 antigen	Cd1d1	Mouse CD1.1 mRNA, complete cds.	0.507265703	3 F1|3 48.0 cM	1894	M63695
119	98507_at	nuclear receptor subfamily 1, group D, member 1	Nr1d1	UI-M-AM1-afw-b-05-0-UI.s1 NIH_BMAP_MAM_N Mus musculus cDNA clone UI-M-AM1-afw-b-05-0-UI 3', mRNA sequence.	0.531526645	11 D	390397	AI834950

Genes italicised indicate those that have passed the Benjamini-Hochberg false discovery rate procedure.